

Evaluation of ultrasound in juvenile idiopathic arthritis

Thesis by

Nina Martine Krafft Sande



Institute of Clinical Medicine

Faculty of Medicine

University of Oslo

2023



Division of Surgery, Inflammatory medicine and Transplantation
Department of Rheumatology, Dermatology- and Infectious diseases

Oslo University Hospital

Oslo, Norway

© **Nina Martine Krafft Sande, 2024**

*Series of dissertations submitted to the
Faculty of Medicine, University of Oslo*

ISBN 978-82-348-0406-9

All rights reserved. No part of this publication may be reproduced or transmitted, in any form or by any means, without permission.

Cover: UiO.

Print production: Graphic center, University of Oslo.

Table of Contents

Acknowledgements	5
Funding	7
Abbreviations	8
Summary of thesis	10
Norsk sammendrag	13
List of papers	16
1. Introduction and background	17
1.1 Juvenile idiopathic arthritis	17
1.1.1 Diagnosis and classification	17
1.1.2 Epidemiology	19
1.1.3 Pathogenesis	19
1.1.4 Management	21
1.1.5 Prognosis and prognostic factors.....	22
1.2 Assessment of disease activity	23
1.2.1 Clinical joint examination	23
1.2.2 Biochemical and immunological markers.....	24
1.2.3 Paediatric core set outcome variables	24
1.2.4 Composite measures of disease activity.....	25
1.2.5 Imaging in JIA.....	27
1.3 Ultrasound	30
1.3.1 Ultrasound physics	31
1.3.2 Musculoskeletal ultrasound in healthy children.....	32
1.3.3 Musculoskeletal ultrasound in patients with JIA	35
1.3.5 Ultrasonographic scoring systems for synovitis in JIA.....	37
2. General aim and research questions	39
2.1 General aim	39

2.2 Research questions	39
3. Material and methods	40
3.1 Study design	40
3.2 Study population	40
3.3 Data collection	41
3.3.1 Demographic variables and laboratory measures.....	41
3.3.2 Clinical variables.....	42
3.3.3 Ultrasound	42
3.3.4 Whole-body Magnetic Resonance Imaging	44
3.4 Statistics	45
3.4.1 Descriptive statistics.....	45
3.4.2 Reliability	45
3.4.3 Associations	46
3.4.4 Validity.....	47
3.5 Ethical considerations	48
4. Summary of results	50
4.1 Paper I	50
4.2 Paper II	51
4.3 Paper III	52
5. Discussion	53
5.1 Methodological aspects	53
5.1.1 Study design	53
5.1.2 Representativeness of study population	54
5.1.3 Data collection.....	55
5.1.4 Statistical considerations	58
5.2 Main results	60
5.2.1 Development of an image acquisition protocol.....	60
5.2.2 Development of a joint-specific scoring system and reference atlas	61
5.2.3 Reliability of the joint-specific scoring system with reference atlas	63

5.2.5 Associations between PD findings and BM synovitis, and clinical arthritis	64
5.2.6 Correlations between ultrasound and whole-body MRI and clinical assessment ...	65
6. Conclusions	69
6.1 Answer to research questions.....	69
6.2 Clinical implications and further research	70
6.3 Dissemination.....	70
7. Errata	72
8. References	73
9. Papers I-III.....	84

Acknowledgements

The work included in this thesis would not have been possible without the contribution of many people, to whom I am truly grateful.

First of all, I would like to thank my main supervisor, **Pernille Boyesen**. Your advice, feedback and encouragement have been invaluable. Thank you for challenging me to work independently and at the same time guiding me in the right direction throughout these years. Thank you for your patience and for believing in me.

I would also like to thank my co-supervisors for their support. **Berit Flatø**, thank you for your guidance and for sharing your enormous knowledge about paediatric rheumatology and research. I am impressed by your working capacity. **Vibke Lilleby**, thank you for your valuable input and advice, and for our good discussions concerning musculoskeletal ultrasound in children.

I am grateful to all my co-authors: **Anna-Birgitte Aga** for your prompt and constructive advice and for always being supportive, **Hilde Berner Hammer** for introducing me to musculoskeletal ultrasound and for always being interested and enthusiastic, **Johannes Roth** for sharing your broad knowledge about musculoskeletal ultrasound in children and for your cooperation, **Eva Kirkhus** for participating in this project and for sharing your extensive knowledge about MRI in children, and **Anders Høye Tomterstad** for your important contribution concerning the whole-body MRI protocol. Thank you for all your feedback.

I would like to thank **Øystein Horgmo** for taking the nice photographs of the ultrasound probe positions used in the reference atlases. I also thank **David Swanson**, **Cathrine Brunborg** and **Lien My Diep** for statistical advice and help in the calculations.

This project would not have been possible without the *participating patients* and *their caregivers*, and I am truly grateful to every one of you.

I would also like to thank the *Norwegian Rheumatism Association* and the *DAM foundation* for believing in this project and for the financial support. I am thankful to *Oslo University*

Hospital for the support they provide their researchers and the *University of Oslo* for facilitating my PhD project.

I am thankful to *Øyvind Molberg* for believing in this project and for offering me my first permanent position as a physician, and to *Helena Andersson* for making the Department of Rheumatology at Rikshospitalet a stimulating workplace.

Thanks to my good PhD colleagues *Ingrid Jyssum* and *Sigrid Hestetun* for the many hours discussing statistics, theory of science and “PhD issues”. Thank you for your valuable support, optimism and friendship. I would also like to thank my *PhD colleagues* at the REMEDY center for inspiring and educative meetings at “Journal Club”, and my *colleagues* at the Department of Rheumatology and at “Bygg 14” at Rikshospitalet for creating a friendly and welcoming work environment.

I am grateful to my good friends, *Ida, Kristin, Cecilie* and *Nina* for always being supportive, kind and caring. Thank you for all our conversations, trips and runs during this PhD period and for making me laugh even in difficult times.

I also want to thank my sisters and brother, *Siri Jo, Rikke* and *Halvor* for inspiring me and encouraging me. Thank you to my *family-in-law* for always being kind and supportive. The warmest thanks to my parents, *Henny* and *Alex* for being such great role models, for your endless love and for always being there for me.

Finally, I want to thank my husband, *Lars Øivind* for your love, patience and support. Thank you *Mikkel* and *Maria*, our wonderful children, for your encouraging little notes and sweet comments. To me, you are everything.

Funding

This PhD-fellowship was funded by the DAM foundation through the Norwegian Rheumatism Association. Institutional support was provided by the administration at Oslo University Hospital, Rikshospitalet.

The funders have not been involved in study design, data collection, data analyses, data interpretation or writing of the manuscripts.

Abbreviations

ACR	American College of Rheumatology
ANA	Antinuclear Antibody
Anti-CCP	Antibodies to Cyclic Citrullinated Peptide
BM	Brightness Mode (B-mode)
BME	Bone Marrow Oedema
CD	Colour Doppler
CHAQ	Childhood Health Assessment Questionnaire
CR	Conventional Radiography
CRP	C-Reactive Protein
DIP	Distal Interphalangeal
DMARD	Disease Modifying Anti-Rheumatic Drug
FOV	Field Of View
ESPR	European Society of Paediatric Radiology
ESR	Erythrocyte Sedimentation Rate
ESSR	European Society of Musculoskeletal Radiology
EULAR	European League Against Rheumatism
GE	General Electric
HLA	Human Leucocyte Antigen
ICC	Intraclass Correlation Coefficient
IL	Interleukin
ILAR	International League of Associations for Rheumatology
IP	Interphalangeal
IQR	Interquartile Range
JADAS	Juvenile Arthritis Disease Activity Score
JAMRI	Juvenile Idiopathic Arthritis Magnetic Resonance Imaging
JIA	Juvenile Idiopathic Arthritis
JSpADA	Juvenile Spondyloarthritis Disease Activity
LOM	Limited range Of Motion
MCP	Metacarpophalangeal
MHz	Megahertz
MRI	Magnetic Resonance Imaging

MTP	Metatarsophalangeal
NPV	Negative Predictive Value
OMERACT	Outcome Measures in Rheumatology
OUH	Oslo University Hospital
PACS	Picture Archiving and Communications Systems
PD	Power Doppler
PGA	Parent/patient Global Assessment of well being
PhGA	Physician Global Assessment of disease activity
PIP	Proximal Interphalangeal
PPV	Positive Predictive Value
PReS	Paediatric Rheumatology European Society
PRF	Pulse Repetition Frequency
PRINTO	Paediatric Rheumatology International Trials Organisation
RA	Rheumatoid Arthritis
RF	Rheumatoid Factor
SPSS	Statistical Package for the Social Sciences
T	Tesla
TE	Echo Time
TNF	Tumour Necrosis Factor
TR	Repetition Time
TSE	Turbo Spin Echo
VAS	Visual Analogue Scale

Summary of thesis

Juvenile idiopathic arthritis (JIA) is the most common rheumatic disease in children and is characterised by joint inflammation that begins before 16 years of age and persists for at least 6 weeks. Reliable and valid methods to detect and quantify joints with inflammation and to assess disease activity is important in the management of patients with JIA. Ultrasound is a non-invasive and well-accepted bedside tool that is increasingly being used in the evaluation of synovitis (joint inflammation). However, the interpretation of ultrasound images in children can be difficult due to the unique features of the growing skeleton. In addition, few data exist on the assessment of Doppler findings (vascularisation) in patients with JIA, which is one of the most difficult ultrasonographic features to interpret in children because of normal vascularisation that must not be misinterpreted as pathological findings. Over the last few years, there has been an increasing focus on standardising the use of ultrasound in children. Definitions for ultrasonographic features of joints in healthy children and preliminary ultrasound definitions for synovitis have been developed, but there is no agreement on how to scan all paediatric joints or how to grade the severity of synovitis. Furthermore, the validity of ultrasound detected synovitis in patients with JIA is still not well known.

The objectives of this thesis were to develop a standardised ultrasonographic scanning protocol and a semiquantitative joint-specific scoring system for synovitis with age-divided reference atlas for patients with JIA. Further, to explore Doppler ultrasound findings in joints with B-mode (BM) synovitis, and to test the reliability and validity of the ultrasonographic scoring system with reference atlas.

The project had a cross-sectional design including patient with JIA, aged 1-18 years old. First, experienced rheumatologists developed a standardised ultrasonographic scanning protocol and a semiquantitative (grades 0-3) joint-specific scoring system for BM synovitis for frequently affected joints in patients with JIA. This was done through a consensus process consisting of literature review, discussions and practical training. The joint regions included were the anterior elbow, posterior elbow, radiocarpal, midcarpal, metacarpophalangeal 2-3 (dorsal), proximal interphalangeal 2-3 (volar and dorsal), hip, knee (suprapatellar recess and lateral parapatellar recess), tibiotalar, talonavicular, anterior subtalar, posterior subtalar and metatarsophalangeal 2-3 joints. Ultrasonographic images that had been collected from the in- and outpatient

rheumatology clinic at Oslo University Hospital, were used to develop reference atlases with images that corresponded to the joint-specific scoring system. For BM synovitis, four atlases were developed according to age-related changes (2-4 years, 5-8 years, 9-12 years and 13-18 years). For Doppler findings, an atlas for power Doppler (PD) activity was developed without dividing into different age-groups. The system was then tested for inter-reader and intra-reader reliability on still images with different levels of synovitis, and in a live exercise including ten patients with JIA.

The ultrasonographic scanning protocol and the joint-specific scoring system with reference atlas were then used to describe ultrasound Doppler findings in joint regions with BM synovitis in 27 patients with JIA who were assessed clinically and with ultrasound. Associations between PD findings and BM synovitis, clinical arthritis and measures of disease activity were further explored.

Finally, the validity of ultrasound and the novel joint-specific scoring system were examined by comparing ultrasound findings of synovitis with findings of joint inflammation on whole-body MRI and clinical examination, and with the disease activity measure 71-joints Juvenile Arthritis Disease Activity Score (JADAS71). Twenty-seven patients with active JIA, who were already referred to a magnetic resonance imaging (MRI) or whole-body MRI examination on clinical indication, were examined clinically, with non-contrast enhanced whole-body MRI and ultrasound. For each patient, a sum score for joint inflammation found on ultrasound (PD and BM synovitis), on whole-body MRI (effusion/synovial thickening) and on clinical joint examination (active joint) was calculated to examine correlations at patient level. Ultrasound findings of synovitis at joint level were also explored using whole-body MRI or clinical joint examination as reference.

The scanning protocol and the joint-specific scoring system with reference atlas demonstrated moderate to excellent inter-reader reliability and good to excellent intra-reader reliability for BM synovitis scoring, and good to excellent inter-reader and intra-reader reliability for PD activity scoring on still images. The inter-reader reliability was moderate to excellent for both BM synovitis and PD activity scoring in the live exercise.

Abnormal Doppler activity was most frequently found in the lateral parapatellar recess of the knee joint. PD grade 1 was found in joints with BM grade 1, 2 and 3, but PD grade 2 and 3 were

only found in joint regions with BM grade 2 and 3. Increasing Doppler grades were significantly associated with greater severity BM synovitis grades and with the presence of clinical arthritis.

Ultrasound synovitis sum scores were significantly correlated with whole-body MRI effusion/synovial thickening sum scores and with the JADAS71. Ultrasound synovitis sum scores were moderately correlated with clinical active joint sum scores. Ultrasound findings of synovitis demonstrated high specificity, but lower sensitivity at joint level when using whole-body MRI or clinical joint examination as reference.

The findings presented in this thesis indicate that the developed ultrasonographic scanning protocol and the joint-specific scoring system for synovitis with age-divided reference atlas for patients with JIA are reliable and valid tools in the assessment of joint inflammation. Further, that ultrasound synovitis sum scores can reflect overall disease activity in patients with JIA and may be a useful outcome measure in future research and clinical practice.

Norsk sammendrag

Juvenil idiopatisk artritt (JIA) er den vanligste revmatiske sykdommen hos barn, og er karakterisert av leddbetennelse som oppstår før 16 års alder og som varer i minst 6 uker.

Det er viktig å ha pålitelige og valide metoder i oppfølgingen av pasienter med JIA slik at man kan oppdage og gradere alvorligheten av ledd med betennelse, samt vurdere sykdomsaktiviteten. Ultralyd er en ikke-invasiv og godt tolerert metode som kan gjøres ved sengekanten, og blir i økende grad benyttet i evalueringen av synovitt (leddbetennelse). Tolkning av ultralydbilder hos barn kan imidlertid være vanskelig fordi barn har et skjelett i vekst. I tillegg finnes det få data om Dopplerfunn (vaskularisering) hos pasienter med JIA. Dette er en av de vanskeligste funnene å vurdere på ultralyd hos barn i vekst fordi de også har normal vaskularisering som ikke må forveksles med patologiske funn. I løpet av de seneste årene har det vært et økende fokus på å standardisere bruken av ultralyd hos barn. Det har blitt utviklet definisjoner for ultralydfunn i ledd hos friske barn og foreløpige definisjoner for synovitt på ultralyd. Det er imidlertid ingen enighet om hvordan ultralydundersøkelse av alle ledd hos barn skal utføres, eller hvordan alvorligheten av synovitt skal graderes. Videre er validiteten av synovittfunn på ultralyd hos pasienter med JIA lite kjent.

Hensikten med denne avhandlingen var å utarbeide en standardisert ultralydundersøkelse og et semikvantitativt leddspesifikt skåringssystem for synovitt med aldersinndelt ultralyd referanseatlas for pasienter med JIA. I tillegg ønsket vi å undersøke ultralyd Dopplerfunn i ledd som hadde B-mode (BM) synovitt, samt teste reliabiliteten og validiteten av skåringssystemet med referanseatlas.

Prosjektet hadde et tverrsnitts design og inkluderte pasienter med JIA i alderen 1-18 år. Først utviklet erfarne revmatologer en standardisert ultralydundersøkellesesprotokoll og et semikvantitativt (gradene 0-3) leddspesifikt skåringssystem for BM synovitt for ledd som ofte er affisert hos pasienter med JIA. Dette ble gjort gjennom en konsensusprosess bestående av litteraturgjennomgang, diskusjoner og praktisk trening. Leddområdene som ble inkludert var anteriore albue, posteriore albue, radiokarpal, midkarpal, metakarpofalangeal 2-3 (dorsal), proksimale interphalangeal 2-3 (volar og dorsal), hofte, kne (suprapatellare recess og laterale parapatellare recess), talokrural, talonavikular, anteriore subtalar, posteriore subtalar og metatarsofalangeal 2-3 ledd. Til slutt ble ultralydbilder, som hadde blitt samlet fra

revmatologisk poliklinikk og sengepost ved Oslo Universitetssykehus, brukt til å lage referanseatlas med ultralydbilder som korresponderte til det leddspesifikke skåringssystemet. Det ble laget fire atlas for BM synovitt i henhold til aldersrelaterte forandringer (2-4 år, 5-8 år, 9-12 år og 13-18 år). For Dopplerfunn ble et atlas for power Doppler (PD) aktivitet laget uten å dele inn i ulike aldersgrupper. Skåringssystemet ble deretter testet for interleser og intraleser reliabilitet på ultralydbilder med ulike grader av leddbetennelse, og i en «live» øvelse som inkluderte ti pasienter med JIA.

Ultralydprotokollen og det leddspesifikke skåringssystemet med referanseatlas ble deretter benyttet til å beskrive Dopplerfunn i ledd med BM synovitt hos 27 pasienter med JIA som ble undersøkt med klinisk leddundersøkelse og med ultralyd. Assosiasjoner mellom PD aktivitet og BM synovitt, klinisk artritt og mål på sykdomsaktivitet ble deretter undersøkt.

Validiteten av ultralyd og det nye leddspesifikke skåringssystemet ble undersøkt ved å sammenligne funn av synovitt på ultralyd med funn av leddbetennelse på helkroppsmagnetiske resonans (MR) og klinisk leddundersøkelse, og med 71-ledds «Juvenile Arthritis Disease Activity Score» (JADAS71), som er et validert mål på sykdomsaktivitet. Tjuesyv pasienter med aktiv JIA, som allerede var henvist til en MR eller helkroppsmr-undersøkelse på klinisk indikasjon, ble undersøkt med klinisk leddundersøkelse, ultralyd og helkroppsmr-uten kontrast. For hver pasient ble en sumskår for leddinflammasjon funnet på ultralyd (PD og BM synovitt), helkroppsmr (effusjon/synovial fortykning) og ved klinisk leddundersøkelse (aktive ledd) kalkulert. De ulike sumskårene ble sammenlignet for å undersøke om de var korrelert på pasientnivå. Funn av synovitt på ultralyd ble også undersøkt på leddnivå ved å bruke helkroppsmr eller klinisk leddundersøkelse som referanse.

Ultralydundersøkelsesprotokollen og det leddspesifikke skåringssystemet med referanseatlas viste moderat til perfekt interleser reliabilitet, og god til perfekt intraleser reliabilitet for skåring av BM synovitt, og god til perfekt intra- og interleser reliabilitet for skåring av PD aktivitet på ultralydbilder. Interleser reliabilitet for skåring av både BM synovitt og PD aktivitet var moderat til perfekt i øvelsen der pasienter med JIA ble undersøkt.

Vi fant at unormal Doppler aktivitet var mest hyppig i kneleddet, nærmere bestemt den laterale parapatellare recess. PD grad 1 ble sett i leddregioner med BM grad 1, 2 og 3, men PD grad 2

og 3 ble kun funnet i leddregioner med BM grad 2 og 3. Økende Doppler grad var signifikant assosiert med høyere BM alvorlighetsgrad og med tilstedeværelse av klinisk artritt.

Ultralyd synovitt sumskår var signifikant korrelert med helkropps-MR effusjon/synovial fortykning sumskår og med JADAS71. Ultralyd synovitt sumskår var moderat korrelert med klinisk aktiv ledd sumskår. Funn av synovitt på ultralyd viste høy spesifisitet, men lavere sensitivitet på leddnivå når helkropps-MR eller klinisk leddundersøkelse ble brukt som referanse.

Funnene som er presentert i denne avhandlingen indikerer at den nyutviklede ultralydundersøkelsesprotokollen og det leddspesifikke skåringsystemet med aldersinndelt referanseatlas for pasienter med JIA er pålitelige og valide verktøy i evalueringen av leddinflammasjon. I tillegg tyder funnene på at en ultralyd synovitt sumskår reflekterer sykdomsaktivitet hos pasienter med JIA og kan være et nyttig utfallsmål i fremtidig forskning og klinisk praksis.

List of papers

I. Nina Krafft Sande, Pernille Bøyese, Anna-Birgitte Aga, Hilde Berner Hammer, Berit Flatø, Johannes Roth, Vibke Lilleby. *Development and reliability of a novel ultrasonographic joint-specific scoring system for synovitis with reference atlas for patients with juvenile idiopathic arthritis*. RMD Open 2021;7:e001581. doi: 10.1136/rmdopen-2021-001581

II. Nina Krafft Sande, Vibke Lilleby, Anna-Birgitte Aga, Eva Kirkhus, Berit Flatø, Pernille Bøyese. *Associations between power Doppler ultrasound findings and B-mode synovitis and clinical arthritis in juvenile idiopathic arthritis using a standardised scanning approach and scoring system*. RMD Open 2023;9:e002937. doi:10.1136/rmdopen-2022-002937

III. Nina Krafft Sande, Eva Kirkhus, Vibke Lilleby, Ander H. Tomterstad, Anna-Birgitte Aga, Berit Flatø, Pernille Bøyese. *Validity of ultrasound synovitis in juvenile idiopathic arthritis: comparison with whole-body magnetic resonance imaging and clinical assessment*. Submitted

1. Introduction and background

1.1 Juvenile idiopathic arthritis

Juvenile Idiopathic Arthritis (JIA) is a chronic inflammatory disease characterised by joint inflammation (arthritis) that leads to pain, swelling and stiffness of the affected joint with subsequent joint damage and functional loss. Extra-articular manifestations such as uveitis and psoriasis are also seen (1). The distribution and the number of affected joints, laboratory measurements such as C-reactive protein (CRP), erythrocyte sedimentation rate (ESR), antinuclear antibodies (ANA) and rheumatoid factor (RF) play important roles in the diagnosis, evaluation of disease activity, treatment, and prognosis of JIA (1-3). Today, clinical joint examination is considered the standard evaluation of arthritis but can be challenging in children due to vague symptoms and complex anatomical regions (4, 5). Ultrasound and magnetic resonance imaging (MRI) have shown to be more sensitive in the detection of arthritis than clinical joint examination, and during the last decades there has been an increasing focus on these imaging modalities in the evaluation of disease activity in patients with JIA (6, 7).

1.1.1 Diagnosis and classification

There are no diagnostic criteria for JIA, but classification criteria are often used for diagnosis and treatment stratification. Classification criteria aim to get homogenous populations for research purposes (8). However, it is important to emphasise that classification criteria are not synonymous with diagnostic criteria which strive to be correct at the patient level. JIA is a heterogeneous disease and to be able to conduct studies and compare cohorts, a common nomenclature is important. The International League of Associations for Rheumatology (ILAR) developed classification criteria for JIA in 1997 by consensus based on expert opinion (9). The classification has later been modified. According to the most recent revision, JIA is defined as arthritis of unknown aetiology that starts before 16 years of age and last for at least 6 weeks, and is further classified into seven subgroups based on clinical characteristics and specific exclusion criteria during the first 6 months: systemic arthritis, oligoarthritis, RF positive polyarthritis, RF negative polyarthritis, psoriatic arthritis, enthesitis related arthritis and undifferentiated arthritis, (**Table 1**) (8).

Table 1. The International League of Associations for Rheumatology (ILAR) classification criteria for juvenile idiopathic arthritis (JIA) (8).

JIA subgroup	Classification criteria	Exclusion criteria
Systemic arthritis	Arthritis with or preceded by quotidian fever of at least 2 weeks duration and one or more of the following: 1. Evanescent erythematous rash, 2. Lymph node enlargement, 3. Hepatomegaly and/or splenomegaly, 4. Serositis	a, b, c, d
Oligoarthritis persistent	Arthritis affecting 4 or fewer joints during first 6 months	a, b, c, d, e
Oligoarthritis extended	Arthritis affecting 4 or fewer joints during first 6 months, extending to more than 4 joints after 6 months	a, b, c, d, e
Rheumatoid factor negative polyarthritis	Arthritis affecting 5 or more joints during the first 6 months. Rheumatoid factor negative	a, b, c, d, e
Rheumatoid factor positive polyarthritis	Arthritis affecting 5 or more joints during the first 6 months. Rheumatoid factor positive on at least two occasions taken more than 3 months apart	a, b, c, e
Psoriatic arthritis	Arthritis and psoriasis, or arthritis and at least two of: 1. Dactylitis, 2. Nail pitting or onycholysis, 3. Psoriasis in first-degree relative	b, c, d, e
Enthesitis-related arthritis	Arthritis and enthesitis, or arthritis or enthesitis with at least two of: 1. History of sacroiliac joint tenderness and/or inflammatory lumbosacral pain, 2. HLA-B27 positive, 3. Arthritis in male over 6 years of age, 4. Anterior uveitis, 5. History of ankylosing spondylitis, enthesitis related arthritis, sacroiliitis with inflammatory bowel disease, Reiter's syndrome, or acute anterior uveitis in first-degree relative	a, d, e
Undifferentiated arthritis	Arthritis that does not fulfil the criteria in any category or in 2 or more of the categories	

Exclusion criteria:

- a. Psoriasis or a history of psoriasis in the patient or first-degree relative
- b. Arthritis in an HLA-B27 positive male beginning after the 6th birthday
- c. Ankylosing spondylitis, enthesitis related arthritis, sacroiliitis with inflammatory bowel disease, Reiter's syndrome, or acute anterior uveitis, or a history of one of these disorders in a first-degree relative
- d. The presence of IgM rheumatoid factor on at least 2 occasions at least 3 months apart
- e. The presence of systemic JIA in the patient.

The Paediatric Rheumatology International Trials Organisation (PRINTO) has started a process to revise the current ILAR classification criteria. The aim is to use an evidence-based approach

to distinguish the types of arthritis seen only in children from those with a similar disease observed in adults (10).

1.1.2 Epidemiology

JIA is the most common chronic rheumatic disease in childhood (1). An overall incidence rate of 7.8/100 000 and prevalence of 32.6/100 000 have been reported in Caucasians (11). In Norway, the annual incidence rate of JIA has varied from 14.0 to 22.6/100 000 (12-14). The pooled incidence has been reported to be 10/100 000 for girls and 5.7/100 000 for boys, and the pooled prevalence to be 19.4/100 000 for girls and 11/100 000 for boys (11). JIA is generally more common in girls than in boys except for systemic arthritis, where the distribution between boys and girls is equal, and for enthesitis-related arthritis which is more common in boys than in girls (1). The most common subgroup in western European countries is oligoarthritis. The percentage distribution between the different subtypes of JIA is: systemic arthritis (4-17%), oligoarthritis (27-56%), RF positive polyarthritis (2-7%), RF negative polyarthritis (11-28%), enthesitis-related arthritis (3-11%), psoriatic arthritis (2-11%) and undifferentiated arthritis (11-21%) (1).

The most frequently affected joints in JIA are the knee, ankle, wrist and finger joints (14-16). However, the number of joints with arthritis and the pattern of joint involvement vary in the different subgroups. Patients with oligoarthritis often have asymmetric arthritis that mainly affects the knee and ankle joints. Patients with RF positive polyarthritis often present with symmetric arthritis affecting the small joints in the finger and toes but can also affect large joints, while RF negative polyarthritis has a more heterogenous joint involvement. In psoriatic arthritis, both small and large joints can be affected. Patients with enthesitis-related arthritis often have affection of the lower extremities and entheses, but arthritis can also be found in the sacroiliac joint and the spine. In systemic arthritis, the joint distribution is often polyarticular and symmetric (1, 2, 17).

1.1.3 Pathogenesis

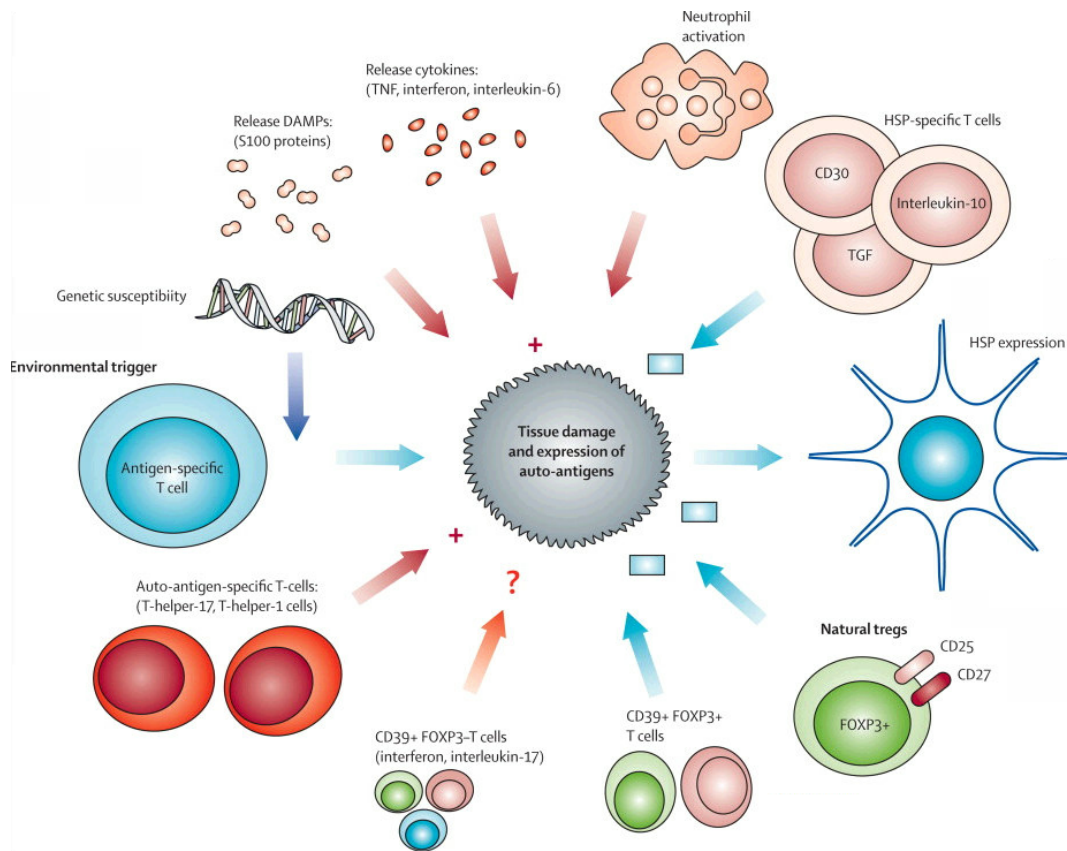
JIA is a complex multifactorial disease where the exact cause and pathogenesis are unknown but probably include both genetic and environmental risk factors (**Figure 1**) (2).

Associations between human leucocyte antigen (HLA) class I and HLA class II alleles and JIA have been reported, and T-cells have been shown to be important in the disease course (18-20). This indicates that the patient's biology is important in the pathogenesis.

Environmental factors are also believed to be significant contributors to the development of JIA. Breastfeeding and household siblings have been proposed as protective factors, but the results are conflicting, and the studies conducted are of variable quality (21). Vaccinations, infections, antibiotic exposure and caesarean section delivery have been suggested as potential triggers of the disease or harmful factors but have not been properly confirmed due to lack of controlled, prospective studies (19, 21).

Arthritis is characterised by joint swelling caused by increased synovial fluid and hyperplasia of the synovial lining. This inflammation can finally lead to cartilage damage and bone erosions (1). The pathogenic process in the joints involves infiltration of inflammatory cells and activation of different molecules, including cytokines and chemokines, that act as key mediators of inflammation (2, 18, 19). The cytokine pattern varies in the different JIA subgroups but are not subgroup specific. Knowledge about the wide range of cells and molecules involved in the pathogenesis of JIA have become important in the development of new drugs (2, 22).

Figure 1. Illustration of the proposed pathogenesis of juvenile idiopathic arthritis (2).



Abbreviations: DAMP: Damage-Associated Molecular Pattern molecules, HSP: Heat-Shock Protein, TGF: Tumour Growth Factor, TNF: Tumour Necrosis Factor.

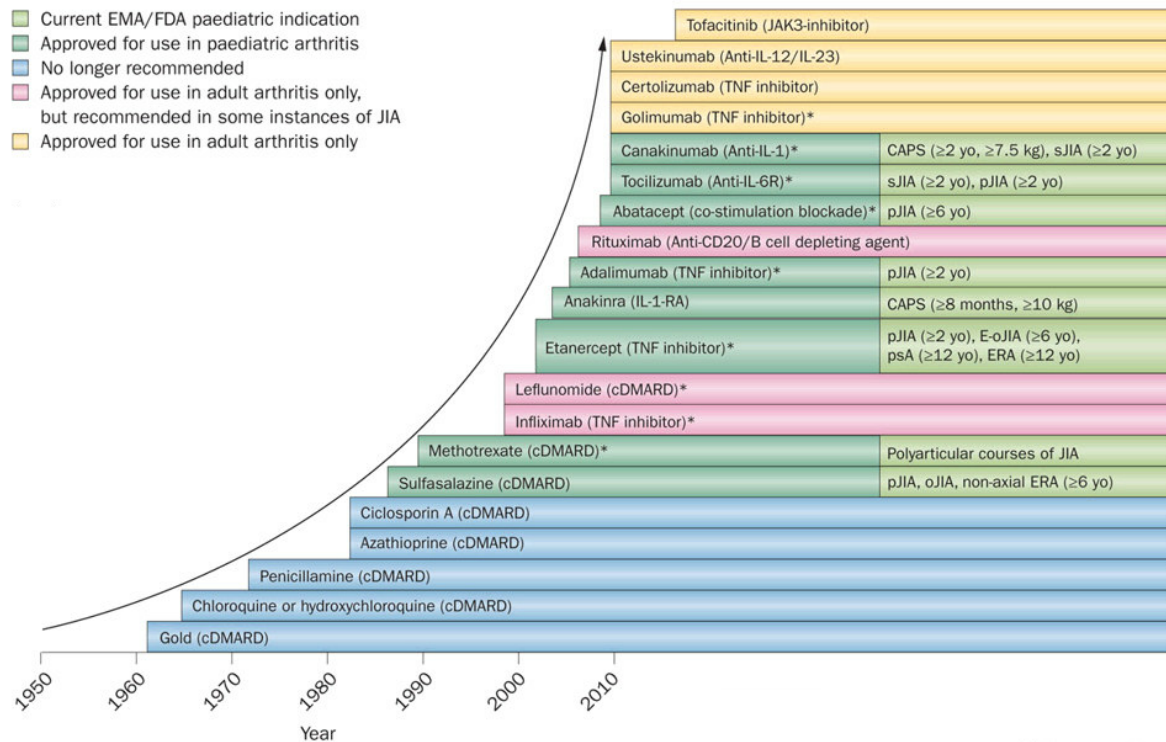
Published by Prakken et al in the Lancet, 2011 (2). Reprinted with permission from Elsevier.

1.1.4 Management

Over the last decades there has been a significant development in the treatment of JIA (**Figure 2**) (23, 24). First with the conventional synthetic disease modifying antirheumatic drug (DMARD) Methotrexate (25, 26), and later with selective immune inhibitors (biologic DMARDs) targeting tumour necrosis factor-alfa (TNF-alfa), interleukin -1 (IL-1), IL-6, and T-cell co-stimulation (27-33). In addition to systemic treatment, intra-articular glucocorticoid injections are often used to relieve symptoms and reduce swelling (34-36). In patients with moderate to high disease activity, a limited course of oral glucocorticoids (< 3 months) can also be used as adjunctive therapy (34). Since JIA is a heterogeneous disease divided into seven subgroups, the treatment recommendations vary, and both national and international treatment recommendations have been developed (34, 37). In all subgroups, increasing evidence suggests

that early initiation of aggressive treatment with tight control and treating to target is of great importance to improve outcome and to avoid permanent damage (23, 38-42).

Figure 2. Development of new drugs in the treatment of juvenile idiopathic arthritis (23).



Abbreviations: CAPS: Cryopyrin-associated Autoinflammatory Syndromes, cDMARD: Conventional Disease-Modifying Drug, EMA: European Medicines Agency, E-oJIA: Extended oligoarticular Juvenile Idiopathic Arthritis, ERA: Enthesitis Related Arthritis, IL1-RA: Interleukin-1 Receptor Antagonist, JIA: Juvenile Idiopathic Arthritis, oJIA: oligoarticular Juvenile Idiopathic Arthritis, pJIA: polyarticular Juvenile Idiopathic Arthritis, psA: psoriatic Arthritis, sJIA: systemic Juvenile Idiopathic Arthritis, TNFi: Tumor Necrosis Factor inhibitor, yo: years old.

Published by Hinze et al in Nature Reviews Rheumatology, 2015 (23). Reprinted with permission from Springer Nature.

1.1.5 Prognosis and prognostic factors

The prognosis in JIA is related to outcomes such as physical function, pain, disability and growth disturbances. Over the last decades JIA prognosis has improved, largely due to the development of new effective drugs (23, 43). However, still less than 50% achieve sustained remission (44). The evaluation of prognostic factors is therefore of importance in the treatment decisions. Young age and greater extension of arthritis at onset, high disease activity, diagnostic delay, presence of RF, ANA, HLA-B27, CRP, long duration of elevated ESR, and morning stiffness are negative prognostic factors (45-49). The autoantibodies ANA and RF also have a prognostic value. A positive ANA is often associated with uveitis, while RF, that is only found

in RF positive polyarthritis, is associated with a more severe course of the disease (2, 3, 50). In addition, early radiographic changes, patterns of joint involvement, including the hip, ankle, wrist, finger joints and cervical spine, are indicators of poor outcome (16, 46, 51-53). Some studies suggest that subclinical arthritis on ultrasound is a predictor of flare, but the results are conflicting (54-56).

1.2 Assessment of disease activity

Assessment of disease activity is important in treatment stratification and in the follow-up of patients with JIA to evaluate treatment effect and to monitor the course of the disease.

1.2.1 Clinical joint examination

Evaluation of arthritis in patients with JIA is traditionally assessed by clinical joint examination. A clinically inflamed joint is often referred to as active arthritis, and defined as the presence of swelling or, if swelling is not present, limitation of motion (LOM) accompanied by pain, tenderness or both (57). However, the interpretation of active arthritis (an active joint) in children with JIA can be difficult due to complex anatomic regions and subcutaneous adipose tissue that can mask anatomical landmarks. In addition, the child can have difficulties expressing and localising pain, and it can be challenging for the physician to distinguish joint pain caused by arthritis from other diseases or injuries. The reliability of clinical joint examination in children with JIA has been shown to be poor (58). In clinical trials, it is recommended to examine the following joints: the temporomandibular, sternoclavicular, acromioclavicular, shoulder, elbow, wrist, metacarpophalangeal (MCP)1-5, proximal interphalangeal (PIP)1-5, distal interphalangeal (DIP)2-5, hip, knee, ankle, subtalar, intertarsal, metatarsophalangeal (MTP)1-5, toe 1-5, and the sacroiliac joints bilaterally, the cervical spine, thoracic spine and lumbar spine (59-62). However, the sacroiliac joint and the thoracic and lumbar spine are often excluded, and reduced joint counts to be used in clinical trials as surrogates for the whole joint count have been proposed (63). The number of joints with clinical active arthritis (as defined by the American College of Rheumatology (ACR) criteria: presence of swelling (not due to currently inactive synovitis or due to bony enlargement) or, if no swelling is present, LOM accompanied by heat, pain or tenderness, and the number of joints

with LOM) are considered core outcome variables to be included in the evaluation of patients with JIA in clinical trials (59).

1.2.2 Biochemical and immunological markers

The most often measured inflammatory markers are CRP and ESR. They are often, but not always, elevated in JIA patients with active disease (3). CRP and ESR are also included in composite disease activity scores for patients with JIA (64, 65). However, these markers are not specific for JIA and can be elevated in other inflammatory disorders and infections.

ANA, RF and HLA-B27 are important immunological markers in the classification and prognosis of JIA (3). Anti-cyclic citrullinated peptide (anti-CCP) antibody plays an important diagnostic and predictive role in rheumatoid arthritis (RA) (66, 67). Anti-CCP has also been found in different JIA subgroups, most often in RF positive polyarthritis (68-70). RF positive polyarthritis is regarded to be much like adult RA (2). However, the reported prevalence of anti-CCP in JIA varies (70), and a negative test does not exclude the diagnosis. In addition, anti-CCP is not included in the classification criteria.

1.2.3 Paediatric core set outcome variables

The ACR has developed a core set of outcome variables that should be used in clinical trials (59). These variables are considered as the core set variables in the evaluation of patients with JIA who receive a treatment intervention, to define if there has been any improvement of the disease course (**Table 2**).

Table 2. Core set of outcome variables in juvenile idiopathic arthritis to be used in clinical trials (59).

Core variables
<ul style="list-style-type: none">• Physician global assessment of disease activity (PhGA)• Patient/parent global assessment of overall well-being (PGA)• The Childhood Health Assessment Questionnaire (CHAQ)• Erythrocyte sedimentation rate (ESR)• Number of joints with active arthritis• Number of joints with limited range of motion (LOM)

The physician's evaluation of disease activity is important in the management of patients with JIA and in the choice and adjustment of medications. In clinical trials, this is reported as the physician global assessment of disease activity (PhGA) measured on a 0-10 cm visual analogue scale (VAS) where 0 = no activity and 10 = maximum activity (59). The patient's perspective, including factors that are not measured by the physician, such as quality of life, fatigue and pain, has gained more focus and is important in medical decision-making and patient compliance. The patient/parent's perception of health in JIA, is reported as the patient/parent global assessment of overall well-being (PGA), measured on a 0-10 cm VAS where 0 = very well, and 10 = very poor (59). The Childhood Health Assessment Questionnaire (CHAQ) is a questionnaire to measure the functional and physical ability of a child with JIA. The CHAQ assess the patient's function in eight different areas and consists of 30 questions, each scored from 0-3 (0 = no difficulty, 1 = some difficulty, 2 = much difficulty, 3 = unable to do). A higher score indicates worse disability (71). A Norwegian version of the CHAQ has been developed and has proven to be a reliable and valid instrument (72). The ESR is used as a biochemical marker of response. ESR can be elevated in other conditions than JIA and can even be normal during a study period. However, since there are no biochemical markers of inflammation in JIA, the ESR is often used in clinical trials. The last two core outcome variables have been discussed previously in this thesis (section 1.2.1) and include the number of joints with active arthritis and the number of joints with LOM.

The use of these six core variables help to standardise the evaluation of patients with JIA in clinical trials and makes it possible to compare results in studies. In addition, many of the variables are used in composite scores to assess disease activity.

1.2.4 Composite measures of disease activity

No single marker can reflect all aspects of JIA. Composite scores have therefore been developed, where individual measures of inflammation are combined into a composite index. Composite scores for assessment of disease activity enable the clinicians to evaluate and to quantify the disease activity.

The Juvenile Arthritis Disease Activity Score (JADAS) was developed in 2009 and was the first composite score for disease activity in patients with JIA (64). The JADAS consists of four measurements: total active joint count, PhGA (0-10 cm VAS), PGA (0-10 cm VAS), and ESR normalised to a 0-10 scale. The normalised ESR is calculated using this formula: (measured

ESR (mm/hour) – 20) / 10, where values < 20 mm/hour = 0 points and values >120 mm/hour = 10 points. The JADAS is calculated as the sum of the scores of these four measurements. During the last few years, several versions of the JADAS have been developed (73):

1. The **JADAS10** is based on the count of active joints up to a maximum of 10 joints, any joint count higher than 10, still only gives 10 points in the score. Range scores 0-40 (64).
2. The **JADAS27**, where selected joints (the cervical spine, elbow, wrist, MCP 1-3, PIP 1-5, hip, knee and ankle joints) are included. Range scores 0-57 (64).
3. The **JADAS71** includes 71 joints, the thoracic and lumbar spine and sacroiliac joint are not included. Range scores 0-101 (64).
4. The **JADAS-CRP** where ESR is substituted with CRP (65).
5. The clinical JADAS (**cJADAS**) (first named the JADAS3), including total active joint count, PhGA and PGA (74).
6. The Juvenile Spondyloarthritis Disease Activity (**JSpADA**) index where eight items are included; arthritis, enthesitis, patient assessment of pain, acute phase reactants, morning stiffness, clinical sacroiliitis, uveitis and back mobility. Range scores: 0-8 (75).

The cut-off values for disease activity states in the JADAS10 have been discussed and new cut-off values have been proposed for the inactive, minimal, moderate and high disease activity states in JIA based on subjective disease assessment by the treating physician (**Table 3**) (76).

Table 3. An overview of the Juvenile Arthritis Disease Activity Score for 10 joints (JADAS10) and the JADAS71 cut-off values for different disease activity states in oligoarthritis and polyarthritis (76-78).

	JADAS10* cut-off values (77, 78)	JADAS10** cut off values (76)	JADAS71* cut off values (77, 78)
Oligoarthritis disease activity state			
Inactive disease	≤ 1	≤ 1.4	≤ 1
Minimal disease activity	1.1 – 2.0	1.5 – 4	1.1 – 2.0
Moderate disease activity	2.1 – 4.2	4.1 – 13	2.1 – 4.2
High disease activity	> 4.2	> 13	> 4.2
Polyarthritis disease activity state			
Inactive disease	≤ 1	≤ 2.7	≤ 1
Minimal disease activity	1.1 – 3.8	2.8 – 6	1.1 – 3.8
Moderate disease activity	3.9 – 10.5	6.1 – 17	3.9 – 10.5
High disease activity	> 10.5	> 17	> 10.5

* (2012-2014), **(2021)

Abbreviations: JADAS10: Juvenile Arthritis Disease Activity Score for 10 joints, JADAS71: Juvenile Arthritis Disease Activity Score for 71 joints.

1.2.5 Imaging in JIA

Imaging has become an important tool in the evaluation of patients with JIA. The European League Against Rheumatism (EULAR) Paediatric Rheumatology European Society (PReS) has developed points to consider for the use of imaging in diagnosis and follow-up of patients with JIA (6).

Conventional radiography

Conventional radiography (CR) has traditionally been an important imaging modality in JIA. CR is useful in the exclusion of other diagnoses causing joint pain, and radiography is cheap and readily available. In the evaluation of joint inflammation, CR findings include soft tissue swelling, joint effusion, growth disturbances, joint damage and osteopenia but these findings are nonspecific (79-81). In addition, CR expose the child to ionising radiation which is a great limitation.

Ultrasound

Ultrasound is useful in the evaluation of inflammatory arthritis and has become an important tool in the assessment of joints in patients with JIA. The imaging modality is well accepted by children, there is no ionising radiation, ultrasound does not require sedation or general anaesthesia and there is no need for intravenous contrast. Ultrasound can be performed bedside in the clinic, and many joints can be assessed at the same visit. Important structures like soft tissue, cartilage, synovial membrane, tendons, bursae and entheses can be evaluated, and joint effusion can be clearly visualised (7, 80, 82). In addition, ultrasound can improve intra-articular glucocorticoid injections by directly visualising the inflamed joint or tendinitis and the position of the needle, and thereby reduce side effects and improve the treatment effect (83-86). In the evaluation of arthritis, ultrasound is superior to clinical joint examination (87-90). However, ultrasound waves cannot penetrate bone and are therefore unable to assess bone marrow oedema (BME) and certain joints like the cervical spine. In addition, ultrasound has shown to have limited ability to evaluate the sacroiliac joint and the temporomandibular joint (6, 91, 92).

During the last decades there has been an increasing focus on ultrasound in the assessment of joints in children with JIA (7, 80, 93-97), and a process to standardise the use of ultrasound in the evaluation of the paediatric joints has started.

Magnetic Resonance Imaging (MRI)

MRI is a tomographic imaging technique. Contrast enhanced MRI is considered the gold standard in the evaluation of joint inflammation as it allows the study of all relevant structures involved in the inflammatory process (7, 80, 98). MRI is the only imaging modality that can detect BME which may indicate active inflammation in the bone and has shown to be a predictor of joint damage progression in patients with RA (99, 100). However, the exact meaning of BME in children is still uncertain (7, 101, 102). MRI is superior in the evaluation of active inflammation in joints like the temporomandibular joint, the sacroiliac joint and the cervical spine (6, 91, 92, 103). In addition, MRI findings of subclinical synovitis in patients with JIA who are in remission may be a predictor of disease flare (104).

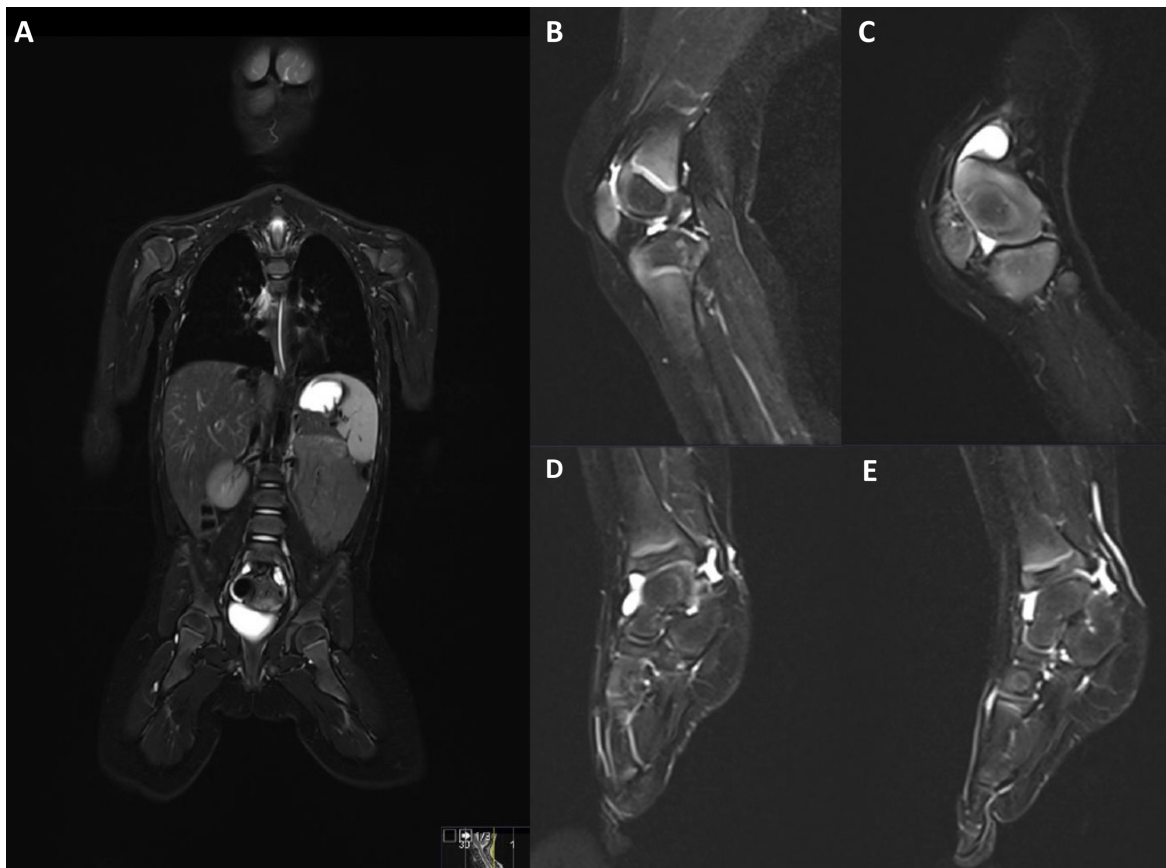
In JIA, synovial hypertrophy on MRI is defined as enhancing thickened synovium (105). Contrast-enhanced MRI has shown to have an important diagnostic value and is considered superior in the evaluation of synovitis compared to non-contrast enhanced MRI (101, 106).

MRI is favourable in children because there is no ionising radiation. However, important limitations are that MRI requires sedation in younger children and is time-consuming, especially when using contrast that prolongs the examination time. In addition, there is a risk of allergic reactions to contrast, and some studies have suggested that repeated contrast (gadolinium)-enhanced MRI examinations may lead to gadolinium deposition in the brain (107). Other limitations are high costs and low availability, and that only one joint or joint area is evaluated in each session.

Whole-body MRI is often used in the assessment of vasculopathies, and in neoplastic, infectious and inflammatory conditions in children (108-110). Whole-body MRI techniques can depict the entire axial skeleton and peripheral joints in one scan with the possibility to evaluate the activity and extent of rheumatological diseases in the same session (**Figure 3**) (111, 112). The use of contrast in whole-body MRI is demanding due to variable post-injection delay in the body that can lead to different synovial contrast enhancement and misinterpretation of findings (113).

A consensus-driven whole-body MRI proposal for image acquisition and scoring of disease activity in JIA has recently been developed (113, 114). Images include water sensitive sequences without contrast enhancement. The scoring system is divided in three: for peripheral and chest joints, for axial joints, and for entheses. The chosen key findings for scoring peripheral and chest joints are effusion/synovial thickening, BME and pericapsular soft tissue inflammation. Effusion and synovial thickening are proposed to be scored altogether as it is difficult to separate these findings without intravenous contrast (114).

Figure 3. Non-contrast enhanced whole-body magnetic resonance imaging (MRI) examination (T2 turbo spin echo Dixon sequence) in a 2-year old. Illustration of the whole-body MRI examination (A). Sagittal MRI scan of the right knee (B). Sagittal MRI scan of the left knee showing effusion (C). Sagittal MRI scan of the right ankle showing synovial effusion in the tibiotalar and the subtalar joints (D). Sagittal MRI scan of the left ankle showing synovial effusion in the tibiotalar and subtalar joints (E).



Images courtesy of Department of Radiology, Oslo University Hospital

1.3 Ultrasound

The first clinically important description of musculoskeletal ultrasound was published in 1972 where ultrasound was used to distinguish between Baker's cysts and thrombophlebitis (115). In 1978, the first use of ultrasound to demonstrate synovitis in the knee joint in patients with RA was published (116). However, it was not until about thirty years ago that ultrasound was used to evaluate joints in children with JIA (117).

1.3.1 Ultrasound physics

Ultrasound technology is based on sound waves. Sound can be described as longitudinal mechanical waves that travel through a medium such as water, air, and tissue. The medium is needed to propagate the sound wave, and therefore sound cannot travel through vacuum (118). Ultrasonographic images are formed by a three-step process: First the production of sound waves, then the reflection of the sound waves (echoes), and finally the conversion of these echoes into an image (119, 120).

Ultrasound waves are produced from piezoelectric crystals of the ultrasound transducer. The quality of the ultrasound waves can be influenced by the frequency of waves, and the size and form of the transducer (121). The reflection of an ultrasound wave is called an echo. The ultrasound wave will interact with tissue as it travels through a medium caused by the acoustic property of the tissue it passes. The acoustic impedance of a tissue is the product of the density and the speed of sound. The difference in acoustic impedance of adjacent tissues will determine the amount of the reflected echo (122). Strong echoes will be white (echoic or hyperechoic) on an ultrasonographic image, weaker echoes will be grey (hypoechoic), and if there are no echoes, the ultrasound image will be black (anechoic) (**Figure 4**) (119, 123).

Figure 4. Ultrasonographic image of the elbow, anterior scan showing different echogenicity.



Image courtesy of Department of Rheumatology, Oslo University Hospital

The ultrasound beam energy is also attenuated, or weakened, as it passes through tissue. The attenuation varies with the frequency of ultrasound. A high frequency ultrasound beam gives better resolution but are attenuated more than a low frequency beam and are therefore not as

penetrating (122, 123). In musculoskeletal ultrasound, high frequencies are suitable for superficial joints like the finger and toe joints, but lower frequencies are needed to visualise joints like the knee and hip joints. The frequencies used in musculoskeletal ultrasound ranges from 3.5 to 20 Megahertz (MHz) (124).

Brightness mode and Doppler mode

Brightness mode or B-mode (BM) is the basic mode used for converting echoes into images in medical ultrasound. The BM provides a two dimensional black and white image seen on the ultrasound screen (121). In musculoskeletal ultrasound, the BM is well suited for the evaluation of synovitis, tenosynovitis, enthesitis, bone erosions and cartilage (82).

The vascularisation in joints and tissues is detected with Doppler ultrasonography. The Doppler effect is a change in frequency of the ultrasound wave caused by a moving reflector. In the human body, the moving reflectors are the blood cells (122). There are two main types of Doppler modes used in musculoskeletal ultrasound: colour Doppler (CD) and power Doppler (PD). The direction of blood flow (movement) is shown in CD, where flow away from the probe is coloured blue and towards the probe is coloured red. PD displays the strength or power of the Doppler signal, and not the direction or the velocity of flow (122, 125). Doppler signals can be present in inflamed joints in children, but Doppler activity can also be seen in normal joints in healthy children (126).

1.3.2 Musculoskeletal ultrasound in healthy children

Ultrasound is well suited for the use in children as it is non-invasive and easily repeatable.

The use of ultrasound requires training, especially in children due to the unique features of the growing skeleton (96, 103). Children have a different skeleton than adults because their bones are not entirely ossified yet (**Figure 5**). In addition to the hyaline cartilage in the articular cartilage, the child's skeleton consists of different amounts of unossified hyaline cartilage in the epiphysis (127). The cartilage thickness and the degree of ossification varies according to the age and stage of maturity and must be considered when performing ultrasound in children (**Figure 6**) (127-130). It is important that these structural differences between adults and children are not misinterpreted as pathological findings.

Figure 5. Illustration of a growing bone showing different levels of vascularisation and ossification.

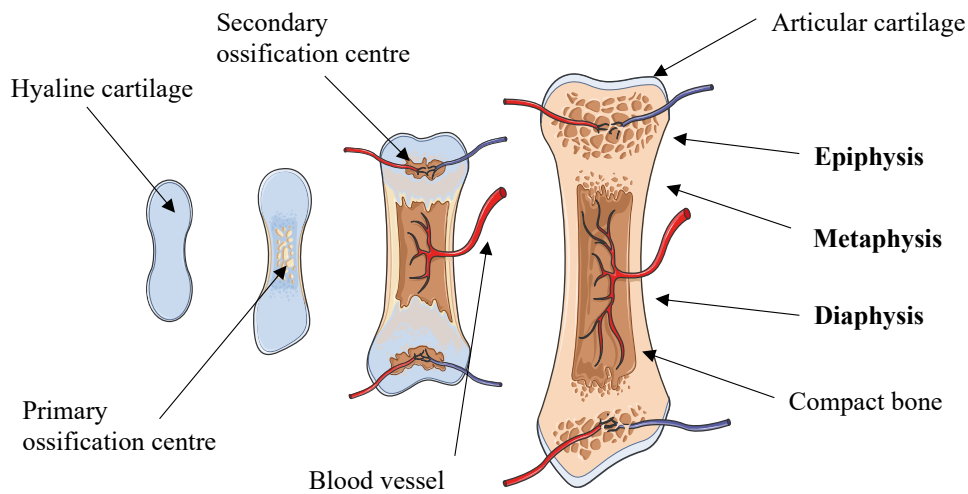
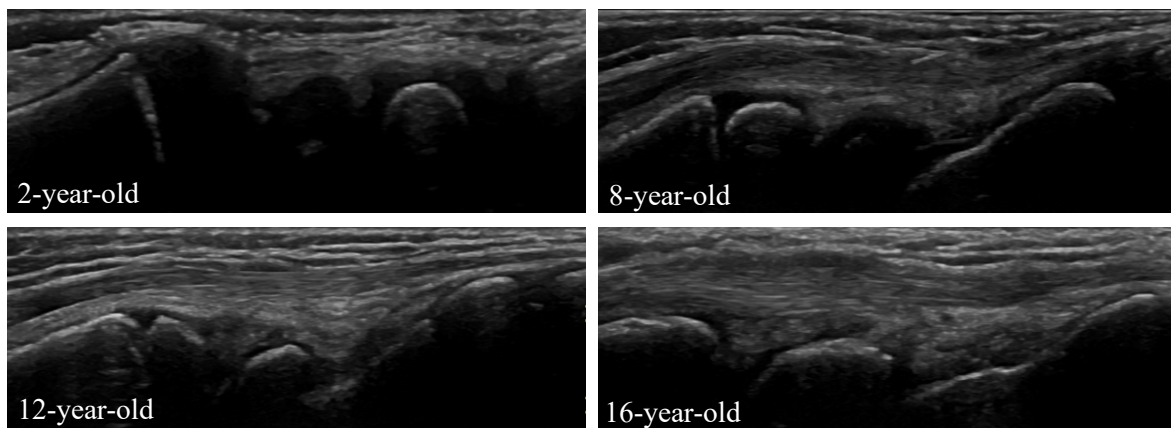


Figure modified with text and markings (arrows) after adaption of “Bone growth” from Servier Medical Art by Servier, licensed under a Creative Commons Attribution 3-0 unported license.

Figure 6. Ultrasound images of the wrist joint (radiocarpal and midcarpal joints) in four different age groups showing varying degrees of ossification.



Images courtesy of Department of Rheumatology, Oslo University Hospital.

Standardisation of musculoskeletal ultrasound in healthy children

A thorough knowledge of the age-dependent variability in joints is important to be able to interpret and distinguish the different components on ultrasound in children (**Figure 7**). An early approach was the description of the joint recess of the hip, knee, wrist, MCP and PIP joints and of the finger flexor tendon sheets in healthy children (131). Then, the establishment of age- and sex-related normal reference values for cartilage thickness of the knee, wrist, MCP2

and PIP2 joints (128). In recent years, the Outcome Measures of Rheumatology (OMERACT) ultrasound paediatric group has started a process of standardising ultrasound in children. The group first developed BM definitions for ultrasound findings in joints in healthy children through a consensus process that was validated in practical exercises (**Table 4**) (127). Further, age-related vascularisation and ossification of joints in healthy children have been described (126).

Table 4. The definitions of the ultrasonographic features of joints in healthy children developed by the OMERACT (127).

Component	Definitions
Hyaline cartilage	The hyaline cartilage will present as a well-defined anechoic structure (with/without bright echoes/dots) that is non-compressible. The cartilage surface can (but does not have to) be detected as a hyperechoic line.
Secondary ossification centre	With advancing maturity, the epiphyseal secondary ossification centre will appear as a hyperechoic structure, with a smooth or irregular surface within the cartilage.
Normal joint capsule	A hyperechoic structure which can (but does not have to) be seen over bone, cartilage and other intraarticular tissue of the joint.
Normal synovial membrane	Under normal circumstances, the thin synovial membrane is undetectable.
Growth plate	The ossified portion of articular bone is detected as a hyperechoic line. Interruptions of this hyperechoic line may be detected at the growth plate and at the junction of two or more ossification centres.

Figure 7. Ultrasonographic image of a metacarpophalangeal joint showing the cartilage surface, the growth plate and the epiphyseal secondary ossification centre.

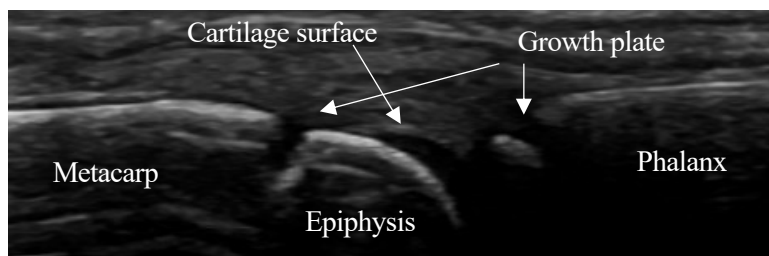


Image courtesy of Department of Rheumatology, Oslo University Hospital.

Scanning protocols in healthy children

One of the major limitations of ultrasound is that the method is operator dependent. To be able to understand and to compare findings, it is important that the sonographer knows how to conduct an ultrasonographic joint examination and that different sonographers do it similarly. In the standardisation process, the OMERACT ultrasound paediatric group developed a standardised scanning approach for the paediatric knee, ankle, wrist and MCP2 joints (132). The scanning protocol describes the positioning of the patient and the transducer placement and movement (from medial to lateral in longitudinal scan, and proximal to distal in transverse). In addition, important anatomic landmarks that must be present in the ultrasonographic image to ensure a similar scanning of the joints are described (132).

Vascularisation in joints in healthy children

In a growing child, physiological vascularisation will be present in many joint structures including the fat pad, short bone, epiphysis and physis, and can be detected as Doppler signals on ultrasound (126, 132). Development of a clear definition of physiological vascularisation on ultrasound has shown to be difficult, especially because of the changes in the skeleton during maturation. Instead, descriptions and statements of normal Doppler findings in healthy children have been developed and include for instance that physiological vascularisation can be seen as Doppler signals in the joint structures at all ages during growth, and that its intraarticular anatomical position is joint- and age-dependent (133).

1.3.3 Musculoskeletal ultrasound in patients with JIA

Musculoskeletal ultrasound has been shown to be more sensitive than clinical examination in the evaluation of joint inflammation (6). During the last decades there has been an increasing focus on ultrasound when assessing joints in patients with JIA and thus also a need for standardisation of the use of this imaging modality in these patients (134).

Standardisation of musculoskeletal ultrasound in JIA

As previously described, the interpretation of ultrasound findings in children is challenging. To be able to assess synovitis in children with JIA, there must be clear definitions of what is pathological. The OMERACT paediatric ultrasound group has developed preliminary definitions for sonographic features of synovitis in children through a consensus process, the overarching principle is that synovitis in children includes BM and Doppler (colour or power Doppler) findings (**Table 5**) (135).

Table 5. The preliminary ultrasound definitions for synovitis in children developed by the OMERACT paediatric ultrasound group (135).

Component	Definition
Synovitis	Can be detected based on B-mode findings alone, but not on Doppler findings alone.
B-mode findings	Include synovial effusion and synovial hypertrophy.
Synovial effusion	Abnormal, intraarticular, anechoic or hypoechoic material that is displaceable.
Synovial hypertrophy	Abnormal, intraarticular, anechoic or hypoechoic material that is nondisplaceable.
Doppler findings	Must be found within synovial hypertrophy to be considered as a sign of synovitis.

Scanning protocols in JIA:

Ultrasonographic scanning protocols are necessary to be able to perform ultrasound examinations reliably and comparably. Many studies involving children with JIA have used scanning approaches developed for adults, but they may not be applicable to growing children (6, 94). As previously described, a scanning protocol for some joints (knee, ankle, wrist and second MCP joints), that can be used in children regardless of age, has been developed (132). In addition, an image acquisition protocol for the paediatric knee has been established (136). However, patients with JIA can have affection of many other joints, and a joint-specific scanning protocol for multiple joints is needed.

Vascularisation in joints in JIA

One of the most challenging joint components to interpret on ultrasound in children is Doppler signals. It is essential to distinguish between normal vascularisation and pathological Doppler signals as a sign of synovitis (**Figure 8**). The preliminary OMERACT ultrasound definitions for synovitis in children state that only Doppler signals present within synovial hypertrophy are pathological (135). There are limited data on the evaluation of Doppler findings in children with JIA (83, 84, 89, 137, 138).

Figure 8. Ultrasound image of the third proximal interphalangeal joint showing abnormal power Doppler signals.

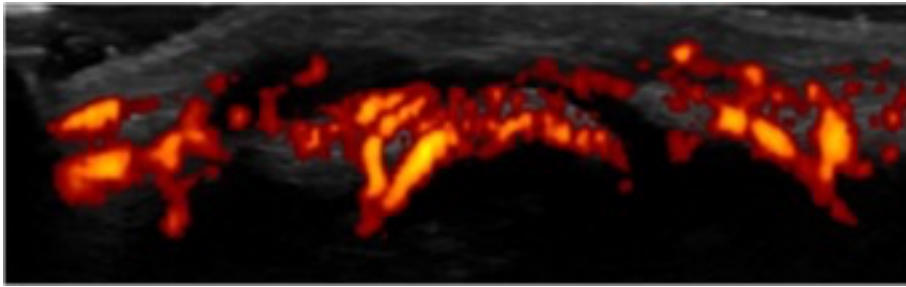


Image courtesy of Department of Rheumatology, Oslo University Hospital.

Which joints to assess

Children do not always report pain and some, especially the youngest, have difficulty in expressing and localising pain. It is well known that children are often impatient, and it is therefore not feasible to assess all joints with ultrasound at each clinical visit. Findings of synovitis on ultrasound in patients with JIA have been described to be most common in the knee, elbow, wrist, MCP, PIP, ankle, and MTP-joints (89, 138, 139).

In adults with RA many reduced joint scores for assessing synovitis on ultrasound have been developed to increase feasibility (140, 141). However, it is difficult to implement these scores in patients with JIA since the pattern of joint involvement vary in the different subgroups. Collado et al. found that ultrasound of 10 joints (knee, ankle, elbow, wrist, second MCP joints bilaterally) in patients with JIA, reflected the inflammatory activity equally well as a 44 joint ultrasound assessment (138). However, which joints that should be examined by ultrasound to assess overall disease activity in JIA is not clear.

1.3.5 Ultrasonographic scoring systems for synovitis in JIA

To quantify findings on ultrasound and to evaluate the extent of the disease, a scoring system for synovitis is needed. Ultrasonographic scoring systems and reference atlas in adults with RA have been developed (142-144). However, they cannot be directly applied to children because of the changing skeleton during growth.

Single standard scoring system

There has been a lack of consensus on an ultrasonographic scoring system for patients with JIA. Collado et al. developed a single standard semiquantitative scoring system (grades 0-3) for synovitis (PedSyns) for the elbow, radiocarpal, tibiotalar, mid-foot and finger joints (138). This scoring system includes scoring for BM and Doppler findings without being joint specific. The BM scoring system uses the shape and the extension of the joint recess in relation to the diaphysis of articulating bones to score the different grades of synovitis. The PedSyns scores Doppler findings as no flow (grade 0), single-vessels (grade 1), confluent vessels (grade 2) and vessels in more than half of the intraarticular area (grade 3) (138).

Joint-specific scoring system

A joint-specific scoring system for the paediatric knee joint was recently developed and includes a scoring system for the suprapatellar view and the parapatellar view for BM and Doppler findings (136). The BM scoring system uses the quadriceps tendon as an important anatomic landmark to describe the extension of the effusion/synovial hypertrophy. For instance, the difference between grade 1 and grade 2 is whether the effusion/synovial hypertrophy extends $< 50\%$ or $> 50\%$ of the visualised portion of the quadriceps tendon. That is, the extension is measured as the distance of the tendon, and not an intraarticular area. When scoring BM findings in the parapatellar recess, the entire intraarticular space is divided by thirds, and then graded according to how much of that intraarticular space is taken up by the synovial distention. The Doppler signals are scored as no Doppler signals (grade 0), 1-3 signals within the area of synovial hypertrophy (grade 1), > 3 or confluent signals in $< 50\%$ of the area of the synovial hypertrophy (grade 2), and confluent signals present in $> 50\%$ of the area of synovial hypertrophy (grade 3) (136).

The two scoring systems described do not fully cover all the different joints that can be affected in patients with JIA. To reliably quantify ultrasound findings in multiple joints, there is a need for reliable and valid joint-specific scoring system.

2. General aim and research questions

2.1 General aim

The general aim of this thesis was to evaluate ultrasound in patients with JIA by developing a standardised ultrasonographic scanning protocol and a semiquantitative joint-specific scoring system for synovitis with age-divided reference atlas, and to test the reliability and the validity of the system.

2.2 Research questions

- At joint level, can ultrasound assessment of synovitis in patients with JIA be performed reliably when using a semiquantitative joint-specific ultrasonographic scoring system with reference atlas? (Paper I)
- At patient level, can ultrasound assessment of synovitis in patients with JIA be performed reliably when using a semiquantitative joint-specific ultrasonographic scoring system with reference atlas? (Paper I)
- Are PD findings associated with B-mode synovitis and clinical arthritis at joint level? (Paper II)
- Are PD findings associated with age, JIA subgroups and the JADAS10 at joint level? (Paper II)
- Are ultrasound synovitis sum scores correlated with whole-body MRI effusion/synovial thickening sum scores? (Paper III)
- Are ultrasound synovitis sum scores correlated with measures of disease activity? (Paper III)
- What is the diagnostic performance of ultrasound in detecting synovitis using whole-body MRI or clinical joint examination as reference? (Paper III)

3. Material and methods

3.1 Study design

The analysis and results in this thesis are based on cross-sectional studies involving ultrasound from three different projects.

In the first project, an image acquisition protocol and a semiquantitative joint-specific scoring system with reference atlas were developed through a consensus process. Inter-reader and intra-reader reliability tests of the scoring system with reference atlas were performed on still images for BM scoring with four readers and for PD scoring with three readers. Then, a cross-sectional live reliability exercise including patients with JIA with three readers was conducted.

The second project was a cross-sectional study including 27 patients with JIA with suspected clinical arthritis. Associations between PD ultrasound findings and BM synovitis, clinical arthritis, patient characteristics, and measures of disease activity were explored.

In the third project, ultrasound detected synovitis was compared with whole-body MRI findings of effusion/synovial thickening and clinical assessment of disease activity in a cross-sectional study including 27 patients with active JIA.

3.2 Study population

The images used in the development of the ultrasonographic age-divided reference atlases and in the still-images exercises were collected during routine ultrasound examination of patients with JIA attending the paediatric rheumatology clinic at Oslo University Hospital (OUH) as part of clinical practice.

The participants in the live reliability exercise in paper I, and the participants in paper II and III, were recruited from the in-and outpatient paediatric rheumatology clinic at OUH in the period September 2020 to December 2022. Inclusion criteria were patients fulfilling the ILAR criteria for JIA (8), age between 1 and 18 years old and presence of active arthritis or suspected

clinical arthritis, that is an assumed flare that needed treatment adjustment. In the third project, the participants also had to be referred to an MRI or whole-body MRI examination on clinical indication to be included. Overview of the study populations in each paper are presented in **Table 6**. The only exclusion criteria were serious comorbidity or contraindication to general anaesthesia. Signed informed consent was obtained by parents, and from patients when aged 16 years and older.

Table 6. Overview of the study populations included in papers I, II and III.

	Anonymised images from JIA patients attending the OUH paediatric rheumatology clinic (n≈5000)	JIA patients attending the OUH paediatric rheumatology clinic (n=10)	JIA patients attending the OUH paediatric rheumatology clinic and referred to MRI (n=27)
Development of the ultrasonographic atlas and still-images reliability exercise (Paper I)	(n≈5000)		
Live exercise to test reliability (Paper I)		(n=10)	
Associations between PD and BM and clinical assessment (Paper II)		(n=10)	(n=17)
Correlations between ultrasound and whole-body MRI and clinical assessment (Paper III)			(n=27)

Abbreviations: JIA: Juvenile Idiopathic Arthritis, OUH: Oslo University Hospital, N: number, MRI: Magnetic Resonance Imaging, PD: Power Doppler, BM: B-mode

3.3 Data collection

3.3.1 Demographic variables and laboratory measures

Demographic variables such as diagnose, age, sex, duration of JIA and medications used were collected in the live exercise and in the second and third projects. Blood samples including CRP and SR were measured, and RF, Anti-CCP and ANA status were reported. The blood samples were taken as part of routine clinical evaluation. No blood samples were taken only for the cause of the project.

3.3.2 Clinical variables

Experienced rheumatologists performed 71-joints clinical examination in each patient, assessing joint tenderness, swollen joint count and limitation of motion. Active uveitis, duration of morning stiffness and symptoms of systemic JIA were also recorded. PhGA and PGA, both measured on a 0-10 cm VAS, were registered. The JADAS was calculated for 10 joints (JADAS10) and 71 joints (JADAS71).

3.3.3 Ultrasound

In the first project, an ultrasonographic image acquisition protocol and a semiquantitative joint-specific scoring system with age-divided reference atlas were developed.

Image acquisition protocol

Seven rheumatologists (NKS, PB, ABA, HBH, BF, JR, VL) developed an ultrasonographic image acquisition protocol for joints that are frequently affected in children with JIA. This was done through a consensus process including literature review, discussions, face-to-face meetings and training exercises. Important anatomic landmarks and positioning of the patient during the examination were key issues that were discussed. The joint regions included in the final protocol were the anterior elbow, posterior elbow, radiocarpal, midcarpal, MCP2-3 (dorsal), PIP2-3 (dorsal and volar), hip, knee (suprapatellar recess and lateral parapatellar recess), tibiotalar, talonavicular, anterior subtalar, posterior subtalar and MTP2-3 (dorsal). Two views were included for some joints to provide a better understanding of the pathology in the joint.

Image collection

Ultrasound images of joints from patients with JIA attending the paediatric rheumatology clinic at OUH had been collected and stored on two General Electric (GE) Logiq S8 ultrasound machines with linear probes (6-15 MHz) and hockey sticks (8-18 MHz) as part of daily clinical practice. Approximately 5000 ultrasound images were then selected and categorised joint-wise in four different age groups (2-3 years, 5-8 years, 9-12 years, 13-18 years) according to age-related changes (132). The images were stored anonymously and served as a database to be used in the project.

Development of an ultrasonographic scoring system

After literature review and discussions among the seven rheumatologists related to synovitis findings and severity, a semiquantitative (grades 0-3) joint-specific scoring system for BM-synovitis was developed. Scoring of BM synovitis of the knee joint followed a recently published scoring system for this joint that had shown good reliability (136). Synovitis findings were defined according to the preliminary definitions for sonographic features of synovitis in children (135). The scoring system for Doppler findings followed a scoring system developed for Doppler activity that we found applicable to all joints (136).

Development of reference atlases

BM images that corresponded to the image acquisition protocol and scoring system for each joint were selected to develop four age-divided reference atlases for BM synovitis (2-4 years, 5-8 years, 9-12 years and 13-18 years). PD images were also selected for each joint, without taking age into account, to create a reference atlas for PD activity. Two BM images and seven PD images, that we could not find on our machines, were added to the atlases from a collaborating centre (Division of Paediatric Dermatology and Rheumatology, Children's Hospital of Eastern Ontario) who used GE Logiq E9 ultrasound machines with linear probes (6-15 MHz) or hockey sticks (8-18 MHz).

Still images reliability testing

Inter-reader and intra-reader reliability were tested on still images. For BM synovitis scoring, 370 BM images from the database of 5000 images were used. The images had varying degrees of BM findings, and all age-groups were represented. The images were scored joint wise by four rheumatologists (NKS, PB, JR, VL). Inter-reader and intra-reader reliability exercises for PD activity were performed by three rheumatologists (NKS, PB, VL) scoring 37 images with different degrees of PD activity, that also were selected from the database of 5000 images.

Live reliability testing

Three rheumatologists (NKS, PB, VL) performed a live inter-reader reliability exercise including ten patients with JIA. One GE Logiq S8 machine with linear probe (6-15 MHz) and hockey stick (8-18 MHz) and standardised settings for BM and PD (pulse repetition frequency (PRF) 0.6 kHz, frequency 7.7 MHz and low wall filter) was used. The 19 joint regions included in the image acquisition protocol were assessed bilaterally with ultrasound in each patient. BM and PD findings were scored semiquantitatively (grades 0-3) at the time of acquisition.

Doppler findings and validity

In the second and third project, the ultrasound examinations were performed by one rheumatologist (NKS) using the new image acquisition protocol and joint-specific scoring system for synovitis with age-divided reference atlas as reference. In the second project, 18 joint regions were assessed bilaterally (the hip joint was excluded since Doppler findings were not assessed in the hip). In the third project, the joint regions assessed were the same 19 joint regions (14 joints) as in the first project. The ultrasound examinations were done bilaterally and scored semiquantitatively (grades 0-3) for BM and PD-findings in both projects. The same ultrasound machine, a GE Logiq S8 with linear probe (6-15 MHz) and hockey stick (8-18 MHz) and the same settings for BM and PD used in the first project, were used in both projects.

3.3.4 Whole-body Magnetic Resonance Imaging

In the third project, the included patients also underwent a whole-body MRI examination.

Image acquisition protocol

Non-contrast enhanced whole-body MRI was performed using Avanto fit 1.5Tesla (T), Aera 1.5T and Vida Fit 3T (Siemens Healthineers, Erlangen, Germany), with local receiver coils covering the whole body. General anaesthesia was given to patients under five years of age to avoid motion artefacts during the examination, which is routine practice at our clinic. The protocol comprised T2 Turbo spin echo (TSE) Dixon sequences: coronal plane from the skull base to the thighs, oblique coronal plane in the sacroiliac joints, and sagittal plane in the spine and in both knees and ankles. The image acquisition parameters were preset: repetition time (TR) >2000ms/echo time (TE) 92-111ms, Field of View (FOV) 15-35 cm, slice thickness 3-4 mm, and in-plane resolution 0.39-0.55 mm².

Scoring of whole-body MRI findings

All images were deidentified and analysed using Sectra Picture Archiving and Communications Systems (PACS). The whole-body MRI images were scored by one radiologist (EK) with broad experience in musculoskeletal MRI (over 20 years) according to a newly developed whole-body MRI scoring system for JIA (114). Effusion/synovial thickening was defined as hyperintense signal intensity within the joint space distending the joint capsule on fluid sensitive sequence, according to the MRI in JIA (JAMRI) OMERACT working group (114). Findings of effusion/synovial thickening in 14 joints (elbow, radiocarpal, midcarpal, MCP2-3,

PIP2-3, hip, knee, tibiotalar, talonavicular, subtalar, MTP2-3) were scored as absent, mild or moderate (grades 0-2) in large joints including the elbows, hips and knees, and as absent or present (grades 0-1) in small joints (114).

3.4 Statistics

Statistical Package for the Social Sciences (SPSS) version 27 was used for analyses in the first paper. Stata version 17 was used in the second paper, and SPSS version 29 was used in the third paper. P-values < 0.05 were considered statistically significant. Statisticians David Swanson, Cathrine Brunborg and Lien My Diep at Oslo Centre for Biostatistics and Epidemiology were consulted regarding the use of statistical methods and analyses.

3.4.1 Descriptive statistics

Continuous data were presented as mean (range), median (range) or median with interquartile range (IQR), as appropriate. Categorical variables were presented as numbers with percentages of total.

3.4.2 Reliability

In paper I, we explored the reliability of the developed semiquantitative joint-specific scoring system with reference atlas. First, in a still images inter-reader and intra-reader reliability exercise at joint level for BM synovitis scoring with four readers. Then, in a still images inter-reader and intra-reader reliability exercise for PD activity scoring at joint level with three readers. Finally, in a real-time live scoring exercise at patient level using ultrasound sum scores to test inter-reader reliability with three readers. In the calculation of the sum score, one view was selected from joints that were assessed from two views to avoid increased weighting of these joints. The sum scores included the following joint regions: anterior elbow, radiocarpal, midcarpal, MCP2-3 dorsal, PIP2-3 volar, hip, knee (suprapatellar recess), tibiotalar, talonavicular, anterior subtalar, MTP2-3 dorsal (28 joints in total). Separate BM synovitis and PD activity sum scores (range 0-84) were calculated for each patient.

To assess the reliability, intraclass correlation coefficient (ICC, absolute-agreement, two-way mixed-effects model) and weighted kappa were calculated (145, 146). For inter-reader reliability, we used average measure ICC (avmICC) and Light's weighted kappa. For intra-reader reliability, we used single measure ICC (smICC), and Cohens weighted kappa. ICC and kappa values were interpreted as fair: 0.20-0.40, moderate: 0.41-0.6, good: 0.61-0.8 and excellent: >0.81 (147).

Missing data

In the live reliability exercise, the anterior elbow was not assessed with ultrasound in one of the patients and therefore missing. Sum scores for each patient were calculated without any missing values.

3.4.3 Associations

In paper II, we investigated if increasing PD grades were associated with increasing BM grades and with the presence of clinical arthritis at joint level. In addition, we explored if PD findings were associated with age, sex, JIA subgroup, disease duration and with the JADAS10 at joint level. Eighteen joint regions (anterior elbow, posterior elbow, radiocarpal, midcarpal, MCP2-3 (dorsal), PIP2-3 (volar and dorsal), knee (suprapatellar recess and lateral parapatellar recess), tibiotalar, talonavicular, anterior subtalar, posterior subtalar and MTP2-3 (dorsal) were evaluated. To capture all PD findings within synovial hypertrophy (135), the chosen cut-off for abnormal BM and PD findings was grade ≥ 1 .

To assess the associations, we used multilevel mixed effects ordered logistic regression model to account for the within-patient (random intercept) effect. All analyses were adjusted for joint regions and side (left and right). Further adjustments, including age and sex were done to examine if the associations were altered.

Missing data

One joint region (anterior elbow) was not examined with ultrasound, but no other joints that were assessed with ultrasound were missing. Missing values for other variables were not included in the calculations.

3.4.4 Validity

In paper III, we examined the validity of ultrasound detected synovitis by comparing ultrasound with whole-body MRI and clinical assessment of disease activity.

At patient level, we compared sum scores from ultrasound, whole-body MRI and clinical joint examinations. The joints included in the sum score were the elbow, radiocarpal, midcarpal, MCP2-3, PIP2-3, hip, knee, tibiotalar, talonavicular, subtalar, MTP2-3 bilaterally (28 joints in total). For joints assessed from two views with ultrasound, the scan with the highest BM and PD score were used in the sum score. For ultrasound, a synovitis sum score was calculated for BM scores and PD scores (range 0-84) and for a combined score (BM + PD scores (range 0-168)) for each patient. For whole-body MRI an effusion/synovial thickening sum score was calculated (range 0-34), and for clinical examination an active joint sum score (range 0-71) was calculated for each patient.

We used Spearman correlation coefficient (r_s) to calculate associations between ultrasound synovitis sum scores, whole-body MRI effusion/synovial thickening sum scores and active joint sum scores. We also compared ultrasound synovitis sum scores with JADAS71, CPR, ESR, PhGA and PGA. We defined the strength of the Spearman's correlation coefficient (r_s) as: very weak: 0.0-0.19, weak: 0.2-0.39, moderate: 0.4-0.59, strong: 0.6-0.79, very strong: 0.8-1.0, in line with other studies evaluating ultrasound (148, 149).

At joint level, we calculated sensitivity, specificity, positive predictive value (PPV) and negative predictive value (NPV) for findings of synovitis on ultrasound using effusion/synovial thickening on whole-body MRI or active joints on clinical examination as reference. The chosen cut-off for abnormality was BM grade ≥ 2 for ultrasound findings, and grade ≥ 1 for whole-body MRI effusion/synovial thickening findings.

Missing data

At patient level, sum scores were calculated without any missing values. The JADAS71 was not calculated if data from any of the four components included in the JADAS were missing (n = 2, one PhGA/one PGA). At joint level, only joints with complete ultrasound, whole-body MRI and clinical joint examination data were included in the analyses. If a joint was missing (n = 32 for whole-body MRI, and n = 4 for ultrasound) the joint was excluded from the analyses.

3.5 Ethical considerations

This project involved children and adolescents with JIA. Children are often referred to as a vulnerable group in research ethics and therefore require special ethical considerations. The Declaration of Helsinki emphasises that research on vulnerable groups can only be justified if their needs are taken into account and the research cannot be carried out on a non-vulnerable group (150). The primary aim of this project was to evaluate ultrasound in children and adolescents with JIA and the ultrasound examinations could therefore not be done in adults because of the special anatomy in the growing child.

The project was approved by the Norwegian Regional Committee for Medical and Health Research Ethics (REK 2018/805) and the Data Protection Office at OUH (18/11742 and 18/12493). The study was conducted in accordance with the Declaration of Helsinki.

An important aspect in research is that participation is voluntary and informed consent is required. In the Declaration of Helsinki, it is accepted that informed consent can be given by authorised representatives for persons who cannot give informed consent themselves. However, it is emphasised that even though the main objective with medical research is to generate new knowledge, the rights of the individual participants must come first (150). According to the Patient and User Rights Act (Pasient- og brukerrettighetsloven), a child who has reached the age of 7 years should receive information and state their opinion before decisions about personal matters. When a child is 12 years old, great emphasis must be placed on what the child says (151).

In this project, information sheets, with text adjusted for children and adolescents in different age groups (under 12 years of age, 12-16 years of age, over 16 years of age and to parents) were made and signed informed consent was obtained by parents, and patients when aged 16 years and older. In addition, all participant and parents were thoroughly informed about the project orally and we were available to answer any questions related to the project. We talked to the participants about the ultrasound and the whole-body MRI examinations, and they could visit the MRI suite before the examination if they wanted to. For all participants, and especially children who were not able to express their opinion (many young children were included), it was important for us to inform and talk to the parents about the project so that they could be comfortable giving an informed consent for their child. The participants and their parents were

told that they could withdraw their consent at any time if they wanted to, without giving any reason, and that this would not affect their treatment.

Research involving children can only be performed if there is a reason to believe that the results may be of use to the participants or other individuals with the same age-specific disease (152). As previously described, there is a need for knowledge about ultrasound in patients with JIA to be able to standardise the method with reliable and valid scanning protocols and scoring systems. The thorough ultrasound examinations that were done in this project could potentially discover more findings than a normal clinical examination and might therefore be useful in the further treatment decisions of the patient. In addition, if the image acquisition protocol and scoring system proved to be reliable and valid tools it could provide a more homogenous and accurate interpretation of ultrasonographic findings in patients with JIA. Then the results could also be of benefit for other children and adolescents with JIA who are examined with ultrasound in future clinical practice.

4. Summary of results

4.1 Paper I

Development and reliability of a novel ultrasonographic joint-specific scoring system for synovitis with reference atlas for patients with juvenile idiopathic arthritis

The objectives of this study were to develop a standardised ultrasonographic image acquisition protocol and a joint-specific scoring system for synovitis with age-divided reference atlas in patients with JIA. Then to assess the reliability of the system on still images and in a live exercise.

Through literature review, discussions, practical training and consensus, an image acquisition protocol for frequently affected joints in JIA was developed. The joints included were the anterior elbow, posterior elbow, radiocarpal, midcarpal, MCP2-3 (dorsal), PIP2-3 (dorsal and volar), hip, knee (suprapatellar and lateral parapatellar recess), tibiotalar, talonavicular, anterior subtalar, posterior subtalar and MTP2-3 (dorsal) joints. Then a semiquantitative joint-specific scoring system, ranging from grade 0 (normal findings) to grade 3 (severe findings), was established. Finally, ultrasonographic reference atlases, corresponding to the joint-specific scoring system for BM synovitis, were developed for four age groups (2-4 years, 5-8 years, 9-12 years and 13-18 years) according to age-related changes. In addition, a reference atlas for PD activity was formed.

BM synovitis scoring on still images at joint level showed good to excellent intra-reader reliability (smICC range 0.75-0.95, weighted kappa range 0.63-0.91), and moderate to excellent inter-reader reliability (avmICC range 0.89-0.99, weighted kappa range 0.50-0.91). Intra-reader reliability for PD activity scoring on still images from all joints included in the scoring exercise combined was excellent, and inter-reader reliability was good to excellent. In the live scoring exercise, the inter-reader reliability was moderate to excellent for both BM synovitis and PD activity scoring.

Our findings suggest that a standardised ultrasound examination and a joint-specific scoring system with reference atlas can be valuable in the evaluation of joint inflammation in patients with JIA in clinical practice and in research.

4.2 Paper II

Associations between power Doppler ultrasound findings and B-mode synovitis and clinical arthritis in juvenile idiopathic arthritis using a standardised scanning approach and scoring system

The objectives of this study were to describe PD findings in patients with JIA with suspected clinical arthritis, and to examine if PD ultrasound findings were associated with BM synovitis and clinical arthritis, using a standardised ultrasound examination protocol and a semiquantitative joint-specific scoring system.

Ultrasound was performed in 27 patients with JIA. Twenty-one of the patients (77.8%) were girls. Seventeen patients had oligoarthritis (63.0%), five had RF negative polyarthritis (18.5%), three had RF positive polyarthritis (11.1%) and two patients had psoriatic arthritis (7.4%). The median number of joints with clinical arthritis was 2 (IQR 1-4).

A total of 971 joint regions were evaluated with ultrasound. BM synovitis (grade ≥ 1) was found in 129 joint regions, and abnormal PD signals were detected in 45 of these (34.9%). In joint regions with BM synovitis, PD grade 1 was detected in 18 joint regions, PD grade 2 in 20 joint regions and PD grade 3 in 7 joint regions. PD grade 1 was found in 4/48 (8.3%) joint regions with BM grade 1, in 7/47 (14.9%) joint regions with BM grade 2, and in 7/34 (20.6%) joint regions with BM grade 3. PD grades 2 and 3 were only found in joint regions that had BM grades 2 or 3.

We found that increasing PD grades were associated with higher BM grades (OR = 5.0, 95% CI: 2.7 - 9.1, $p < 0.001$) and with clinical arthritis (OR = 7.4, 95% CI: 2.6 - 21.0, $p < 0.001$).

Our findings suggest that the use of a standardised ultrasound examination and a semiquantitative joint-specific scoring system can make the assessment of abnormal Doppler signals more accurate in children and may reflect disease activity in patients with JIA.

4.3 Paper III

Validity of ultrasound synovitis in juvenile idiopathic arthritis: comparison with whole-body magnetic resonance imaging and clinical assessment

The objective of this paper was to assess the construct validity of ultrasound in patients with JIA by comparing findings of synovitis on ultrasound with non-contrast enhanced whole-body MRI findings of effusion/synovial thickening and clinical assessment of disease activity.

A total of 27 patients with JIA were included. Twenty-four patients (89%) were girls. Thirteen patients had oligoarthritis (48.1%), five had RF negative polyarthritis (18.5%), five had RF positive polyarthritis (18.5%), three had psoriatic arthritis (11.1%) and one patient had undifferentiated arthritis (3.7%). The median number of active joints was 4 (IQR 2-6) and the median JADAS71 was 13.4 (IQR 9.4-28.6).

At patient level, sum scores for ultrasound synovitis and whole-body MRI effusion/synovial thickening showed strong correlation ($r_s = 0.74$, $p < 0.01$). Ultrasound synovitis sum scores were also strongly correlated with JADAS71 ($r_s = 0.71$, $p < 0.01$). Ultrasound synovitis sum scores and active joint sum scores were moderately correlated ($r_s = 0.57$, $p < 0.01$).

At joint level, a total of 692 joints were assessed with ultrasound, whole-body MRI and clinical examination. On ultrasound and whole-body MRI, 58/692 joints (8.4%) had findings of synovitis or effusion/synovial thickening, whereas 566/692 joints (81.8%) had normal finding on both imaging modalities. On ultrasound and clinical joint examination, 58/692 joints (8.4%) had findings of joint inflammation, while 562/692 joints (81.2%) had normal findings. Ultrasound assessed synovitis at joint level showed high specificity, but lower sensitivity using effusion/synovial thickening on whole-body MRI or active joints on clinical examination as reference.

These findings suggest that ultrasound synovitis sum scores can reflect disease activity and may be a valuable outcome measure in clinical practice and research.

5. Discussion

5.1 Methodological aspects

In this section, the strengths and limitations of the study design and the statistical methods used in this project will be discussed.

5.1.1 Study design

All three papers are based on cross-sectional data and the project had an observational design. The focus of this project was to develop an ultrasonographic scanning protocol and a semiquantitative joint-specific scoring system with age-divided reference atlas in patients with JIA. Further to test the reliability of the system and the validity of ultrasound assessed synovitis, and to explore associations and frequencies of abnormal ultrasound findings in patients with JIA.

The cross-sectional design is well suited to assess frequencies, reliability, associations, and correlations. However, because we did not have longitudinal data, we could not explore risk, causal relationships or make conclusions about the prognostic meaning of ultrasound findings over time.

Observational studies can be influenced by selection bias, information bias and confounding factors (153). We performed reliability testing in multiple joints on still images and in a live exercise including patients with JIA. In the still images reliability exercise, a test-retest was performed with at least two weeks apart. Before the second scoring the images were rearranged by a person that did not participate in the exercise. All readers were blinded for the rearrangement, thus limiting recall bias. Only ten patients were assessed by three rheumatologists for inter-reader reliability in the live exercise in paper I, and we did not perform intra-reader reliability testing, which is a limitation. This was done for feasibility reasons in a challenging clinical setting during the COVID-19 pandemic. However, there are few ultrasound studies that test reliability in a real time setting in patients with JIA (89, 154). It is difficult to perform both inter-reader and intra-reader live reliability ultrasound exercises in children as they are often impatient. In addition, one must consider the ethical aspects of performing many examinations by several physicians when the participants are children.

5.1.2 Representativeness of study population

The methods used to select participants in a study can give selection bias that can affect the implementation of the results to the general population (153). If the participants are not representative of the population you want to study, the external validity can be reduced. All the patients that participated in this project fulfilled the ILAR classification criteria for JIA (8). Patients were consecutively included from the paediatric rheumatology clinic at OUH. We included boys and girls in all age-groups (1-18 years old) with clinical active arthritis or with suspected clinical arthritis. The one-centre design may limit the generalisability, but the paediatric rheumatology unit at OUH treats patients from all over the South-Eastern region of Norway. We therefore believe that the study population is representative of patients with JIA seen in clinical practice. In addition, the broad inclusion criteria and few exclusion criteria enabled this project to include patients with different levels of disease activity and with established or newly onset JIA which strengthen the external validity. In the third paper, all patients had to be referred to an MRI or whole-body MRI on clinical indication to be included. Since some joints are more difficult to evaluate than others, both clinically and with ultrasound, patients with symptoms from these joint regions are often referred to an MRI for further evaluation. This could have led to inclusion of more patients with affection of specific joints in our study and given a selection bias.

The low number of included patients is a limitation. This is often seen in ultrasound studies involving children (139, 155-158). Most patients in our study were girls and had oligoarthritis. However, oligoarthritis is the most common JIA subgroup and JIA is more common in girls than in boys (1). The low number of patients made us unable to stratify analyses for subgroups separately, which is a limitation, but synovitis findings are not known to be specific for JIA subgroups and is less likely to influence the generalisability. If we had included more patients, we might have seen more of the different JIA subgroups and perhaps detected additional findings in some joints. However, we had enough strength to find significant associations in this project, which means that we had an adequate number of patients to be able to answer the research questions.

Another limitation is that we did not include healthy controls. In the first project, our main aim was to develop a scoring system with reference atlas for patients with JIA, not to compare findings between healthy children and patients with JIA. However, in the development of the scoring system, we considered relevant studies in which ultrasound findings in healthy children

were described (126, 127, 129, 132, 133, 159). In the second paper, the aim was to describe PD findings in joints with BM synovitis in patients with JIA. By doing this, we excluded joints that had BM grade 0. If we had included healthy children, the results from the ultrasound findings in the joints of these children would probably be omitted in the analysis since we would expect normal findings. However, since there is no defined cut-off level for pathology on ultrasound in children, it can be difficult to conclude with what is a normal finding, and by including healthy children this might have been highlighted better. In the third paper the aim was not to define what is normal and what is pathological, but to validate the system by comparing findings on ultrasound with findings on whole-body MRI and clinical examination in patients with JIA. Healthy children were therefore not included.

5.1.3 Data collection

Ultrasound

A strength of this project is the extensive collection of ultrasonographic images, and that many joints were examined with ultrasound. Two GE Logiq S8 and one GE Logiq E9 ultrasound machines were used to collect the still images that were used in the reliability exercises on still images and in the reference atlases. However, the same ultrasound machine, a GE Logiq S8, was used in the live reliability exercise in paper I and in all ultrasound examinations in paper II and III. The preliminary definitions for ultrasound features of synovitis in children were used in all papers (135).

In paper I and III, sum scores were calculated for each patient. Since some joints were evaluated from more than one view with ultrasound, we decided to use one of the views in the calculations to avoid increased weighting of these joints. In paper I we used the view we believed to be most sensitive. In paper III we used the view with the highest BM and PD score to assess the overall disease activity in each patient. We may have found other results if we for instance had used the average score from the two views in the calculations as done by others (149).

Room temperature and pre or post examinations were not standardised and could have had an impact on our findings, especially concerning PD activity since a change in temperature can cause variability in the vascularisation with less flow in cold temperatures. It has been shown that low skin temperature can result in reduced Doppler activity in the wrist joint in RA patients (160). Other factors that can influence the interpretation of PD findings are tension in the muscles or movement of the patient (motion artefacts), or if the examiner has too much pressure

applied to the transducer as this will lead to decreased flow (125). Motion of the patient could have made us register more PD activity than it was, whereas cold temperatures and too much pressure could have made us register less PD activity. However, we strived to make the examination as comfortable as possible and made sure that the patients were not cold. The use of different ultrasound machines and settings has been shown to affect Doppler findings in patients with RA (161). We used the same ultrasound machine in all examinations with standardised settings for PD with low PRF and low wall filter and the ultrasonographer tried to use as little pressure as possible on the probe. In addition, the colour box was always placed at the top of the image to avoid reverberation artefacts, as recommended by others (125).

A strength of the study is that the rheumatologist was blinded to clinical and whole-body MRI findings. In addition, in paper II and III the same ultrasonographer performed all ultrasound examinations and used the same ultrasound machine with standardised settings and a standardised scanning protocol. We did not perform reliability studies in these papers, but the ultrasonographer had shown moderate to excellent reliability in paper I and has broad experience in musculoskeletal ultrasound.

Clinical assessment, measures of disease activity and laboratory analyses

Several rheumatologists performed the clinical joint examinations. No practical training or reliability exercises were done prior to this study, which is a limitation. However, all were experienced physicians and used to perform standardised joint examinations in a research setting. The lack of reliability testing means that the between-scorer variability is not known in this study and may have affected the number of reported active joints.

It was the treating rheumatologist who performed the clinical joint examination and was therefore informed about the medical history and clinical symptoms of the patients. The lack of blinding is a limitation and may have affected their interpretation of findings. Especially in paper III where the participants already were referred to an MRI. This may have led to a higher number of joints being scored as active because the rheumatologist might have expected to find arthritis there. This may have given a performance bias that could have influenced the study results.

In paper II and III the treating rheumatologists assessed the PhGA. It has been discussed if the interpretation of disease activity can be influenced by other factors, and that some physicians

do not always score 0 (in the VAS) even in the presence of disease remission (162). However, the PhGA and PGA are part of the core set of outcome variables used in clinical trials in patients with JIA and are also part of the JADAS. We therefore wanted to assess both the PhGA and PGA in this study. We only included patients with suspected clinical arthritis or active arthritis, and this may have led to better utilisation of the VAS scale by the physicians. In addition, the treating physicians, who scored the PhGA, were experienced rheumatologists and had all clinical data available. The PGA was completed by the participants or the parents. There are many factors affecting a patient's symptoms, for instance the sensation of pain. It can be difficult to distinguish if the pain is caused by active arthritis or other causes (163). These factors could potentially have led to a misinterpretation and inaccurate scoring of PGA, and subsequently the calculation of JADAS. This could have affected the results in paper II (association with PD activity) and paper III (correlation with ultrasound).

The JADAS is a validated and often used disease activity measurement in JIA. Our results can therefore easily be compared with other studies. In paper II, we chose to use the JADAS10 with the 2021 cut-offs for disease activity states (76). The JADAS10 is widely used and is easy to perform in the clinic. We also believe that the new cut-offs for disease activity states are more relevant and useful in clinical practice. We used the JADAS71 in paper III since we wanted to include all the joints that were assessed by clinical joint examination to evaluate the overall disease activity in the patients.

Blood samples and the laboratory analysis were done on clinical indication and performed by trained personnel. The blood samples were analysed at the same laboratory using nationally accredited analyses. This could have reduced the effect of random errors.

Whole-body MRI

Contrast-enhanced MRI is considered the gold standard in the evaluation of joint inflammation (80, 164). Because we wanted to assess many joints in each patient, whole-body MRI was chosen as the comparator to ultrasound as it can depict the entire body in one session (164). Using contrast in whole-body MRI to assess multiple joints is challenging as the prolonged scan time can lead to incorrect interpretation of synovial contrast enhancement (113). We therefore did not use contrast, which might have affected our findings since MRI without contrast has been shown to have lower ability to evaluate synovitis (106). The JAMRI OMERACT working group has proposed effusion/synovial thickening, BME, and pericapsular

soft tissue inflammation as inflammatory items for scoring peripheral and chest joints in a recently developed whole-body MRI scoring system (114). In this study, we used effusion/synovial thickening as the inflammatory item on whole-body MRI as we found this most comparable to findings of synovitis on ultrasound.

MRI is time consuming and general anaesthesia is required for the youngest patients so they can remain still during the session. This is a great limitation. Another challenge in this study was that some joints were outside the field of view and was therefore not depicted (elbow joints), and some joints were difficult to evaluate due to the small size (PIP joints). Ultrasound and clinical joint examination could have detected synovitis in these joints, but since missing joints for any modality (ultrasound, whole-body MRI or clinical examination) were excluded in the analysis, the joints were not included in the calculations at joint level. We could therefore have missed many findings, and this may have affected the sensitivity and specificity.

For feasibility reasons, one experienced musculoskeletal radiologist scored the whole-body MRI images only once. A strength is that she was blinded to clinical and ultrasound findings, but the single assessment of the images may have caused poorer data quality and lower associations with ultrasound findings.

5.1.4 Statistical considerations

Reliability

The Kappa is a statistical measure of agreement between readers or among repeated measures by a single reader. Kappa takes the possibility of the agreement occurring by chance into account (165). The ICC is another method for assessing agreement where the extent of the disagreement is included, meaning that larger sizes of disagreement, gives lower ICC than smaller (145, 146).

To test intra-reader reliability, we used the Cohen's weighted kappa, that allocates weights to different categories to reflect the degree of disagreement between readers (166, 167). We evaluated pairs of scoring by the same reader that were scored with two to three weeks in between. The two-way mixed effects model ICC was used to test the reliability of the specific readers that participated in the exercise (146). Since the Cohen's kappa is suitable for two

readers and we had three or four readers in the inter-reader reliability exercise, we used the Light's weighted kappa by calculating the mean kappa for all reader pairs (145).

We chose to include both ICC and Kappa as measures of reliability seeing that they are both commonly used in papers examining reliability in musculoskeletal ultrasound. In this way the results are easily understood and comparable to studies that have chosen to use one of the two methods.

Associations

Standard statistical methods assume independent observations. However, sometimes the observations are not independent of each other. Multilevel analyses take dependency of the observations into account (168). This is useful in settings where you have repeated or correlated measurements.

We explored associations between PD activity grades and BM synovitis grades and clinical arthritis. Since we evaluated many joints in the same patient (repeated measurements on the same individual), the data was not independent, and we had to take this into consideration in the calculations. In cooperation with a statistician, we used multilevel mixed-effects ordered logistic regression analyses with random intercept for patients to account for within-patient effect, and because we had an ordinal endpoint.

Validity

Validity tells you how accurately a method measures something. There exist four main types of validity: content, face, criterion and construct validity (169, 170). We tested the construct validity, meaning that the test (ultrasound) was compared with other tests (whole-body MRI, clinical assessment) measuring the same concept (joint inflammation). To explore the validity of ultrasound detected synovitis we used correlation, sensitivity and specificity.

At patient level we used correlation analyses to evaluate the associations between joint inflammation sum scores. Since the data in our study was not normally distributed, we used Spearman's correlation coefficient (r_s). This correlation is calculated by replacing the actual values from the included variables with ranks (171, 172). At joint level, we used sensitivity and specificity to assess the diagnostic performance of ultrasound. We used binary outcomes (presence/absence) for findings of synovitis, effusion/synovial thickening and active joints in

the calculations. The sensitivity reflects the true positive rate, while specificity reflects the true negative rate. Sensitivity and specificity are inversely related (173, 174).

5.2 Main results

In this section, the main results according to the specific research questions in this thesis will be interpreted, discussed, and compared to other related studies.

5.2.1 Development of an image acquisition protocol

In this project an image acquisition protocol for frequently affected joints in JIA was first established. The protocol was built upon existing approaches but adjusted to be suitable for the different paediatric joints (124, 132, 136).

Previous scanning approaches used in ultrasound studies with children have mainly used protocols developed for adults with RA (124). However, there was a need for a scanning approach specially designed for children. Prior to the development of our protocol, two protocols for children had been developed, but only for a limited number of joints (knee, wrist, MCP2 and ankle joints) (132, 136). We decided to use the scans of the wrist (radiocarpal and midcarpal) and the knee joint from these scanning protocols as we found them applicable. For the remaining joints the scanning protocol was developed through the consensus process described in section 3.3.3. For some joints, we decided to include two views to provide a better understanding of the pathology in the joint and seeing that two views could have an added value, as also suggested by others (136). The consensus process was not done by a Delphi (175). Since we did not use this validated method, it can be difficult to reproduce the consensus process. A bias could have occurred if the participants were worried about how their opinions would be viewed by the others since proposals were not shared anonymously. However, a Delphi can be time consuming, and it can be difficult to define what is meant by consensus and when this is reached. The rheumatologists involved in our consensus process had considerable experience (5-20 years) in musculoskeletal ultrasound and methodological experience from the OMERACT. In addition, the development of the protocol was dynamic where the different proposals were tested in practical exercises to assess the applicability.

Another ultrasonographic scanning approach for multiple joints in children was recently published (149). The protocol is very comprehensive (52 different views in BM, whereas 19 views in ours) and may not be feasible in daily clinical practice. Most of the joints included in the scanning protocol are the same as ours, but they have included the shoulder and the radioulnar joints. They have also included the interphalangeal (IP) joint, and all MCP, PIP and MTP joints. In addition, several joints are assessed from more than one view. The biceps- and the ankle tendons are also included in their scanning protocol. A limitation in our study is that we did not include the shoulder and the radioulnar joints in our protocol. This was done because we only included the most frequently affected joints in JIA, but since there are patients with arthritis in these joints it would have been favourable to have included them in our protocol. The optimal number of joints that needs to be assessed to evaluate disease activity is not standardised. Collado et al. evaluated a 44 joint model versus a 10 joint model (bilateral knee, ankle, wrist, elbow and MCP2 joints) and found the 10 joint model to be valid and to have a higher responsiveness to change than the 44 joint model (138). However, it is uncertain how well this model will work in other patient samples.

5.2.2 Development of a joint-specific scoring system and reference atlas

Scoring system

An ultrasonographic semiquantitative joint-specific scoring system for synovitis in patients with JIA was presented in paper I. A specific scoring of BM findings ranging from grade 0 (normal) to grade 3 (severe) was developed for each joint. The scoring system for Doppler activity followed a newly developed semiquantitative scoring system that could be applied to all joints (136).

The choice of a semiquantitative score was done in accordance with what had been done previously (89, 136, 138). In addition, a semiquantitative scoring has shown to have better reliability than a binary scoring (143). Prior to our study, only one joint-specific scoring system for the paediatric knee joint existed (136). The OMERACT paediatric ultrasound group had proposed a single standard scoring system, but this has not been published (176). In a recent study, Rossi-Semerano et al., used a modified version of this scoring system to account for the different anatomy in the joints they evaluated (177). Another single standard scoring system had been published prior to our study, but this scoring system did not seem to be applicable to all joints either (138). As previously described (section 1.3.5), the BM scoring in this system is based on the shape and extension of the joint recess in relation to the bone diaphysis and is

therefore not applicable to joints where an articulating bone does not have a diaphysis, like for instance the ankle joint. Our joint-specific scoring system for synovitis in JIA allows for a clear assessment of the specific paediatric joint that is being evaluated.

Shortly after the publication of our scoring system, another joint-specific scoring system for children was published (149). There are many similarities in these scoring systems, including the descriptions of BM grades (0-3) in some joints and the Doppler scoring. The main differences are that they also have included scoring of the shoulder, IP and radioulnar joints, and scoring from more views for the wrist and the MCP joints. In addition, scoring of the biceps and ankle tendons are included. However, the scoring of the tendons in the ankle is not tendon-specific, and the scoring is binary (presence/absence). In addition, it does not consider the newly published consensus for ultrasound definitions of tenosynovitis in JIA (178). Other differences are that they use the terminology “ α -line” and “ β -line”, and we use “imaginary line”, but the descriptions of the lines are almost the same in the two scoring systems. When developing our scoring system, we especially focused on the distribution of synovial hypertrophy/effusion in the joints and discovered that the use of an imaginary line could help to distinguish different degrees of synovitis. In some joints this line complied to the joint capsule, but in others it did not (for instance the elbow), and to harmonise the scoring system we chose to implement the “imaginary line”. We included the nomenclature “mild, moderate and severe” (for grades 1, 2, and 3) to elaborate the severity of the findings in each joint. This is also included in the other scoring system but only for some joints, and they use “mild, moderate and marked”. The many similarities between the systems may indicate that the international ultrasound communities have similar interpretation of findings in the paediatric joint.

Reference atlas

Four reference atlases for BM scoring of synovitis, comprising of 224 distinctive BM images, divided in four age-groups (2-4 years, 5-8 years, 9-12 years and 13-18 years), and a reference atlas for scoring of PD activity, comprising of 51 PD images were produced in paper I.

Because interpretation of ultrasound images in the growing skeleton is difficult, we saw the importance of a reference atlas. The joint-specific ultrasonographic atlas developed by Hammer et al. for patients with RA has shown high reliability (142), but cannot be directly applied to children because of the unique growing skeleton. The differences seen in the skeleton during growth were also the reason why we decided to make four reference atlases in accordance with

age-related changes (132). Our reference atlas can provide an additional tool when scoring synovitis in children of different ages by finding the best matching image in the reference atlas. The reference atlas for PD activity is not age-divided. This was done because our intention was to have images of the different PD signals corresponding to the scoring system, not the age-variability. In addition, since PD signals need to be found within synovial hypertrophy to be considered as a sign of synovitis (135), evaluation of BM findings must be performed first. This can be done by using the scoring system with age-divided reference atlas for BM synovitis where the age-related changes can be clearly identified.

A limitation is that we could not find representative images of all grades for all joints in the atlases (anterior elbow for PD grade 3, MCP2-3 and MTP2-3 for BM grade 2 and 3 in the age-group 2-4 years, and MCP2-3 for BM grade 3 in the age group 5-8 years). However, we added images of these grades from other age-groups (5-8 years and 9-12 years), so the sonographer can be able to compare images.

5.2.3 Reliability of the joint-specific scoring system with reference atlas

We demonstrated moderate to excellent reliability for BM synovitis scoring, and good to excellent reliability for PD activity scoring on still images. The reliability for BM synovitis and PD activity scoring in a live exercise, was moderate to excellent.

The readers in the reliability exercises were all experienced rheumatologists and had participated in the development of the scoring system, which could have affected the results. However, it is recommended to perform calibration before reliability exercises. In addition, others who have evaluated scoring systems, have performed several reliability tests during the study period where modifications of the system have been done until acceptable reliability is achieved (136, 149, 179). We therefore believe that our results are representative.

A strength of this study is that reliability testing was performed on many joints from all age groups (2-18 years), and that reliability was performed on both still images and in a live exercise. Our results from the still image reliability exercises are comparable with results from other ultrasound studies testing reliability on still images in patients with JIA (136, 149, 177, 179, 180). In ultrasound reliability studies in adult patients with RA, both inter-reader and intra-reader reliability testing in patients are often performed (142-144, 181). A limitation in our study is that we did not perform an intra-reader reliability live scoring. As previously described

(section 5.1.1.) this was done for feasibility reasons in a clinical setting during the COVID-19 pandemic. To the best of our knowledge, only one ultrasound study in children has tested both inter-reader and intra-reader reliability in live exercises, but only a few joints were examined (154). Another ultrasound study that performed a live reliability exercise in children reported inter-reader reliability (89). The results presented in this study are comparable to our results.

Another limitation in our study is that only ten patients with JIA were assessed in the live exercise. However, we had power to show moderate to excellent reliability and others have shown that the same number of patients may give enough power to test reliability (142, 181, 182).

5.2.5 Associations between PD findings and BM synovitis, and clinical arthritis

In this study we found that at joint level, increasing PD grades were significantly associated with higher BM grades and with clinical arthritis.

To our knowledge, no other studies have explored the associations between ultrasound PD grades and BM grades in patients with JIA. As previously discussed in this thesis, interpretation of Doppler signals in paediatric joints is challenging, but it is very important to distinguish between normal and pathological findings. To help distinguish between these findings, the proposed definitions for synovitis in children underline that abnormal Doppler signals must be intrasynovial, not just intraarticular (135).

We detected abnormal PD signals in 45 of 129 joint regions that had BM synovitis (grade ≥ 1). PD grades 0 and 1 were found in joint regions with BM grade 1, 2 and 3, but PD grade 2 and 3 were only detected in joint regions that had BM grade 2 or 3. This may indicate that the joint-specific scoring system harmonises with the severity of synovitis.

The preliminary definitions for sonographic features of synovitis in children emphasise that Doppler signals must be detected within synovial hypertrophy to be considered as a sign of synovitis. In addition, that synovitis can be based on BM findings alone but not Doppler findings alone (135). There were many joint regions that had BM synovitis where we did not find abnormal PD signals in our study, suggesting that BM synovitis without PD findings could be more common in patients with JIA. Other explanations to our findings could be that our patients had a low-grade disease, or that the BM findings were remnants of previous synovitis

(158). It could also be that synovial effusion is more common than synovial hypertrophy in patients with JIA. Doppler signals cannot be detected in synovial effusion, whereas BM synovitis can be based on synovial effusion alone (135). However, since we did not distinguish between synovial effusion and synovial hypertrophy in our scoring of BM synovitis, we could not explore this further. Another possible explanation could be that BM grade 1 represents normal findings since there are no defined cut-off grade for what is pathological. However, there were some joints with BM grade 1 that also had PD grade 1, and since PD signals only were scored within synovial hypertrophy, we believe that our findings represent abnormal PD signals.

We did not find synovial hypertrophy or effusion in any MCP joints and could therefore not look for PD signals there. As the MCP2 joint is known to be frequently affected in JIA (132, 156, 177), our results could have been affected by the limited number of patients, but most JIA subgroups were represented. It could also be because of the small size of the joint or that the joint was assessed from one view, as opposed to the PIP joints that were assessed from two views and synovitis was detected in those joints. The use of a dorsal or a volar ultrasound scan of the MCP joints is inconsistent in children (135, 154, 156, 177). In our study, the knee joint was also assessed from two views according to our scanning protocol. A high number of abnormal PD signals were detected in the lateral parapatellar recess, while BM synovitis without PD findings were more common in the suprapatellar recess. To assess the joints from more than one view may seem to have an added value. However, in a clinical setting it can be difficult to evaluate several joints from more views because young children are often impatient.

The number of patients is also a limitation in this study. As previously mentioned, this is a challenge in paediatric ultrasound studies, especially when evaluating more than one joint. However, as many as 971 joint regions were examined clinically and with ultrasound, and the associations were explored at joint level. In addition, we used the same ultrasound machine with standardised settings in all examinations.

5.2.6 Correlations between ultrasound and whole-body MRI and clinical assessment

At patient level, we found a strong correlation between ultrasound synovitis sum scores and whole-body MRI effusion/synovial thickening sum scores. We also detected a strong correlation between ultrasound synovitis sum scores and the JADAS71. The correlation between ultrasound synovitis sum scores and clinical active joint sum score was moderate.

To the best of our knowledge, this is the first study comparing ultrasound detected synovitis in multiple joints with MRI in patients with JIA. Interestingly many joints with effusion/synovial thickening were detected on whole-body MRI even though we did not use contrast and had lower resolution than a standard MRI examination. We therefore believe that the MRI images acquired in this study enabled a comparison between ultrasound and whole-body MRI findings of joint inflammation.

We found a strong correlation between ultrasound synovitis sum scores and the JADAS71. Others have reported a poor or moderate correlation between ultrasound and the JADAS (89, 149). The JADAS consists of four items (number of active joints, PhGA, PGA and ESR) that all can affect the final score. We found a strong correlation between ultrasound synovitis sum scores and PhGA. Vega-Fernandez et al. reported a variable correlation between ultrasound and PhGA, finding weak correlation at a baseline visit, and moderate to strong correlation at follow up (183). Others have reported a poor correlation (89). A poor agreement in scoring PhGA among physicians in JIA patients with low or no disease activity have been reported (184), and physicians around the world tend to score the PhGA differently (185). In our study, there were experienced rheumatologists that had clinical information available and were used to evaluate PhGA in a research setting, that scored the PhGA. In addition, we only had patients with suspected or active arthritis. This could have contributed to the strong correlation between ultrasound and PhGA found in our study. We found a weak, not statistically significant correlation between PGA and ultrasound synovitis sum scores. A poor correlation has also been reported by others (89). As previously described (section 5.1.3) the PGA can be challenging to score. It can be difficult to distinguish between symptoms of JIA and symptoms from other causes. It has been shown that the parents and physicians often disagree in the evaluation of disease activity, especially if the patient has pain as this can affect the parent's evaluation of the child's well-being (186-188). While ultrasound evaluate the inflammation at a precise location, the PGA may be affected by other confounding factors. This may have affected the scoring of PGA and could be a reason to the low correlation found in our study.

It is important to emphasise these issues since both PhGA and PGA are part of the core set of outcome variables used in clinical trials and part of the JADAS that is often used as a disease activity measurement in patients with JIA. One may consider if ultrasound can provide a more

unbiased evaluation of the total inflammatory activity and be used as an outcome measure of disease activity. However, a limitation of ultrasound is that it is operator dependent.

At joint level, the sensitivity was low, which may indicate that ultrasound is too cautious in finding synovitis and could miss pathology in a joint. This again may lead to treatment delay and potential joint damage. On the other hand, we found a high specificity, which means that if ultrasound does not detect synovitis in a joint, one can be quite certain that there is no pathology in that joint. The PPV and NPV is related to the prevalence of the disease (174). In general, there were few joints with inflammatory findings in our study which may have resulted in high NPV and lower PPV. The participants in this study were all referred to an MRI or whole-body MRI on clinical indication. Joints that are difficult to evaluate clinically or with ultrasound are often referred to a contrast enhanced MRI for further evaluation. The affected joints could therefore have been complex and difficult to evaluate with ultrasound, and this may have contributed to the low sensitivity between ultrasound and whole-body MRI in our study. We also found a low sensitivity between ultrasound and clinical joint examination. The rheumatologist who performed the clinical joint examination was not blinded to the patient's symptoms, medical history, or previous findings, but the sonographer was blinded to all clinical information except for the age. This could have influenced the findings, and thus also the results.

Whole-body MRI detected abnormalities in some joints more frequently than ultrasound, while ultrasound found abnormalities more often than whole-body MRI in other joints. This might have been because of the complex anatomy in some joints (189-191), and that the positioning of the joints differed in the two examinations which could have altered the distribution of the effusion, as also suggested by others (157). We used non-contrast enhanced whole-body MRI findings of joint inflammation as reference to validate ultrasound findings of synovitis. At present, contrast enhanced MRI is considered the gold standard in the evaluation of synovitis and considered to be more sensitive in detecting joint inflammation than non-contrast enhanced MRI (80, 106, 164). It is therefore possible that the whole-body MRI examination may have underestimated the overall disease burden.

Our findings of a strong correlation between ultrasound synovitis sum scores and whole-body MRI effusion/synovial thickening sum scores at patient level and low sensitivity between

ultrasound and whole-body MRI at joint level suggest that these modalities can measure the overall disease activity, but the imaging properties are different.

6. Conclusions

6.1 Answer to research questions

Regarding the specific research questions of this thesis presented in section 2.2 we were able to draw the following conclusions:

- At joint level, ultrasound assessment of synovitis in patients with JIA can be performed reliably when using a semiquantitative joint-specific ultrasonographic scoring system with reference atlas (Paper I)
- At patient level, ultrasound assessment of synovitis in patients with JIA can be performed reliably when using a semiquantitative joint-specific ultrasonographic scoring system with reference atlas (Paper I)
- PD findings are associated with BM-synovitis and with the presence of clinical arthritis at joint level (Paper II)
- PD findings are not associated with age, JIA subgroups or the JADAS10 at joint level (Paper II)
- Ultrasound synovitis sum scores are strongly correlated with whole-body MRI effusion/synovial thickening sum scores (Paper III)
- Ultrasound synovitis sum scores are strongly correlated with the JADAS71 and moderately with clinical active joint sum scores (Paper III)
- Ultrasound showed high specificity but lower sensitivity in detecting synovitis using whole-body MRI or clinical joint examination as reference (Paper III)

6.2 Clinical implications and further research

Detection of joints with inflammation is important in the diagnosis, treatment, and follow-up of patients with JIA. Clinical joint examination can be challenging in children and reliable and valid measures to evaluate disease activity are needed.

Our results suggest that the use of a standardised ultrasound examination and a semiquantitative joint-specific scoring system with age-divided reference atlas can be useful when evaluating disease activity, and that ultrasound may be a valuable outcome measure in patients with JIA.

Since the use of ultrasound in JIA has evolved in recent years, it would have been a great advantage if the international community could work together to establish scanning protocols and a scoring system that could be used worldwide. The EULAR-PreS has developed points to consider for the use of imaging in diagnosis and follow-up of patients with JIA (6). In addition, the European Society of Musculoskeletal Radiology (ESSR) arthritis subcommittee and the European Society of Paediatric Radiology (ESPR) have proposed points to consider concerning imaging in children with suspected or known JIA (192). There are still many countries where ultrasound is being performed by radiologists, but this could potentially lead to diagnostic and treatment delay. There seems to be a growing interest to educate rheumatologists in paediatric ultrasound, and procedures for the content, conduct and format of EULAR/PreS paediatric ultrasound courses have recently been published (193).

6.3 Dissemination

The image acquisition protocol and ultrasonographic joint-specific scoring system with age-divided reference atlas developed in this thesis are already being used in clinical practice and research in Norway. Ultrasound courses and training in the scoring system have been held for medical doctors in all health-regions in Norway. In addition, instructional videos for ultrasound joint examination in children have been developed with both Norwegian and English audio and are available online.

The image acquisition protocol and scoring system are being used by study personnel in the “MyJIA trial” which is a randomised, open, prospective, multi-centre clinical study involving patients with JIA starting biologic treatment. The ultrasound data will be analysed to explore baseline and longitudinal changes in ultrasound assessed synovitis in patients treated with biological medications. In addition, the ability of ultrasound to discriminate between treatment arms will be assessed.

The image acquisition protocol and scoring system will also be implemented in the “MOVE JIA trial”. This is a 3-armed randomised, prospective, multi-centre clinical trial involving patients with JIA in sustained remission who either continue stable dose methotrexate and TNF-alfa inhibitors or withdraw either methotrexate or TNF-alfa inhibitors. Ultrasound data will be used to explore if ultrasound findings can predict a flare.

7. Errata

Paper II

In the caption to Figure 2 it is incorrectly written “Longitudinal dorsal scan of the knee joint (lateral parapatellar recess) showing BM synovitis (C), and BM synovitis with abnormal PD signals (grade 3) (D).” The correct is “Transverse scan of the knee joint (lateral parapatellar recess) showing BM synovitis (C), and BM synovitis with abnormal PD signals (grade 3) (D).”

Errata list

Page	Line	Original text	Corrected text
Abbreviations		Added: PRF Pulse Repetition Frequency	
22	2	..(23, 38-42)	..(23, 38-42).
24	7	..patients JIA..	..patients with JIA..
29	5	..may led to..	..may lead to..
43	31	..pulse repetition frequency..	..pulse repetition frequency (PRF)..
44	4	In the second, project..	In the second project,..
51	12	..five had RF negative polyarthritis (33.3%)..	..five had RF negative polyarthritis (18.5%)..
55	15	GE Logic S8..	GE Logiq S8..
56	22	..is not known in..	..is not known in this study..
60	21	..developed thorough..	..developed through..
63	21	..experienced rheumatologist..	..experienced rheumatologists..
65	33	..sum scores the JADAS71..	..sum scores and the JADAS71..
66	16	..score tend to score..	..tend to score..
69	5	..precented..	..presented..
70	13	..scoring system..	..a scoring system..

8. References

1. Ravelli A, Martini A. Juvenile idiopathic arthritis. *Lancet*. 2007;369:767-78.
2. Prakken B, Albani S, Martini A. Juvenile idiopathic arthritis. *Lancet*. 2011;377:2138-49.
3. Swart JF, de Roock S, Prakken BJ. Understanding inflammation in juvenile idiopathic arthritis: How immune biomarkers guide clinical strategies in the systemic onset subtype. *Eur J Immunol*. 2016;46:2068-77.
4. Rooney ME, McAllister C, Burns JF. Ankle disease in juvenile idiopathic arthritis: ultrasound findings in clinically swollen ankles. *J Rheumatol*. 2009;36:1725-9.
5. Pascoli L, Wright S, McAllister C, et al. Prospective evaluation of clinical and ultrasound findings in ankle disease in juvenile idiopathic arthritis: importance of ankle ultrasound. *J Rheumatol*. 2010;37:2409-14.
6. Colebatch-Bourn AN, Edwards CJ, Collado P, et al. EULAR-PreS points to consider for the use of imaging in the diagnosis and management of juvenile idiopathic arthritis in clinical practice. *Ann Rheum Dis*. 2015;74:1946-57.
7. Collado P, Malattia C. Imaging in paediatric rheumatology: Is it time for imaging? *Best Pract Res Clin Rheumatol*. 2016;30:720-35.
8. Petty RE, Southwood TR, Manners P, et al. International League of Associations for Rheumatology classification of juvenile idiopathic arthritis: second revision, Edmonton, 2001. *J Rheumatol*. 2004;31:390-2.
9. Petty RE, Southwood TR, Baum J, et al. Revision of the proposed classification criteria for juvenile idiopathic arthritis: Durban, 1997. *J Rheumatol*. 1998;25:1991-4.
10. Martini A, Ravelli A, Avcin T, et al. Toward New Classification Criteria for Juvenile Idiopathic Arthritis: First Steps, Pediatric Rheumatology International Trials Organization International Consensus. *J Rheumatol*. 2019;46:190-7.
11. Thierry S, Fautrel B, Lemelle I, et al. Prevalence and incidence of juvenile idiopathic arthritis: a systematic review. *Joint Bone Spine*. 2014;81:112-7.
12. Moe N, Rygg M. Epidemiology of juvenile chronic arthritis in northern Norway: a ten-year retrospective study. *Clin Exp Rheumatol*. 1998;16:99-101.
13. Berntson L, Andersson Gare B, Fasth A, et al. Incidence of juvenile idiopathic arthritis in the Nordic countries. A population based study with special reference to the validity of the ILAR and EULAR criteria. *J Rheumatol*. 2003;30:2275-82.
14. Riise Ø R, Handeland KS, Cvancarova M, et al. Incidence and characteristics of arthritis in Norwegian children: a population-based study. *Pediatrics*. 2008;121:e299-306.
15. Sharma S, Sherry DD. Joint distribution at presentation in children with pauciarticular arthritis. *J Pediatr*. 1999;134:642-3.
16. Eng SWM, Aeschlimann FA, van Veenendaal M, et al. Patterns of joint involvement in juvenile idiopathic arthritis and prediction of disease course: A prospective study with multilayer non-negative matrix factorization. *PLoS Med*. 2019;16:e1002750.
17. Martini A, Lovell DJ. Juvenile idiopathic arthritis: state of the art and future perspectives. *Ann Rheum Dis*. 2010;69:1260-3.
18. Prahalad S, Glass DN. A comprehensive review of the genetics of juvenile idiopathic arthritis. *Pediatr Rheumatol Online J*. 2008;6:11.
19. Prakken BJ, Albani S. Using biology of disease to understand and guide therapy of JIA. *Best Pract Res Clin Rheumatol*. 2009;23:599-608.
20. Henderson LA, Volpi S, Frugoni F, et al. Next-Generation Sequencing Reveals Restriction and Clonotypic Expansion of Treg Cells in Juvenile Idiopathic Arthritis. *Arthritis Rheumatol*. 2016;68:1758-68.

21. Horton DB, Shenoi S. Review of environmental factors and juvenile idiopathic arthritis. *Open Access Rheumatol.* 2019;11:253-67.
22. Giancane G, Alongi A, Ravelli A. Update on the pathogenesis and treatment of juvenile idiopathic arthritis. *Curr Opin Rheumatol.* 2017;29:523-9.
23. Hinze C, Gohar F, Foell D. Management of juvenile idiopathic arthritis: hitting the target. *Nat Rev Rheumatol.* 2015;11:290-300.
24. Ruperto N, Martini A. Current and future perspectives in the management of juvenile idiopathic arthritis. *Lancet Child Adolesc Health.* 2018;2:360-70.
25. Giannini EH, Brewer EJ, Kuzmina N, et al. Methotrexate in resistant juvenile rheumatoid arthritis. Results of the U.S.A.-U.S.S.R. double-blind, placebo-controlled trial. The Pediatric Rheumatology Collaborative Study Group and The Cooperative Children's Study Group. *N Engl J Med.* 1992;326:1043-9.
26. Ruperto N, Murray KJ, Gerloni V, et al. A randomized trial of parenteral methotrexate comparing an intermediate dose with a higher dose in children with juvenile idiopathic arthritis who failed to respond to standard doses of methotrexate. *Arthritis Rheum.* 2004;50:2191-201.
27. Lovell DJ, Giannini EH, Reiff A, et al. Etanercept in children with polyarticular juvenile rheumatoid arthritis. Pediatric Rheumatology Collaborative Study Group. *N Engl J Med.* 2000;342:763-9.
28. Lovell DJ, Ruperto N, Goodman S, et al. Adalimumab with or without methotrexate in juvenile rheumatoid arthritis. *N Engl J Med.* 2008;359:810-20.
29. Horneff G, Fitter S, Foeldvari I, et al. Double-blind, placebo-controlled randomized trial with adalimumab for treatment of juvenile onset ankylosing spondylitis (JoAS): significant short term improvement. *Arthritis Res Ther.* 2012;14:R230.
30. Ruperto N, Lovell DJ, Quartier P, et al. Abatacept in children with juvenile idiopathic arthritis: a randomised, double-blind, placebo-controlled withdrawal trial. *Lancet.* 2008;372:383-91.
31. Brunner HI, Ruperto N, Zuber Z, et al. Efficacy and safety of tocilizumab in patients with polyarticular-course juvenile idiopathic arthritis: results from a phase 3, randomised, double-blind withdrawal trial. *Ann Rheum Dis.* 2015;74:1110-7.
32. Quartier P, Allantaz F, Cimaz R, et al. A multicentre, randomised, double-blind, placebo-controlled trial with the interleukin-1 receptor antagonist anakinra in patients with systemic-onset juvenile idiopathic arthritis (ANAJIS trial). *Ann Rheum Dis.* 2011;70:747-54.
33. Ruperto N, Brunner HI, Quartier P, et al. Two randomized trials of canakinumab in systemic juvenile idiopathic arthritis. *N Engl J Med.* 2012;367:2396-406.
34. Ringold S, Angeles-Han ST, Beukelman T, et al. 2019 American College of Rheumatology/Arthritis Foundation Guideline for the Treatment of Juvenile Idiopathic Arthritis: Therapeutic Approaches for Non-Systemic Polyarthritis, Sacroiliitis, and Enthesitis. *Arthritis Care Res (Hoboken).* 2019;71:717-34.
35. Lanni S, Bertamino M, Consolaro A, et al. Outcome and predicting factors of single and multiple intra-articular corticosteroid injections in children with juvenile idiopathic arthritis. *Rheumatology (Oxford).* 2011;50:1627-34.
36. Ravelli A, Davi S, Bracciolini G, et al. Intra-articular corticosteroids versus intra-articular corticosteroids plus methotrexate in oligoarticular juvenile idiopathic arthritis: a multicentre, prospective, randomised, open-label trial. *Lancet.* 2017;389:909-16.
37. Oslo Universitetssykehus. NAKBUR. Behandlingsplaner ved Barneleddgikt (JIA) 2019 [updated 22. Feb. 2021; cited 2023 18. Oct]. Available from: <https://www.oslo-universitetssykehus.no/fag-og-forskning/nasjonale-og-regionale-tjenester/nasjonal-kompetansetjeneste-for-barne-og-ungdomsrevmatologi/behandlingsplaner-ved-barneleddgikt-jia-2019/>.

38. Wallace CA, Giannini EH, Spalding SJ, et al. Trial of early aggressive therapy in polyarticular juvenile idiopathic arthritis. *Arthritis Rheum.* 2012;64:2012-21.
39. Wallace CA, Giannini EH, Spalding SJ, et al. Clinically inactive disease in a cohort of children with new-onset polyarticular juvenile idiopathic arthritis treated with early aggressive therapy: time to achievement, total duration, and predictors. *J Rheumatol.* 2014;41:1163-70.
40. Ravelli A, Consolaro A, Horneff G, et al. Treating juvenile idiopathic arthritis to target: recommendations of an international task force. *Ann Rheum Dis.* 2018;77:819-28.
41. Hissink Muller P, Brinkman DMC, Schonenberg-Meinema D, et al. Treat to target (drug-free) inactive disease in DMARD-naive juvenile idiopathic arthritis: 24-month clinical outcomes of a three-armed randomised trial. *Ann Rheum Dis.* 2019;78:51-9.
42. Ramanan AV, Sage AM. Treat to Target (Drug-Free) Inactive Disease in JIA: To What Extent Is This Possible? *J Clin Med.* 2022;11.
43. Giancane G, Muratore V, Marzetti V, et al. Disease activity and damage in juvenile idiopathic arthritis: methotrexate era versus biologic era. *Arthritis Res Ther.* 2019;21:168.
44. Shoop-Worrall SJW, Kearsley-Fleet L, Thomson W, et al. How common is remission in juvenile idiopathic arthritis: A systematic review. *Semin Arthritis Rheum.* 2017;47:331-7.
45. Flatø B, Lien G, Smerdel A, et al. Prognostic factors in juvenile rheumatoid arthritis: a case-control study revealing early predictors and outcome after 14.9 years. *J Rheumatol.* 2003;30:386-93.
46. Ravelli A, Martini A. Early predictors of outcome in juvenile idiopathic arthritis. *Clin Exp Rheumatol.* 2003;21:S89-93.
47. Flatø B, Aasland A, Vinje O, et al. Outcome and predictive factors in juvenile rheumatoid arthritis and juvenile spondyloarthritis. *J Rheumatol.* 1998;25:366-75.
48. van Dijkhuizen EH, Wulffraat NM. Early predictors of prognosis in juvenile idiopathic arthritis: a systematic literature review. *Ann Rheum Dis.* 2015;74:1996-2005.
49. Rypdal V, Arnstad ED, Aalto K, et al. Predicting unfavorable long-term outcome in juvenile idiopathic arthritis: results from the Nordic cohort study. *Arthritis Res Ther.* 2018;20:91.
50. Gilliam BE, Chauhan AK, Low JM, et al. Measurement of biomarkers in juvenile idiopathic arthritis patients and their significant association with disease severity: a comparative study. *Clin Exp Rheumatol.* 2008;26:492-7.
51. Selvaag AM, Flatø B, Dale K, et al. Radiographic and clinical outcome in early juvenile rheumatoid arthritis and juvenile spondyloarthritis: a 3-year prospective study. *J Rheumatol.* 2006;33:1382-91.
52. Beukelman T, Patkar NM, Saag KG, et al. 2011 American College of Rheumatology recommendations for the treatment of juvenile idiopathic arthritis: initiation and safety monitoring of therapeutic agents for the treatment of arthritis and systemic features. *Arthritis Care Res (Hoboken).* 2011;63:465-82.
53. Al-Matar MJ, Petty RE, Tucker LB, et al. The early pattern of joint involvement predicts disease progression in children with oligoarticular (pauciarticular) juvenile rheumatoid arthritis. *Arthritis Rheum.* 2002;46:2708-15.
54. Magni-Manzoni S, Scirè CA, Ravelli A, et al. Ultrasound-detected synovial abnormalities are frequent in clinically inactive juvenile idiopathic arthritis, but do not predict a flare of synovitis. *Ann Rheum Dis.* 2013;72:223-8.
55. Miotto ESB, Mitraud SAV, Furtado RNV, et al. Patients with juvenile idiopathic arthritis in clinical remission with positive power Doppler signal in joint ultrasonography have an increased rate of clinical flare: a prospective study. *Pediatr Rheumatol Online J.* 2017;15:80.

56. De Lucia O, Ravagnani V, Pregolato F, et al. Baseline ultrasound examination as possible predictor of relapse in patients affected by juvenile idiopathic arthritis (JIA). *Ann Rheum Dis.* 2018;77:1426-31.
57. Ravelli A, Viola S, Ruperto N, et al. Correlation between conventional disease activity measures in juvenile chronic arthritis. *Ann Rheum Dis.* 1997;56:197-200.
58. Guzmán J, Burgos-Vargas R, Duarte-Salazar C, et al. Reliability of the articular examination in children with juvenile rheumatoid arthritis: interobserver agreement and sources of disagreement. *J Rheumatol.* 1995;22:2331-6.
59. Giannini EH, Ruperto N, Ravelli A, et al. Preliminary definition of improvement in juvenile arthritis. *Arthritis Rheum.* 1997;40:1202-9.
60. Brewer EJ, Jr., Bass J, Baum J, et al. Current proposed revision of JRA Criteria. JRA Criteria Subcommittee of the Diagnostic and Therapeutic Criteria Committee of the American Rheumatism Section of The Arthritis Foundation. *Arthritis Rheum.* 1977;20:195-9.
61. Cassidy JT, Levinson JE, Bass JC, et al. A study of classification criteria for a diagnosis of juvenile rheumatoid arthritis. *Arthritis Rheum.* 1986;29:274-81.
62. Printo_Rheumatologic exam 2013 [cited 2023 19. Oct]. Available from: https://www.printo.it/docs/PRINTO-PRCSG_rheuma_exam_VAS_0-100_mm.pdf.
63. Bazso A, Consolaro A, Ruperto N, et al. Development and testing of reduced joint counts in juvenile idiopathic arthritis. *J Rheumatol.* 2009;36:183-90.
64. Consolaro A, Ruperto N, Bazso A, et al. Development and validation of a composite disease activity score for juvenile idiopathic arthritis. *Arthritis Rheum.* 2009;61:658-66.
65. Nordal EB, Zak M, Aalto K, et al. Validity and predictive ability of the juvenile arthritis disease activity score based on CRP versus ESR in a Nordic population-based setting. *Ann Rheum Dis.* 2012;71:1122-7.
66. Nishimura K, Sugiyama D, Kogata Y, et al. Meta-analysis: diagnostic accuracy of anti-cyclic citrullinated peptide antibody and rheumatoid factor for rheumatoid arthritis. *Ann Intern Med.* 2007;146:797-808.
67. Avouac J, Gossec L, Dougados M. Diagnostic and predictive value of anti-cyclic citrullinated protein antibodies in rheumatoid arthritis: a systematic literature review. *Ann Rheum Dis.* 2006;65:845-51.
68. van Rossum M, van Soesbergen R, de Kort S, et al. Anti-cyclic citrullinated peptide (anti-CCP) antibodies in children with juvenile idiopathic arthritis. *J Rheumatol.* 2003;30:825-8.
69. Avcin T, Cimaz R, Falcini F, et al. Prevalence and clinical significance of anti-cyclic citrullinated peptide antibodies in juvenile idiopathic arthritis. *Ann Rheum Dis.* 2002;61:608-11.
70. Wang Y, Pei F, Wang X, et al. Meta-analysis: diagnostic accuracy of anti-cyclic citrullinated peptide antibody for juvenile idiopathic arthritis. *J Immunol Res.* 2015;2015:915276.
71. Singh G, Athreya BH, Fries JF, et al. Measurement of health status in children with juvenile rheumatoid arthritis. *Arthritis Rheum.* 1994;37:1761-9.
72. Flatø B, Sørskaar D, Vinje O, et al. Measuring disability in early juvenile rheumatoid arthritis: evaluation of a Norwegian version of the childhood Health Assessment Questionnaire. *J Rheumatol.* 1998;25:1851-8.
73. Consolaro A, Giancane G, Schiappapietra B, et al. Clinical outcome measures in juvenile idiopathic arthritis. *Pediatr Rheumatol Online J.* 2016;14:23.
74. McErlane F, Beresford MW, Baildam EM, et al. Validity of a three-variable Juvenile Arthritis Disease Activity Score in children with new-onset juvenile idiopathic arthritis. *Ann Rheum Dis.* 2013;72:1983-8.

75. Weiss PF, Colbert RA, Xiao R, et al. Development and retrospective validation of the juvenile spondyloarthritis disease activity index. *Arthritis Care Res (Hoboken)*. 2014;66:1775-82.
76. Trincianti C, Van Dijkhuizen EHP, Alongi A, et al. Definition and Validation of the American College of Rheumatology 2021 Juvenile Arthritis Disease Activity Score Cutoffs for Disease Activity States in Juvenile Idiopathic Arthritis. *Arthritis Rheumatol*. 2021;73:1966-75.
77. Consolaro A, Bracciolini G, Ruperto N, et al. Remission, minimal disease activity, and acceptable symptom state in juvenile idiopathic arthritis: defining criteria based on the juvenile arthritis disease activity score. *Arthritis Rheum*. 2012;64:2366-74.
78. Consolaro A, Ruperto N, Bracciolini G, et al. Defining criteria for high disease activity in juvenile idiopathic arthritis based on the juvenile arthritis disease activity score. *Ann Rheum Dis*. 2014;73:1380-3.
79. Sheybani EF, Khanna G, White AJ, et al. Imaging of juvenile idiopathic arthritis: a multimodality approach. *Radiographics*. 2013;33:1253-73.
80. Damasio MB, Malattia C, Martini A, et al. Synovial and inflammatory diseases in childhood: role of new imaging modalities in the assessment of patients with juvenile idiopathic arthritis. *Pediatr Radiol*. 2010;40:985-98.
81. van Rossum MA, Zwinderman AH, Boers M, et al. Radiologic features in juvenile idiopathic arthritis: a first step in the development of a standardized assessment method. *Arthritis Rheum*. 2003;48:507-15.
82. Collado Ramos P. Ultrasound imaging in juvenile idiopathic arthritis for the rheumatologist. *Clin Exp Rheumatol*. 2014;32:S34-41.
83. Laurell L, Court-Payen M, Nielsen S, et al. Ultrasonography and color Doppler in juvenile idiopathic arthritis: diagnosis and follow-up of ultrasound-guided steroid injection in the ankle region. A descriptive interventional study. *Pediatr Rheumatol Online J*. 2011;9:4.
84. Laurell L, Court-Payen M, Nielsen S, et al. Ultrasonography and color Doppler in juvenile idiopathic arthritis: diagnosis and follow-up of ultrasound-guided steroid injection in the wrist region. A descriptive interventional study. *Pediatr Rheumatol Online J*. 2012;10:11.
85. Young CM, Shiels WE, 2nd, Coley BD, et al. Ultrasound-guided corticosteroid injection therapy for juvenile idiopathic arthritis: 12-year care experience. *Pediatr Radiol*. 2012;42:1481-9.
86. Peters SE, Laxer RM, Connolly BL, et al. Ultrasound-guided steroid tendon sheath injections in juvenile idiopathic arthritis: a 10-year single-center retrospective study. *Pediatr Rheumatol Online J*. 2017;15:22.
87. Nielsen HE, Strandberg C, Andersen S, et al. Ultrasonographic examination in juvenile idiopathic arthritis is better than clinical examination for identification of intraarticular disease. *Dan Med J*. 2013;60:A4669.
88. Breton S, Jousse-Joulin S, Cangemi C, et al. Comparison of clinical and ultrasonographic evaluations for peripheral synovitis in juvenile idiopathic arthritis. *Semin Arthritis Rheum*. 2011;41:272-8.
89. Magni-Manzoni S, Epis O, Ravelli A, et al. Comparison of clinical versus ultrasound-determined synovitis in juvenile idiopathic arthritis. *Arthritis Rheum*. 2009;61:1497-504.
90. Filippou G, Cantarini L, Bertoldi I, et al. Ultrasonography vs. clinical examination in children with suspected arthritis. Does it make sense to use poliarticular ultrasonographic screening? *Clin Exp Rheumatol*. 2011;29:345-50.
91. Müller L, Kellenberger CJ, Cannizzaro E, et al. Early diagnosis of temporomandibular joint involvement in juvenile idiopathic arthritis: a pilot study comparing clinical examination and ultrasound to magnetic resonance imaging. *Rheumatology (Oxford)*. 2009;48:680-5.

92. Weiss PF, Arabshahi B, Johnson A, et al. High prevalence of temporomandibular joint arthritis at disease onset in children with juvenile idiopathic arthritis, as detected by magnetic resonance imaging but not by ultrasound. *Arthritis Rheum.* 2008;58:1189-96.
93. Lanni S, Martini A, Malattia C. Heading toward a modern imaging approach in juvenile idiopathic arthritis. *Curr Rheumatol Rep.* 2014;16:416.
94. Laurell L, Court-Payen M, Boesen M, et al. Imaging in juvenile idiopathic arthritis with a focus on ultrasonography. *Clin Exp Rheumatol.* 2013;31:135-48.
95. Malattia C, Tzaribachev N, van den Berg JM, et al. Juvenile idiopathic arthritis - the role of imaging from a rheumatologist's perspective. *Pediatr Radiol.* 2018;48:785-91.
96. Magni-Manzoni S. Ultrasound in juvenile idiopathic arthritis. *Pediatr Rheumatol Online J.* 2016;14:33.
97. Lanni S, Wood M, Ravelli A, et al. Towards a role of ultrasound in children with juvenile idiopathic arthritis. *Rheumatology (Oxford).* 2013;52:413-20.
98. Ording Muller LS, Humphries P, Rosendahl K. The joints in juvenile idiopathic arthritis. *Insights Imaging.* 2015;6:275-84.
99. Haavardsholm EA, Bøyesen P, Østergaard M, et al. Magnetic resonance imaging findings in 84 patients with early rheumatoid arthritis: bone marrow oedema predicts erosive progression. *Ann Rheum Dis.* 2008;67:794-800.
100. Bøyesen P, Haavardsholm EA, Ostergaard M, et al. MRI in early rheumatoid arthritis: synovitis and bone marrow oedema are independent predictors of subsequent radiographic progression. *Ann Rheum Dis.* 2011;70:428-33.
101. Hemke R, Kuijpers TW, Nusman CM, et al. Contrast-enhanced MRI features in the early diagnosis of Juvenile Idiopathic Arthritis. *Eur Radiol.* 2015;25:3222-9.
102. Müller LS, Avenarius D, Damasio B, et al. The paediatric wrist revisited: redefining MR findings in healthy children. *Ann Rheum Dis.* 2011;70:605-10.
103. Magni-Manzoni S, Malattia C, Lanni S, et al. Advances and challenges in imaging in juvenile idiopathic arthritis. *Nat Rev Rheumatol.* 2012;8:329-36.
104. Nusman CM, Hemke R, Lavini C, et al. Dynamic contrast-enhanced magnetic resonance imaging can play a role in predicting flare in juvenile idiopathic arthritis. *Eur J Radiol.* 2017;88:77-81.
105. Hemke R, van Rossum MA, van Veenendaal M, et al. Reliability and responsiveness of the Juvenile Arthritis MRI Scoring (JAMRIS) system for the knee. *Eur Radiol.* 2013;23:1075-83.
106. Hemke R, Kuijpers TW, van den Berg JM, et al. The diagnostic accuracy of unenhanced MRI in the assessment of joint abnormalities in juvenile idiopathic arthritis. *Eur Radiol.* 2013;23:1998-2004.
107. Guo BJ, Yang ZL, Zhang LJ. Gadolinium Deposition in Brain: Current Scientific Evidence and Future Perspectives. *Front Mol Neurosci.* 2018;11:335.
108. Davis JT, Kwatra N, Schooler GR. Pediatric whole-body MRI: A review of current imaging techniques and clinical applications. *J Magn Reson Imaging.* 2016;44:783-93.
109. Eutsler EP, Khanna G. Whole-body magnetic resonance imaging in children: technique and clinical applications. *Pediatr Radiol.* 2016;46:858-72.
110. Korchi AM, Hanquinet S, Anooshiravani M, et al. Whole-body magnetic resonance imaging: an essential tool for diagnosis and work up of non-oncological systemic diseases in children. *Minerva Pediatr.* 2014;66:169-76.
111. Dimitriou C, Boitsios G, Badot V, et al. Imaging of Juvenile Idiopathic Arthritis. *Radiol Clin North Am.* 2017;55:1071-83.
112. Aquino MR, Tse SM, Gupta S, et al. Whole-body MRI of juvenile spondyloarthritis: protocols and pictorial review of characteristic patterns. *Pediatr Radiol.* 2015;45:754-62.

113. Panwar J, Patel H, Tolend M, et al. Toward Developing a Semiquantitative Whole Body-MRI Scoring for Juvenile Idiopathic Arthritis: Critical Appraisal of the State of the Art, Challenges, and Opportunities. *Acad Radiol.* 2021;28:271-86.
114. Panwar J, Tolend M, Redd B, et al. Consensus-driven conceptual development of a standardized whole body-MRI scoring system for assessment of disease activity in juvenile idiopathic arthritis: MRI in JIA OMERACT working group. *Semin Arthritis Rheum.* 2021;51:1350-9.
115. McDonald DG, Leopold GR. Ultrasound B-scanning in the differentiation of Baker's cyst and thrombophlebitis. *Br J Radiol.* 1972;45:729-32.
116. Cooperberg PL, Tsang I, Truelove L, et al. Gray scale ultrasound in the evaluation of rheumatoid arthritis of the knee. *Radiology.* 1978;126:759-63.
117. Sureda D, Quiroga S, Arnal C, et al. Juvenile rheumatoid arthritis of the knee: evaluation with US. *Radiology.* 1994;190:403-6.
118. Lieu D. Ultrasound physics and instrumentation for pathologists. *Arch Pathol Lab Med.* 2010;134:1541-56.
119. Jacobson JA, van Holsbeeck MT. Musculoskeletal ultrasonography. *Orthop Clin North Am.* 1998;29:135-67.
120. Hangiandreou NJ. AAPM/RSNA physics tutorial for residents. Topics in US: B-mode US: basic concepts and new technology. *Radiographics.* 2003;23:1019-33.
121. Abu-Zidan FM, Hefny AF, Corr P. Clinical ultrasound physics. *J Emerg Trauma Shock.* 2011;4:501-3.
122. Bushberg JT, Seibert JA, Leidholdt JR. EM, et al. The essential physics of medical imaging. 2nd ed. Philadelphia: Lippincott Williams & Wilkins; 2002.
123. Aldrich JE. Basic physics of ultrasound imaging. *Crit Care Med.* 2007;35:S131-7.
124. Backhaus M, Burmester GR, Gerber T, et al. Guidelines for musculoskeletal ultrasound in rheumatology. *Ann Rheum Dis.* 2001;60:641-9.
125. Torp-Pedersen ST, Terslev L. Settings and artefacts relevant in colour/power Doppler ultrasound in rheumatology. *Ann Rheum Dis.* 2008;67:143-9.
126. Windschall D, Collado P, Vojinovic J, et al. Age-Related Vascularization and Ossification of Joints in Children: An International Pilot Study to Test Multiobserver Ultrasound Reliability. *Arthritis Care Res (Hoboken).* 2020;72:498-506.
127. Roth J, Jousse-Joulin S, Magni-Manzoni S, et al. Definitions for the sonographic features of joints in healthy children. *Arthritis Care Res (Hoboken).* 2015;67:136-42.
128. Spannow AH, Pfeiffer-Jensen M, Andersen NT, et al. Ultrasonographic measurements of joint cartilage thickness in healthy children: age- and sex-related standard reference values. *J Rheumatol.* 2010;37:2595-601.
129. Windschall D, Trauzeddel R, Haller M, et al. Pediatric musculoskeletal ultrasound: age- and sex-related normal B-mode findings of the knee. *Rheumatol Int.* 2016;36:1569-77.
130. Trauzeddel R, Lehman H, Trauzeddel RF, et al. Age dependent ultrasound B-mode findings of the elbow joint in healthy children and adolescents. *Rheumatol Int.* 2019;39:1007-18.
131. Collado P, Naredo E, Calvo C, et al. Assessment of the joint recesses and tendon sheaths in healthy children by high-resolution B-mode and power Doppler sonography. *Clin Exp Rheumatol.* 2007;25:915-21.
132. Collado P, Vojinovic J, Nieto JC, et al. Toward Standardized Musculoskeletal Ultrasound in Pediatric Rheumatology: Normal Age-Related Ultrasound Findings. *Arthritis Care Res (Hoboken).* 2016;68:348-56.
133. Collado P, Windschall D, Vojinovic J, et al. Amendment of the OMERACT ultrasound definitions of joints' features in healthy children when using the DOPPLER technique. *Pediatr Rheumatol Online J.* 2018;16:23.

134. Collado P, Jousse-Joulin S, Alcalde M, et al. Is ultrasound a validated imaging tool for the diagnosis and management of synovitis in juvenile idiopathic arthritis? A systematic literature review. *Arthritis Care Res (Hoboken)*. 2012;64:1011-9.
135. Roth J, Ravagnani V, Backhaus M, et al. Preliminary Definitions for the Sonographic Features of Synovitis in Children. *Arthritis Care Res (Hoboken)*. 2017;69:1217-23.
136. Ting TV, Vega-Fernandez P, Oberle EJ, et al. Novel Ultrasound Image Acquisition Protocol and Scoring System for the Pediatric Knee. *Arthritis Care Res (Hoboken)*. 2019;71:977-85.
137. Shanmugavel C, Sodhi KS, Sandhu MS, et al. Role of power Doppler sonography in evaluation of therapeutic response of the knee in juvenile rheumatoid arthritis. *Rheumatol Int*. 2008;28:573-8.
138. Collado P, Naredo E, Calvo C, et al. Reduced joint assessment vs comprehensive assessment for ultrasound detection of synovitis in juvenile idiopathic arthritis. *Rheumatology (Oxford)*. 2013;52:1477-84.
139. Haslam KE, McCann LJ, Wyatt S, et al. The detection of subclinical synovitis by ultrasound in oligoarticular juvenile idiopathic arthritis: a pilot study. *Rheumatology (Oxford)*. 2010;49:123-7.
140. Backhaus M, Ohrndorf S, Kellner H, et al. Evaluation of a novel 7-joint ultrasound score in daily rheumatologic practice: a pilot project. *Arthritis Rheum*. 2009;61:1194-201.
141. Naredo E, Rodríguez M, Campos C, et al. Validity, reproducibility, and responsiveness of a twelve-joint simplified power doppler ultrasonographic assessment of joint inflammation in rheumatoid arthritis. *Arthritis Rheum*. 2008;59:515-22.
142. Hammer HB, Bolton-King P, Bakkeheim V, et al. Examination of intra and interrater reliability with a new ultrasonographic reference atlas for scoring of synovitis in patients with rheumatoid arthritis. *Ann Rheum Dis*. 2011;70:1995-8.
143. D'Agostino MA, Terslev L, Aegerter P, et al. Scoring ultrasound synovitis in rheumatoid arthritis: a EULAR-OMERACT ultrasound taskforce-Part 1: definition and development of a standardised, consensus-based scoring system. *RMD Open*. 2017;3:e000428.
144. Terslev L, Naredo E, Aegerter P, et al. Scoring ultrasound synovitis in rheumatoid arthritis: a EULAR-OMERACT ultrasound taskforce-Part 2: reliability and application to multiple joints of a standardised consensus-based scoring system. *RMD Open*. 2017;3:e000427.
145. Hallgren KA. Computing Inter-Rater Reliability for Observational Data: An Overview and Tutorial. *Tutor Quant Methods Psychol*. 2012;8:23-34.
146. Koo TK, Li MY. A Guideline of Selecting and Reporting Intraclass Correlation Coefficients for Reliability Research. *J Chiropr Med*. 2016;15:155-63.
147. Landis JR, Koch GG. The measurement of observer agreement for categorical data. *Biometrics*. 1977;33:159-74.
148. Hammer HB, Michelsen B, Sexton J, et al. Swollen, but not tender joints, are independently associated with ultrasound synovitis: results from a longitudinal observational study of patients with established rheumatoid arthritis. *Ann Rheum Dis*. 2019;78:1179-85.
149. Vega-Fernandez P, Ting TV, Oberle EJ, et al. Musculoskeletal Ultrasound in Childhood Arthritis Limited Examination: A Comprehensive, Reliable, Time-Efficient Assessment of Synovitis. *Arthritis Care Res (Hoboken)*. 2021.
150. World Medical Association Declaration of Helsinki: ethical principles for medical research involving human subjects. *Jama*. 2013;310:2191-4.
151. Lovdata. 2001. Lov om pasient- og brukerrettigheter (pasient- og brukerrettighetsloven). Kapittel 4. [updated 1. July 2023; cited 2023 17. Oct]. Available from: https://lovdata.no/dokument/NL/lov/1999-07-02-63/KAPITTEL_4#KAPITTEL_4.

152. Lovdata. 2009. Lov om medisinsk og helsefaglig forskning (helseforskningsloven). Kapittel 4. [updated 2. July 2021; cited 2023 17. Oct]. Available from: https://lovdata.no/dokument/NL/lov/2008-06-20-44/KAPITTEL_4#KAPITTEL_4.
153. Rothman KJ. Epidemiology - An Introduction. 2nd ed. Oxford: Oxford University Press; 2012.
154. Ventura-Rios L, Faugier E, Barzola L, et al. Reliability of ultrasonography to detect inflammatory lesions and structural damage in juvenile idiopathic arthritis. *Pediatr Rheumatol Online J*. 2018;16:58.
155. Eich GF, Hallé F, Hodler J, et al. Juvenile chronic arthritis: imaging of the knees and hips before and after intraarticular steroid injection. *Pediatr Radiol*. 1994;24:558-63.
156. Karmazyn B, Bowyer SL, Schmidt KM, et al. US findings of metacarpophalangeal joints in children with idiopathic juvenile arthritis. *Pediatr Radiol*. 2007;37:475-82.
157. Laurell L, Court-Payen M, Nielsen S, et al. Comparison of ultrasonography with Doppler and MRI for assessment of disease activity in juvenile idiopathic arthritis: a pilot study. *Pediatr Rheumatol Online J*. 2012;10:23.
158. Rebollo-Polo M, Koujok K, Weisser C, et al. Ultrasound findings on patients with juvenile idiopathic arthritis in clinical remission. *Arthritis Care Res (Hoboken)*. 2011;63:1013-9.
159. Rosendahl K, Bruserud IS, Oehme N, et al. Normative ultrasound references for the paediatric wrist; dorsal soft tissues. *RMD Open*. 2018;4:e000642.
160. Ellegaard K, Torp-Pedersen S, Henriksen M, et al. Influence of recent exercise and skin temperature on ultrasound Doppler measurements in patients with rheumatoid arthritis--an intervention study. *Rheumatology (Oxford)*. 2009;48:1520-3.
161. Torp-Pedersen S, Christensen R, Szkudlarek M, et al. Power and color Doppler ultrasound settings for inflammatory flow: impact on scoring of disease activity in patients with rheumatoid arthritis. *Arthritis Rheumatol*. 2015;67:386-95.
162. Consolaro A, Negro G, Lanni S, et al. Toward a treat-to-target approach in the management of juvenile idiopathic arthritis. *Clin Exp Rheumatol*. 2012;30:S157-62.
163. Stinson JN, Kavanagh T, Yamada J, et al. Systematic review of the psychometric properties, interpretability and feasibility of self-report pain intensity measures for use in clinical trials in children and adolescents. *Pain*. 2006;125:143-57.
164. Malattia C, Tolend M, Mazzoni M, et al. Current status of MR imaging of juvenile idiopathic arthritis. *Best Pract Res Clin Rheumatol*. 2020;34:101629.
165. Rigby AS. Statistical methods in epidemiology. v. Towards an understanding of the kappa coefficient. *Disabil Rehabil*. 2000;22:339-44.
166. Cohen J. Weighted kappa: nominal scale agreement with provision for scaled disagreement or partial credit. *Psychol Bull*. 1968;70:213-20.
167. Gisev N, Bell JS, Chen TF. Interrater agreement and interrater reliability: key concepts, approaches, and applications. *Res Social Adm Pharm*. 2013;9:330-8.
168. Twisk JWR. Applied multilevel analysis. Cambridge: Cambridge University Press; 2006.
169. Boers M, Brooks P, Strand CV, et al. The OMERACT filter for Outcome Measures in Rheumatology. *J Rheumatol*. 1998;25:198-9.
170. Boers M, Kirwan JR, Wells G, et al. Developing core outcome measurement sets for clinical trials: OMERACT filter 2.0. *J Clin Epidemiol*. 2014;67:745-53.
171. Mukaka MM. Statistics corner: A guide to appropriate use of correlation coefficient in medical research. *Malawi Med J*. 2012;24:69-71.
172. Schober P, Boer C, Schwarte LA. Correlation Coefficients: Appropriate Use and Interpretation. *Anesth Analg*. 2018;126:1763-8.

173. Parikh R, Mathai A, Parikh S, et al. Understanding and using sensitivity, specificity and predictive values. *Indian J Ophthalmol*. 2008;56:45-50.
174. Monaghan TF, Rahman SN, Agudelo CW, et al. Foundational Statistical Principles in Medical Research: Sensitivity, Specificity, Positive Predictive Value, and Negative Predictive Value. *Medicina (Kaunas)*. 2021;57.
175. Barrett D, Heale R. What are Delphi studies? *Evid Based Nurs*. 2020;23:68-9.
176. Vojinovic J, Magni-Manzoni S, Collado P, et al. SAT0636 Ultrasonography definitions for synovitis grading in children: the omeract pediatric ultrasound task force. *Ann Rheum Dis*. 2017;76:1015.
177. Rossi-Semerano L, Breton S, Semerano L, et al. Application of the OMERACT synovitis ultrasound scoring system in juvenile idiopathic arthritis: a multicenter reliability exercise. *Rheumatology (Oxford)*. 2020.
178. Collado P, Martire MV, Lanni S, et al. OMERACT International Consensus for Ultrasound Definitions of Tenosynovitis in Juvenile Idiopathic Arthritis: Systematic Literature Review and Delphi Process. *Arthritis Care Res (Hoboken)*. 2023;75:2277-84.
179. Vega-Fernandez P, De Ranieri D, Oberle E, et al. Comprehensive and reliable sonographic assessment and scoring system for inflammatory lesions of the pediatric ankle. *Rheumatology (Oxford)*. 2022.
180. Vega-Fernandez P, Esteban Y, Oberle E, et al. Reliability of the Pediatric Specific Musculoskeletal Ultrasound Scoring Systems for the Elbow, Wrist, and Finger Joints. *J Rheumatol*. 2022.
181. Bruyn GAW, Siddle HJ, Hanova P, et al. Ultrasound of Subtalar Joint Synovitis in Patients with Rheumatoid Arthritis: Results of an OMERACT Reliability Exercise Using Consensual Definitions. *J Rheumatol*. 2019;46:351-9.
182. Haavardsholm EA, Ostergaard M, Ejbjerg BJ, et al. Reliability and sensitivity to change of the OMERACT rheumatoid arthritis magnetic resonance imaging score in a multireader, longitudinal setting. *Arthritis Rheum*. 2005;52:3860-7.
183. Vega-Fernandez P, Oberle EJ, Henrickson M, et al. Musculoskeletal Ultrasound and the Assessment of Disease Activity in Juvenile Idiopathic Arthritis. *Arthritis Care Res (Hoboken)*. 2023;75:1815-20.
184. Taylor J, Giannini EH, Lovell DJ, et al. Lack of Concordance in Interrater Scoring of the Provider's Global Assessment of Children With Juvenile Idiopathic Arthritis With Low Disease Activity. *Arthritis Care Res (Hoboken)*. 2018;70:162-6.
185. Backström M, Tarkiainen M, Gottlieb BS, et al. Paediatric rheumatologists do not score the physician's global assessment of juvenile idiopathic arthritis disease activity in the same way. *Rheumatology (Oxford)*. 2023;62:3421-6.
186. Consolaro A, Vitale R, Pistorio A, et al. Physicians' and parents' ratings of inactive disease are frequently discordant in juvenile idiopathic arthritis. *J Rheumatol*. 2007;34:1773-6.
187. Palmisani E, Solari N, Magni-Manzoni S, et al. Correlation between juvenile idiopathic arthritis activity and damage measures in early, advanced, and longstanding disease. *Arthritis Rheum*. 2006;55:843-9.
188. Sztajn bok F, Coronel-Martinez DL, Diaz-Maldonado A, et al. Discordance between physician's and parent's global assessments in juvenile idiopathic arthritis. *Rheumatology (Oxford)*. 2007;46:141-5.
189. Lanni S, Bovis F, Ravelli A, et al. Delineating the Application of Ultrasound in Detecting Synovial Abnormalities of the Subtalar Joint in Juvenile Idiopathic Arthritis. *Arthritis Care Res (Hoboken)*. 2016;68:1346-53.
190. Remedios D, Martin K, Kaplan G, et al. Juvenile chronic arthritis: diagnosis and management of tibio-talar and sub-talar disease. *Br J Rheumatol*. 1997;36:1214-7.

191. Lanni S, Marafon DP, Civino A, et al. Comparison Between Clinical and Ultrasound Assessment of the Ankle Region in Children With Juvenile Idiopathic Arthritis. *Arthritis Care Res (Hoboken)*. 2021;73:1180-6.
192. Hemke R, Herregods N, Jaremko JL, et al. Imaging assessment of children presenting with suspected or known juvenile idiopathic arthritis: ESSR-ESPR points to consider. *Eur Radiol*. 2020;30:5237-49.
193. Magni-Manzoni S, Muratore V, Vojinović J, et al. Procedures for the content, conduct and format of EULAR/PReS paediatric musculoskeletal ultrasound courses. *RMD Open*. 2022;8.

9. Papers I-III

ORIGINAL RESEARCH

Development and reliability of a novel ultrasonographic joint-specific scoring system for synovitis with reference atlas for patients with juvenile idiopathic arthritis

Nina Krafft Sande ¹, Pernille Bøyesen ¹, Anna-Birgitte Aga,¹
Hilde Berner Hammer ^{2,3}, Berit Flatø,^{1,3} Johannes Roth,⁴ Vibke Lilleby¹

To cite: Sande NK, Bøyesen P, Aga A-B, *et al.* Development and reliability of a novel ultrasonographic joint-specific scoring system for synovitis with reference atlas for patients with juvenile idiopathic arthritis. *RMD Open* 2021;7:e001581. doi:10.1136/rmdopen-2021-001581

► Additional supplemental material is published online only. To view, please visit the journal online (<http://dx.doi.org/10.1136/rmdopen-2021-001581>).

Received 12 January 2021
Revised 3 March 2021
Accepted 2 April 2021



© Author(s) (or their employer(s)) 2021. Re-use permitted under CC BY-NC. No commercial re-use. See rights and permissions. Published by BMJ.

For numbered affiliations see end of article.

Correspondence to
Dr Nina Krafft Sande;
ninamkrafft@hotmail.com

ABSTRACT

Objective To develop an ultrasonographic image acquisition protocol and a joint-specific scoring system for synovitis with reference atlas in patients with juvenile idiopathic arthritis (JIA) and to assess the reliability of the system.

Methods Seven rheumatologists with extensive ultrasound experience developed a scanning protocol and a semiquantitative joint-specific scoring system for B-mode (BM) synovitis for the elbow, wrist, metacarpophalangeal 2–3, proximal interphalangeal 2–3, hip, knee, ankle and metatarsophalangeal 2–3 joints. An ultrasonographic reference atlas for BM synovitis, divided in four age groups (2–4, 5–8, 9–12, 13–18 years), and power Doppler (PD) activity was then developed. Reliability was assessed for all joints on still images and in a live exercise including 10 patients with JIA, calculated by intraclass correlation coefficient (ICC) and weighted kappa.

Results A scanning protocol and scoring system for multiple joints with reference atlas composed of images with four different score levels for BM and PD were developed. Still image scoring for BM synovitis on joint level showed good to excellent intra-reader reliability (ICC/kappa ranges: 0.75–0.95/0.63–0.91) and moderate to excellent inter-reader reliability (ICC/kappa ranges: 0.89–0.99/0.50–0.91). Still image scoring for PD activity showed excellent intra-reader and inter-reader reliability (ICC/kappa: 0.96/0.91 and ICC/kappa: 0.97/0.80, respectively). In the live scoring, inter-reader reliability (ICC/kappa) was moderate to excellent for BM synovitis (0.94/0.51) and PD activity (0.91/0.60).

Conclusion An ultrasonographic image acquisition protocol and joint-specific scoring system with reference atlas were developed and demonstrated moderate to excellent reliability for scoring of synovitis in patients with JIA. This can be a valuable tool in clinical practice and future research.

INTRODUCTION

Persistent joint inflammation is the hallmark feature in juvenile idiopathic arthritis

Key messages

What is already known about this subject?

► Ultrasound is an important tool in the evaluation of joint inflammation but can be difficult to interpret in children.

What does this study add?

► A novel, reliable joint-specific scoring system for synovitis with reference atlas for frequently affected joints in JIA was developed.

How might this impact on clinical practice or further developments?

► The combination of a defined joint-specific scoring system with reference atlas for assessing synovitis may introduce an intuitive and feasible implementation of ultrasound in patients with JIA.

(JIA).¹ If not properly reversed by treatment this inflammation can ultimately destroy the joints, explaining why JIA used to be one of the most disabling childhood diseases.¹ Over the last 20 years the development of new effective drugs has improved the outcome of JIA and reduced the burden of disease for the afflicted children.^{2,3} Still, less than half of these patients achieve sustained inactive disease.⁴

The challenge of achieving inactive disease in JIA relates closely to the challenge of monitoring disease activity to detect persistent joint inflammation, and step up therapy when required. Symptoms and clinical signs of joint inflammation can be difficult to assess and interpret in children due to vague complaints and clinically challenging anatomical regions.^{5,6} This emphasises the need for sensitive measures of joint inflammation to assess disease activity and treatment response.⁷

Ultrasound is an important tool in the evaluation of joint inflammation and provides a unique possibility for systematically assessing all joints in one single bedside examination.^{8,9} Ultrasound is well suited for use in children, is relatively cheap and feasible, and does not require sedation or exposure to ionising radiation. However, ultrasound interpretation in children requires thorough knowledge of the age-dependent variability in the maturing skeleton.^{8,10-12} The Outcome Measures in Rheumatology (OMERACT) ultrasound paediatric group has started the process of standardising ultrasound assessments in children. The group has developed definitions of sonographic features of joints and descriptions of scanning approaches for the knee, ankle, wrist and second metacarpophalangeal (MCP) joints in healthy children, and preliminary ultrasound definitions of synovitis.^{11,13,14} However, an ultrasonographic scoring system has so far not been published by OMERACT. The use of an ultrasonographic atlas as reference for scoring of synovitis in patients with rheumatoid arthritis has shown high reliability,¹⁵ but cannot be directly applied to children due to their distinctive anatomy during growth. To our knowledge, two scoring systems in JIA exist.^{16,17} One, the scoring system of paediatric synovitis (PedSynS), proposes a single standard scoring system but does not clearly apply to all joints.¹⁶ The second offers joint-specific scoring for the knee but cannot be applied to other joints.¹⁷ The two scoring systems have made important contributions to standardise the use of ultrasound in patients with JIA. However, they do not fully encompass the heterogeneous joint distribution in these patients. In an effort to further broaden the application and feasibility of musculoskeletal ultrasound in JIA, we wanted to examine if a joint-specific approach and an ultrasonographic reference atlas for patients with JIA could improve the feasibility of ultrasound examination and scoring of synovitis in these patients.

The objectives of this study were to develop an ultrasonographic image acquisition protocol and a semiquantitative joint-specific scoring system with an age-divided reference atlas for scoring of synovitis in patients with JIA, and to assess the reliability of the scoring system.

METHODS

The study was performed at Oslo University Hospital (OUH) at the Department of Rheumatology from January 2018 to October 2020 and conducted through the following six steps: Development of an ultrasonographic image acquisition protocol and still image collection (step 1 and 2), development of a semiquantitative joint-specific scoring system with reference atlas (step 3 and 4), reliability testing of the scoring system with reference atlas including a still image scoring (step 5) and a live exercise (step 6), (flowchart in online supplemental figure 1).

Development of an image acquisition protocol

In the first step, one adult and six paediatric rheumatologists with extensive experience in musculoskeletal

ultrasound (5–20 years) developed an image acquisition protocol for frequently affected joints in JIA (anterior elbow, posterior elbow, radiocarpal, midcarpal, MCP2–3 (dorsal), proximal interphalangeal (PIP) 2–3 (dorsal and volar), hip, knee (suprapatellar recess and lateral parapatellar recess), tibiotalar, talonavicular, anterior subtalar, posterior subtalar and metatarsophalangeal (MTP) 2–3 (dorsal)). Different views for some joints were chosen to provide additional information when scoring synovitis, i.e. the anterior and posterior elbow were considered to be recesses of the same joint. The protocol was built on established scanning approaches.^{13,15,17,18} However, since only a few scanning procedures have previously been described for children,^{13,17} the image acquisition protocol was adjusted and further specified to be applicable for paediatric joints through a consensus process driven by literature review, discussions and face-to-face meetings including two live exercises where seven patients with JIA (ages 3–16 years), who volunteered to participate, were assessed. The first session was held in May 2018 (NKS, A-BA, HBH, VL), the second in June 2018 (NKS, A-BA, HBH, BF, JR, VL). General aspects like defining important anatomical landmarks and the optimal position of the patient to acquire a good image were discussed. Joint-specific landmarks were included as part of the image acquisition protocol to ensure a standardised scanning position. For the wrist, the validated scanning procedure by Collado *et al* was applied.¹³ For the knee, the scanning procedure published by Ting *et al* was used.¹⁷ For the remaining joints, the image acquisition protocol including landmarks was developed through the consensus process described above. Finally, a protocol with specific instructions for each joint was developed and full consensus among the rheumatologists was reached.

Collection of still images

In the second step, ultrasonographic images of joints with different degrees of pathology were collected from the inpatient and outpatient rheumatology clinics at OUH according to the predefined image acquisitions. The images were collected during routine ultrasound examination as part of daily clinical practice. Two GE Logiq S8 ultrasound machines with linear probes (6–15 MHz) and hockey sticks (8–18 MHz) were used to acquire and collect the images. Approximately 5000 images were obtained and categorised jointwise in four age groups according to age-related changes; 2–4, 5–8, 9–12, 13–18 years.¹³ The images served as a database for the third step.

Development of an ultrasonographic scoring system and reference atlas

In the third step, the rheumatologists performed a literature review and discussed important aspects related to synovitis in different joints in patients with JIA. They also reviewed ultrasonographic images (obtained from the database of 5000 images) with different degrees of B-mode (BM) synovitis. They decided for a joint-specific scoring

system because a single standard system did not clearly apply to all joints. A semiquantitative scoring system (0–3) was chosen in accordance with what has previously been done.^{16 17 19} Sonographic features of synovitis were defined according to the OMERACT ultrasound group.¹⁴ Based on this, the rheumatologists proposed scores for different grades and joints and discussed the suggestions on teleconferences, mail correspondence and face-to-face meetings. The nomenclature ‘mild, moderate and severe’ was included in the joint-specific scoring system to further elaborate the severity of the findings. Through this dynamic process a preliminary four-point semiquantitative joint-specific scoring system for BM synovitis, ranging from grade 0 (normal) to grade 3 (severe) for each joint was developed and full consensus reached among the rheumatologists. The scoring system for the knee was built on a newly published system that displayed good reliability, and was in accordance with our aim of developing a joint-specific scoring system.¹⁷

Scoring of Doppler activity was applied to Doppler signals detected within synovial hypertrophy (BM score >grade 0), harmonising with the joint-specific scoring system for BM synovitis, and in accordance with the definitions developed by the OMERACT ultrasound group where Doppler signals must be detected within synovial hypertrophy to be considered as a sign of synovitis.¹⁴ The scoring system for Doppler activity followed Ting *et al.*¹⁷ Power Doppler (PD) was chosen instead of colour Doppler because the participating rheumatologists used PD in their daily clinical practice and had more experience with this method.

In the fourth step, NKS selected BM images from the collection of 5000 images in the database that best corresponded to the scoring system for each joint in the four age ranges to establish an age-divided reference atlas for scoring of BM synovitis. All selected images were reviewed and approved by the research group. The reference atlas was finally composed of 224 characteristic BM images (14 joint regions with four different score levels in four age-groups). Representative PD images were selected by NKS from the database of 5000 images without accounting for an equal distribution of images from all age groups to develop a reference atlas for scoring of PD activity. Eventually, the reference atlas consisted of 51 distinctive PD images (13 joint regions (the hip was not included as PD signals are rarely found in this joint) with four different score levels). Due to missing images for some grades in our database, two BM and seven PD images were added to the atlas by JR working at a collaborating centre using GE Logiq E9 ultrasound machines with linear probes (6–15 MHz) or hockey sticks (8–18 MHz).

During a meeting in October 2019 the feasibility and face validity of the system with reference atlas were tested by four rheumatologists (NKS, PB, VL, JR) in a scoring exercise consisting of 69 ultrasonographic still images of joints with different degrees of pathology from patients with JIA (ages 2–18 years). The images were randomly selected by NKS from the database of 5000 images.

Then a live exercise performing ultrasound of the joints included in the image acquisition protocol was done bilaterally in four patients with JIA (ages 2–15 years). The assessors were blinded to each other’s scoring and clinical information, but the patient’s age was known. The images were scored individually according to the system and saved for a following discussion concerning the scoring of the images obtained. Feasibility was assessed by the time spent performing the ultrasound examination and scoring of pathology defined to be within 30 min, and the tolerance of the examined children.

The definitions and scores were thoroughly discussed during the still image scoring and live scoring exercises. The main sources of initial disagreement concerned the development of suitable scores for the subtalar, wrist and finger joints, where the distribution of synovial hypertrophy/effusion was discussed in detail. The rheumatologists agreed on the use of percentages to differentiate grades in some joints and that the terms ‘without overall convex shape’ and ‘clearly convex shape’ could distinguish between grades 2 and 3 in the MCP, PIP and MTP joints. They also found that scoring of the knee joint (suprapatellar recess) in the youngest children could underestimate the degree of pathology due to their relatively shorter femur and made adjustments in the protocol. In case of disagreement, ultrasonographic images were reviewed and scoring feasibility discussed to reach harmonisation of the scoring definitions. During these exercises the system was adjusted, and the reference atlas improved accordingly by including images that satisfied the criteria to the scoring system. Finally, 100% consensus was reached among the rheumatologists for the scoring system and atlas.

Reliability testing of the scoring system with reference atlas on still images

The fifth step was conducted in December 2019/January 2020 where the same group (NKS, PB, VL, JR) performed an intra-reader and inter-reader reliability study. From the database of 5000 images, NKS selected 370 ultrasonographic still images of joints with different degrees of BM synovitis from patients with JIA (ages 2–18 years), consisting of at least 20 images from each joint included in the scoring system for BM synovitis. The number of images per age varied for each joint, but every joint had images from all four age groups. The images were scored jointwise with the novel scoring system and atlas for BM synovitis as reference. The rheumatologists were blinded to each other’s scoring and clinical information. The images were rearranged for a second round of scoring that was done at least 2 weeks later. To assess reliability of the scoring system and atlas for PD activity, three rheumatologists (NKS, PB, VL) scored 37 ultrasonographic still images of joints with different degrees of PD activity selected by NKS from the database of 5000 images. After 3 weeks, the images were rearranged, and a second PD scoring was performed.

Reliability testing of the scoring system with reference atlas in a live exercise

The sixth step was a live scoring exercise including 10 consecutive patients fulfilling the International League of Associations for Rheumatology (ILAR) criteria for JIA,²⁰ attending the paediatric rheumatology clinic at OUH in the period September/October 2020. Signed informed consent was obtained by patients and/or parents. Each patient was assessed bilaterally by three rheumatologists (NKS, PB, VL) within 1–2 days, performing ultrasound of the joints included in the image acquisition protocol using a GE Logiq S8 machine with linear probe (6–15 MHz) and standardised settings for BM and PD (pulse repetition frequency 0.6 kHz, frequency 7.7 MHz and low wall filter). The rheumatologists were blinded to each other's scoring and clinical information and had digital and printed versions of the scoring system and atlas available during the examinations. The assessed joints were used to derive separate BM synovitis and PD activity sum scores. For the joints assessed from two views, one view was selected to avoid increased weighting of these joints. The ultrasound sum score included the anterior elbow, radiocarpal, midcarpal, MCP2–3 dorsal, PIP2–3 volar, hip, knee (suprapatellar recess), tibiotalar, talonavicular, anterior subtalar and MTP2–3 dorsal joints.

Patient and public involvement

Patients have not actively participated in the planning of this study. However, the patients included in the study and the Norwegian Rheumatism Association have endorsed the project and voiced that this is of true interest to the patient community, especially concerning the national and international disparity in the use of ultrasound. Study results will be disseminated to patients and the public through the patient organisation's website and newsletter.

Statistics

Descriptive statistics were calculated as mean (range) and median (range), as appropriate. Reliability testing in the still image exercise was performed on a joint level for BM scoring, and on all joints included in the scoring exercise combined for PD scoring. In the live exercise, separate ultrasound sum scores for BM synovitis and PD activity were calculated and used for reliability testing. Reliability was calculated by intraclass correlation coefficient (ICC, absolute-agreement, two-way mixed-effects model) and weighted kappa with linear weights.²¹ Intra-reader reliability was calculated as single measure (sm) ICC and Cohen's weighted kappa, reported as mean (SD) between readers. Inter-reader reliability was calculated as average measure (avm) ICC, with 95% CI and Light's weighted kappa (SD). ICC and kappa values 0.2–0.4 were considered fair, 0.41–0.6 moderate, 0.61–0.8 good and >0.81 excellent. Analyses were performed using SPSS V.27.

RESULTS

An ultrasonographic image acquisition protocol for frequently affected joints in JIA was first established (table 1). A semiquantitative joint-specific scoring system (table 2) with an age-divided reference atlas for scoring of BM synovitis and a reference atlas for scoring of PD activity in patients with JIA was then developed. The atlas is shown with example illustrations in figure 1A–D and figure 2. For the full scoring system and atlas see online supplementary file. Feasibility assessment showed that the time spent on the ultrasound examination and scoring of pathology was attainable within 30 min and was well tolerated by the participants.

Reliability for BM synovitis scoring on still images

Intra-reader reliability for BM synovitis scoring on still images on a joint level was good to excellent (smICC range 0.75–0.95 and weighted kappa range 0.63–0.91). Inter-reader reliability for BM synovitis scoring on still images, assessed by avmICC (range) for each joint was excellent (0.89–0.99) and weighted kappa (range) was moderate to excellent (0.50–0.91). Jointwise results for the BM synovitis still image scoring are presented in table 3.

Reliability for PD activity scoring on still images

Intra-reader reliability for PD activity scoring on still images from all joints included in the scoring exercise combined was excellent (smICC (SD) 0.96 (0.03) and weighted kappa (SD) 0.91 (0.06)). Inter-reader reliability for PD activity scoring on still images from all joints included in the scoring exercise combined, was good to excellent (avmICC (95% CI) 0.97 (0.94 to 0.98) and weighted kappa (SD) 0.80 (0.06)).

Reliability for BM synovitis and PD activity scoring in live exercise

Ten patients, seven girls and three boys were included in the live scoring exercise with a median age (range) 7.5 years (3–10 years). Seven patients had oligoarthritis (70%), three patients had rheumatoid factor-negative polyarthritis (30%). Median disease duration (range) was 10 months (0–65 months). Five patients were treated with methotrexate, one with etanercept, one with nonsteroidal anti-inflammatory drug (NSAID)s and three patients were without systemic treatment. The number of patients assessed in each age group was two in group 1 (ages 2–4 years), five in group 2 (ages 5–8 years) and three in group 3 (ages 9–12 years). Ultrasound findings of a BM synovitis score ≥ 1 were present in 29 of 280 joint regions (10.4%) and a PD activity score ≥ 1 in 13 of the 29 joints with BM synovitis (44.8%). The most frequently affected joints (number) were the knee (9), anterior elbow (5) and anterior subtalar (3) for BM synovitis, and the radiocarpal (4) and knee (3) for PD activity. Mean (range) ultrasound sum scores for BM synovitis and PD activity were 7.5 (5.8–9.6) and 2.2 (1.8–2.9), respectively. Inter-reader reliability (avmICC (95% CI)) for BM synovitis

Table 1 Ultrasonographic image acquisition protocol for frequently affected joints in juvenile idiopathic arthritis

Regions	Image acquisition protocol
General remarks	The scanning will be done bilaterally. The left side of the screen is proximal, the right side distal. The probe will be moved across the joint for the specified scans. Scoring of BM and PD should be done at the area of the maximal distension of the synovial recess and the maximum amount of PD while keeping the bony landmarks clearly in view. PD will only be done when the BM score is 1 or more. The Doppler box should be placed to cover the entire joint and extend to the top of the image to be aware of reverberation artefacts.
Anterior elbow	The subject will be in a supine position, but the scanning can also be done with the subject on the parents' lap. The elbow should be in full extension and supination of the lower arm for a longitudinal anterior scan of the elbow (humeroradial) joint. Landmarks: (1) The distal humerus and (2) The radius
Posterior elbow	The subject will be in a supine position, but the scanning can also be done with the subject on the parents' lap. The elbow should be flexed at 90 degrees with the forearm resting on the stomach. A longitudinal posterior scan of the elbow (humeroulnar) joint. Landmarks: (1) The distal humerus and (2) The olecranon (ulna)
Radiocarpal and midcarpal	The subject will be in a sitting position, the hands palm-side down in a neutral position on an examination table and resting the elbow on the table. A longitudinal dorsal scan of the radiocarpal and midcarpal joints at the sagittal midline of the wrist, including the distal radius, the lunate and the capitate bone. Landmarks: (1) The distal end of diaphysis and epiphysial cartilage of radius and (2) The dorsal recess of the radiocarpal and midcarpal joints and over them (3) A compartment of the extensor tendons according to the area imaged ¹³
MCP2–3, dorsal	The subject will be in a sitting position with the hands palm-side down in a neutral position on an examination table. A longitudinal dorsal scan of the MCP2 and MCP3 joints. Landmarks: (1) The head of metacarpal bone (2/3 of the image) and (2) The base of proximal phalanx (1/3 of the image)
PIP2–3, dorsal	The subject will be in a sitting position with the hands palm-side down in a neutral position on an examination table. A longitudinal dorsal scan of the PIP2 and PIP3 joints. Landmarks: (1) The head of proximal phalanx (2/3 of the image) and (2) The base of middle phalanx (1/3 of the image)
PIP2–3, volar	The subject will be in a sitting position with the hands palm-side up in a neutral position on an examination table. A longitudinal volar scan of the PIP2 and PIP3 joints. Landmarks: (1) The head of the proximal phalanx, (2) The base of the middle phalanx and (3) The flexor tendon
Hip	The subject will be in a supine position with the hip in a neutral position, slightly externally rotated. A longitudinal anterior scan parallel to the femoral neck of the hip joint. Landmarks: (1) The femoral head and (2) The femoral neck.
Knee, suprapatellar recess	The subject will be in a supine position. The knee should be flexed at 30 degrees, and images taken after the subject completes flexion and extension three times. A longitudinal scan of the suprapatellar joint space. For the youngest subjects the patella should fill 1/3 of the image to compensate for the relatively shorter femur (to not underestimate the scoring). Landmarks: (1) The proximal third of the patella and (2) A clearly visualised quadriceps tendon ¹⁷
Knee, lateral parapatellar recess	The subject will be in a supine position. The knee should be flexed at 30 degrees. For the lateral parapatellar recess the image will be obtained with the probe in transverse position over the mid-patella with both the patella and femur in view. Landmarks: (1) The superior edge of the patella and (2) The femoral condyle ¹⁷
Tibiotalar	The subject will be in a supine position with the knee at 90 degrees flexion and the foot sole-side down. A longitudinal scan of the tibiotalar joint. Landmarks: (1) The distal end of the tibia and (2) The talus
Talonavicular	The subject will be in a supine position with the knee at 90 degrees flexion and the foot sole-side down. A longitudinal scan of the talonavicular joint. Landmarks: (1) The talus and (2) The navicular bone

Continued

Table 1 Continued

Regions	Image acquisition protocol
Anterior subtalar	The subject will be in a supine position with the forefoot/ankle in slight eversion. The probe will be positioned at 45 degrees pointing to the heel and then moved proximally and distally. A medial scan of the anterior subtalar joint. Landmarks: (1) The talus and (2) The sustentaculum tali (calcaneus)
Posterior subtalar	The subject will be in a supine position with the forefoot/ankle in slight inversion. The probe will be positioned along the sinus tarsi perpendicular to the sole, and then moved posteriorly. If no distension is seen, the image will be taken visualising the joint with the peroneus tendons. A lateral scan of the posterior subtalar joint. Landmarks: (1) The talus and (2) The calcaneus
MTP2–3 dorsal	The subject will be in a supine position with the knee at 90 degrees flexion and the foot sole-side down. A longitudinal dorsal scan of the MTP2 and MTP3 joints. Landmarks: (1) The head of metatarsal bone (2/3 of the image) and (2) The base of the proximal phalanx (1/3 of the image)

BM, B-mode; MCP, metacarpophalangeal; MTP, metatarsophalangeal; PD, power Doppler; PIP, proximal interphalangeal.

and PD activity ultrasound sum scores were 0.94 (0.72 to 0.99) and 0.91 (0.74 to 0.97), respectively. Weighted kappa (SD) was 0.51 (0.09) for BM synovitis and 0.60 (0.12) for PD activity.

DISCUSSION

For the first time we present an ultrasonographic image acquisition protocol and a semiquantitative joint-specific scoring system for synovitis with an age-divided reference atlas for BM synovitis and a reference atlas for PD activity for frequently affected joints in patients with JIA. The present study demonstrated overall moderate to excellent reliability.

The image acquisition protocol ensured a standardised ultrasound examination in the practical sessions and live scoring exercises. Some of the views were adapted and adjusted from the OMERACT ultrasound paediatric group.¹³ Their scanning approaches showed to be applicable in children regardless of age. In our study, the image acquisition protocol was easily learnt and highly feasible, probably because of the thorough descriptions and illustrative ultrasound images with important anatomical landmarks for each joint. As the pattern of joint involvement seems to be of prognostic importance,^{22 23} a standardised and systematic ultrasound examination might be able to improve assessment of disease activity and individualise treatment in patients with JIA.

The novel scoring system proposes joint-specific scores for frequently affected joints in JIA. A single standard paediatric scoring system may have some limitations in that it does not clearly apply to all joints.¹⁶ For instance, grade 2 and grade 3 BM synovitis in the PedSynS is partly defined by whether or not the joint recess is extending over the bone diaphysis.¹⁶ The score may be difficult to use for joints adjacent to short bones without diaphysal bone structures. A joint-specific scoring system for the knee in patients with JIA was recently developed and demonstrated good reliability.¹⁷ This provided the basis for our further development of joint-specific scores for frequently affected joints in JIA. The suprapatellar recess

was first scored with the scoring system presented by Ting *et al.*¹⁷ However, in the smallest children we discovered that this system could underestimate the degree of pathology due to their relatively shorter femur. In the image acquisition protocol, we therefore added that for the youngest children the patella should fill a third of the image on the ultrasound screen when scoring for pathology.

The variable sonoanatomy in the growing child may lead to pitfalls even when performed by experienced rheumatologists, and there is a lack of published age-specific and joint-specific imaging data in the literature. The images used in this study were selected from our database consisting of approximately 5000 ultrasonographic images. These images were collected during routine ultrasound examination as part of daily clinical practice from patients with JIA attending our inpatient and outpatient clinics. We therefore believe that our selection of images is representative of the patients with JIA seen in clinical practice. The comprehensive ultrasonographic atlas consisting of 224 BM images of normal and inflamed joints divided in four age groups and 51 images with semiquantitative scores for the presence of PD activity, enables the sonographer to recognise age-specific and joint-specific ultrasonographic findings of synovitis and to score ultrasound images according to the best possible match in the reference atlas. The combination of a defined joint-specific scoring system with reference atlas for assessing synovitis may introduce an intuitive and feasible implementation of ultrasound in patients with JIA.

The still image scoring exercise demonstrated moderate to excellent reliability for all joints. At joint level, the scoring of BM synovitis in our study showed the highest ICC and kappa values for the posterior elbow, knee, tibiotalar, anterior subtalar and the MTP joints (table 3). The good reliability for the scoring of the knee was in accordance with data reported by Ting *et al.*¹⁷

The subtalar joint is one of the most difficult joints to assess clinically in the ankle, but this joint is often

Table 2 Ultrasonographic semiquantitative joint-specific scoring system for BM in juvenile idiopathic arthritis

Joint	Semiquantitative scoring system, BM
Anterior elbow	<p>0: No or minimal synovial hypertrophy/effusion</p> <p>1: Mild synovial hypertrophy/effusion</p> <p>2: Moderate synovial hypertrophy/effusion up to, but not beyond the imaginary line*</p> <p>3: Severe synovial hypertrophy/effusion beyond the imaginary line* and a clearly convex shape</p> <p>* <i>The line above the radial fossa; between the proximal end of the fossa to the top of the cartilage over the capitulum humeri</i></p>
Posterior elbow	<p>0: No or minimal synovial hypertrophy/effusion</p> <p>1: Mild synovial hypertrophy/effusion, filling up to 25% of the fossa</p> <p>2: Moderate synovial hypertrophy/effusion filling up to 50% of the fossa, but not beyond the imaginary line*</p> <p>3: Severe synovial hypertrophy/effusion filling more than 50% of the fossa and/or extending beyond the imaginary line*</p> <p>* <i>The line above the fossa olecrani; between the proximal end of the fossa to the top of the cartilage of the trochlea humeri</i></p>
Radiocarpal and midcarpal	<p>0: No sign of synovial hypertrophy/effusion</p> <p>1: Mild synovial hypertrophy/effusion</p> <p>2: Moderate synovial hypertrophy/effusion up to, but not beyond the imaginary line*</p> <p>3: Severe synovial hypertrophy/effusion with a convex shape extending beyond the imaginary line* and can push up the extensor tendons</p> <p>* <i>The line between the top of the cartilage of the distal end of the radius to the top of the cartilage of the capitate (just proximal to the CMC joint)</i></p>
MCP2–3, dorsal	<p>0: No sign of synovial hypertrophy/effusion</p> <p>1: Mild synovial hypertrophy/effusion but not beyond the imaginary line*</p> <p>2: Moderate synovial hypertrophy/effusion extending beyond the imaginary line*, but without overall convex shape</p> <p>3: Severe synovial hypertrophy/effusion extending beyond the imaginary line* with a clearly convex shape</p> <p>* <i>The line between the top of the cartilage of the distal end of the metacarpal to the top of the cartilage of the proximal end of the phalanx</i></p>
PIP2–3, dorsal	<p>0: No sign of synovial hypertrophy/effusion</p> <p>1: Mild synovial hypertrophy/effusion but not beyond the imaginary line*</p> <p>2: Moderate synovial hypertrophy/effusion extending beyond the imaginary line*, but without overall convex shape</p> <p>3: Severe synovial hypertrophy/effusion extending beyond the imaginary line* with a clearly convex shape</p> <p>* <i>The line between the top of the cartilage of the distal end of the proximal phalanx to the top of the cartilage of the proximal end of the middle phalanx</i></p>
PIP2–3, volar	<p>0: No sign of synovial hypertrophy/effusion</p> <p>1: Mild synovial hypertrophy/effusion, possible to extend proximally but without convex shape</p> <p>2: Moderate synovial hypertrophy/effusion extending over the proximal phalanx with convex shape, but not filling the joint space between proximal and middle phalanx</p> <p>3: Severe synovial hypertrophy/effusion extending over the proximal phalanx and filling the joint space between proximal and middle phalanx with an overall convex shape</p>
Hip	<p>0: No sign of synovial hypertrophy/effusion</p> <p>1: Mild synovial hypertrophy/effusion, but just a 'slit' of fluid between the two layers of the capsule</p> <p>2: Moderate synovial hypertrophy/effusion leading to a straight line/minimal convex shape of the capsule</p> <p>3: Severe synovial hypertrophy/effusion with a clearly convex shape, the effusion can also extend proximally over the femoral head</p>
Knee, suprapatellar recess	<p>0: 'Slit' of fluid/synovium without elevation of the prepatellar fat pad but with only minimal extension beyond the prepatellar fat pad</p> <p>1: Mild synovial hypertrophy/effusion with elevation of the prepatellar fat pad and extension proximally <50% of the visualised portion of the quadriceps tendon</p> <p>2: Moderate synovial hypertrophy/effusion elevating the prepatellar fat pad with extension proximally >50% of the visualised portion of the quadriceps tendon</p> <p>3: Significant distension of the suprapatellar recess throughout the image, and with the most proximal portion of the synovial recess being >50% of the maximum distension of the recess</p>

Continued

Table 2 Continued

Joint	Semiquantitative scoring system, BM
Knee, lateral parapatellar recess	<p>0: Empty parapatellar recess but a minimal bulge of synovial hypertrophy/effusion may be found extending to the patellofemoral joint line</p> <p>1: Synovial hypertrophy/effusion filling <1/3 of the full area of the parapatellar recess</p> <p>2: Synovial hypertrophy/effusion filling between 1/3 to 2/3 of the full area of the parapatellar recess</p> <p>3: Synovial hypertrophy/effusion that fills >2/3 of the full area of the parapatellar recess and clearly pushing up the retinaculum¹⁷</p>
Tibiotalar	<p>0: No sign of synovial hypertrophy/effusion in the tibiotalar joint, but possible to have a minimal amount of fluid in the concave neck of the talus</p> <p>1: Mild synovial hypertrophy/effusion filling the gap between the tibia and the talus and in the concave neck of the talus, but not continuously over the talus</p> <p>2: Moderate synovial hypertrophy/effusion filling <50% of the area between the tibia, the talus and the imaginary line* and continuously over the talus</p> <p>3: Severe synovial hypertrophy/effusion filling >50% of the area between the tibia, the talus and the imaginary line* or beyond the imaginary line*</p> <p>* The line between the top of the cartilage of the distal end of the tibia and the top of the cartilage of the talar head</p>
Talonavicular	<p>0: No sign of synovial hypertrophy/effusion</p> <p>1: Mild synovial hypertrophy/effusion but not beyond the imaginary line*</p> <p>2: Moderate synovial hypertrophy/effusion extending beyond the imaginary line* and proximal with a concave or straight shape</p> <p>3: Severe synovial hypertrophy/effusion extending beyond the imaginary line* and over the talus with a convex shape clearly pushing up the joint capsule</p> <p>* The line between the top of the cartilage of the head of the talus to the top of the cartilage of the navicular bone</p>
Anterior subtalar	<p>0: No sign of synovial hypertrophy/effusion</p> <p>1: Mild synovial hypertrophy/effusion covering up to 25% of the straight part of the talus</p> <p>2: Moderate synovial hypertrophy/effusion covering up to 50% of the straight part of the talus</p> <p>3: Severe synovial hypertrophy/effusion covering more than 50% of the straight part of the talus</p>
Posterior subtalar	<p>0: No sign of synovial hypertrophy/effusion</p> <p>1: Mild synovial hypertrophy/effusion filling the gap between the talus and the calcaneus</p> <p>2: Moderate synovial hypertrophy/effusion extending beyond the talus and the calcaneus but not with a convex shape</p> <p>3: Severe synovial hypertrophy/effusion extending beyond the talus and the calcaneus with a convex shape</p>
MTP2–3 dorsal	<p>0: No sign of synovial hypertrophy/effusion</p> <p>1: Mild synovial hypertrophy/effusion but not beyond the imaginary line*</p> <p>2: Moderate synovial hypertrophy/effusion extending beyond the imaginary line*, but without overall convex shape</p> <p>3: Severe synovial hypertrophy/effusion extending beyond the imaginary line* with a clearly convex shape</p> <p>* The line between the top of the cartilage of the distal end of the metatarsal to the top of the cartilage of the proximal end of the phalanx</p>

BM, B-mode; CMC, carpometacarpal; MCP, metacarpophalangeal; MTP, metatarsophalangeal; PIP, proximal interphalangeal.

involved in patients with JIA.^{6 24 25} To our knowledge, image acquisitions and scoring systems for the paediatric anterior and posterior subtalar joints have not been published before. We therefore included them in our scanning protocol and scoring system, which is also in accordance with suggestions by others.²⁵ In our study, the joint-specific scoring with illustrative images in the reference atlas of the anterior and posterior subtalar joints showed good to excellent reliability.

Interpretation of PD signals in children is complicated due to a variable degree of physiological blood flow within the joint that can easily be misinterpreted as inflammation. The OMERACT ultrasound group has started the

process of defining age-related vascularisation of joints in healthy children,^{13 26} and developed preliminary definitions of synovitis in children which define that Doppler signals must be detected within synovial hypertrophy to be considered as a sign of synovitis.¹⁴ Our reference atlas for scoring of PD activity might improve the feasibility of this ultrasonographic feature, but further studies are needed regarding the detection of abnormal vascularisation in the paediatric joint.

Inter-reader reliability on live scoring has only been reported in few JIA studies. The live scoring of 10 patients with JIA in this study demonstrated good reliability, which

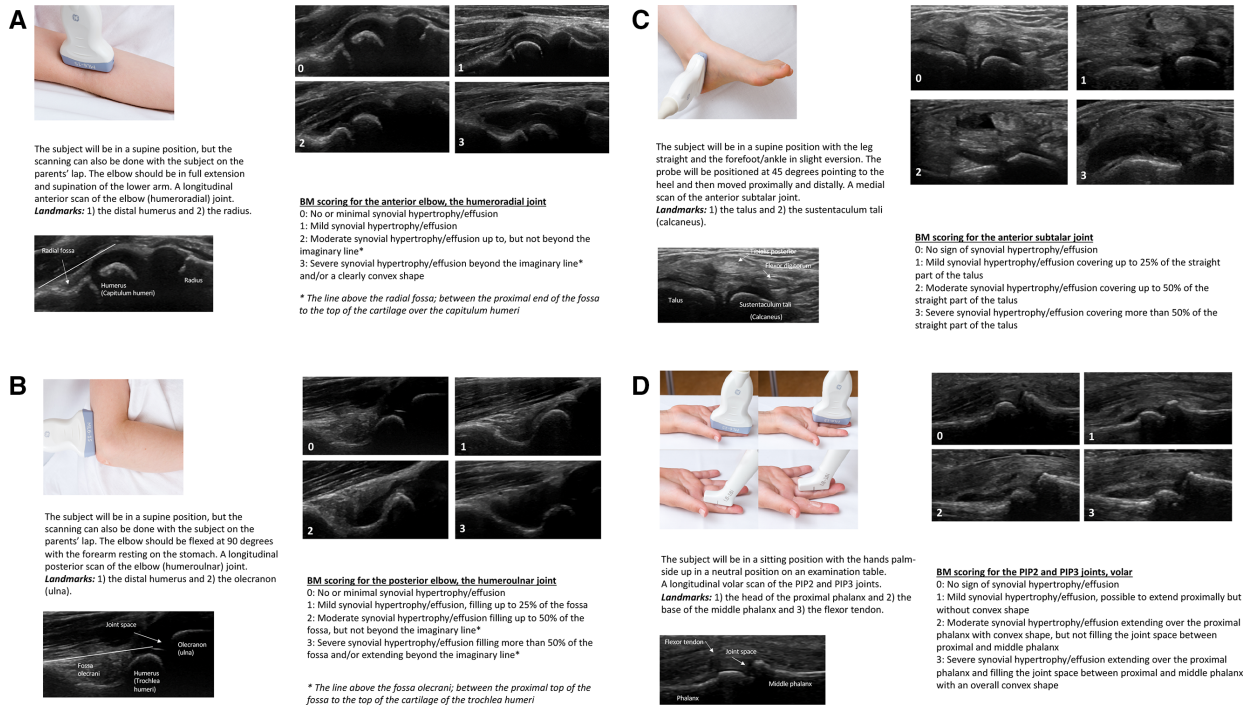


Figure 1 (A–D) Description of ultrasound examination and scoring of B-mode (BM) synovitis from the ultrasonographic BM reference atlas in juvenile idiopathic arthritis (JIA). (A) The elbow joint, longitudinal anterior scan (2–4 years). (B) The elbow joint, longitudinal posterior scan (5–8 years). (C) The anterior subtalar joint, medial scan (9–12 years). (D) The proximal interphalangeal (PIP)2 and PIP3 joints, longitudinal volar scan (13–18 years).

is comparable to the results presented by Magni-Manzoni *et al.*¹⁹

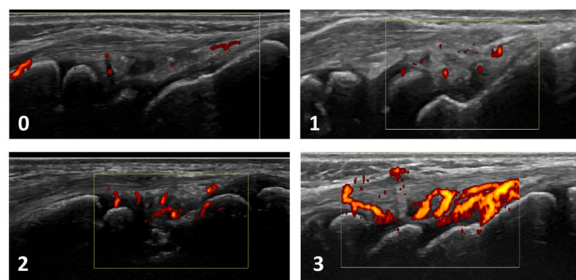
Limitations of this study are the low number of patients included in the live scoring exercise, that only three sonographers participated and that they only scanned the patients once. At the time of our live scoring exercise,

we experienced that the COVID-19 situation made it impossible to conduct a large scoring exercise including more patients and readers. However, we wished to test the scoring system in a live setting and made adaptations to our project within these limitations. Previous studies have shown that inclusion of 10 patients may yield sufficient



The subject will be in a sitting position, the hands palm-side down in a neutral position on an examination table and resting the elbow on the table. A longitudinal dorsal scan of the radiocarpal and midcarpal joints at the sagittal midline of the wrist, including the distal radius, the lunate and the capitate bone.

Landmarks: 1) the distal end of diaphysis and epiphyseal cartilage of radius and 2) the dorsal recess of the radiocarpal and midcarpal joints and over them 3) a compartment of the extensor tendons according to the area imaged. (Collado *et al.* 2016)



PD scoring for the radiocarpal and midcarpal joints

- 0: No Doppler signal
- 1: 1-3 signals within the area of synovial hypertrophy only
- 2: > 3 signals or confluent signals present in < 50% of the area of synovial hypertrophy
- 3: Confluent signals present in > 50% of the area of synovial hypertrophy (Ting *et al.* 2019)

Figure 2 Description of ultrasound examination and scoring of power Doppler (PD) activity for the wrist; radiocarpal and midcarpal joints (longitudinal dorsal scan) from the ultrasonographic PD reference atlas in juvenile idiopathic arthritis (JIA).

Table 3 Intra-reader and inter-reader reliability for B-mode (BM) synovitis scoring on still images in juvenile idiopathic arthritis (JIA)

Regions	No. images	Intra-reader reliability		Inter-reader reliability	
		smlICC Mean (SD)	Cohen's weighted kappa Mean (SD)	avmlICC (95% CI)	Light's weighted kappa Mean (SD)
Anterior elbow	25	0.90 (0.03)	0.81 (0.06)	0.96 (0.92 to 0.98)	0.72 (0.09)
Posterior elbow	27	0.93 (0.04)	0.88 (0.06)	0.96 (0.93 to 0.98)	0.76 (0.05)
Radiocarpal	28	0.79 (0.10)	0.67 (0.12)	0.93 (0.87 to 0.96)	0.61 (0.10)
Midcarpal	28	0.89 (0.05)	0.79 (0.08)	0.96 (0.93 to 0.98)	0.73 (0.11)
MCP2–3, dorsal	20	0.75 (0.07)	0.63 (0.07)	0.89 (0.79 to 0.95)	0.50 (0.10)
PIP2–3, dorsal	20	0.87 (0.05)	0.77 (0.07)	0.94 (0.88 to 0.98)	0.64 (0.11)
PIP2–3, volar	30	0.85 (0.07)	0.72 (0.10)	0.95 (0.92 to 0.98)	0.72 (0.10)
Hip	26	0.92 (0.05)	0.84 (0.08)	0.96 (0.93 to 0.98)	0.75 (0.08)
Knee, suprapatellar recess	24	0.95 (0.01)	0.91 (0.02)	0.98 (0.96 to 0.99)	0.86 (0.05)
Knee, lateral parapatellar recess	27	0.88 (0.09)	0.81 (0.13)	0.95 (0.91 to 0.98)	0.70 (0.04)
Tibiotalar	26	0.94 (0.04)	0.90 (0.07)	0.98 (0.96 to 0.99)	0.83 (0.05)
Talonavicular	22	0.87 (0.12)	0.83 (0.13)	0.95 (0.90 to 0.98)	0.69 (0.09)
Anterior subtalar	27	0.95 (0.04)	0.91 (0.07)	0.99 (0.97 to 0.99)	0.91 (0.04)
Posterior subtalar	20	0.86 (0.09)	0.74 (0.08)	0.95 (0.90 to 0.98)	0.75 (0.10)
MTP2–3, dorsal	20	0.94 (0.04)	0.89 (0.08)	0.96 (0.93 to 0.99)	0.79 (0.11)

avmlICC, average measure ICC; ; ICC, intraclass correlation coefficient; MCP, metacarpophalangeal; MTP, metatarsophalangeal; PIP, proximal interphalangeal; smlICC, single measure ICC.

power for reliability testing.^{15 27} We found it feasible for three dedicated rheumatologists to do a live scoring exercise implemented in our daily clinical practice by consecutively including 10 patients with JIA disease flare in need of hospital admission. In this setting, the inter-reader reliability was good, suggesting that the scoring system with atlas is a reliable tool. Examination of potential variability in the reliability of the scoring system with respect to age or disease activity was beyond the scope of this study and should be addressed in future research.

Another limitation is the lack of comparison with healthy subjects. The main target of this study was to develop an ultrasonographic scoring system with reference atlas for patients with JIA and to test the reliability of the system. The study was not designed to compare ultrasonographic findings in healthy children with patients with JIA. However, results from available musculoskeletal ultrasound studies highlighting findings in healthy children were taken into account in the process.^{11–13 26} A comparison of ultrasonographic findings in healthy children with patients with JIA according to the presented scoring system could be a future study of interest.

Other limitations are that we did not have images of all grades in the atlas, and that the reference atlas for scoring of PD activity was not age-divided. However, the main goal for the PD reference atlas is to illustrate different grades of PD signals for each joint and not the age variability. Furthermore, in accordance with the definitions developed by the OMERACT ultrasound group,¹⁴ PD signals must be detected within synovial hypertrophy

to be considered as a sign of synovitis, which will be clearly identified first by using the scoring system and age-divided atlas for BM synovitis as reference. In addition, we will continuously include images in our database and aspire to include the best possible reference images for all grades in the reference atlas.

The strengths of the study are the unique collection of ultrasonographic images with different degrees of pathology in four age ranges and the approach to define individual scores for a substantial number of joints in patients with JIA.

In conclusion, this study presents an ultrasonographic image acquisition protocol and a semiquantitative joint-specific scoring system for synovitis with reference atlas in patients with JIA. The study demonstrated moderate to excellent reliability when used in assessments on still images as well as on patients. We expect that the system can be a valuable tool for clinicians and future research. Future studies are needed for further validation of the scoring system with atlas, such as association to clinical measures of disease activity and the system's sensitivity to change.

Author affiliations

¹Department of Rheumatology, Oslo University Hospital, Oslo, Norway

²Department of Rheumatology, Diakonhjemmet Hospital, Oslo, Norway

³Faculty of Medicine, University of Oslo, Oslo, Norway

⁴Division of Pediatric Dermatology and Rheumatology, Children's Hospital of Eastern Ontario and University of Ottawa, Ottawa, Ontario, Canada

Acknowledgements The authors thank David Swanson, Researcher (statistician), PhD, for statistical advice, and Øystein Horgmo, senior photographer, for taking photographs of probe positioning to the ultrasonographic atlas. The authors also thank all the patients and their families who contributed to this study.

Contributors NKS designed the study, made substantial contributions to acquisition, analysis and interpretation of data and writing the manuscript. PB and VL designed the study, and made substantial contributions to acquisition, interpretation of data and writing the manuscript. JR participated in the study design, made substantial contributions to acquisition, interpretation of data and writing the manuscript. A-BA, HBH and BF participated in the study design and made substantial contributions to data interpretation and writing the manuscript.

Funding The authors have not declared a specific grant for this research from any funding agency in the public, commercial or not-for-profit sectors.

Competing interests HBH reports personal fees from Lilly, personal fees from Novartis, personal fees from AbbVie, personal fees from Roche, outside the submitted work.

Patient consent for publication Not required.

Ethics approval The study was done in accordance with the Declaration of Helsinki and was approved by the Norwegian Regional Committee for Medical and Health Research Ethics (REK 2018/805) and the Data Protection Officer at Oslo University Hospital, Norway (18/11742 and 18/12493). Image storage was approved by the Data Protection Officer at OUH (18/11742).

Provenance and peer review Not commissioned; externally peer reviewed.

Data availability statement Data are available upon reasonable request to the corresponding author.

Open access This is an open access article distributed in accordance with the Creative Commons Attribution Non Commercial (CC BY-NC 4.0) license, which permits others to distribute, remix, adapt, build upon this work non-commercially, and license their derivative works on different terms, provided the original work is properly cited, appropriate credit is given, any changes made indicated, and the use is non-commercial. See: <http://creativecommons.org/licenses/by-nc/4.0/>.

ORCID iDs

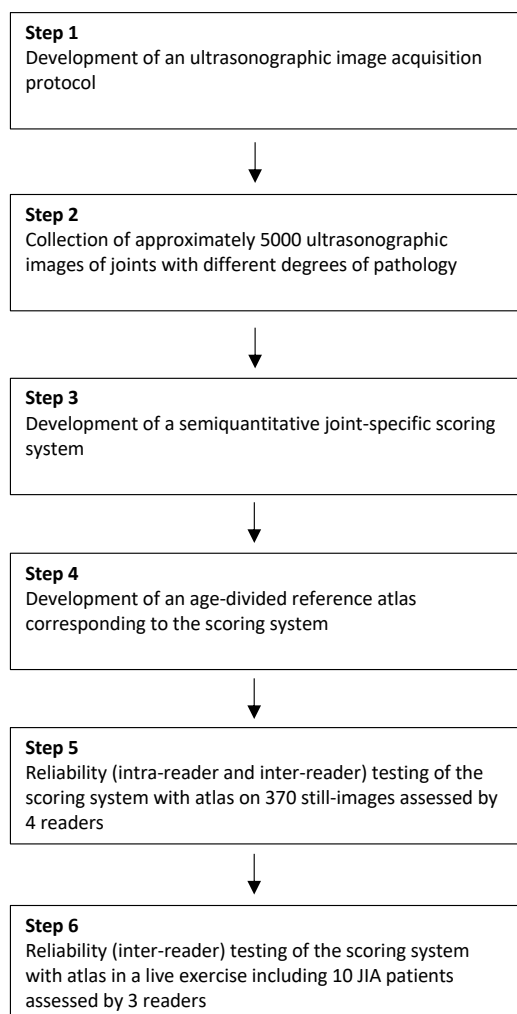
Nina Krafft Sande <http://orcid.org/0000-0003-3461-9525>

Pernille Bøyesen <http://orcid.org/0000-0002-9751-5144>

Hilde Berner Hammer <http://orcid.org/0000-0001-7317-8991>

REFERENCES

- Ravelli A, Martini A. Juvenile idiopathic arthritis. *Lancet* 2007;369:767–78.
- Ringold S, Angeles-Han ST, Beukelman T, et al. 2019 American College of Rheumatology/Arthritis Foundation guideline for the treatment of juvenile idiopathic arthritis: therapeutic approaches for non-systemic polyarthritis, sacroiliitis, and Enthesitis. *Arthritis Care Res* 2019;71:717–34.
- Steigerwald KA, Ilowite NT. Novel treatment options for juvenile idiopathic arthritis. *Expert Rev Clin Pharmacol* 2015;8:559–73.
- Shoop-Worrall SJW, Kearsley-Fleet L, Thomson W, et al. How common is remission in juvenile idiopathic arthritis: a systematic review. *Semin Arthritis Rheum* 2017;47:331–7.
- Rooney ME, McAllister C, Burns JFT. Ankle disease in juvenile idiopathic arthritis: ultrasound findings in clinically swollen Ankles. *J Rheumatol* 2009;36:1725–9.
- Pascoli L, Wright S, McAllister C, et al. Prospective evaluation of clinical and ultrasound findings in ankle disease in juvenile idiopathic arthritis: importance of ankle ultrasound. *J Rheumatol* 2010;37:2409–14.
- Colebatch-Bourn AN, Edwards CJ, Collado P, et al. EULAR-PRReS points to consider for the use of imaging in the diagnosis and management of juvenile idiopathic arthritis in clinical practice. *Ann Rheum Dis* 2015;74:1946–57.
- Lanni S, Wood M, Ravelli A, et al. Towards a role of ultrasound in children with juvenile idiopathic arthritis. *Rheumatology* 2013;52:413–20.
- Windschall D, Malattia C. Ultrasound imaging in paediatric rheumatology. *Best Pract Res Clin Rheumatol* 2020;34:101570.
- Magni-Manzoni S, Malattia C, Lanni S, et al. Advances and challenges in imaging in juvenile idiopathic arthritis. *Nat Rev Rheumatol* 2012;8:329–36.
- Roth J, Jousse-Joulin S, Magni-Manzoni S, et al. Definitions for the sonographic features of joints in healthy children. *Arthritis Care Res* 2015;67:136–42.
- Windschall D, Trauzeddel R, Haller M, et al. Pediatric musculoskeletal ultrasound: age- and sex-related normal B-mode findings of the knee. *Rheumatol Int* 2016;36:1569–77.
- Collado P, Vojinovic J, Nieto JC, et al. Toward standardized musculoskeletal ultrasound in pediatric rheumatology: normal age-related ultrasound findings. *Arthritis Care Res* 2016;68:348–56.
- Roth J, Ravagnani V, Backhaus M, et al. Preliminary definitions for the sonographic features of synovitis in children. *Arthritis Care Res* 2017;69:1217–23.
- Hammer HB, Bolton-King P, Bakkeheim V, et al. Examination of intra and interrater reliability with a new ultrasonographic reference atlas for scoring of synovitis in patients with rheumatoid arthritis. *Ann Rheum Dis* 2011;70:1995–8.
- Collado P, Naredo E, Calvo C, et al. Reduced joint assessment vs comprehensive assessment for ultrasound detection of synovitis in juvenile idiopathic arthritis. *Rheumatology* 2013;52:1477–84.
- Ting TV, Vega-Fernandez P, Oberle EJ, et al. Novel ultrasound image acquisition protocol and scoring system for the pediatric knee. *Arthritis Care Res* 2019;71:977–85.
- Backhaus M, Burmester GR, Gerber T, et al. Guidelines for musculoskeletal ultrasound in rheumatology. *Ann Rheum Dis* 2001;60:641–9.
- Magni-Manzoni S, Epis O, Ravelli A, et al. Comparison of clinical versus ultrasound-determined synovitis in juvenile idiopathic arthritis. *Arthritis Rheum* 2009;61:1497–504.
- Petty RE, Southwood TR, Manners P, et al. International League of associations for rheumatology classification of juvenile idiopathic arthritis: second revision, Edmonton, 2001. *J Rheumatol* 2004;31:390–2.
- Hallgren KA. Computing inter-rater reliability for observational data: an overview and tutorial. *Tutor Quant Methods Psychol* 2012;8:23–34.
- Eng SWM, Aeschlimann FA, van Veenendaal M, et al. Patterns of joint involvement in juvenile idiopathic arthritis and prediction of disease course: a prospective study with multilayer non-negative matrix factorization. *PLoS Med* 2019;16:e1002750.
- Flatø B, Lien G, Smerdel A, et al. Prognostic factors in juvenile rheumatoid arthritis: a case-control study revealing early predictors and outcome after 14.9 years. *J Rheumatol* 2003;30:386–93.
- Hendry GJ, Gardner-Medwin J, Steultjens MPM, et al. Frequent discordance between clinical and musculoskeletal ultrasound examinations of foot disease in juvenile idiopathic arthritis. *Arthritis Care Res* 2012;64:441–7.
- Lanni S, Bovis F, Ravelli A, et al. Delineating the application of ultrasound in detecting synovial abnormalities of the Subtalar joint in juvenile idiopathic arthritis. *Arthritis Care Res* 2016;68:1346–53.
- Windschall D, Collado P, Vojinovic J, et al. Age-Related vascularization and ossification of joints in children: an international pilot study to test multiobserver ultrasound reliability. *Arthritis Care Res* 2020;72:498–506.
- Haavardsholm EA, Ostergaard M, Ejbjerg BJ, et al. Reliability and sensitivity to change of the OMERACT rheumatoid arthritis magnetic resonance imaging score in a multireader, longitudinal setting. *Arthritis Rheum* 2005;52:3860–7.

Supplementary Figure 1: The study was conducted through the following six steps

Ultrasonographic atlas for scoring of B-mode (BM) synovitis in patients with juvenile idiopathic arthritis 2-4 years

Nina Krafft Sande et al.

Included joint regions

- Anterior elbow
- Posterior elbow
- Wrist (radiocarpal and midcarpal)
- Metacarpophalangeal (MCP) 2-3 dorsal
- Proximal interphalangeal (PIP) 2-3 dorsal
- Proximal interphalangeal (PIP) 2-3 volar
- Hip
- Knee, suprapatellar recess
- Knee, lateral parapatellar recess
- Tibiotalar
- Talonavicular
- Anterior subtalar
- Posterior subtalar
- Metatarsophalangeal (MTP) 2-3 dorsal

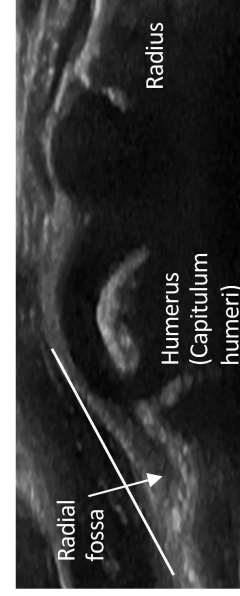
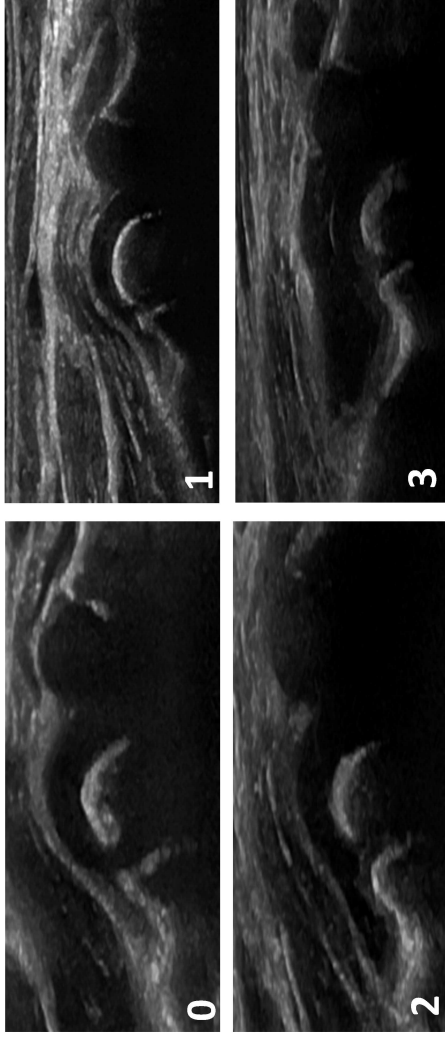


Anterior elbow



The subject will be in a supine position, but the scanning can also be done with the subject on the parents' lap. The elbow should be in full extension and supination of the lower arm. A longitudinal anterior scan of the elbow (humeroradial) joint.

Landmarks: 1) the distal humerus and 2) the radius.



BM scoring for the anterior elbow, the humeroradial joint

- 0: No or minimal synovial hypertrophy/effusion
- 1: Mild synovial hypertrophy/effusion
- 2: Moderate synovial hypertrophy/effusion up to, but not beyond the imaginary line*
- 3: Severe synovial hypertrophy/effusion beyond the imaginary line* and/or a clearly convex shape

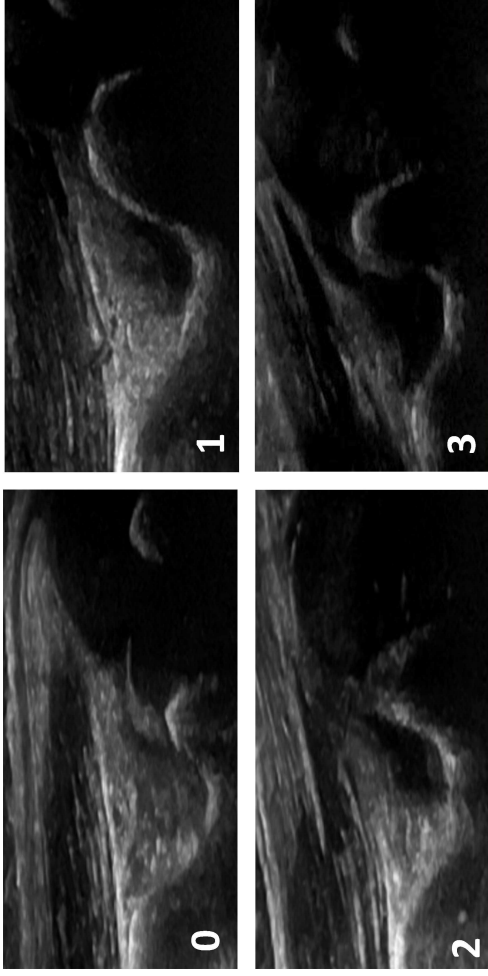
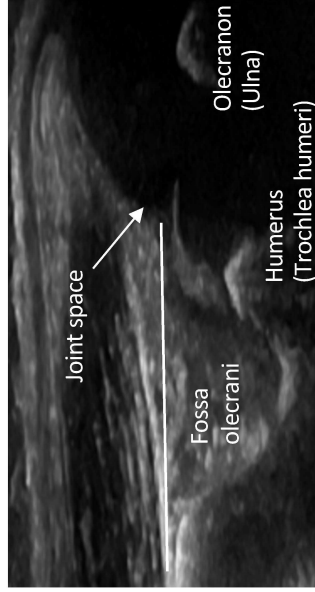
* The line above the radial fossa; between the proximal end of the fossa to the top of the cartilage over the capitulum humeri

Posterior elbow



The subject will be in a supine position, but the scanning can also be done with the subject on the parents' lap. The elbow should be flexed at 90 degrees with the forearm resting on the stomach.

A longitudinal posterior scan of the elbow (humeroulnar) joint. **Landmarks:** 1) the distal humerus and 2) the olecranon (ulna).



BM scoring for the posterior elbow, the humeroulnar joint

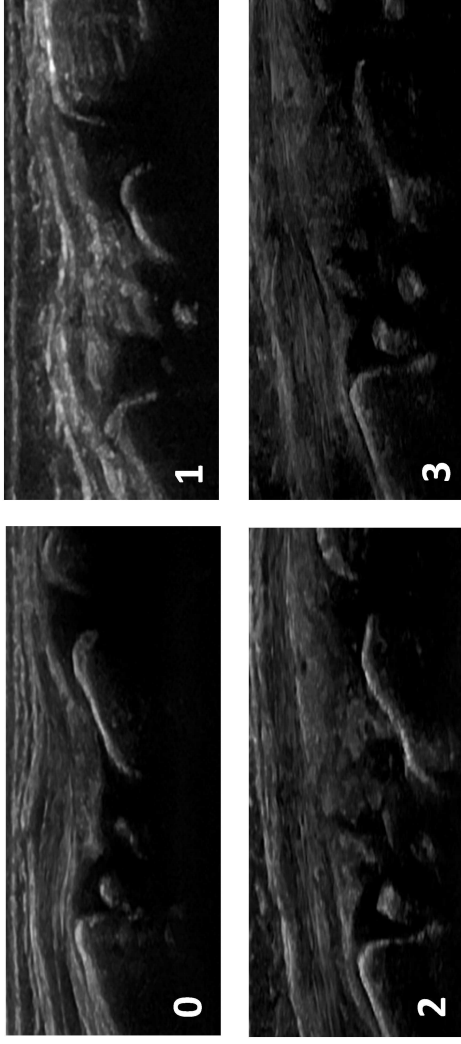
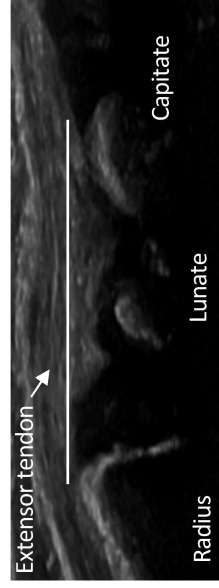
- 0: No or minimal synovial hypertrophy/effusion
- 1: Mild synovial hypertrophy/effusion, filling up to 25% of the fossa
- 2: Moderate synovial hypertrophy/effusion filling up to 50% of the fossa, but not beyond the imaginary line*
- 3: Severe synovial hypertrophy/effusion filling more than 50% of the fossa and/or extending beyond the imaginary line*

* The line above the fossa olecrani; between the proximal top of the fossa to the top of the cartilage of the trochlea humeri

Radiocarpal and midcarpal



The subject will be in a sitting position, the hands palm-side down in a neutral position on an examination table and resting the elbow on the table. A longitudinal dorsal scan of the radiocarpal and midcarpal joints at the sagittal midline of the wrist, including the distal radius, the lunate and the capitate bone.
Landmarks: 1) the distal end of diaphysis and epiphyseal cartilage of radius and 2) the dorsal recess of the radiocarpal and midcarpal joints and over them 3) a compartment of the extensor tendons according to the area imaged.
 (Collado et al. 2016)



BM scoring for the radiocarpal and midcarpal joints

- 0: No sign of synovial hypertrophy/effusion
- 1: Mild synovial hypertrophy/effusion
- 2: Moderate synovial hypertrophy/effusion up to, but not beyond the imaginary line*
- 3: Severe synovial hypertrophy/effusion with a convex shape extending beyond the imaginary line* and can push up the extensor tendons

* The line between the top of the cartilage of the distal end of the radius to the top of the cartilage of the capitate

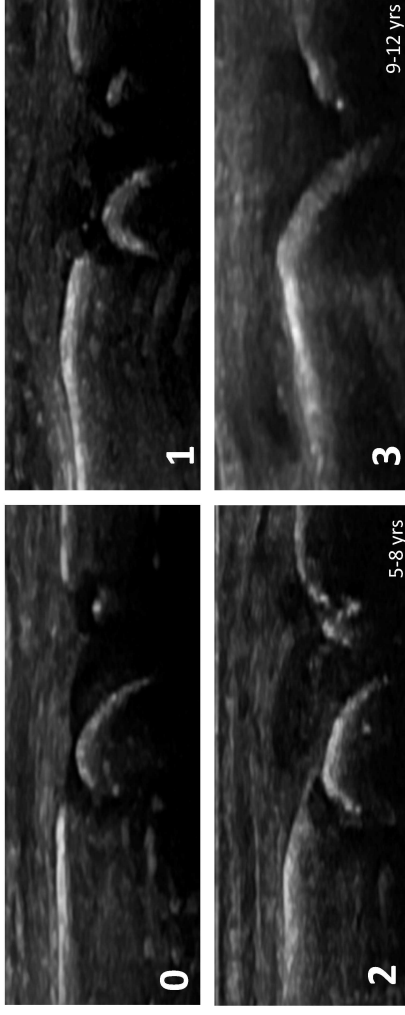
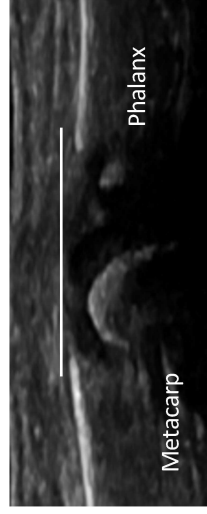
MCP2 - MCP3 dorsal



The subject will be in a sitting position with the hands palm-side down in a neutral position on an examination table.

A longitudinal dorsal scan of the MCP2 and MCP3 joints.

Landmarks: 1) the head of the metacarpal bone (2/3 of the image) and 2) the base of the proximal phalanx (1/3 of the image).



BM scoring for the MCP2 and MCP3 joints, dorsal

- 0: No sign of synovial hypertrophy/effusion
- 1: Mild synovial hypertrophy/effusion but not beyond the imaginary line*
- 2: Moderate synovial hypertrophy/effusion extending beyond the imaginary line*, but without overall convex shape
- 3: Severe synovial hypertrophy/effusion extending beyond the imaginary line* with a clearly convex shape

**The line between the top of the cartilage of the distal end of the metacarp to the top of the cartilage of the proximal end of the phalanx*

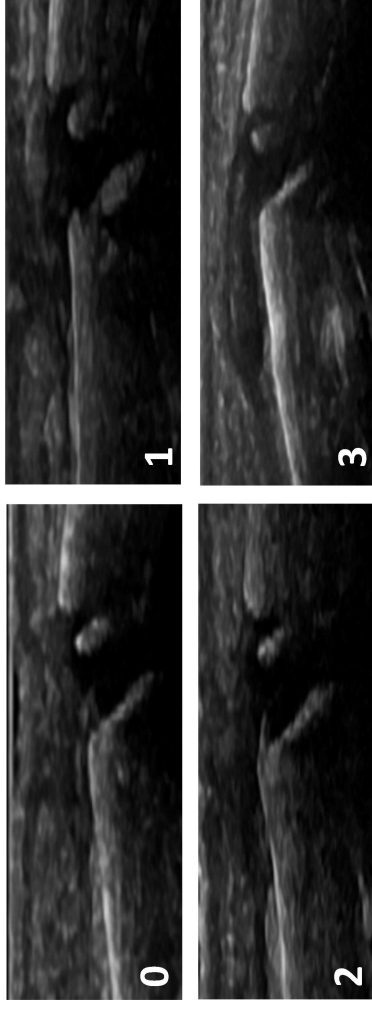
PIP2 - PIP3 dorsal



The subject will be in a sitting position with the hands palm-side down in a neutral position on an examination table.

A longitudinal dorsal scan of the PIP2 and PIP3 joints.

Landmarks: 1) the head of the proximal phalanx (2/3 of the image) and 2) the base of the middle phalanx (1/3 of the image).



BM scoring for the PIP2 and PIP3 joints, dorsal

- 0: No sign of synovial hypertrophy/effusion
- 1: Mild synovial hypertrophy/effusion but not beyond the imaginary line*
- 2: Moderate synovial hypertrophy/effusion extending beyond the imaginary line*, but without overall convex shape
- 3: Severe synovial hypertrophy/effusion extending beyond the imaginary line* with a clearly convex shape

*The line between the top of the cartilage of the distal end of the proximal phalanx to the top of the cartilage of the proximal end of the middle phalanx

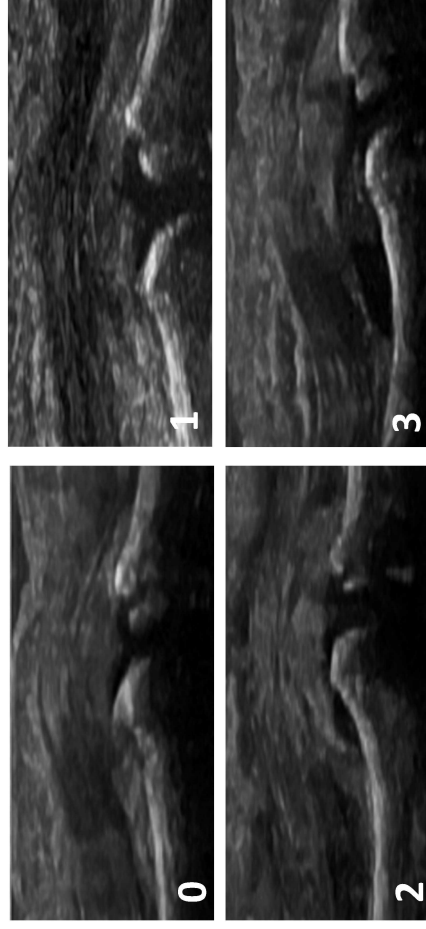
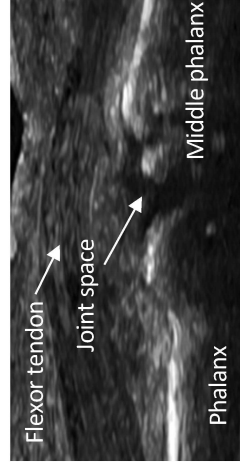
PIP2 - PIP3 volar



The subject will be in a sitting position with the hands palm-side up in a neutral position on an examination table.

A longitudinal volar scan of the PIP2 and PIP3 joints.

Landmarks: 1) the head of the proximal phalanx and 2) the base of the middle phalanx and 3) the flexor tendon.



BM scoring for the PIP2 and PIP3 joints, volar

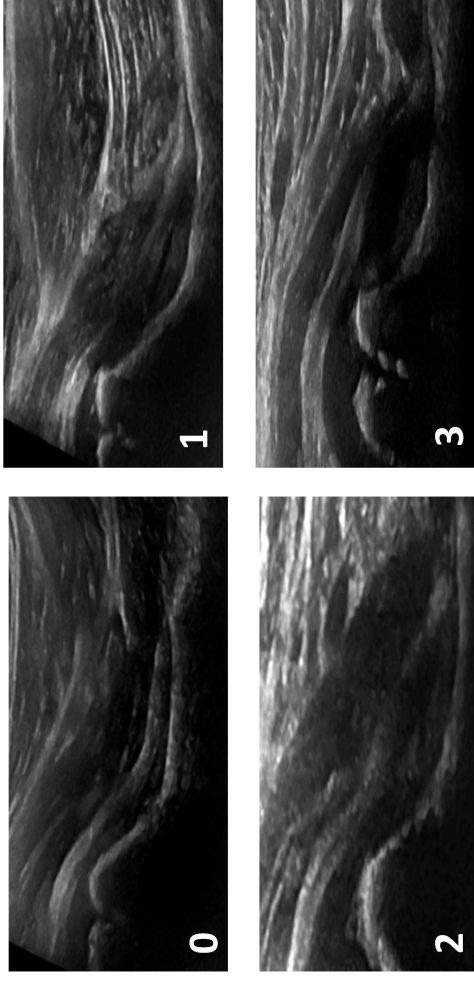
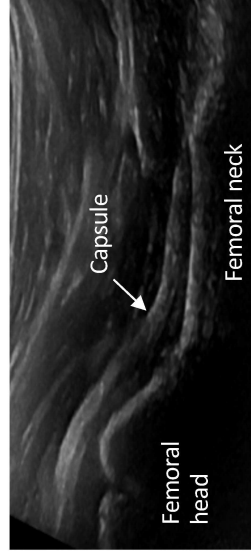
- 0: No sign of synovial hypertrophy/effusion
- 1: Mild synovial hypertrophy/effusion, possible to extend proximally but without convex shape
- 2: Moderate synovial hypertrophy/effusion extending over the proximal phalanx with convex shape, but not filling the joint space between proximal and middle phalanx
- 3: Severe synovial hypertrophy/effusion extending over the proximal phalanx and filling the joint space between proximal and middle phalanx with an overall convex shape

Hip



The subject will be in a supine position with the hip in a neutral position, slightly externally rotated. A longitudinal anterior scan parallel to the femoral neck of the hip joint.

Landmarks: 1) the femoral head and 2) the femoral neck.



BM scoring for the hip joint

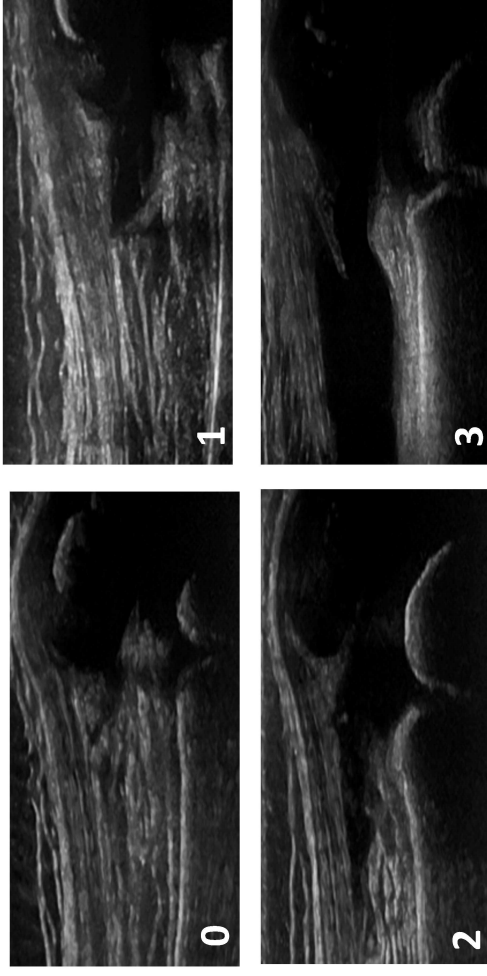
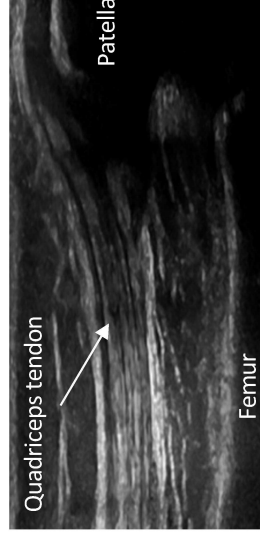
- 0: No sign of synovial hypertrophy/effusion
 1: Mild synovial hypertrophy/effusion, but just a "slit" of fluid between the two layers of the capsule
 2: Moderate synovial hypertrophy/effusion leading to a straight line/minimal convex shape of the capsule
 3: Severe synovial hypertrophy/effusion with a clearly convex shape, the effusion can also extend proximally over the femoral head

Knee, suprapatellar recess



The subject will be in a supine position. The knee should be flexed at 30 degrees, and images taken after the subject completes flexion and extension three times. A longitudinal scan of the suprapatellar joint space. For the youngest subjects, the patella should fill 1/3 of the image to compensate for the relatively shorter femur.

Landmarks: 1) the proximal third of the patella and 2) a clearly visualized quadriceps tendon. (Ting et al. 2019)

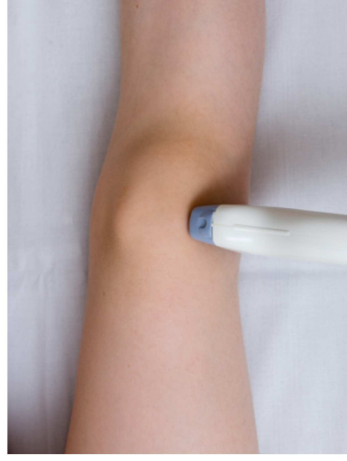


BM scoring for the knee, suprapatellar recess

- 0: "Slit" of fluid/synovium without elevation of the pre-patellar fat pad but with only minimal extension beyond the prepatellar fat pad
- 1: Mild synovial hypertrophy/effusion with elevation of the prepatellar fat pad and extension proximally <50% of the visualized portion of the quadriceps tendon
- 2: Moderate synovial hypertrophy/effusion elevating the pre-patellar fat pad with extension proximally > 50% of the visualized portion of the quadriceps tendon
- 3: Significant distension of the suprapatellar recess throughout the image, and with the most proximal portion of the synovial recess being > 50% of the maximum distension of the recess (Ting et al. 2019)



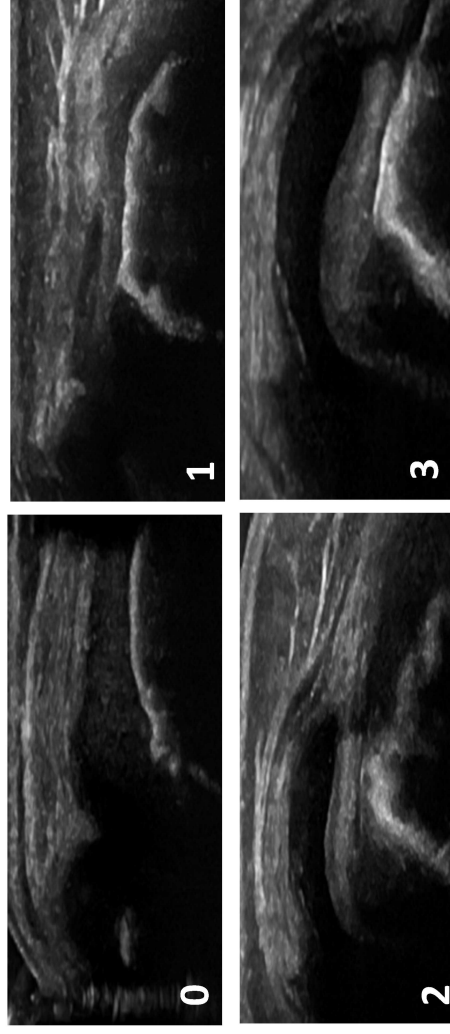
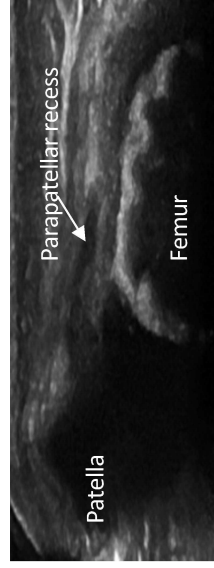
Knee, lateral parapatellar recess



The subject will be in a supine position. The knee should be flexed at 30 degrees. For the lateral parapatellar recess the image will be obtained with the probe in transverse position over the mid-patella with both the patella and femur in view.

Landmarks: 1) the superior edge of the patella and 2) the femoral condyle.

(Ting et al. 2019)



BM scoring for the knee, lateral parapatellar recess

0: Empty parapatellar recess but a minimal bulge of synovial hypertrophy/effusion may be found extending to the patellofemoral joint line

1: Synovial hypertrophy/effusion filling < 1/3 of the full area of the parapatellar recess

2: Synovial hypertrophy/effusion filling between one to two thirds of the full area of the parapatellar recess

3: Synovial hypertrophy/effusion that fills >2/3 of the full area of the parapatellar recess and clearly pushing up the retinaculum
(Ting et al. 2019)

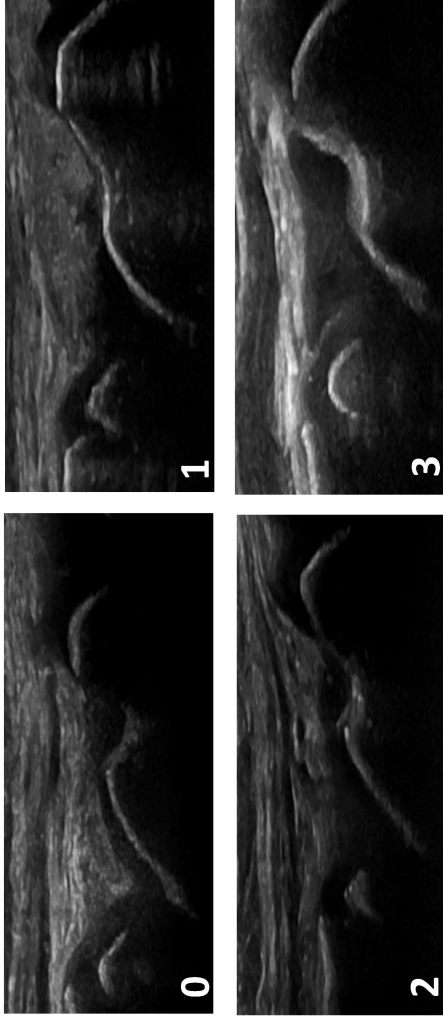
Tibiotalar



The subject will be in a supine position with the knee at 90 degrees flexion and the foot sole-side down.

A longitudinal scan of the tibiotalar joint.

Landmarks: 1) the distal end of the tibia and 2) the talus.



BM scoring for the tibiotalar joint

- 0:** No sign of synovial hypertrophy/effusion in the tibiotalar joint, but possible to have a minimal amount of fluid in the concave neck of the talus
- 1:** Mild synovial hypertrophy/effusion filling the gap between the tibia and the talus and in the concave neck of the talus, but not continuously over the talus
- 2:** Moderate synovial hypertrophy/effusion filling up to 50% of the area between the tibia, the talus and the imaginary line* and continuously over the talus
- 3:** Severe synovial hypertrophy/effusion filling more than 50% of the area between the tibia, the talus and the imaginary line*, or beyond the imaginary line*

*The line between the top of the cartilage of the distal end of the tibia and the top of the cartilage of the talar head

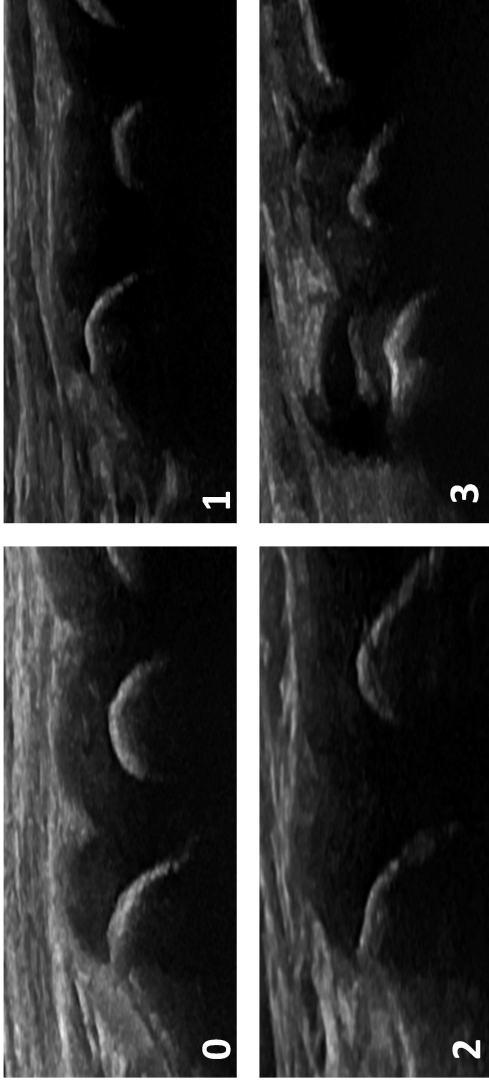
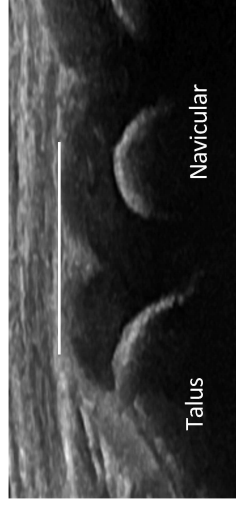
Talonavicular



The subject will be in a supine position with the knee at 90 degrees flexion and the foot sole-side down.

A longitudinal scan of the talonavicular joint.

Landmarks: 1) the talus and 2) the navicular bone.



BMJ scoring for the talonavicular joint

- 0: No sign of synovial hypertrophy/effusion
- 1: Mild synovial hypertrophy/effusion but not beyond the imaginary line*
- 2: Moderate synovial hypertrophy/effusion extending beyond the imaginary line* and proximal with a concave or straight shape
- 3: Severe synovial hypertrophy/effusion extending beyond the imaginary line* and over the talus with a convex shape clearly pushing up the joint capsule

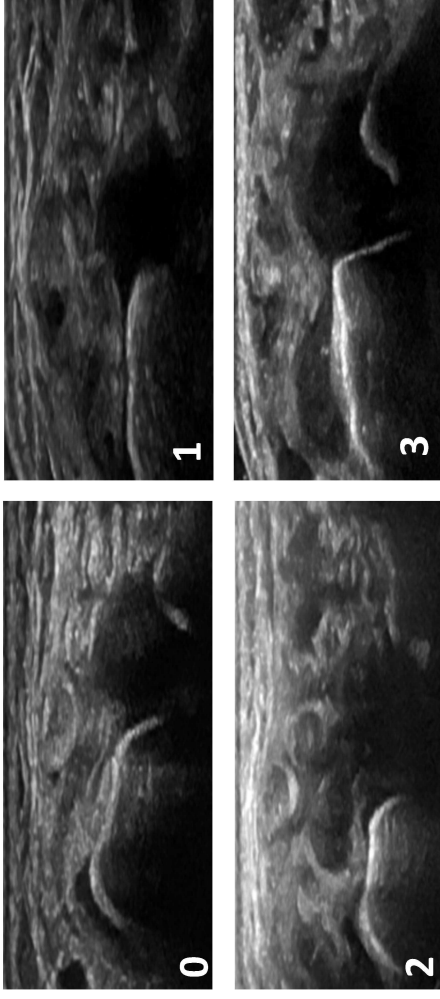
* The line between the top of the cartilage of the head of the talus to the top of the cartilage of the navicular bone

Anterior subtalar



The subject will be in a supine position with the leg straight and the forefoot/ankle in slight eversion. The probe will be positioned at 45 degrees pointing to the heel and then moved proximally and distally. A medial scan of the anterior subtalar joint.

Landmarks: 1) the talus and 2) the sustentaculum tali (calcaneus).



BM scoring for the anterior subtalar joint

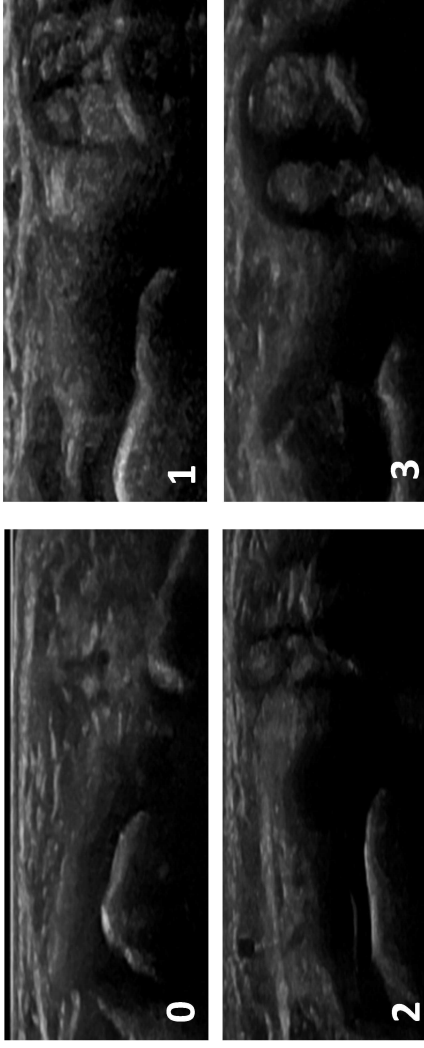
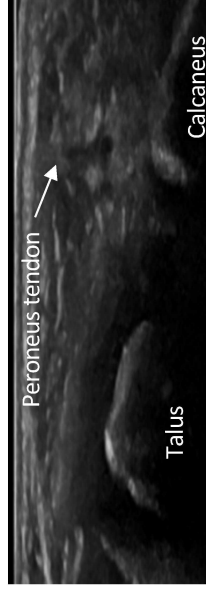
- 0: No sign of synovial hypertrophy/effusion
- 1: Mild synovial hypertrophy/effusion covering up to 25% of the straight part of the talus
- 2: Moderate synovial hypertrophy/effusion covering up to 50% of the straight part of the talus
- 3: Severe synovial hypertrophy/effusion covering more than 50% of the straight part of the talus

Posterior subtalar



The subject will be in a supine position with the leg straight and the forefoot/ankle in slight inversion. The probe will be positioned along the sinus tarsi perpendicular to the sole, and then moved posteriorly. If no distension is seen, the image will be taken visualizing the joint with the peroneus tendons. A lateral scan of the posterior subtalar joint.

Landmarks: 1) the talus and 2) the calcaneus.



BM scoring for the posterior subtalar joint

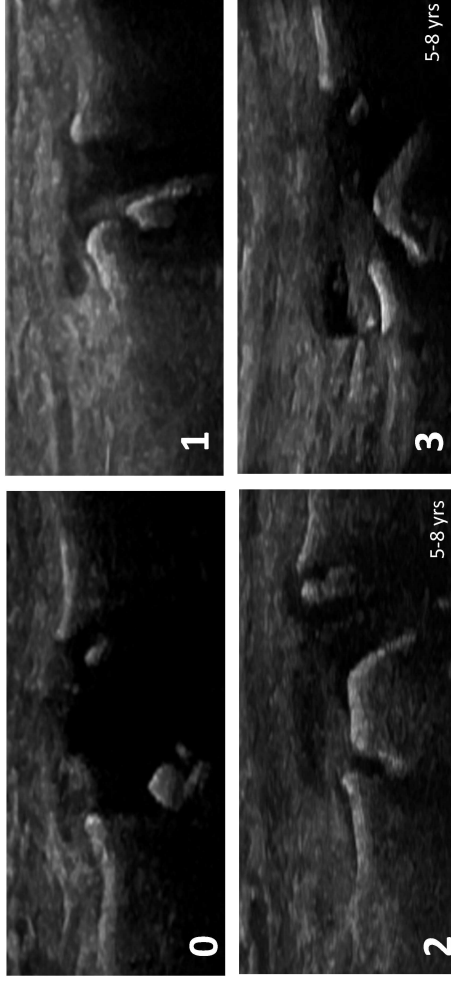
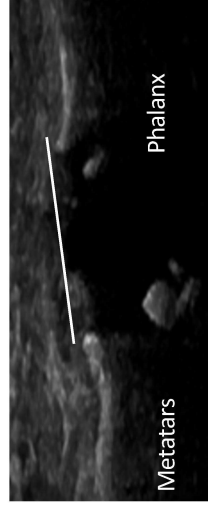
- 0: No sign of synovial hypertrophy/effusion
- 1: Mild synovial hypertrophy/effusion filling the gap between the talus and the calcaneus
- 2: Moderate synovial hypertrophy/effusion extending beyond the talus and the calcaneus but not with a convex shape
- 3: Severe synovial hypertrophy/effusion extending beyond the talus and the calcaneus with a convex shape

MTP2 - MTP3 dorsal



The subject will be in a supine position with the knee at 90 degrees flexion and the foot sole-side down. A longitudinal, dorsal scan of the MTP2 and MTP3 joints.

Landmarks: 1) the head of the metatarsal bone (2/3 of the image) and 2) the base of the proximal phalanx (1/3 of the image).



BM scoring for the MTP2 and MTP3 joints, dorsal

- 0: No sign of synovial hypertrophy/effusion
- 1: Mild synovial hypertrophy/effusion but not beyond the imaginary line*
- 2: Moderate synovial hypertrophy/effusion extending beyond the imaginary line*, but without overall convex shape
- 3: Severe synovial hypertrophy/effusion extending beyond the imaginary line* with a clearly convex shape

* The line between the top of the cartilage of the distal end of the metatars to the top of the cartilage of the proximal end of the phalanx

Ultrasonographic atlas for scoring of B-mode (BM) synovitis in patients with juvenile idiopathic arthritis 13-18 years

Nina Krafft Sande et al.

Included joint regions

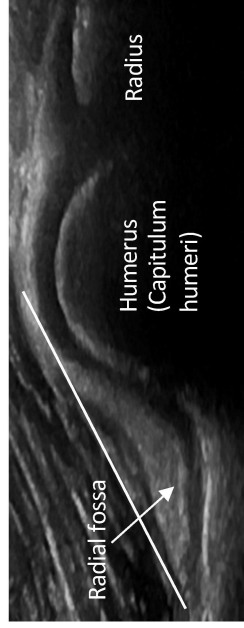
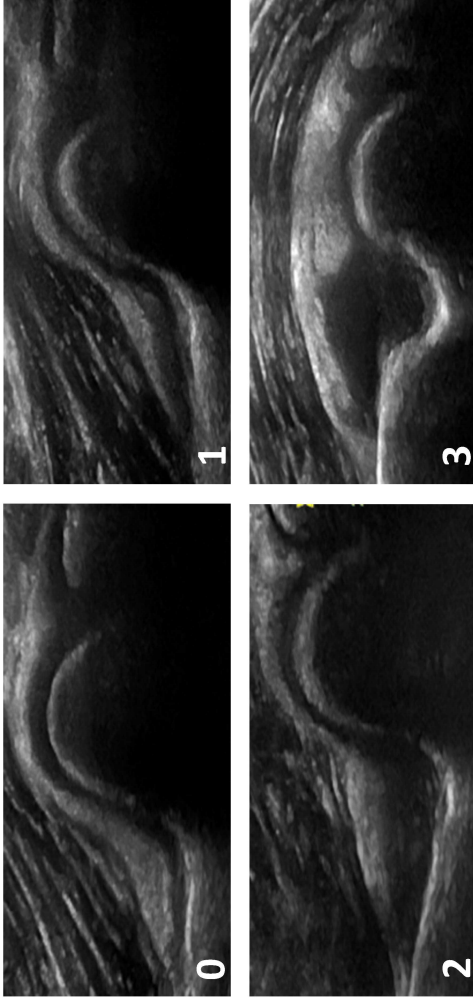
- Anterior elbow
- Posterior elbow
- Wrist (radiocarpal and midcarpal)
- Metacarpophalangeal (MCP) 2-3 dorsal
- Proximal interphalangeal (PIP) 2-3 dorsal
- Proximal interphalangeal (PIP) 2-3 volar
- Hip
- Knee, suprapatellar recess
- Knee, lateral parapatellar recess
- Tibiotalar
- Talonavicular
- Anterior subtalar
- Posterior subtalar
- Metatarsophalangeal (MTP) 2-3 dorsal



Anterior elbow



The subject will be in a supine position. The elbow should be in full extension and supination of the lower arm. A longitudinal anterior scan of the elbow (humeroradial) joint. **Landmarks:** 1) the distal humerus and 2) the radius.



BM scoring for the anterior elbow, the humeroradial joint

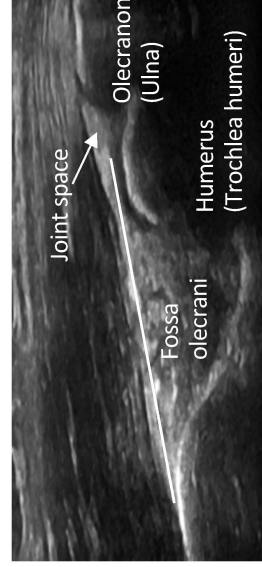
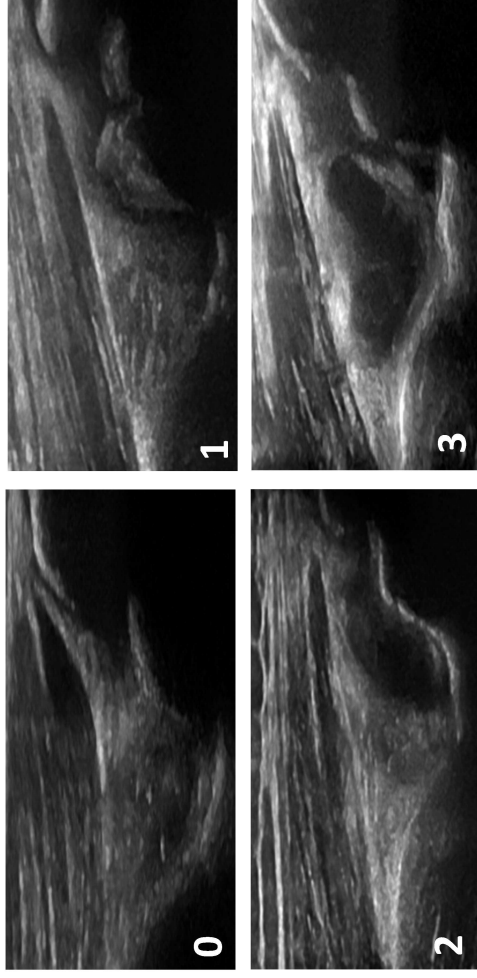
- 0: No or minimal synovial hypertrophy/effusion
- 1: Mild synovial hypertrophy/effusion
- 2: Moderate synovial hypertrophy/effusion up to, but not beyond the imaginary line*
- 3: Severe synovial hypertrophy/effusion beyond the imaginary line* and/or a clearly convex shape

* The line above the radial fossa; between the proximal end of the fossa to the top of the cartilage over the capitulum humeri

Posterior elbow



The subject will be in a supine position. The elbow should be flexed at 90 degrees with the forearm resting on the stomach. A longitudinal posterior scan of the elbow (humeroulnar) joint. **Landmarks:** 1) the distal humerus and 2) the olecranon (ulna).



BM scoring for the posterior elbow, the humeroulnar joint

- 0: No or minimal synovial hypertrophy/effusion
- 1: Mild synovial hypertrophy/effusion, filling up to 25% of the fossa
- 2: Moderate synovial hypertrophy/effusion filling up to 50% of the fossa, but not beyond the imaginary line*
- 3: Severe synovial hypertrophy/effusion filling more than 50% of the fossa and/or extending beyond the imaginary line*

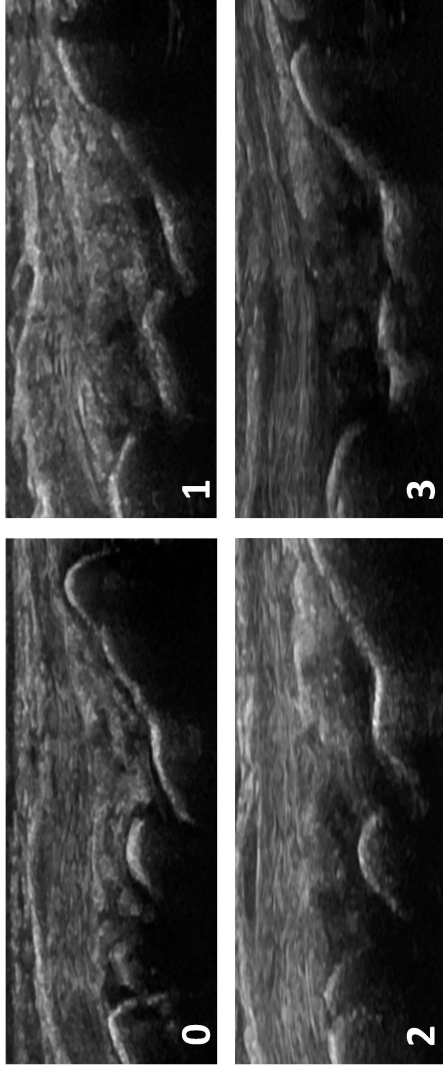
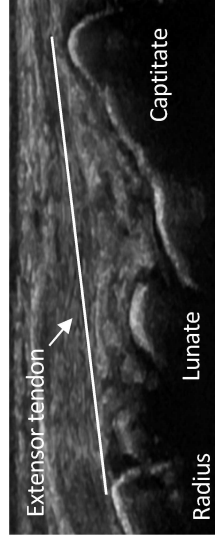
* The line above the fossa olecrani; between the proximal top of the fossa to the top of the cartilage of the trochlea humeri

Radiocarpal and midcarpal



The subject will be in a sitting position, the hands palm-side down in a neutral position on an examination table and resting the elbow on the table. A longitudinal dorsal scan of the radiocarpal and midcarpal joints at the sagittal midline of the wrist, including the distal radius, the lunate and the capitate bone.

Landmarks: 1) the distal end of diaphysis and epiphyseal cartilage of radius and 2) the dorsal recess of the radiocarpal and midcarpal joints and over them 3) a compartment of the extensor tendons according to the area imaged. (Collado et al. 2016)



BM scoring for the radiocarpal and midcarpal joints

- 0: No sign of synovial hypertrophy/effusion
- 1: Mild synovial hypertrophy/effusion
- 2: Moderate synovial hypertrophy/effusion up to, but not beyond the imaginary line*
- 3: Severe synovial hypertrophy/effusion with a convex shape extending beyond the imaginary line* and can push up the extensor tendons

* The line between the top of the cartilage of the distal end of the radius to the top of the cartilage of the capitate

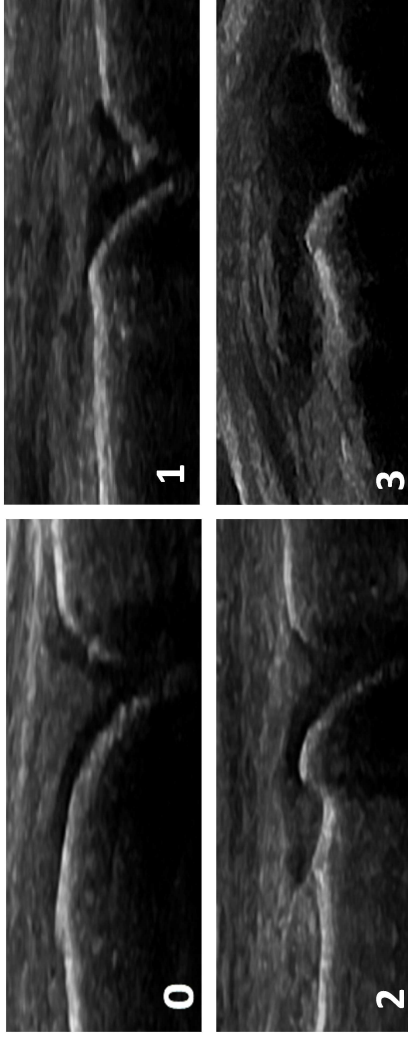
MCP2 - MCP3 dorsal



The subject will be in a sitting position with the hands palm-side down in a neutral position on an examination table.

A longitudinal dorsal scan of the MCP2 and MCP3 joints.

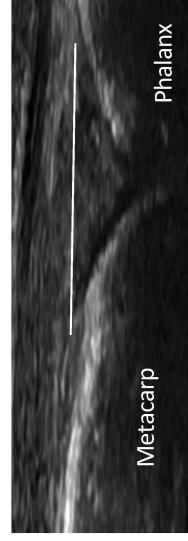
Landmarks: 1) the head of the metacarpal bone (2/3 of the image) and 2) the base of the proximal phalanx (1/3 of the image).



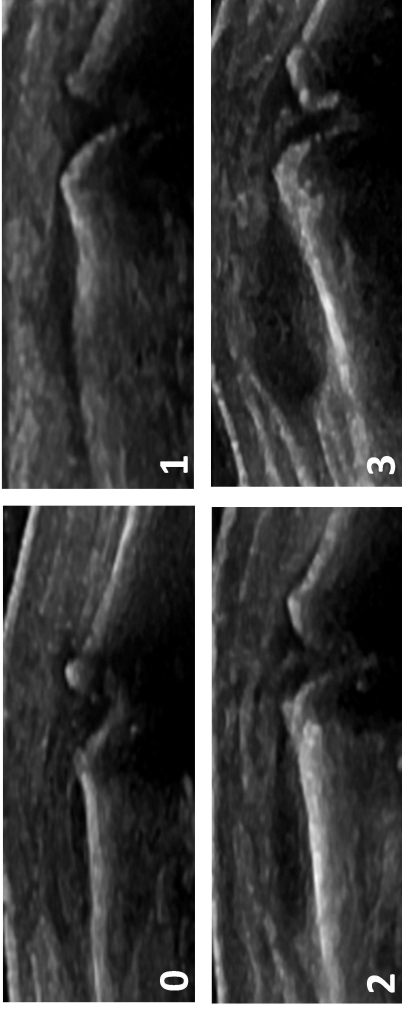
BM scoring for the MCP2 and MCP3 joints, dorsal

- 0: No sign of synovial hypertrophy/effusion
 1: Mild synovial hypertrophy/effusion but not beyond the imaginary line*
 2: Moderate synovial hypertrophy/effusion extending beyond the imaginary line*, but without overall convex shape
 3: Severe synovial hypertrophy/effusion extending beyond the imaginary line* with a clearly convex shape

*The line between the top of the cartilage of the distal end of the metacarp to the top of the cartilage of the proximal end of the phalanx



PIP2 - PIP3 dorsal



The subject will be in a sitting position with the hands palm-side down in a neutral position on an examination table.

A longitudinal dorsal scan of the PIP2 and PIP3 joints.

Landmarks: 1) the head of the proximal phalanx (2/3 of the image) and 2) the base of the middle phalanx (1/3 of the image).



BM scoring for the PIP2 and PIP3 joints, dorsal

- 0: No sign of synovial hypertrophy/effusion
- 1: Mild synovial hypertrophy/effusion but not beyond the imaginary line*
- 2: Moderate synovial hypertrophy/effusion extending beyond the imaginary line*, but without overall convex shape
- 3: Severe synovial hypertrophy/effusion extending beyond the imaginary line* with a clearly convex shape

**The line between the top of the cartilage of the distal end of the proximal phalanx to the top of the cartilage of the proximal end of the middle phalanx*

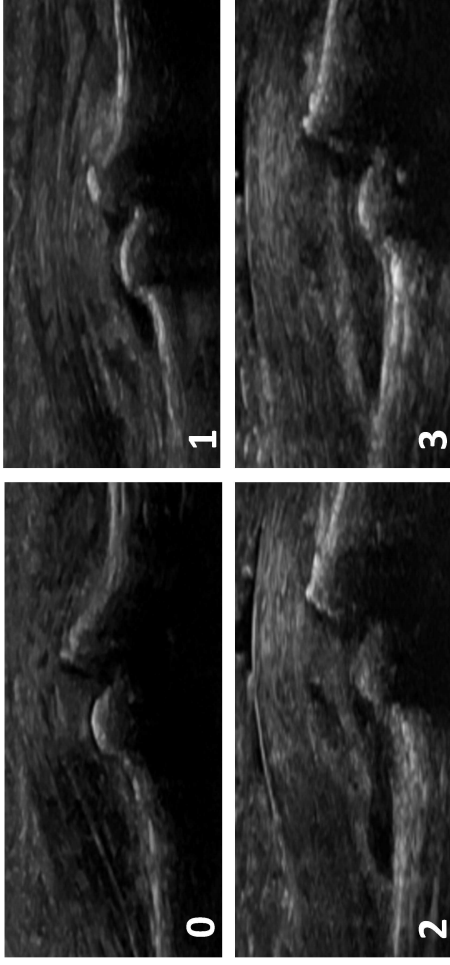
PIP2 - PIP3 volar



The subject will be in a sitting position with the hands palm-side up in a neutral position on an examination table.

A longitudinal volar scan of the PIP2 and PIP3 joints.

Landmarks: 1) the head of the proximal phalanx and 2) the base of the middle phalanx and 3) the flexor tendon.



BM scoring for the PIP2 and PIP3 joints, volar

0: No sign of synovial hypertrophy/effusion

1: Mild synovial hypertrophy/effusion, possible to extend proximally but without convex shape

2: Moderate synovial hypertrophy/effusion extending over the proximal phalanx with convex shape, but not filling the joint space between proximal and middle phalanx

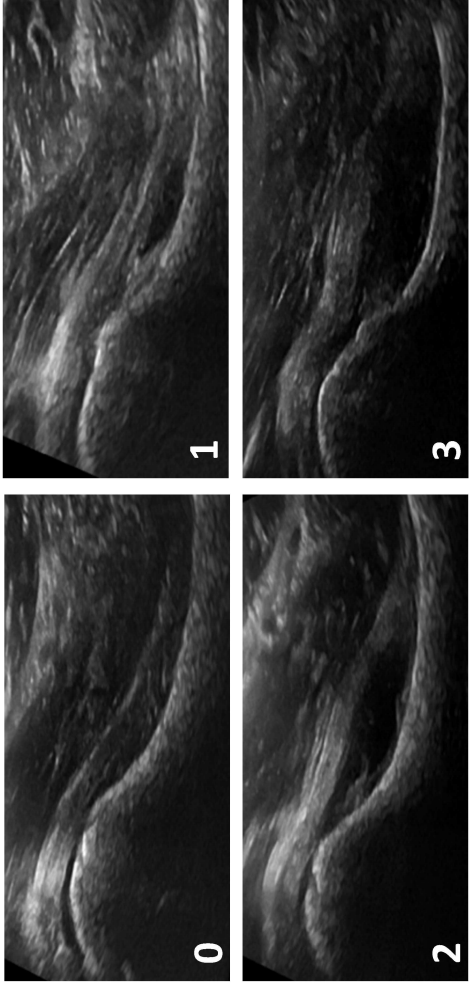
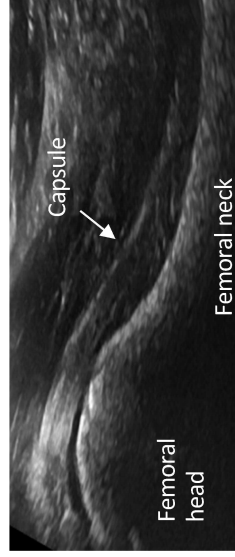
3: Severe synovial hypertrophy/effusion extending over the proximal phalanx and filling the joint space between proximal and middle phalanx with an overall convex shape

Hip



The subject will be in a supine position with the hip in a neutral position, slightly externally rotated. A longitudinal anterior scan parallel to the femoral neck of the hip joint.

Landmarks: 1) the femoral head and 2) the femoral neck.



BM scoring for the hip joint

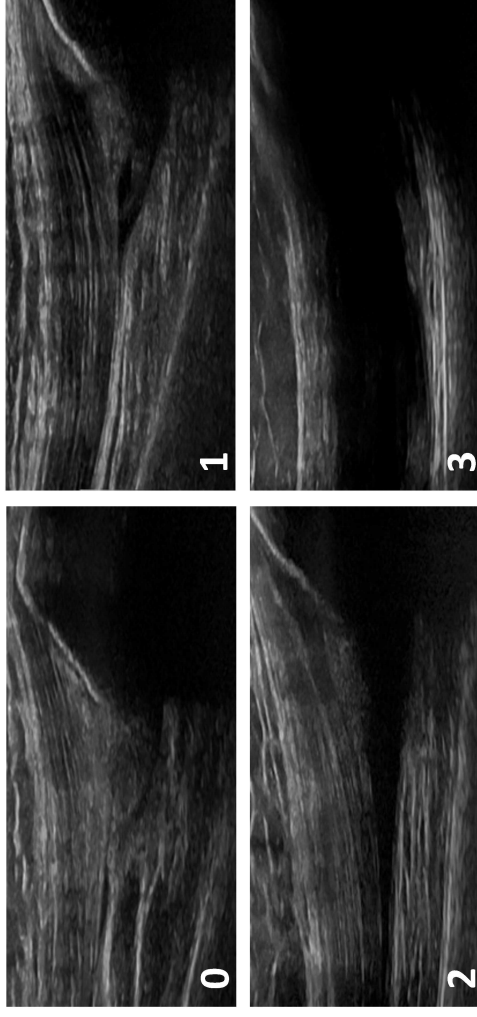
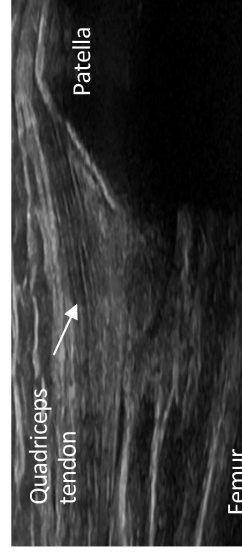
- 0: No sign of synovial hypertrophy/effusion
- 1: Mild synovial hypertrophy/effusion, but just a "slit" of fluid between the two layers of the capsule
- 2: Moderate synovial hypertrophy/effusion leading to a straight line/minimal convex shape of the capsule
- 3: Severe synovial hypertrophy/effusion with a clearly convex shape, the effusion can also extend proximally over the femoral head

Knee, suprapatellar recess



The subject will be in a supine position. The knee should be flexed at 30 degrees, and images taken after the subject completes flexion and extension three times. A longitudinal scan of the suprapatellar joint space.

Landmarks: 1) the proximal third of the patella and 2) a clearly visualized quadriceps tendon. (Ting et al. 2019)



BM scoring for the knee, suprapatellar recess

0: "Slit" of fluid/synovium without elevation of the pre-patellar fat pad but with only minimal extension beyond the prepatellar fat pad

1: Mild synovial hypertrophy/effusion with elevation of the prepatellar fat pad and extension proximally <50% of the visualized portion of the quadriceps tendon

2: Moderate synovial hypertrophy/effusion elevating the pre-patellar fat pad with extension proximally > 50% of the visualized portion of the quadriceps tendon

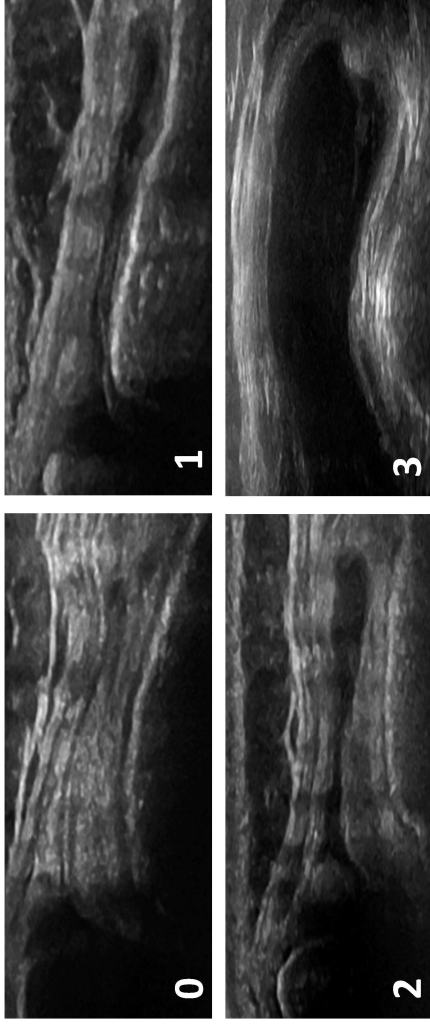
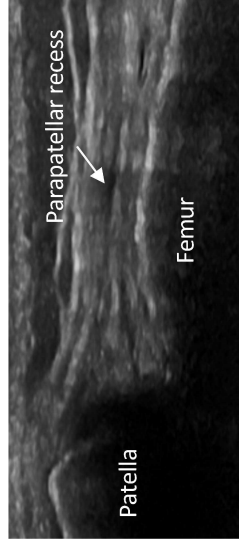
3: Significant distension of the suprapatellar recess throughout the image, and with the most proximal portion of the synovial recess being > 50% of the maximum distension of the recess (Ting et al. 2019)

Knee, lateral parapatellar recess



The subject will be in a supine position. The knee should be flexed at 30 degrees. For the lateral parapatellar recess the image will be obtained with the probe in transverse position over the mid-patella with both the patella and femur in view.

Landmarks: 1) the superior edge of the patella and 2) the femoral condyle.
(Ting et al. 2019)



BM scoring for the knee, lateral parapatellar recess

0: Empty parapatellar recess but a minimal bulge of synovial hypertrophy/effusion may be found extending to the patellofemoral joint line

1: Synovial hypertrophy/effusion filling < 1/3 of the full area of the parapatellar recess

2: Synovial hypertrophy/effusion filling between one to two thirds of the full area of the parapatellar recess

3: Synovial hypertrophy/effusion that fills >2/3 of the full area of the parapatellar recess and clearly pushing up the retinaculum
(Ting et al. 2019)

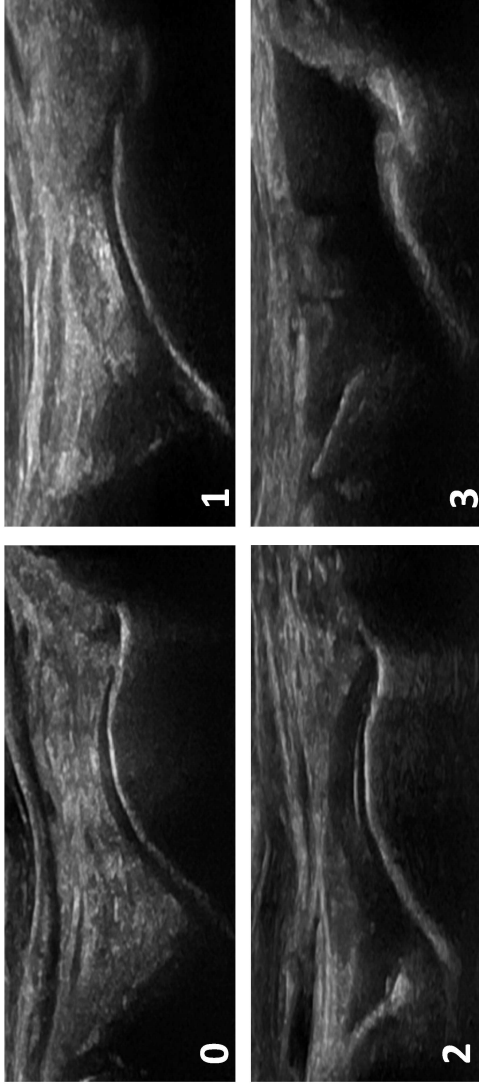
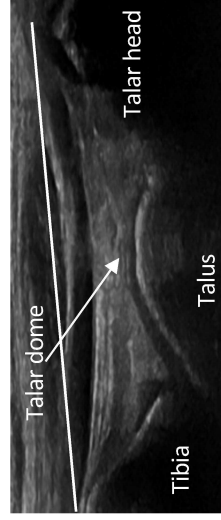
Tibiotalar



The subject will be in a supine position with the knee at 90 degrees flexion and the foot sole-side down.

A longitudinal scan of the tibiotalar joint.

Landmarks: 1) the distal end of the tibia and 2) the talus.



BM scoring for the tibiotalar joint

0: No sign of synovial hypertrophy/effusion in the tibiotalar joint, but possible to have a minimal amount of fluid in the concave neck of the talus

1: Mild synovial hypertrophy/effusion filling the gap between the tibia and the talus and in the concave neck of the talus, but not continuously over the talus

2: Moderate synovial hypertrophy/effusion filling up to 50% of the area between the tibia, the talus and the imaginary line* and continuously over the talus

3: Severe synovial hypertrophy/effusion filling more than 50% of the area between the tibia, the talus and the imaginary line*, or beyond the imaginary line*

*The line between the top of the cartilage of the distal end of the tibia and the top of the cartilage of the talar head

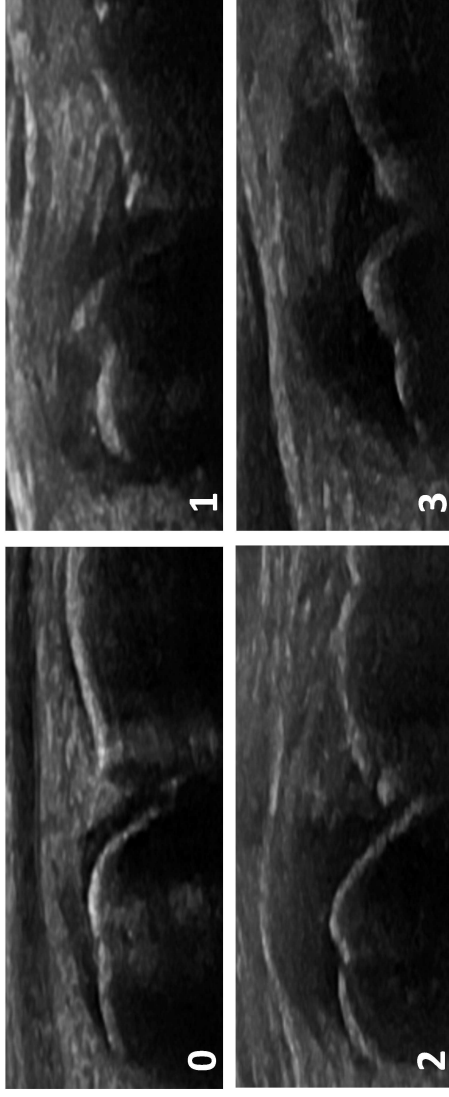
Talonavicular



The subject will be in a supine position with the knee at 90 degrees flexion and the foot sole-side down.

A longitudinal scan of the talonavicular joint.

Landmarks: 1) the talus and 2) the navicular bone.



BM scoring for the talonavicular joint

- 0: No sign of synovial hypertrophy/effusion
- 1: Mild synovial hypertrophy/effusion but not beyond the imaginary line*
- 2: Moderate synovial hypertrophy/effusion extending beyond the imaginary line* and proximal with a concave or straight shape
- 3: Severe synovial hypertrophy/effusion extending beyond the imaginary line* and over the talus with a convex shape clearly pushing up the joint capsule

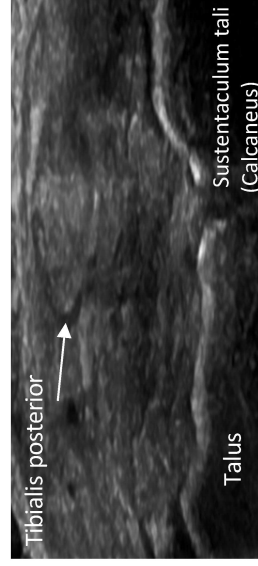
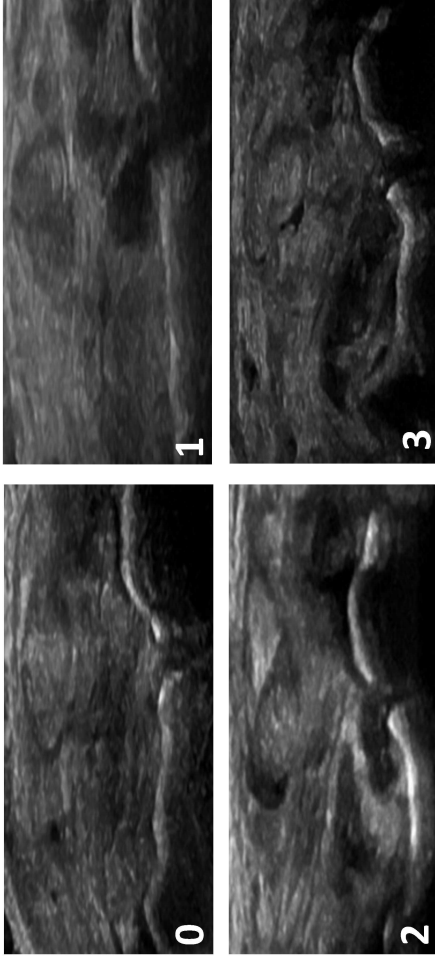
* The line between the top of the cartilage of the head of the talus to the top of the cartilage of the navicular bone

Anterior subtalar



The subject will be in a supine position with the leg straight and the forefoot/ankle in slight eversion. The probe will be positioned at 45 degrees pointing to the heel and then moved proximally and distally. A medial scan of the anterior subtalar joint.

Landmarks: 1) the talus and 2) the sustentaculum tali (calcaneus).



BM scoring for the anterior subtalar joint

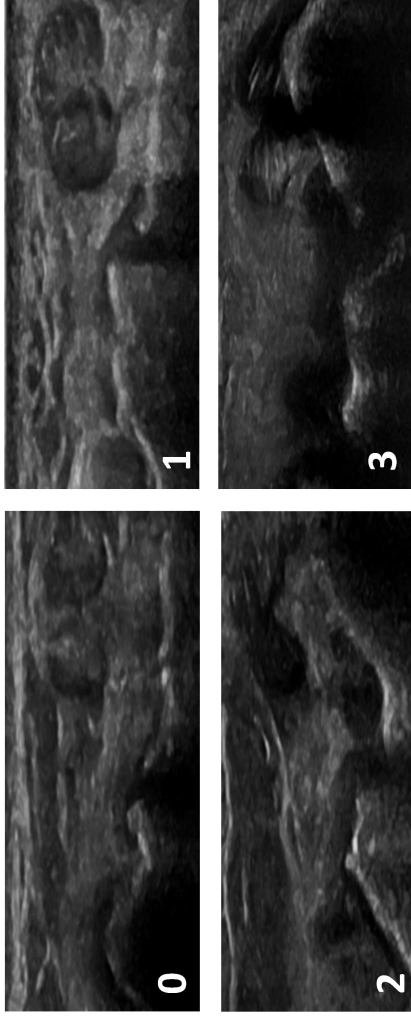
- 0: No sign of synovial hypertrophy/effusion
 1: Mild synovial hypertrophy/effusion covering up to 25% of the straight part of the talus
 2: Moderate synovial hypertrophy/effusion covering up to 50% of the straight part of the talus
 3: Severe synovial hypertrophy/effusion covering more than 50% of the straight part of the talus

Posterior subtalar



The subject will be in a supine position with the leg straight and the forefoot/ankle in slight inversion. The probe will be positioned along the sinus tarsi perpendicular to the sole, and then moved posteriorly. If no distension is seen, the image will be taken visualizing the joint with the peroneus tendons. A lateral scan of the posterior subtalar joint.

Landmarks: 1) the talus and 2) the calcaneus.



BM scoring for the posterior subtalar joint

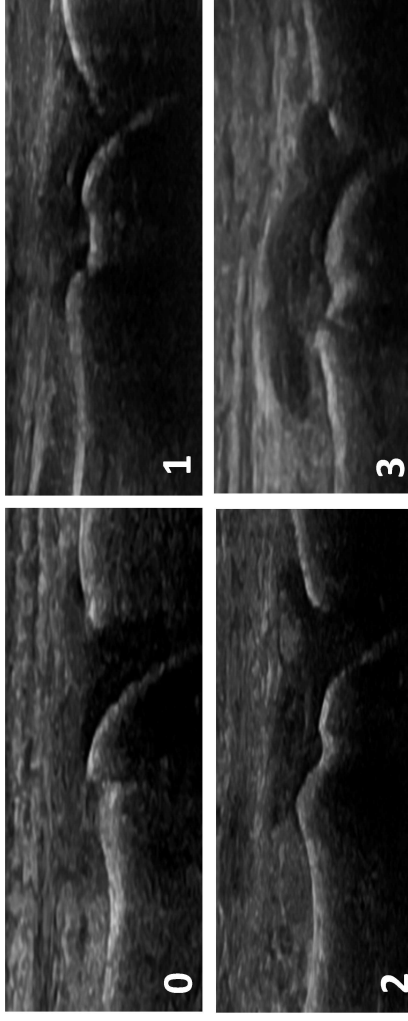
- 0: No sign of synovial hypertrophy/effusion
- 1: Mild synovial hypertrophy/effusion filling the gap between the talus and the calcaneus
- 2: Moderate synovial hypertrophy/effusion extending beyond the talus and the calcaneus but not with a convex shape
- 3: Severe synovial hypertrophy/effusion extending beyond the talus and the calcaneus with a convex shape

MTP2 - MTP3 dorsal



The subject will be in a supine position with the knee at 90 degrees flexion and the foot sole-side down. A longitudinal dorsal scan of the MTP2 and MTP3 joints.

Landmarks: 1) the head of the metatarsal bone (2/3 of the image) and 2) the base of the proximal phalanx (1/3 of the image).



BM scoring for the MTP2 and MTP3 joints, dorsal

- 0: No sign of synovial hypertrophy/effusion
- 1: Mild synovial hypertrophy/effusion but not beyond the imaginary line*
- 2: Moderate synovial hypertrophy/effusion extending beyond the imaginary line*, but without overall convex shape
- 3: Severe synovial hypertrophy/effusion extending beyond the imaginary line* with a clearly convex shape

* The line between the top of the cartilage of the distal end of the metatars to the top of the cartilage of the proximal end of the phalanx

Ultrasonographic atlas for scoring of B-mode (BM) synovitis in patients with juvenile idiopathic arthritis 5-8 years

Nina Krafft Sande et al.

Included joint regions

- Anterior elbow
- Posterior elbow
- Wrist (radiocarpal and midcarpal)
- Metacarpophalangeal (MCP) 2-3 dorsal
- Proximal interphalangeal (PIP) 2-3 dorsal
- Proximal interphalangeal (PIP) 2-3 volar
- Hip
- Knee, suprapatellar recess
- Knee, lateral parapatellar recess
- Tibiotalar
- Talonavicular
- Anterior subtalar
- Posterior subtalar
- Metatarsophalangeal (MTP) 2-3 dorsal

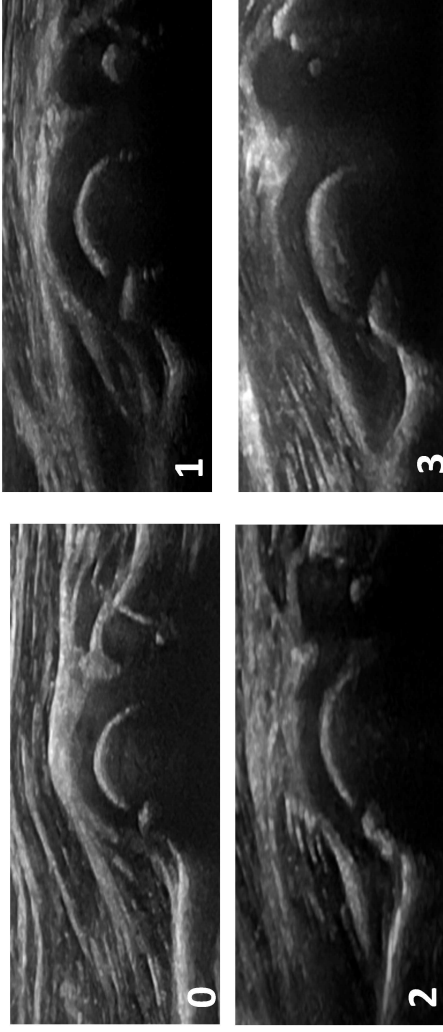
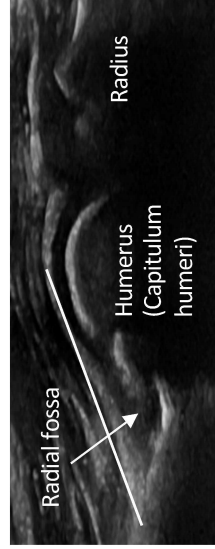


Anterior elbow



The subject will be in a supine position, but the scanning can also be done with the subject on the parents' lap. The elbow should be in full extension and supination of the lower arm. A longitudinal anterior scan of the elbow (humeroradial) joint.

Landmarks: 1) the distal humerus and 2) the radius.



BM scoring for the anterior elbow, the humeroradial joint

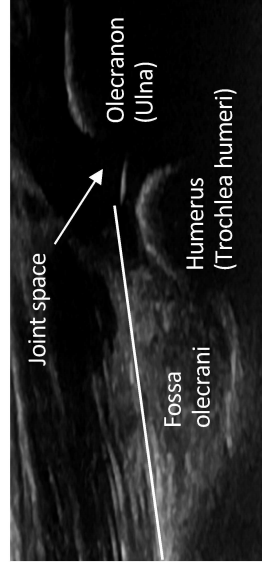
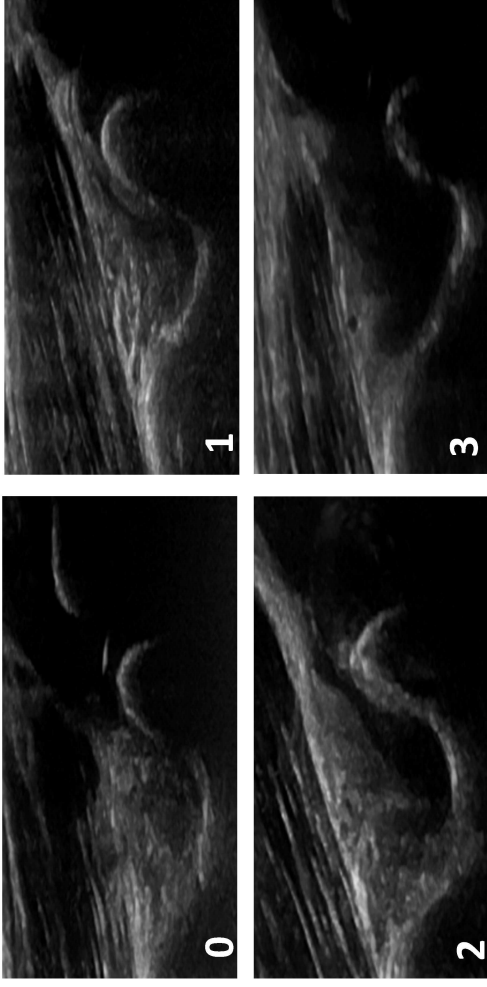
- 0: No or minimal synovial hypertrophy/effusion
- 1: Mild synovial hypertrophy/effusion
- 2: Moderate synovial hypertrophy/effusion up to, but not beyond the imaginary line*
- 3: Severe synovial hypertrophy/effusion beyond the imaginary line* and/or a clearly convex shape

* The line above the radial fossa; between the proximal end of the fossa to the top of the cartilage over the capitulum humeri

Posterior elbow



The subject will be in a supine position, but the scanning can also be done with the subject on the parents' lap. The elbow should be flexed at 90 degrees with the forearm resting on the stomach. A longitudinal posterior scan of the elbow (humeroulnar) joint. **Landmarks:** 1) the distal humerus and 2) the olecranon (ulna).



BM scoring for the posterior elbow, the humeroulnar joint

- 0: No or minimal synovial hypertrophy/effusion
- 1: Mild synovial hypertrophy/effusion filling up to 25% of the fossa
- 2: Moderate synovial hypertrophy/effusion filling up to 50% of the fossa, but not beyond the imaginary line*
- 3: Severe synovial hypertrophy/effusion filling more than 50% of the fossa and/or extending beyond the imaginary line*

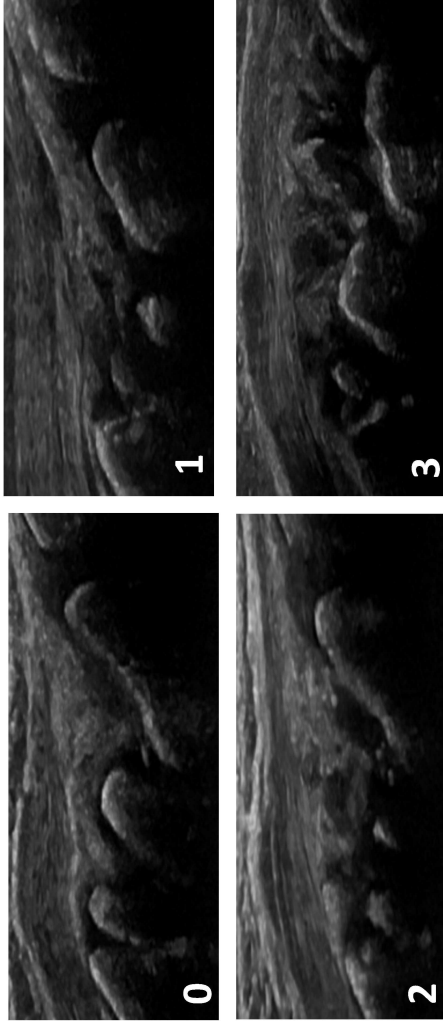
* The line above the fossa olecrani; between the proximal top of the fossa to the top of the cartilage of the trochlea humeri

Radiocarpal and midcarpal



The subject will be in a sitting position, the hands palm-side down in a neutral position on an examination table and resting the elbow on the table. A longitudinal dorsal scan of the radiocarpal and midcarpal joints at the sagittal midline of the wrist, including the distal radius, the lunate and the capitate bone.

Landmarks: 1) the distal end of diaphysis and epiphyseal cartilage of radius and 2) the dorsal recess of the radiocarpal and midcarpal joints and over them 3) a compartment of the extensor tendons according to the area imaged. (Collado et al. 2016)

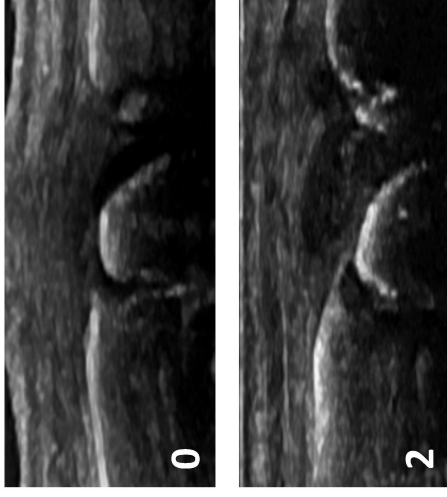


BM scoring for the radiocarpal and midcarpal joints

- 0: No sign of synovial hypertrophy/effusion
- 1: Mild synovial hypertrophy/effusion
- 2: Moderate synovial hypertrophy/effusion up to, but not beyond the imaginary line*
- 3: Severe synovial hypertrophy/effusion with a convex shape extending beyond the imaginary line* and can push up the extensor tendons

* The line between the top of the cartilage of the distal end of the radius to the top of the cartilage of the capitate

MCP2 - MCP3 dorsal



The subject will be in a sitting position with the hands palm-side down in a neutral position on an examination table.

A longitudinal dorsal scan of the MCP2 and MCP3 joints.

Landmarks: 1) the head of the metacarpal bone (2/3 of the image) and 2) the base of the proximal phalanx (1/3 of the image).



BM scoring for the MCP2 and MCP3 joints, dorsal

- 0: No sign of synovial hypertrophy/effusion
 1: Mild synovial hypertrophy/effusion but not beyond the imaginary line*
 2: Moderate synovial hypertrophy/effusion extending beyond the imaginary line*, but without overall convex shape
 3: Severe synovial hypertrophy/effusion extending beyond the imaginary line* with a clearly convex shape

*The line between the top of the cartilage of the distal end of the metacarp to the top of the cartilage of the proximal end of the phalanx

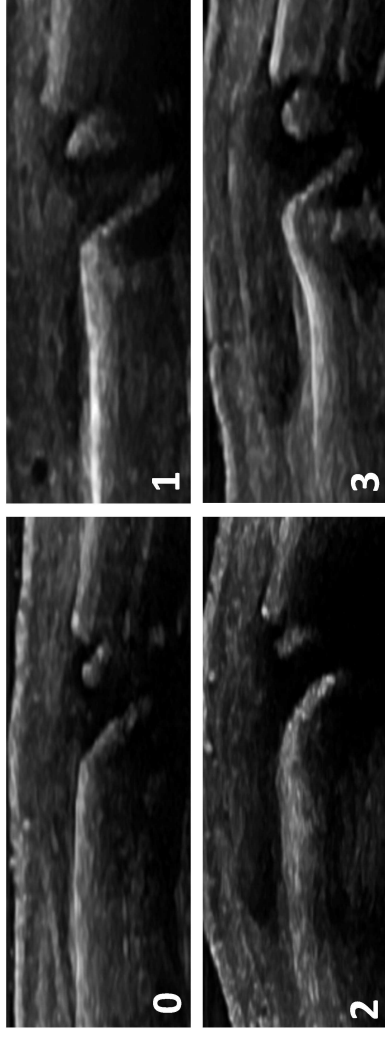
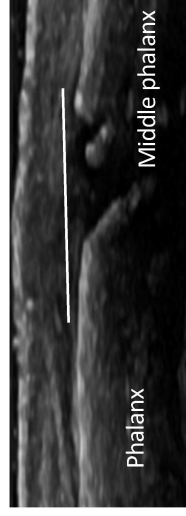
PIP2 - PIP3 dorsal



The subject will be in a sitting position with the hands palm-side down in a neutral position on an examination table.

A longitudinal dorsal scan of the PIP2 and PIP3 joints.

Landmarks: 1) the head of the proximal phalanx (2/3 of the image) and 2) the base of the middle phalanx (1/3 of the image).



BM scoring for the PIP2 and PIP3 joints, dorsal

- 0: No sign of synovial hypertrophy/effusion
- 1: Mild synovial hypertrophy/effusion but not beyond the imaginary line*
- 2: Moderate synovial hypertrophy/effusion extending beyond the imaginary line*, but without overall convex shape
- 3: Severe synovial hypertrophy/effusion extending beyond the imaginary line* with a clearly convex shape

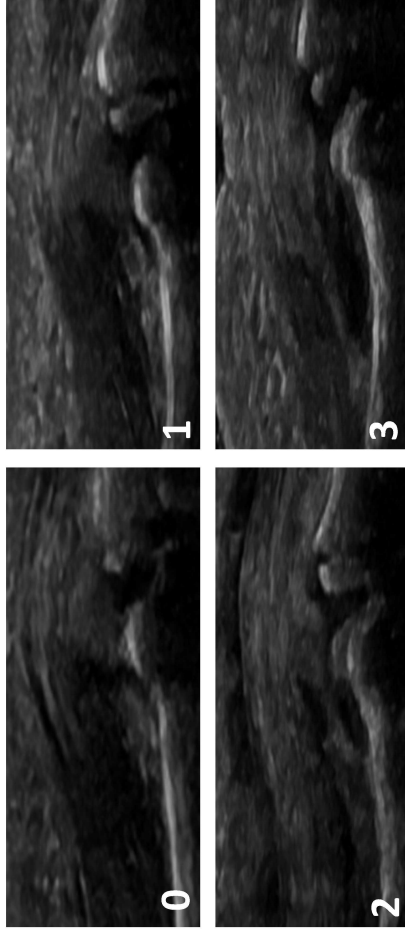
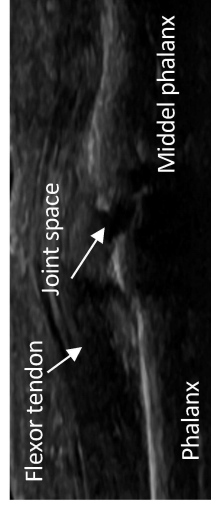
**The line between the top of the cartilage of the distal end of the proximal phalanx to the top of the cartilage of the proximal end of the middle phalanx*

PIP2 - PIP3 volar



The subject will be in a sitting position with the hands palm-side up in a neutral position on an examination table. A longitudinal volar scan of the PIP2 and PIP3 joints.

Landmarks: 1) the head of the proximal phalanx and 2) the base of the middle phalanx and 3) the flexor tendon.



BM scoring for the PIP2 and PIP3 joints, volar

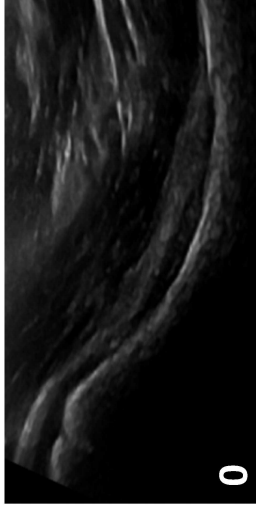
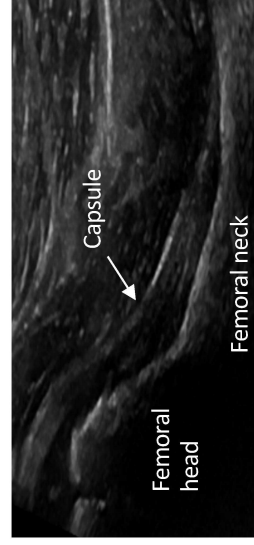
- 0: No sign of synovial hypertrophy/effusion
 1: Mild synovial hypertrophy/effusion, possible to extend proximally but without convex shape
 2: Moderate synovial hypertrophy/effusion extending over the proximal phalanx with convex shape, but not filling the joint space between proximal and middle phalanx
 3: Severe synovial hypertrophy/effusion extending over the proximal phalanx and filling the joint space between proximal and middle phalanx with an overall convex shape

Hip

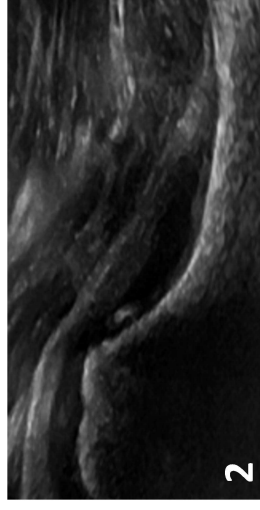
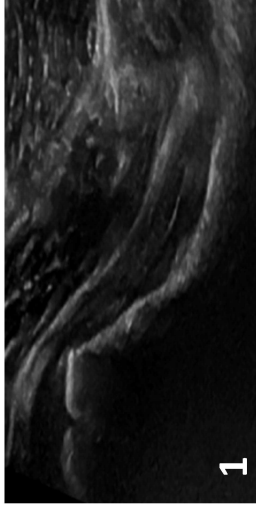


The subject will be in a supine position with the hip in a neutral position, slightly externally rotated. A longitudinal anterior scan parallel to the femoral neck of the hip joint.

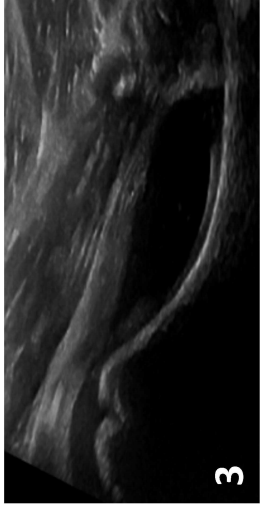
Landmarks: 1) the femoral head and 2) the femoral neck.



1



3



BM scoring for the hip joint

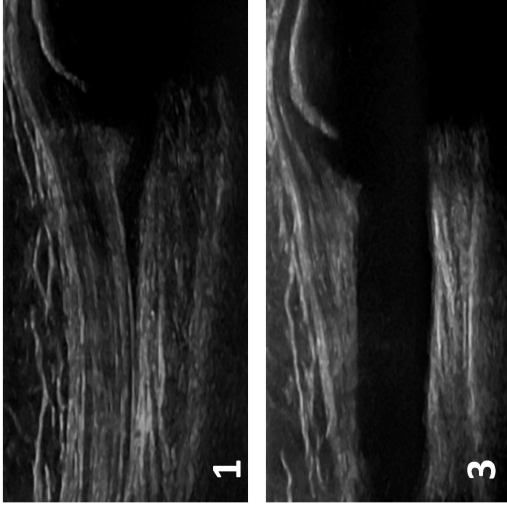
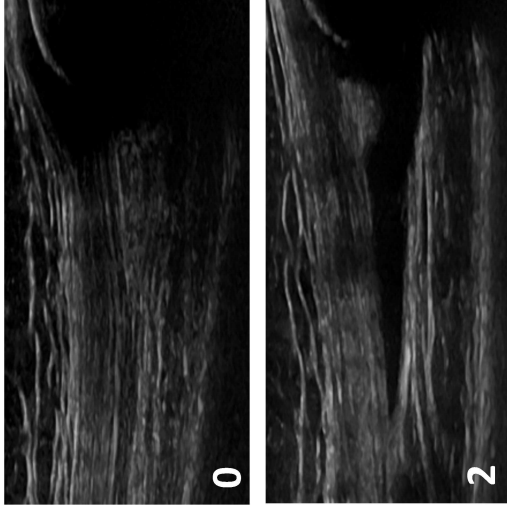
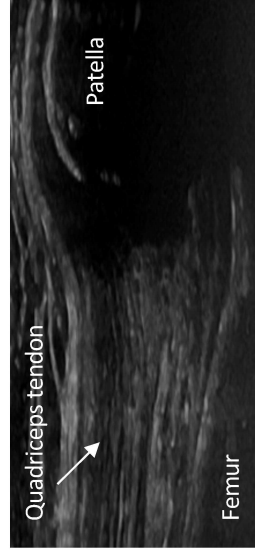
- 0: No sign of synovial hypertrophy/effusion
- 1: Mild synovial hypertrophy/effusion, but just a "slit" of fluid between the two layers of the capsule
- 2: Moderate synovial hypertrophy/effusion leading to a straight line/minimal convex shape of the capsule
- 3: Severe synovial hypertrophy/effusion with a clearly convex shape, the effusion can also extend proximally over the femoral head

Knee, suprapatellar recess



The subject will be in a supine position. The knee should be flexed at 30 degrees, and images taken after the subject completes flexion and extension three times. A longitudinal scan of the suprapatellar joint space. For the youngest subjects, the patella should be 1/3 of the image to compensate for the relatively shorter femur.

Landmarks: 1) the proximal third of the patella and 2) a clearly visualized quadriceps tendon. (Ting et al. 2019)



BM scoring for the knee, suprapatellar recess

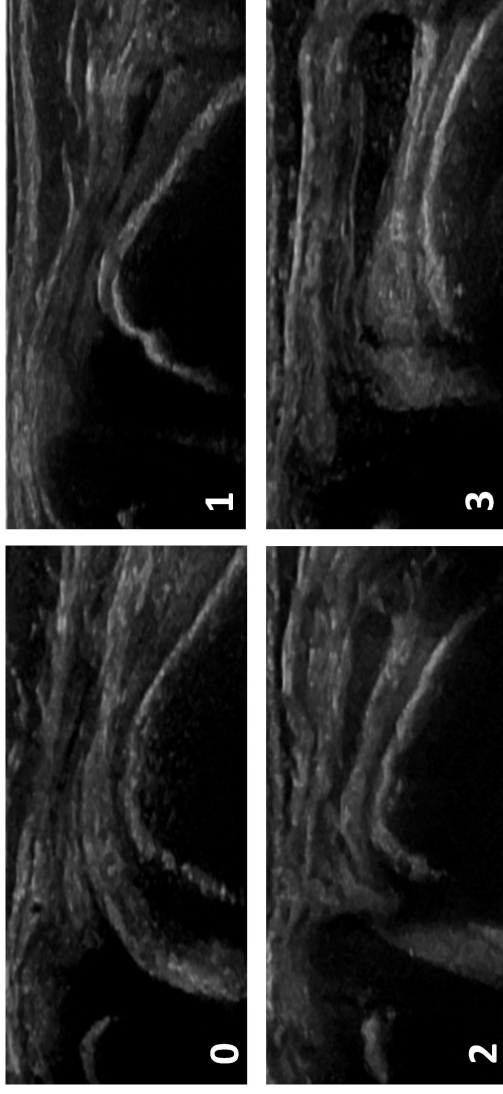
- 0: "Slit" of fluid/synovium without elevation of the pre-patellar fat pad but with only minimal extension beyond the prepatellar fat pad
- 1: Mild synovial hypertrophy/effusion with elevation of the prepatellar fat pad and extension proximally <50% of the visualized portion of the quadriceps tendon
- 2: Moderate synovial hypertrophy/effusion elevating the pre-patellar fat pad with extension proximally > 50% of the visualized portion of the quadriceps tendon
- 3: Significant distension of the suprapatellar recess throughout the image, and with the most proximal portion of the synovial recess being > 50% of the maximum distension of the recess (Ting et al. 2019)

Knee, lateral parapatellar recess



The subject will be in a supine position. The knee should be flexed at 30 degrees. For the lateral parapatellar recess the image will be obtained with the probe in transverse position over the mid-patella with both the patella and femur in view.

Landmarks: 1) the superior edge of the patella and 2) the femoral condyle.
(Ting et al. 2019)



BM scoring for the knee, lateral parapatellar recess

- 0: Empty parapatellar recess but a minimal bulge of synovial hypertrophy/effusion may be found extending to the patellofemoral joint line
- 1: Synovial hypertrophy/effusion filling < 1/3 of the full area of the parapatellar recess
- 2: Synovial hypertrophy/effusion filling between one to two thirds of the full area of the parapatellar recess
- 3: Synovial hypertrophy/effusion that fills >2/3 of the full area of the parapatellar recess and clearly pushing up the retinaculum
(Ting et al. 2019)

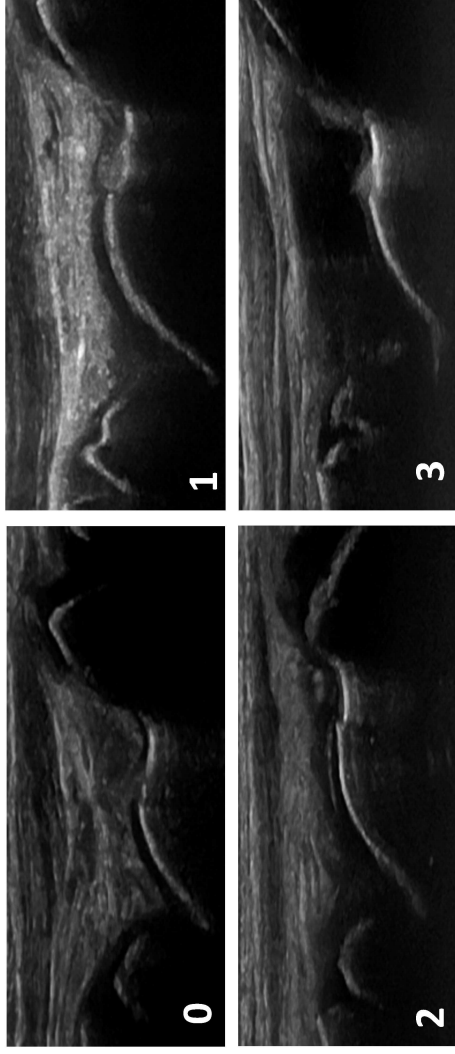
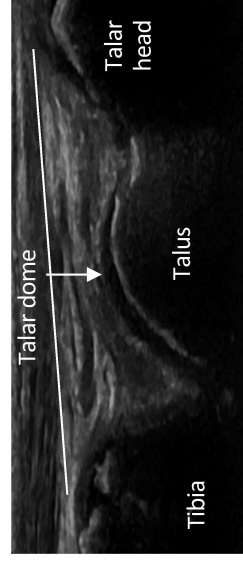
Tibiotalar



The subject will be in a supine position with the knee at 90 degrees flexion and the foot sole-side down.

A longitudinal scan of the tibiotalar joint.

Landmarks: 1) the distal end of the tibia and 2) the talus.



BM scoring for the tibiotalar joint

- 0: No sign of synovial hypertrophy/effusion in the tibiotalar joint, but possible to have a minimal amount of fluid in the concave neck of the talus
- 1: Mild synovial hypertrophy/effusion filling the gap between the tibia and the talus and in the concave neck of the talus, but not continuously over the talus
- 2: Moderate synovial hypertrophy/effusion filling up to 50% of the area between the tibia, the talus and the imaginary line* and continuously over the talus
- 3: Severe synovial hypertrophy/effusion filling more than 50% of the area between the tibia, the talus and the imaginary line*, or beyond the imaginary line*

*The line between the top of the cartilage of the distal end of the tibia and the top of the cartilage of the talar head



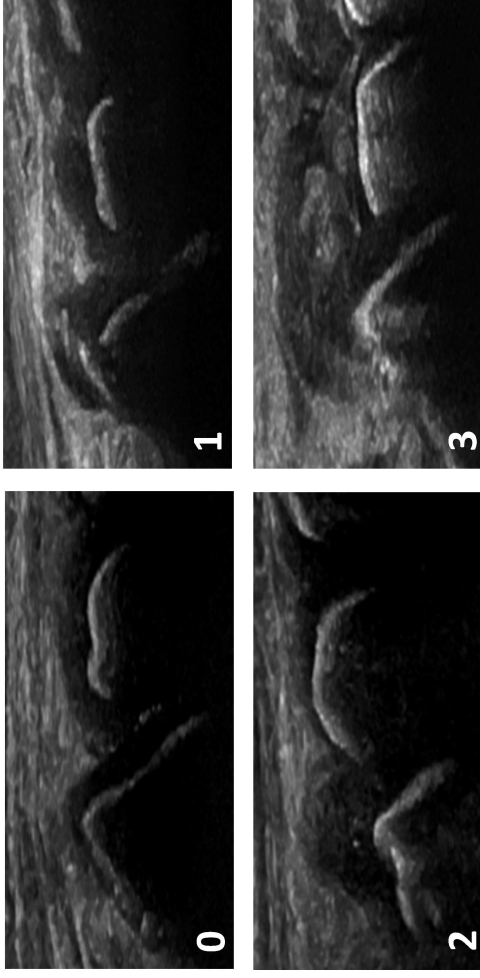
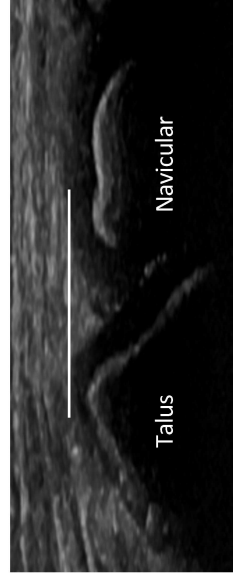
Talonavicular



The subject will be in a supine position with the knee at 90 degrees flexion and the foot sole-side down.

A longitudinal scan of the talonavicular joint.

Landmarks: 1) the talus and 2) the navicular bone.



BM scoring for the talonavicular joint

- 0: No sign of synovial hypertrophy/effusion
- 1: Mild synovial hypertrophy/effusion but not beyond the imaginary line*
- 2: Moderate synovial hypertrophy/effusion extending beyond the imaginary line* and proximal with a concave or straight shape
- 3: Severe synovial hypertrophy/effusion extending beyond the imaginary line* and over the talus with a convex shape clearly pushing up the joint capsule

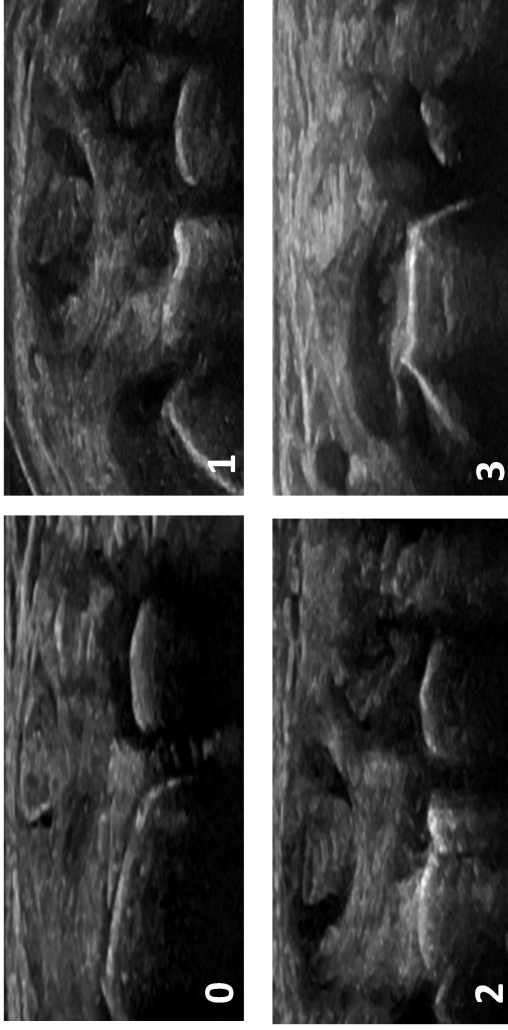
* The line between the top of the cartilage of the head of the talus to the top of the cartilage of the navicular bone

Anterior subtalar



The subject will be in a supine position with the leg straight and the forefoot/ankle in slight eversion. The probe will be positioned at 45 degrees pointing to the heel and then moved proximally and distally. A medial scan of the anterior subtalar joint.

Landmarks: 1) the talus and 2) the sustentaculum tali (calcaneus).



BM scoring for the anterior subtalar joint

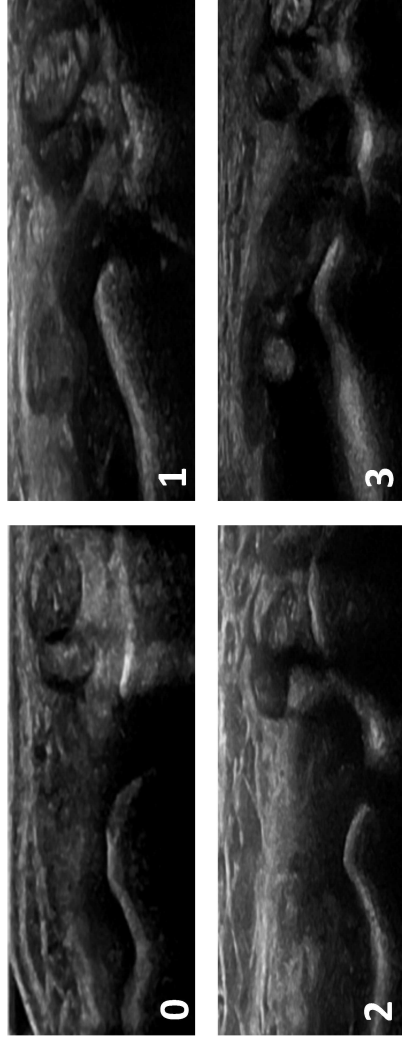
- 0: No sign of synovial hypertrophy/effusion
- 1: Mild synovial hypertrophy/effusion covering up to 25% of the straight part of the talus
- 2: Moderate synovial hypertrophy/effusion covering up to 50% of the straight part of the talus
- 3: Severe synovial hypertrophy/effusion covering more than 50% of the straight part of the talus

Posterior subtalar



The subject will be in a supine position with the leg straight and the forefoot/ankle in slight inversion. The probe will be positioned along the sinus tarsi perpendicular to the sole, and then moved posteriorly. If no distension is seen, the image will be taken visualizing the joint with the peroneus tendons. A lateral scan of the posterior subtalar joint.

Landmarks: 1) the talus and 2) the calcaneus.



BMJ scoring for the posterior subtalar joint

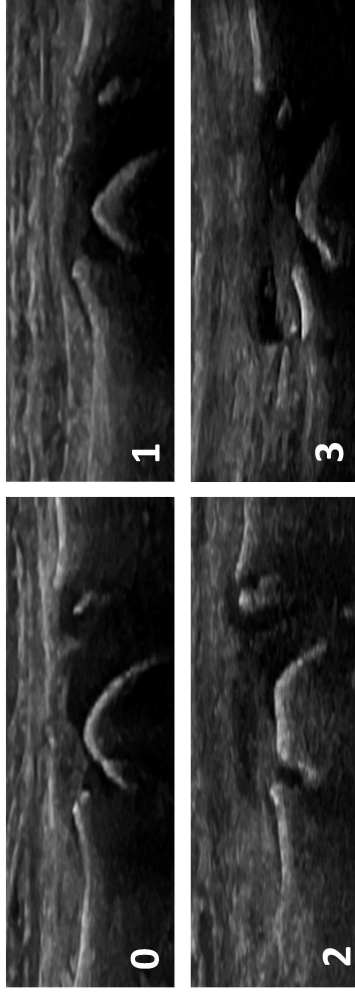
- 0: No sign of synovial hypertrophy/effusion
- 1: Mild synovial hypertrophy/effusion filling the gap between the talus and the calcaneus
- 2: Moderate synovial hypertrophy/effusion extending beyond the talus and the calcaneus but not with a convex shape
- 3: Severe synovial hypertrophy/effusion extending beyond the talus and the calcaneus with a convex shape

MTP2 - MTP3 dorsal



The subject will be in a supine position with the knee at 90 degrees flexion and the foot sole-side down. A longitudinal dorsal scan of the MTP2 and MTP3 joints.

Landmarks: 1) the head of the metatarsal bone (2/3 of the image) and 2) the base of the proximal phalanx (1/3 of the image).



BM scoring for the MTP2 and MTP3 joints, dorsal

- 0: No sign of synovial hypertrophy/effusion
- 1: Mild synovial hypertrophy/effusion but not beyond the imaginary line*
- 2: Moderate synovial hypertrophy/effusion extending beyond the imaginary line*, but without overall convex shape
- 3: Severe synovial hypertrophy/effusion extending beyond the imaginary line* with a clearly convex shape

* The line between the top of the cartilage of the distal end of the metatars to the top of the cartilage of the proximal end of the phalanx



Ultrasonographic atlas for scoring of power Doppler (PD) activity in patients with juvenile idiopathic arthritis

Nina Krafft Sande et al.



Included joint regions

- Anterior elbow
- Posterior elbow
- Wrist (radiocarpal and midcarpal)
- Metacarpophalangeal (MCP) 2-3 dorsal
- Proximal interphalangeal (PIP) 2-3 dorsal
- Proximal interphalangeal (PIP) 2-3 volar
- Knee, suprapatellar recess
- Knee, lateral parapatellar recess
- Tibiotalar
- Talonavicular
- Anterior subtalar
- Posterior subtalar
- Metatarsophalangeal (MTP) 2-3 dorsal

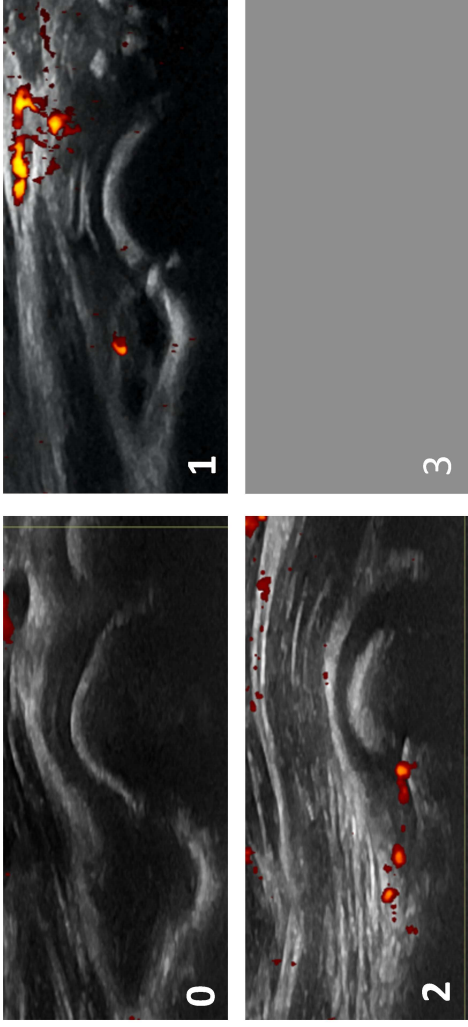
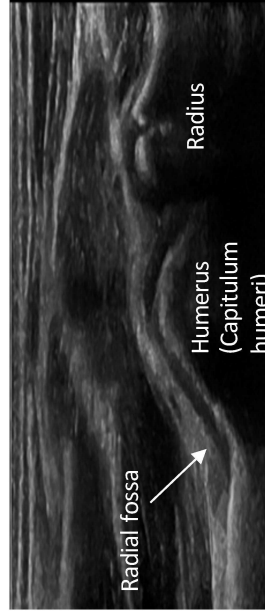


Anterior elbow



The subject will be in a supine position, but the scanning can also be done with the subject on the parents' lap. The elbow should be in full extension and supination of the lower arm. A longitudinal anterior scan of the elbow (humeroradial) joint.

Landmarks: 1) the distal humerus and 2) the radius.



PD scoring for the anterior elbow, the humeroradial joint

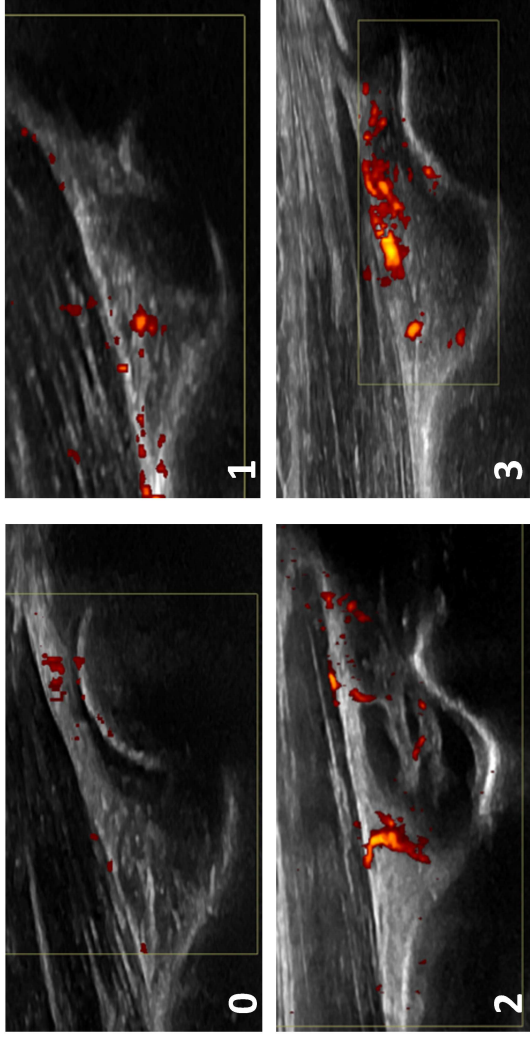
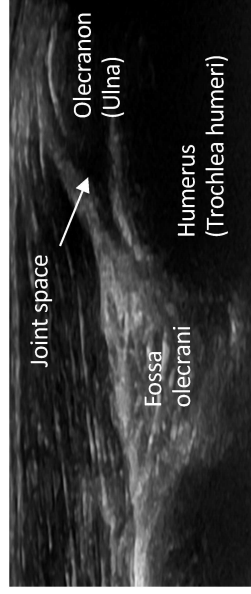
- 0: No Doppler signal
- 1: 1-3 signals within the area of synovial hypertrophy only
- 2: > 3 signals or confluent signals present in < 50% of the area of synovial hypertrophy
- 3: Confluent signals present in > 50% of the area of synovial hypertrophy (Ting et al. 2019)

Posterior elbow



The subject will be in a supine position, but the scanning can also be done with the subject on the parents' lap. The elbow should be flexed at 90 degrees with the forearm resting on the stomach. A longitudinal posterior scan of the elbow (humeroulnar) joint.

Landmarks: 1) the distal humerus and 2) the olecranon (ulna).



PD scoring for the posterior elbow, the humeroulnar joint

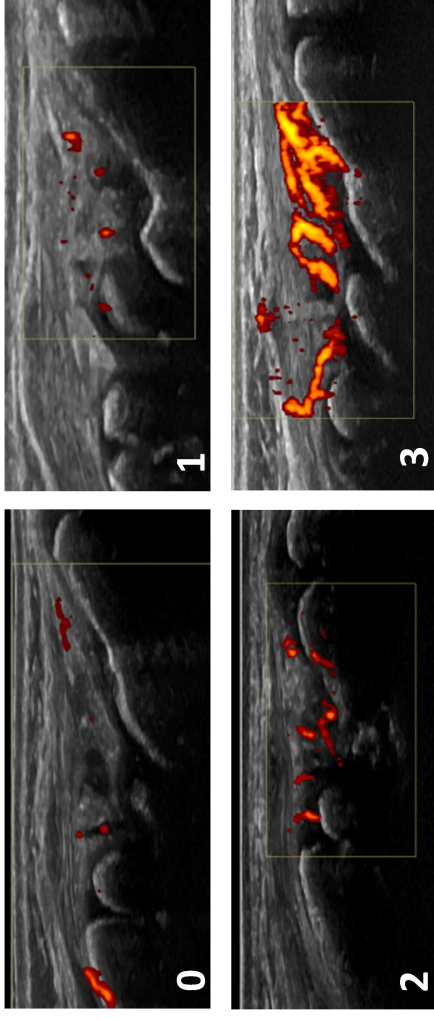
- 0: No Doppler signal
- 1: 1-3 signals within the area of synovial hypertrophy only
- 2: > 3 signals or confluent signals present in < 50% of the area of synovial hypertrophy
- 3: Confluent signals present in > 50% of the area of synovial hypertrophy (Ting et al. 2019)

Radiocarpal and midcarpal



The subject will be in a sitting position, the hands palm-side down in a neutral position on an examination table and resting the elbow on the table. A longitudinal dorsal scan of the radiocarpal and midcarpal joints at the sagittal midline of the wrist, including the distal radius, the lunate and the capitate bone.

Landmarks: 1) the distal end of diaphysis and epiphyseal cartilage of radius and 2) the dorsal recess of the radiocarpal and midcarpal joints and over them 3) a compartment of the extensor tendons according to the area imaged. (Collado et al. 2016)



PD scoring for the radiocarpal and midcarpal joints

- 0: No Doppler signal
- 1: 1-3 signals within the area of synovial hypertrophy only
- 2: > 3 signals or confluent signals present in < 50% of the area of synovial hypertrophy
- 3: Confluent signals present in > 50% of the area of synovial hypertrophy (Ting et al. 2019)

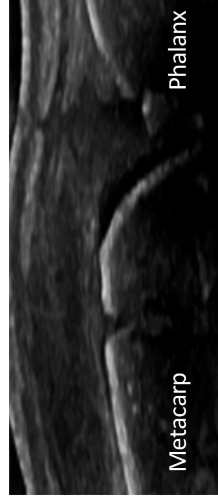
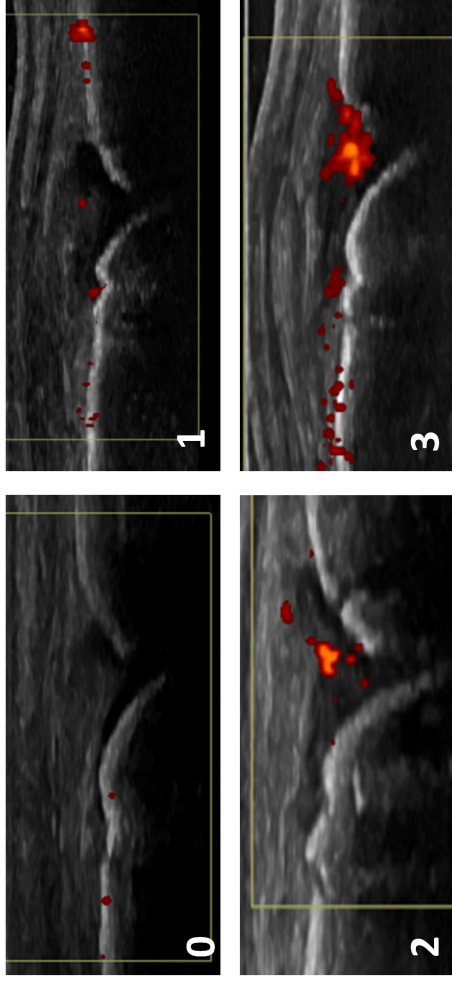
MCP2 - MCP3 dorsal



The subject will be in a sitting position with the hands palm-side down in a neutral position on an examination table.

A longitudinal dorsal scan of the MCP2 and MCP3 joints.

Landmarks: 1) the head of the metacarpal bone (2/3 of the image) and 2) the base of the proximal phalanx (1/3 of the image).



PD scoring for the MCP2 and MCP3 joints, dorsal

- 0: No Doppler signal
- 1: 1-3 signals within the area of synovial hypertrophy only
- 2: > 3 signals or confluent signals present in < 50% of the area of synovial hypertrophy
- 3: Confluent signals present in > 50% of the area of synovial hypertrophy (Ting et al. 2019)

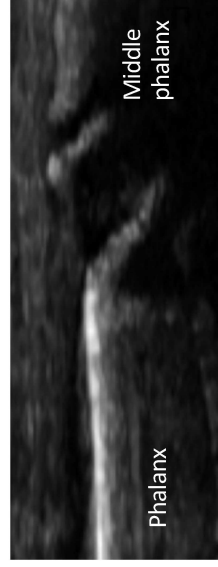
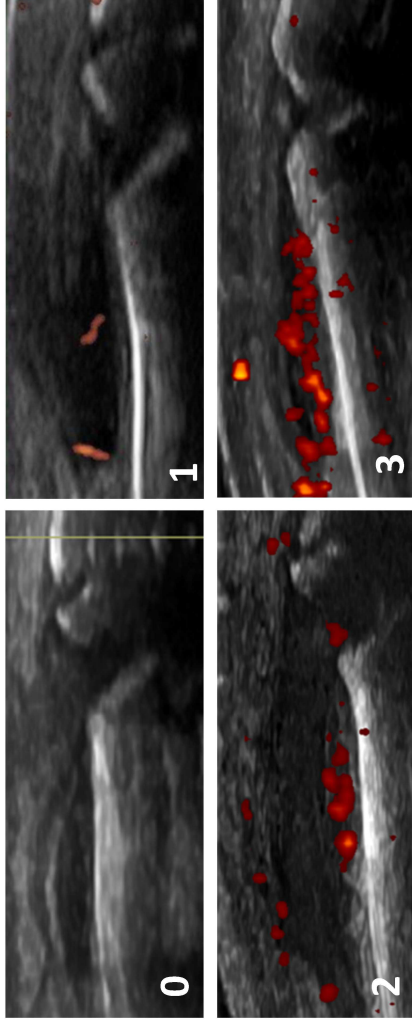
PIP2 - PIP3 dorsal



The subject will be in a sitting position with the hands palm-side down in a neutral position on an examination table.

A longitudinal dorsal scan of the PIP2 and PIP3 joints.

Landmarks: 1) the head of the proximal phalanx (2/3 of the image) and 2) the base of the middle phalanx (1/3 of the image).



PD scoring for the PIP2 and PIP3 joints, dorsal

- 0: No Doppler signal
- 1: 1-3 signals within the area of synovial hypertrophy only
- 2: > 3 signals or confluent signals present in < 50% of the area of synovial hypertrophy
- 3: Confluent signals present in > 50% of the area of synovial hypertrophy (Ting et al. 2019)

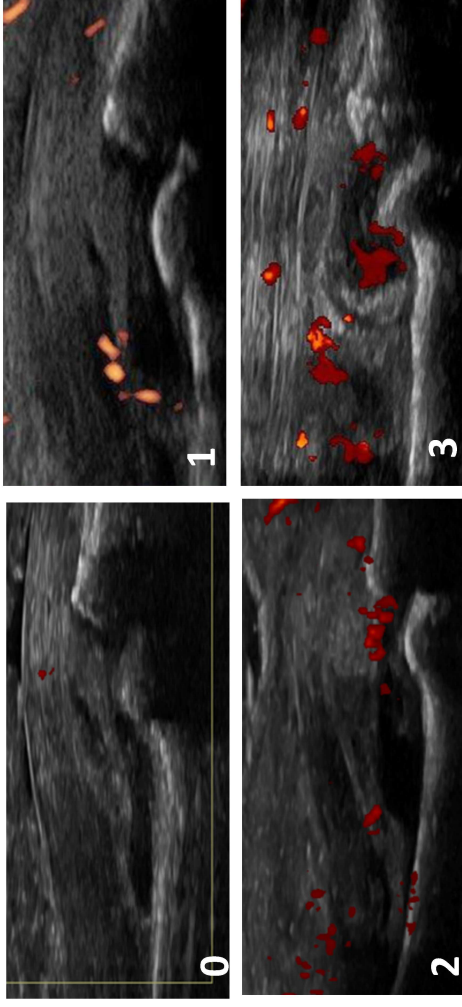
PIP2 - PIP3 volar



The subject will be in a sitting position with the hands palm-side up in a neutral position on an examination table.

A longitudinal volar scan of the PIP2 and PIP3 joints.

Landmarks: 1) the head of the proximal phalanx and 2) the base of the middle phalanx and 3) the flexor tendon.



PD scoring for the PIP2 and PIP3 joints, volar

0: No Doppler signal

1: 1-3 signals within the area of synovial hypertrophy only

2: > 3 signals or confluent signals present in < 50% of the area of synovial hypertrophy

3: Confluent signals present in > 50% of the area of synovial hypertrophy

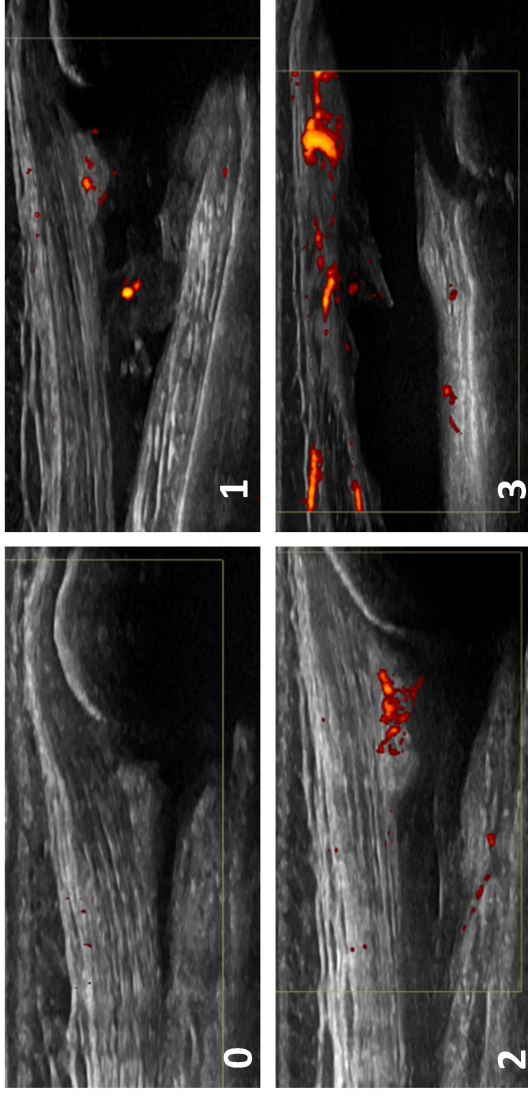
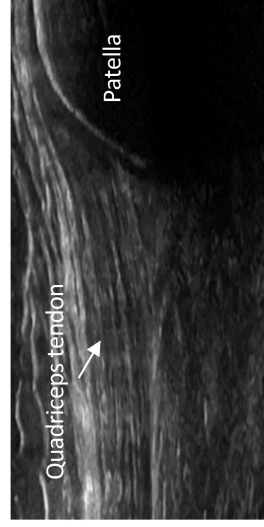
(Ting et al. 2019)

Knee, suprapatellar recess



The subject will be in a supine position. The knee should be flexed at 30 degrees, and images taken after the subject completes flexion and extension three times. A longitudinal scan of the suprapatellar joint space. For the youngest subjects, the patella should fill 1/3 of the image to compensate for the relatively shorter femur.

Landmarks: 1) the proximal third of the patella and 2) a clearly visualized quadriceps tendon.



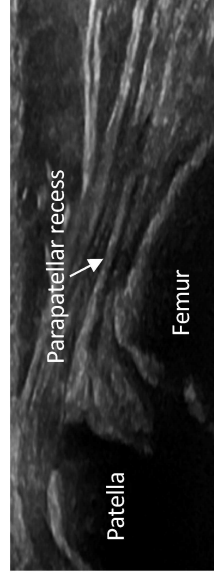
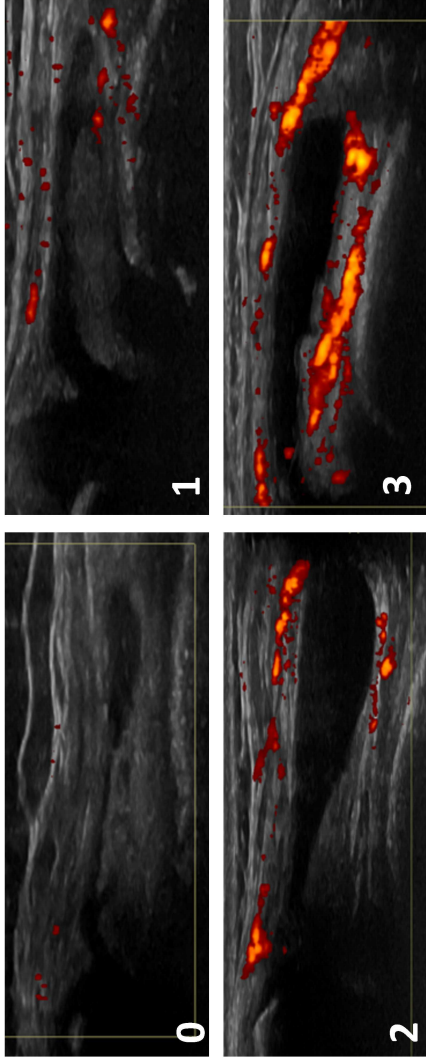
PD scoring for the knee, suprapatellar recess

- 0: No Doppler signal
- 1: 1-3 signals within the area of synovial hypertrophy only
- 2: > 3 signals or confluent signals present in < 50% of the area of synovial hypertrophy
- 3: Confluent signals present in > 50% of the area of synovial hypertrophy (Ting et al. 2019)

Knee, lateral parapatellar recess



The subject will be in a supine position. The knee should be flexed at 30 degrees. For the lateral parapatellar recess the image will be obtained with the probe in transverse position over the mid-patella with both the patella and femur in view.
Landmarks: 1) the superior edge of the patella and 2) the femoral condyle.
 (Ting et al. 2019)



PD scoring for the knee, lateral parapatellar recess

- 0: No Doppler signal
- 1: 1-3 signals within the area of synovial hypertrophy only
- 2: > 3 signals or confluent signals present in < 50% of the area of synovial hypertrophy
- 3: Confluent signals present in > 50% of the area of synovial hypertrophy
 (Ting et al. 2019)

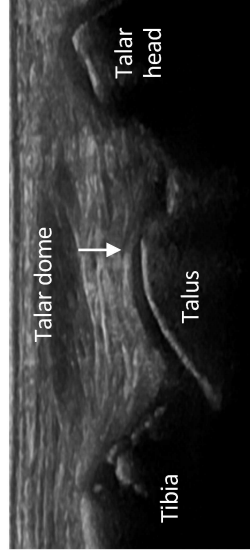
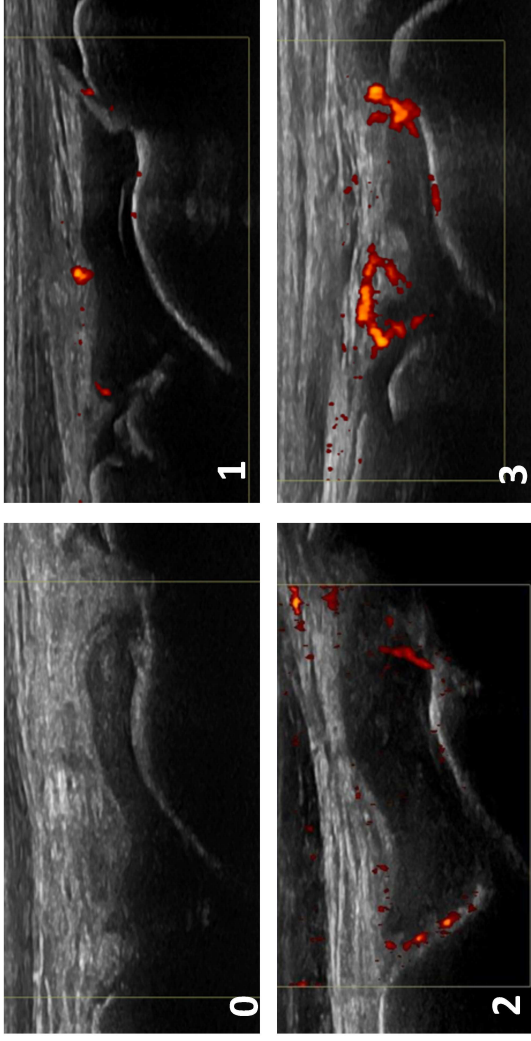
Tibiotalar



The subject will be in a supine position with the knee at 90 degrees flexion and the foot sole-side down.

A longitudinal scan of the tibiotalar joint.

Landmarks: 1) the distal end of the tibia and 2) the talus.



PD scoring for the tibiotalar joint

- 0: No Doppler signal
- 1: 1-3 signals within the area of synovial hypertrophy only
- 2: > 3 signals or confluent signals present in < 50% of the area of synovial hypertrophy
- 3: Confluent signals present in > 50% of the area of synovial hypertrophy (Ting et al. 2019)

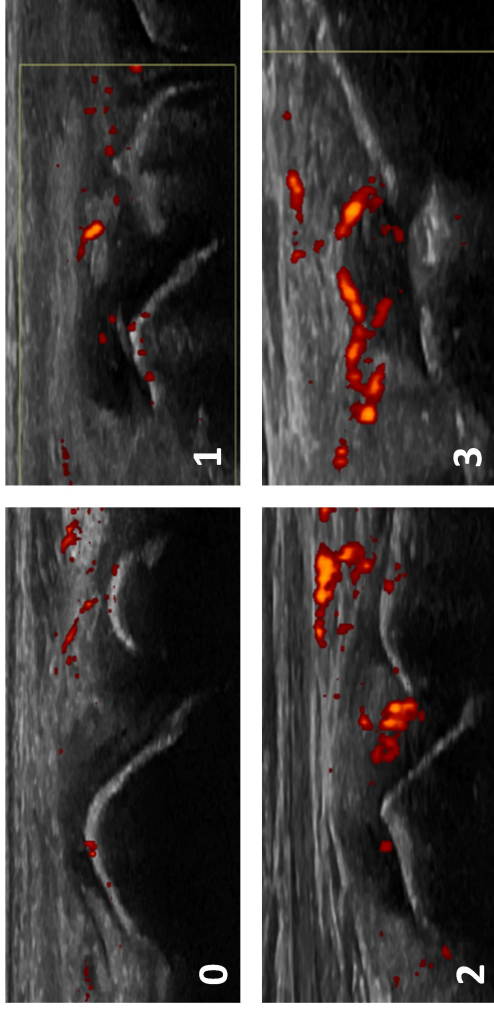
Talonavicular



The subject will be in a supine position with the knee at 90 degrees flexion and the foot sole-side down.

A longitudinal scan of the talonavicular joint.

Landmarks: 1) the talus and 2) the navicular bone.



PD scoring for the talonavicular joint

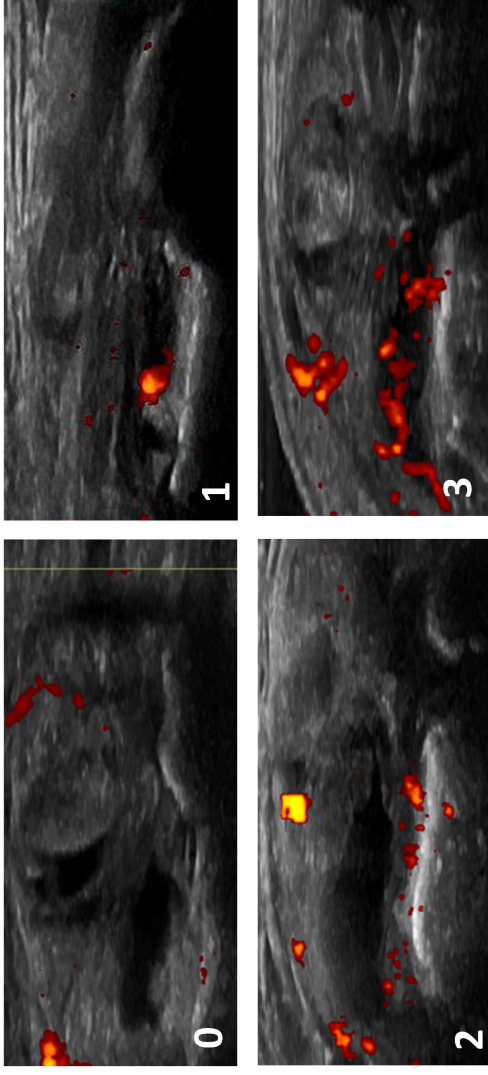
- 0: No Doppler signal
- 1: 1-3 signals within the area of synovial hypertrophy only
- 2: > 3 signals or confluent signals present in < 50% of the area of synovial hypertrophy
- 3: Confluent signals present in > 50% of the area of synovial hypertrophy (Ting et al. 2019)

Anterior subtalar



The subject will be in a supine position with the leg straight and the forefoot/ankle in slight eversion. The probe will be positioned at 45 degrees pointing to the heel and then moved proximally and distally. A medial scan of the anterior subtalar joint.

Landmarks: 1) the talus and 2) the sustentaculum tali (calcaneus).



PD scoring for the anterior subtalar joint

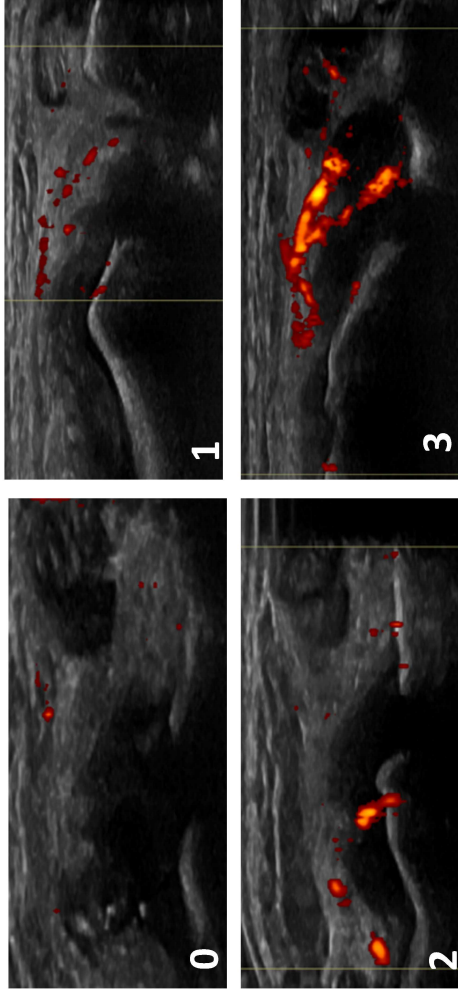
- 0: No Doppler signal
- 1: 1-3 signals within the area of synovial hypertrophy only
- 2: > 3 signals or confluent signals present in < 50% of the area of synovial hypertrophy
- 3: Confluent signals present in > 50% of the area of synovial hypertrophy (Ting et al. 2019)

Posterior subtalar



The subject will be in a supine position with the leg straight and the forefoot/ankle in slight inversion. The probe will be positioned along the sinus tarsi perpendicular to the sole, and then moved posteriorly. If no distension is seen, the image will be taken visualizing the joint with the peroneus tendons. A lateral scan of the posterior subtalar joint.

Landmarks: 1) the talus and 2) the calcaneus.



PD scoring for the posterior subtalar joint

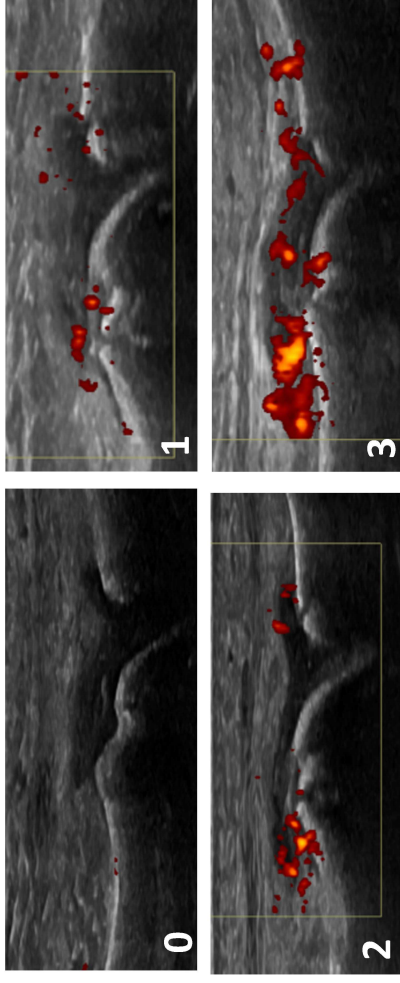
- 0: No Doppler signal
- 1: 1-3 signals within the area of synovial hypertrophy only
- 2: > 3 signals or confluent signals present in < 50% of the area of synovial hypertrophy
- 3: Confluent signals present in > 50% of the area of synovial hypertrophy (Ting et al. 2019)

MTP2 - MTP3 dorsal



The subject will be in a supine position with the knee at 90 degrees flexion and the foot sole-side down. A longitudinal dorsal scan of the MTP2 and MTP3 joints.

Landmarks: 1) the head of the metatarsal bone (2/3 of the image) and 2) the base of the proximal phalanx (1/3 of the image).



PD scoring for the MTP2 and MTP3 joints, dorsal

- 0: No Doppler signal
- 1: 1-3 signals within the area of synovial hypertrophy only
- 2: > 3 signals or confluent signals present in < 50% of the area of synovial hypertrophy
- 3: Confluent signals present in > 50% of the area of synovial hypertrophy (Ting et al. 2019)

Ultrasonographic atlas for scoring of B-mode (BM) synovitis in patients with juvenile idiopathic arthritis 9-12 years

Nina Krafft Sande et al.

Included joint regions

- Anterior elbow
- Posterior elbow
- Wrist (radiocarpal and midcarpal)
- Metacarpophalangeal (MCP) 2-3 dorsal
- Proximal interphalangeal (PIP) 2-3 dorsal
- Proximal interphalangeal (PIP) 2-3 volar
- Hip
- Knee, suprapatellar recess
- Knee, lateral parapatellar recess
- Tibiotalar
- Talonavicular
- Anterior subtalar
- Posterior subtalar
- Metatarsophalangeal (MTP) 2-3 dorsal



Anterior elbow

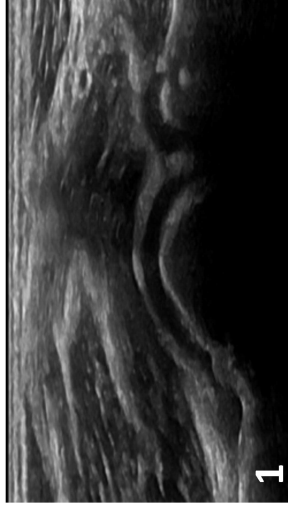


The subject will be in a supine position. The elbow should be in full extension and supination of the lower arm. A longitudinal anterior scan of the elbow (humeroradial) joint.

Landmarks: 1) the distal humerus and 2) the radius.



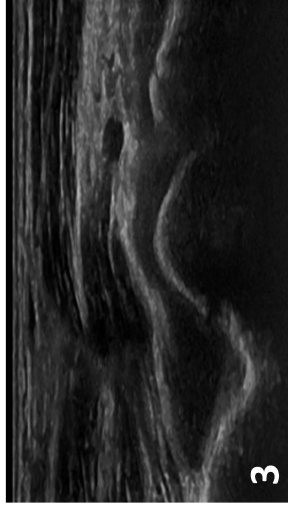
0



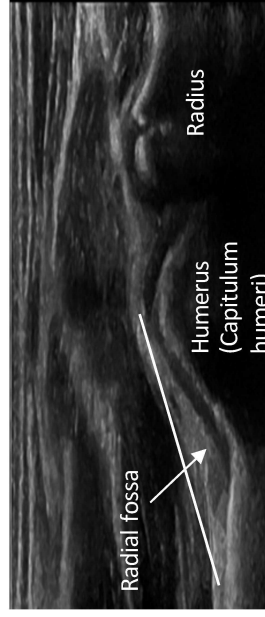
1



2



3



BM scoring for the anterior elbow, the humeroradial joint

0: No or minimal synovial hypertrophy/effusion

1: Mild synovial hypertrophy/effusion

2: Moderate synovial hypertrophy/effusion up to, but not beyond the imaginary line*

3: Severe synovial hypertrophy/effusion beyond the imaginary line* and/or a clearly convex shape

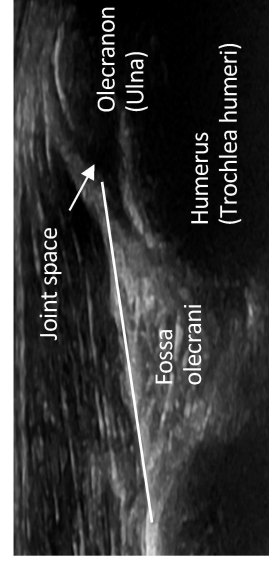
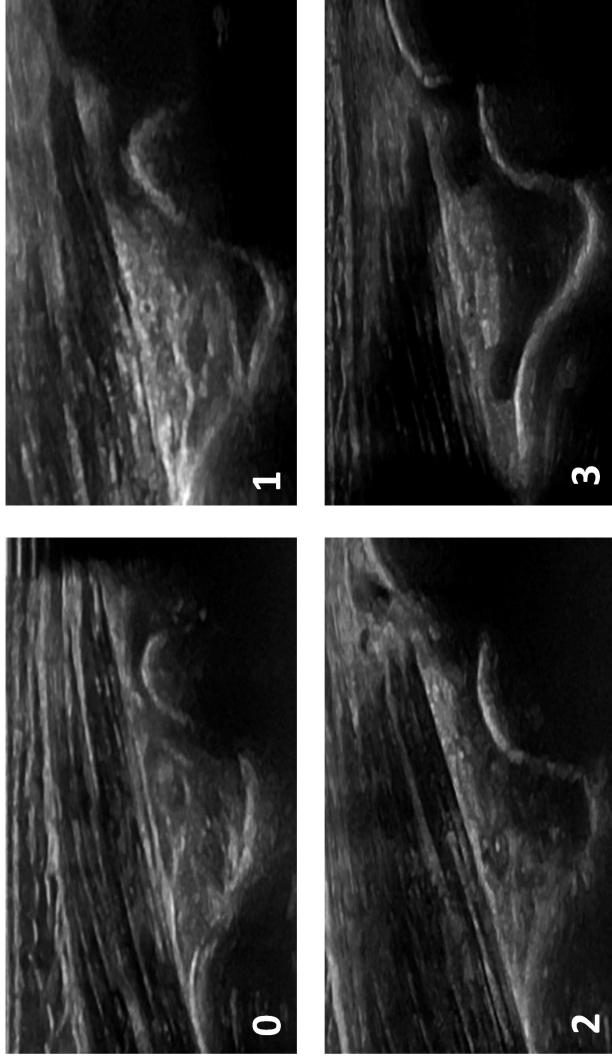
* The line above the radial fossa; between the proximal end of the fossa to the top of the cartilage over the capitulum humeri

Posterior elbow



The subject will be in a supine position. The elbow will be flexed at 90 degrees with the forearm resting on the stomach. A longitudinal posterior scan of the elbow (humeroulnar) joint.

Landmarks: 1) the distal humerus and 2) the olecranon (ulna).



BM scoring for the posterior elbow, the humeroulnar joint

- 0: No or minimal synovial hypertrophy/effusion
 1: Mild synovial hypertrophy/effusion, filling up to 25% of the fossa
 2: Moderate synovial hypertrophy/effusion filling up to 50% of the fossa, but not beyond the imaginary line*
 3: Severe synovial hypertrophy/effusion filling more than 50% of the fossa and/or extending beyond the imaginary line*

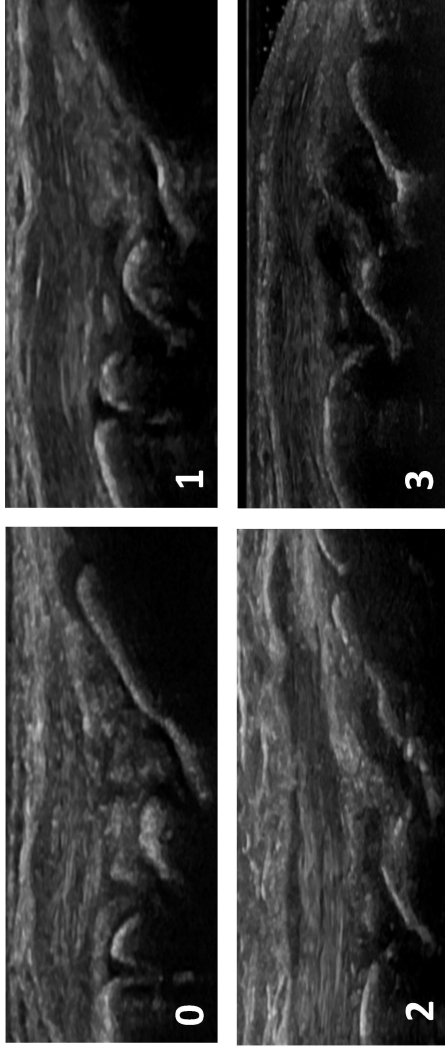
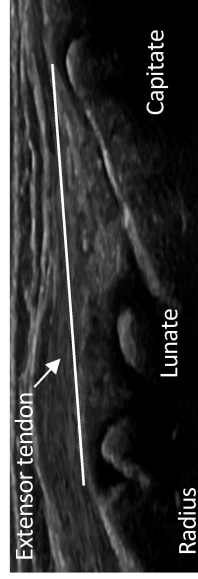
* The line above the fossa olecrani; between the proximal top of the fossa to the top of the cartilage of the trochlea humeri

Radiocarpal and midcarpal



The subject will be in a sitting position, the hands palm-side down in a neutral position on an examination table and resting the elbow on the table. A longitudinal dorsal scan of the radiocarpal and midcarpal joints at the sagittal midline of the wrist, including the distal radius, the lunate and the capitate bone.

Landmarks: 1) the distal end of diaphysis and epiphyseal cartilage of radius and 2) the dorsal recess of the radiocarpal and midcarpal joints and over them 3) a compartment of the extensor tendons according to the area imaged. (Collado et al. 2016)

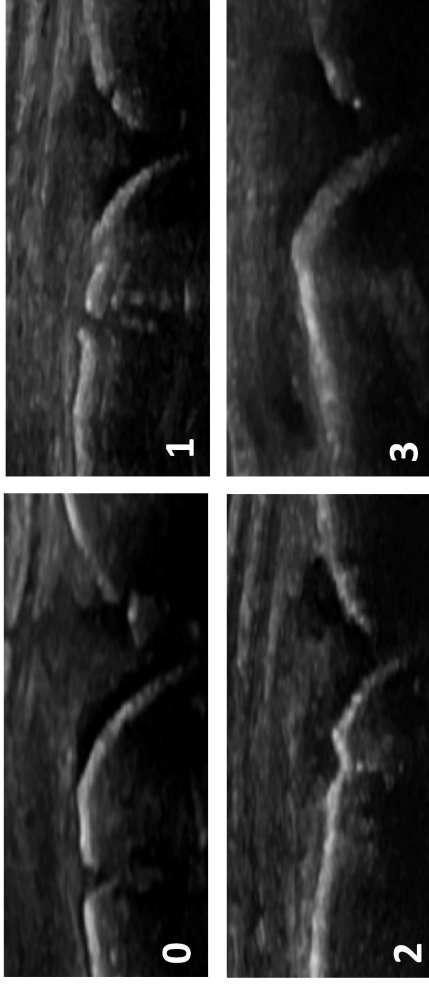


BM scoring for the radiocarpal and midcarpal joints

- 0: No sign of synovial hypertrophy/effusion
- 1: Mild synovial hypertrophy/effusion
- 2: Moderate synovial hypertrophy/effusion up to, but not beyond the imaginary line*
- 3: Severe synovial hypertrophy/effusion with a convex shape extending beyond the imaginary line* and can push up the extensor tendons

* The line between the top of the cartilage of the distal end of the radius to the top of the cartilage of the capitate

MCP2 - MCP3 dorsal



The subject will be in a sitting position with the hands palm-side down in a neutral position on an examination table.

A longitudinal dorsal scan of the MCP2 and MCP3 joints.

Landmarks: 1) the head of the metacarpal bone (2/3 of the image) and 2) the base of the proximal phalanx (1/3 of the image).



BM scoring for the MCP2 and MCP3 joints, dorsal

- 0: No sign of synovial hypertrophy/effusion
- 1: Mild synovial hypertrophy/effusion but not beyond the imaginary line*
- 2: Moderate synovial hypertrophy/effusion extending beyond the imaginary line* , but without overall convex shape
- 3: Severe synovial hypertrophy/effusion extending beyond the imaginary line* with a clearly convex shape

*The line between the top of the cartilage of the distal end of the metacarp to the top of the cartilage of the proximal end of the phalanx

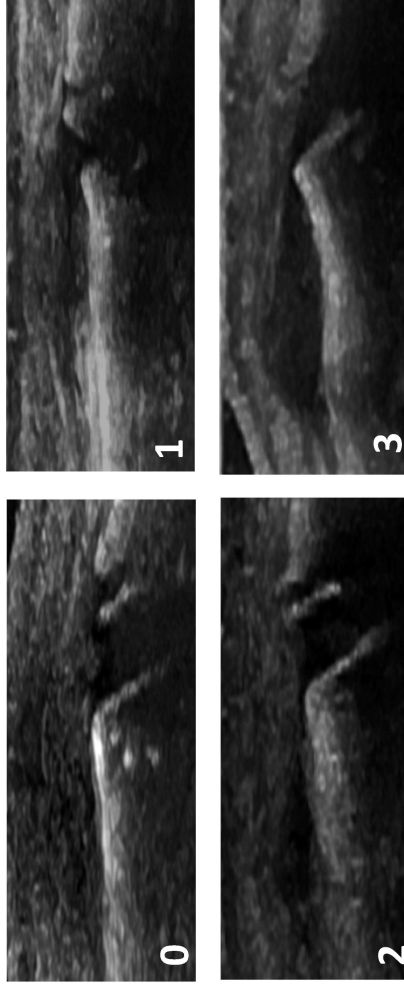
PIP2 - PIP3 dorsal



The subject will be in a sitting position with the hands palm-side down in a neutral position on an examination table.

A longitudinal dorsal scan of the PIP2 and PIP3 joints.

Landmarks: 1) the head of the proximal phalanx (2/3 of the image) and 2) the base of the middle phalanx (1/3 of the image).



BM scoring for the PIP2 and PIP3 joints, dorsal

- 0: No sign of synovial hypertrophy/effusion
- 1: Mild synovial hypertrophy/effusion but not beyond the imaginary line*
- 2: Moderate synovial hypertrophy/effusion extending beyond the imaginary line*, but without overall convex shape
- 3: Severe synovial hypertrophy/effusion extending beyond the imaginary line* with a clearly convex shape

*The line between the top of the cartilage of the distal end of the proximal phalanx to the top of the cartilage of the proximal end of the middle phalanx

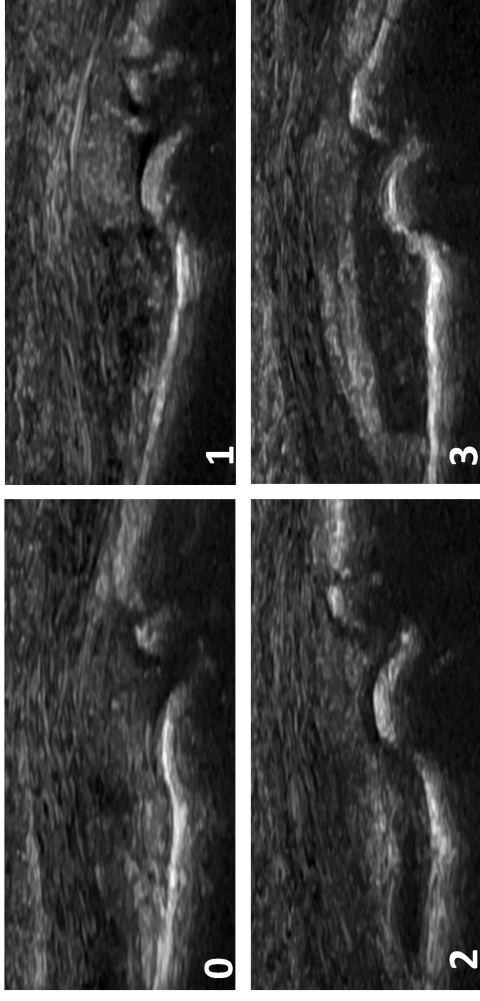
PIP2 - PIP3 volar



The subject will be in a sitting position with the hands palm-side up in a neutral position on an examination table.

A longitudinal volar scan of the PIP2 and PIP3 joints.

Landmarks: 1) the head of the proximal phalanx and 2) the base of the middle phalanx and 3) the flexor tendon.



BM scoring for the PIP2 and PIP3 joints, volar

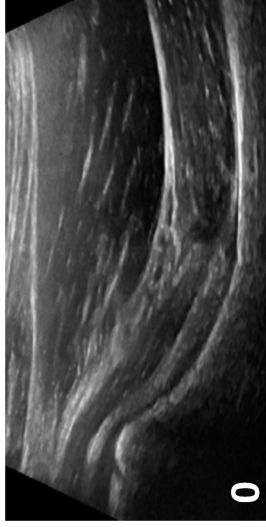
- 0: No sign of synovial hypertrophy/effusion
- 1: Mild synovial hypertrophy/effusion, possible to extend proximally but without convex shape
- 2: Moderate synovial hypertrophy/effusion extending over the proximal phalanx with convex shape, but not filling the joint space between proximal and middle phalanx
- 3: Severe synovial hypertrophy/effusion extending over the proximal phalanx and filling the joint space between proximal and middle phalanx with an overall convex shape

Hip

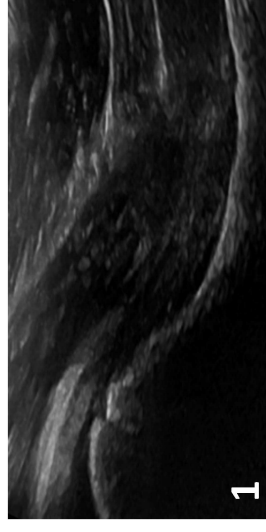


The subject will be in a supine position with the hip in a neutral position, slightly externally rotated. A longitudinal anterior scan parallel to the femoral neck of the hip joint.

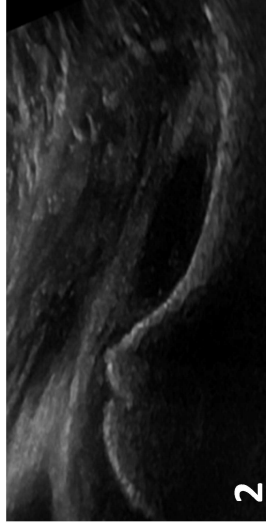
Landmarks: 1) the femoral head and 2) the femoral neck.



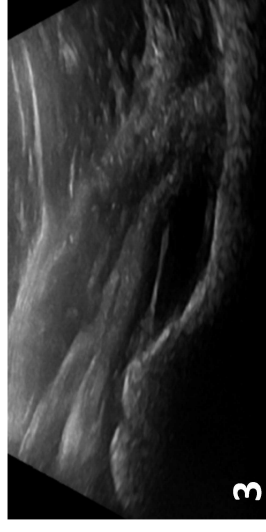
0



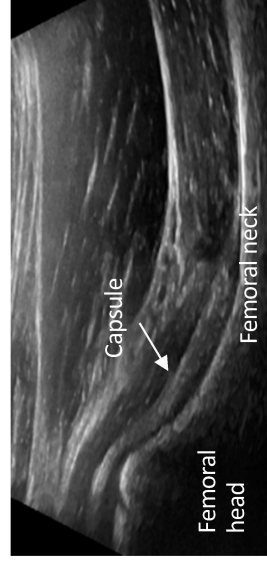
1



2



3



BM scoring for the hip joint

0: No sign of synovial hypertrophy/effusion

1: Mild synovial hypertrophy/effusion, but just a "slit" of fluid between the two layers of the capsule

2: Moderate synovial hypertrophy/effusion leading to a straight line/minimal convex shape of the capsule

3: Severe synovial hypertrophy/effusion with a clearly convex shape, the effusion can also extend proximally over the femoral head

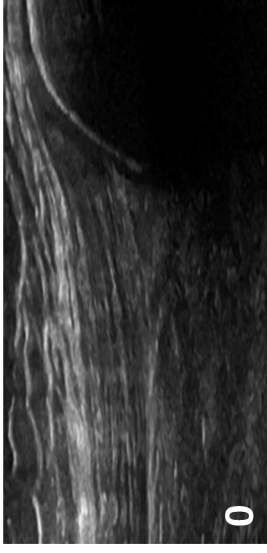
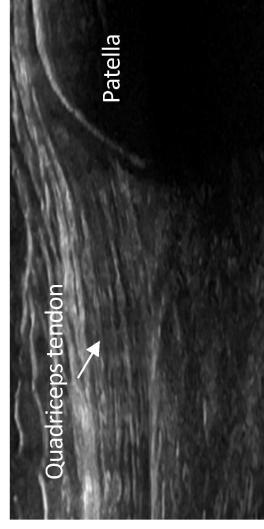
Knee, suprapatellar recess



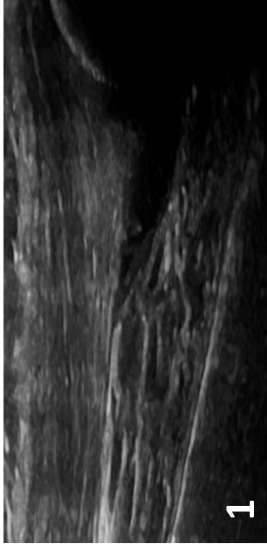
The subject will be in a supine position. The knee should be flexed at 30 degrees, and images taken after the subject completes flexion and extension three times. A longitudinal scan of the suprapatellar joint space.

Landmarks: 1) the proximal third of the patella and 2) a clearly visualized quadriceps tendon.

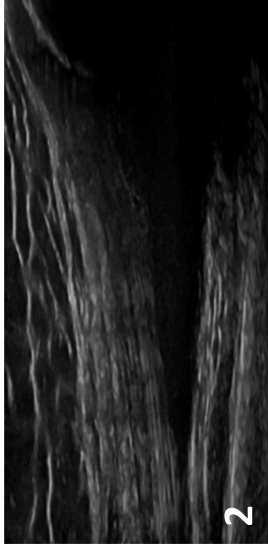
(Ting et al. 2019)



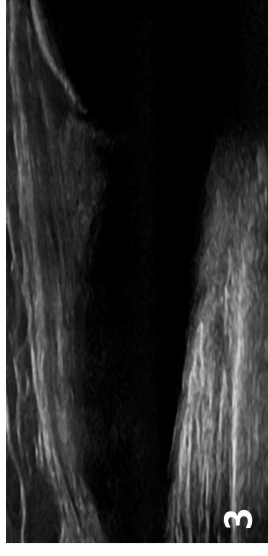
0



1



2



3

BM scoring for the knee, suprapatellar recess

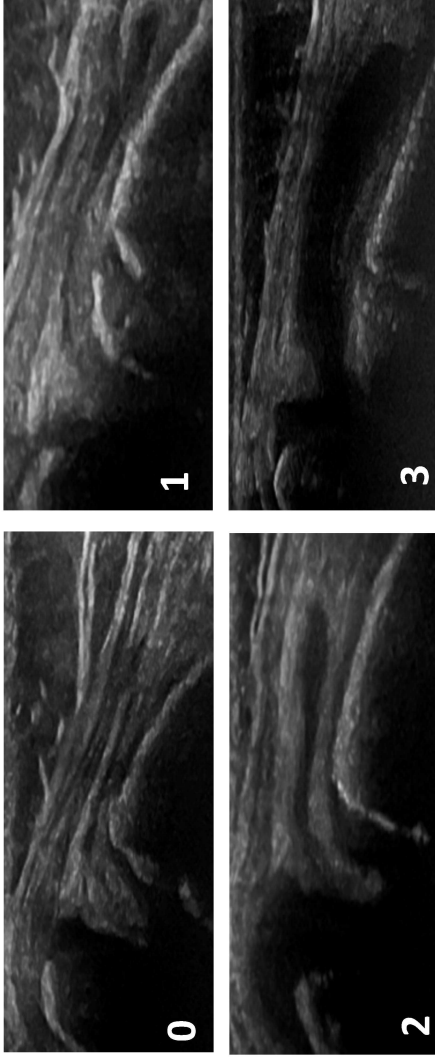
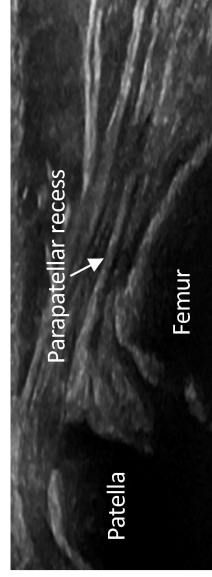
- 0: "Slit" of fluid/synovium without elevation of the pre-patellar fat pad but with only minimal extension beyond the prepatellar fat pad
- 1: Mild synovial hypertrophy/effusion with elevation of the prepatellar fat pad and extension proximally <50% of the visualized portion of the quadriceps tendon
- 2: Moderate synovial hypertrophy/effusion elevating the pre-patellar fat pad with extension proximally > 50% of the visualized portion of the quadriceps tendon
- 3: Significant distension of the suprapatellar recess throughout the image, and with the most proximal portion of the synovial recess being > 50% of the maximum distension of the recess (Ting et al. 2019)

Knee, lateral parapatellar recess



The subject will be in a supine position. The knee should be flexed at 30 degrees. For the lateral parapatellar recess the image will be obtained with the probe in transverse position over the mid-patella with both the patella and femur in view.

Landmarks: 1) the superior edge of the patella and 2) the femoral condyle.
(Ting et al. 2019)



BM scoring for the knee, lateral parapatellar recess

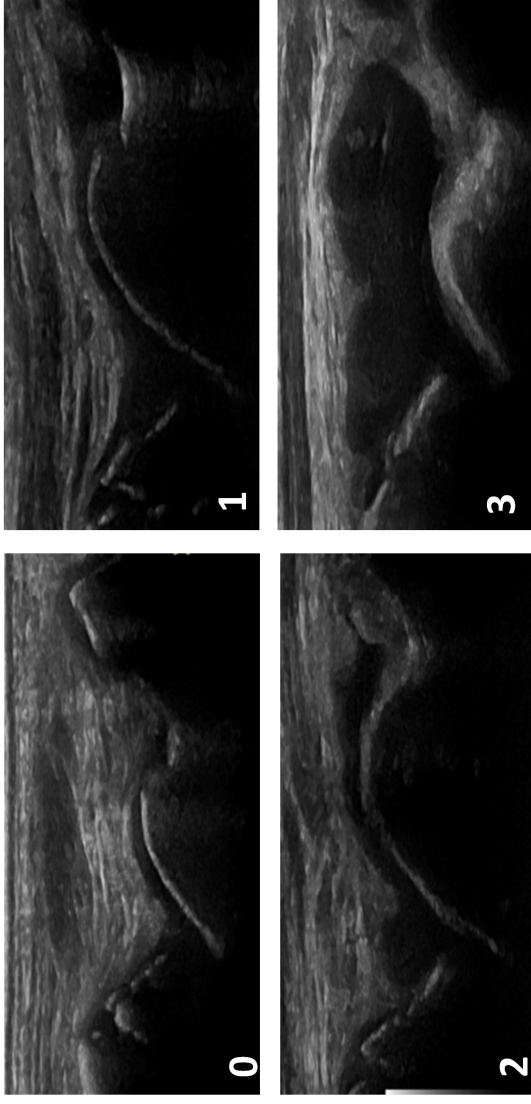
- 0: Empty parapatellar recess but a minimal bulge of synovial hypertrophy/effusion may be found extending to the patellofemoral joint line
- 1: Synovial hypertrophy/effusion filling < 1/3 of the full area of the parapatellar recess
- 2: Synovial hypertrophy/effusion filling between one to two thirds of the full area of the parapatellar recess
- 3: Synovial hypertrophy/effusion that fills >2/3 of the full area of the parapatellar recess and clearly pushing up the retinaculum
(Ting et al. 2019)

Tibiotalar



The subject will be in a supine position with the knee at 90 degrees flexion and the foot sole-side down.
A longitudinal scan of the tibiotalar joint.

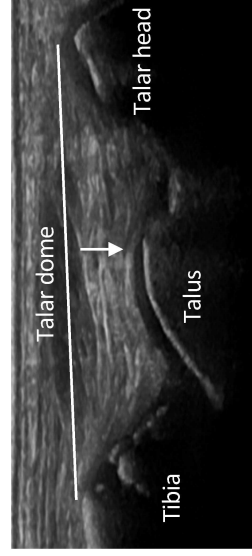
Landmarks: 1) the distal end of the tibia and 2) the talus.



BM scoring for the tibiotalar joint

- 0: No sign of synovial hypertrophy/effusion in the tibiotalar joint, but possible to have a minimal amount of fluid in the concave neck of the talus
- 1: Mild synovial hypertrophy/effusion filling the gap between the tibia and the talus and in the concave neck of the talus, but not continuously over the talus
- 2: Moderate synovial hypertrophy/effusion filling up to 50% of the area between the tibia, the talus and the imaginary line* and continuously over the talus
- 3: Severe synovial hypertrophy/effusion filling more than 50% of the area between the tibia, the talus and the imaginary line*, or beyond the imaginary line*

*The line between the top of the cartilage of the distal end of the tibia and the top of the cartilage of the talar head



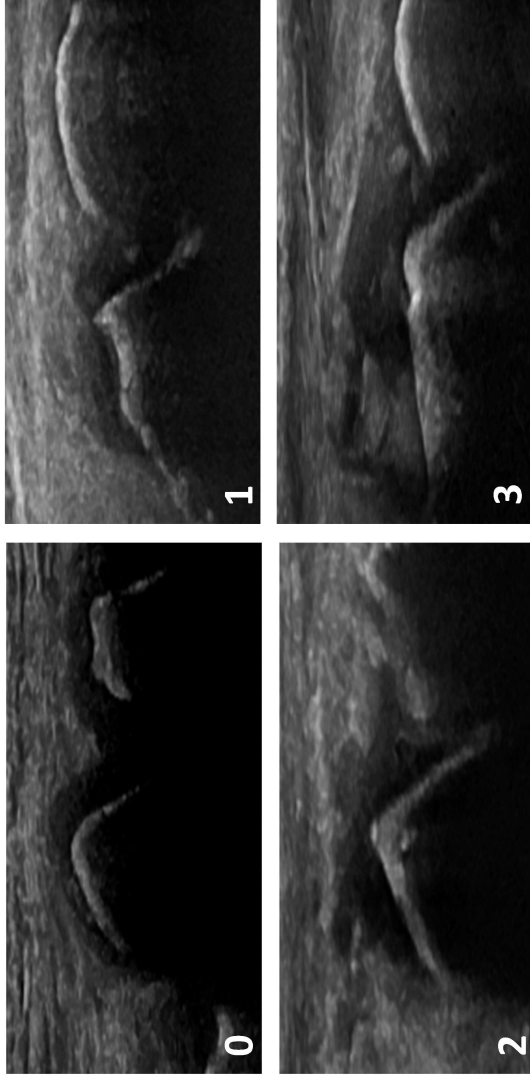
Talonavicular



The subject will be in a supine position with the knee at 90 degrees flexion and the foot sole-side down.

A longitudinal scan of the talonavicular joint.

Landmarks: 1) the talus and 2) the navicular bone.



BM scoring for the talonavicular joint

- 0: No sign of synovial hypertrophy/effusion
- 1: Mild synovial hypertrophy/effusion but not beyond the imaginary line*
- 2: Moderate synovial hypertrophy/effusion extending beyond the imaginary line* and proximal with a concave or straight shape
- 3: Severe synovial hypertrophy/effusion extending beyond the imaginary line* and over the talus with a convex shape clearly pushing up the joint capsule

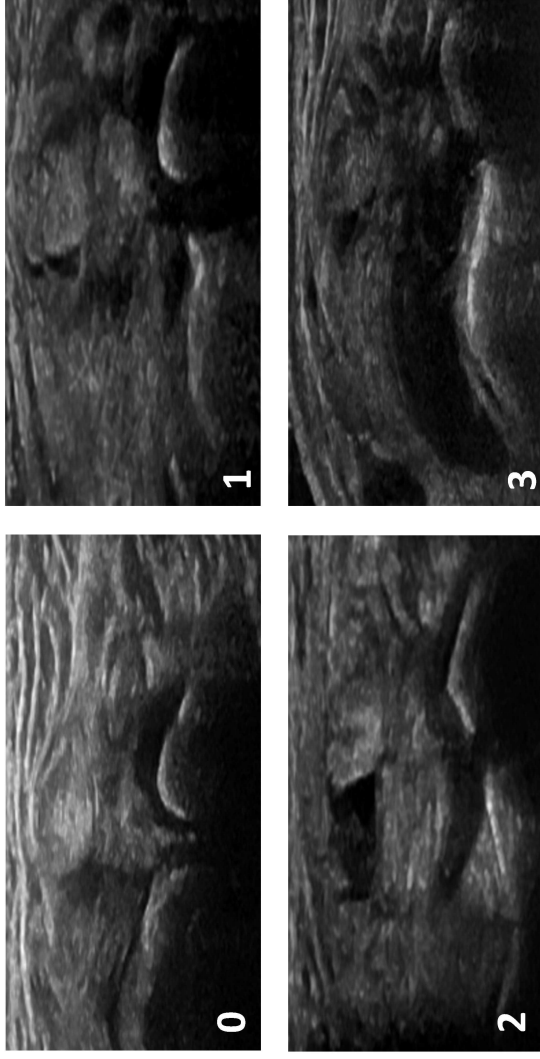
* The line between the top of the cartilage of the head of the talus to the top of the cartilage of the navicular bone

Anterior subtalar



The subject will be in a supine position with the leg straight and the forefoot/ankle in slight eversion. The probe will be positioned at 45 degrees pointing to the heel and then moved proximally and distally. A medial scan of the anterior subtalar joint.

Landmarks: 1) the talus and 2) the sustentaculum tali (calcaneus).



BM scoring for the anterior subtalar joint

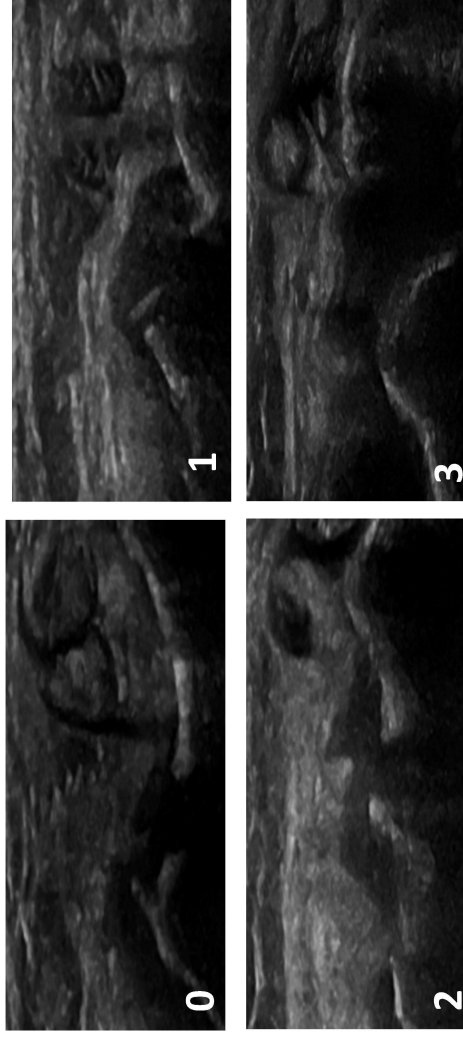
- 0: No sign of synovial hypertrophy/effusion
- 1: Mild synovial hypertrophy/effusion covering up to 25% of the straight part of the talus
- 2: Moderate synovial hypertrophy/effusion covering up to 50% of the straight part of the talus
- 3: Severe synovial hypertrophy/effusion covering more than 50% of the straight part of the talus

Posterior subtalar



The subject will be in a supine position with the leg straight and the forefoot/ankle in slight inversion. The probe will be positioned along the sinus tarsi perpendicular to the sole, and then moved posteriorly. If no distension is seen, the image will be taken visualizing the joint with the peroneus tendons. A lateral scan of the posterior subtalar joint.

Landmarks: 1) the talus and 2) the calcaneus.



BM scoring for the posterior subtalar joint

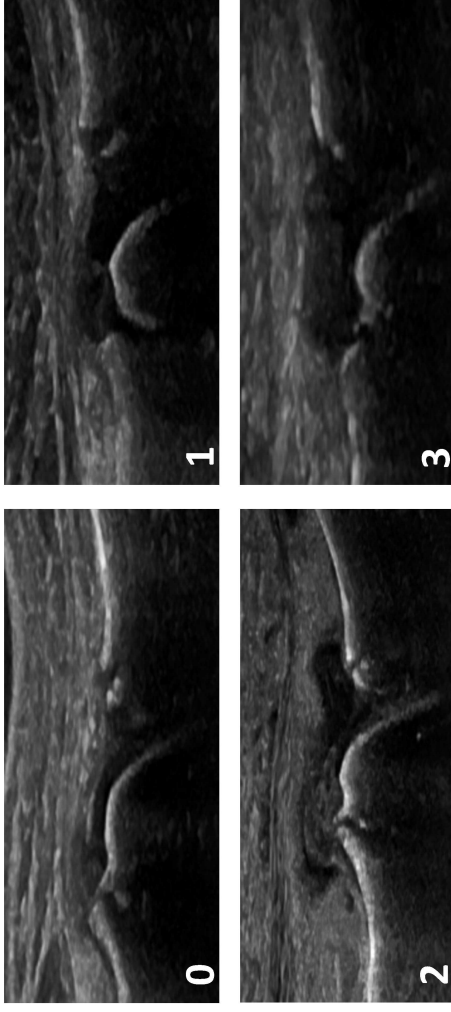
- 0: No sign of synovial hypertrophy/effusion
- 1: Mild synovial hypertrophy/effusion filling the gap between the talus and the calcaneus
- 2: Moderate synovial hypertrophy/effusion extending beyond the talus and the calcaneus but not with a convex shape
- 3: Severe synovial hypertrophy/effusion extending beyond the talus and the calcaneus with a convex shape

MTP2 - MTP3 dorsal



The subject will be in a supine position with the knee at 90 degrees flexion and the foot sole-side down. A longitudinal, dorsal scan of the MTP2 and MTP3 joints.

Landmarks: 1) the head of the metatarsal bone (2/3 of the image) and 2) the base of the proximal phalanx (1/3 of the image).



BM scoring for the MTP2 and MTP3 joints, dorsal

- 0: No sign of synovial hypertrophy/effusion
- 1: Mild synovial hypertrophy/effusion but not beyond the imaginary line*
- 2: Moderate synovial hypertrophy/effusion extending beyond the imaginary line*, but without overall convex shape
- 3: Severe synovial hypertrophy/effusion extending beyond the imaginary line* with a clearly convex shape

* The line between the top of the cartilage of the distal end of the metatars to the top of the cartilage of the proximal end of the phalanx

ORIGINAL RESEARCH

Associations between power Doppler ultrasound findings and B-mode synovitis and clinical arthritis in juvenile idiopathic arthritis using a standardised scanning approach and scoring system

Nina Krafft Sande ^{1,2}, Vibke Lilleby,¹ Anna-Birgitte Aga ¹, Eva Kirkhus,³ Berit Flatø,^{1,2} Pernille Bøyesen ¹

To cite: Sande NK, Lilleby V, Aga A-B, *et al.* Associations between power Doppler ultrasound findings and B-mode synovitis and clinical arthritis in juvenile idiopathic arthritis using a standardised scanning approach and scoring system. *RMD Open* 2023;**9**:e002937. doi:10.1136/rmdopen-2022-002937

► Additional supplemental material is published online only. To view, please visit the journal online (<http://dx.doi.org/10.1136/rmdopen-2022-002937>).

Received 15 December 2022
Accepted 2 March 2023



© Author(s) (or their employer(s)) 2023. Re-use permitted under CC BY-NC. No commercial re-use. See rights and permissions. Published by BMJ.

¹Department of Rheumatology, Oslo University Hospital, Oslo, Norway

²Institute of Clinical Medicine, Faculty of Medicine, University of Oslo, Oslo, Norway

³Department of Radiology, Oslo University Hospital, Oslo, Norway

Correspondence to
Dr Nina Krafft Sande;
ninamkrafft@hotmail.com

ABSTRACT

Objectives To describe power Doppler (PD) ultrasound findings in joint regions with B-mode (BM) synovitis using a standardised scanning protocol and scoring system in patients with juvenile idiopathic arthritis (JIA). Further, to examine associations between PD findings and BM synovitis, clinical arthritis, patient characteristics and disease activity.

Methods In this cross-sectional study, one experienced ultrasonographer, blinded to clinical findings, performed ultrasound examinations in 27 JIA patients with suspected clinical arthritis. The elbow, wrist, metacarpophalangeal 2–3, proximal interphalangeal 2–3, knee, ankle and metatarsophalangeal 2–3 joints were assessed bilaterally and scored semiquantitatively (grades 0–3) for BM and PD findings using a joint-specific scoring system with reference atlas. Multilevel mixed-effects ordered regression models were used to explore associations between PD findings and BM synovitis, clinical arthritis, age, sex, JIA subgroups, disease duration and 10-joint Juvenile Arthritis Disease Activity Score (JADAS10).

Results Twenty-one girls and six boys, median age (IQR) 8 years (6–12 years) were included. Overall, 971 joint regions were evaluated by ultrasound, 129 had BM synovitis and were assessed for PD. PD findings were detected in 45 joint regions (34.9%), most frequently in the parapatellar recess of the knee (24.4%). Increasing PD grades were associated with higher BM grades (OR=5.0, $p<0.001$) and with clinical arthritis (OR=7.4, $p<0.001$) but not with age, sex, JIA subgroups, disease duration or JADAS10.

Conclusion Increasing severity of PD findings were significantly associated with BM synovitis and with clinical arthritis. This suggests that PD signals detected using a standardised ultrasound examination and scoring system can reflect active disease in JIA patients.

INTRODUCTION

Ultrasound is a well-tolerated, non-invasive and easily accessible imaging technique that is well suited for use in children. However, the

WHAT IS ALREADY KNOWN ON THIS TOPIC

⇒ Ultrasound is a valuable tool in the evaluation of synovitis in patients with juvenile idiopathic arthritis (JIA), but the interpretation of Doppler signals in children is challenging due to physiological vascularisation that can be misinterpreted as pathological findings.

WHAT THIS STUDY ADDS

⇒ Power Doppler (PD) findings in multiple joint regions with B-mode (BM) synovitis in patients with JIA were described using a standardised scanning approach and scoring system. Increasing PD grades were significantly associated with higher BM grades and with the presence of clinical arthritis.

HOW THIS STUDY MIGHT AFFECT RESEARCH, PRACTICE OR POLICY

⇒ Doppler signal assessment using a standardised ultrasound examination and a joint-specific scoring system can establish a feasible and more accurate interpretation of disease activity in patients with JIA.

interpretation of ultrasonographic images in children can be challenging due to the unique features of the growing skeleton.^{1–3} The interpretation of Doppler signals in children is especially challenging because of physiological vascularisation during growth. Doppler signals in healthy children can be detected in fat pads, epiphysis, physis and in intracartilaginous regions of small bones.^{4–6} It is important that physiological vascularisation on ultrasound in children is not misinterpreted as pathological vascularisation and a sign of synovitis.

Few data exist on the evaluation of Doppler findings in patients with juvenile idiopathic arthritis (JIA). The studies conducted have

used different scanning approaches, definitions for abnormal Doppler signals and scoring systems.^{7–11} In addition, previous studies have mostly used ultrasound definitions developed for adults with rheumatoid arthritis (RA), which may not be suitable for use in children.^{7–11}

The Outcome Measures in Rheumatology (OMERACT) ultrasound group has made preliminary ultrasound definitions for synovitis in children, including B-mode (BM) and Doppler findings.¹² Only Doppler signals detected within synovial hypertrophy are considered pathologic.¹² The fact that Doppler signals need to be intrasynovial and not just intraarticular is an important differentiation from the definition in adults.¹³

A standardised ultrasound examination and scoring system for Doppler signals are needed to clarify the role of Doppler findings in monitoring disease activity and treatment effects in patients with JIA. A scanning protocol and an ultrasonographic joint-specific semiquantitative scoring system for BM synovitis and power Doppler (PD) activity with reference atlas for patients with JIA have recently been developed and have shown moderate to excellent reliability.¹⁴

As ultrasound is increasingly being used in the evaluation of synovitis in children and has become an important tool in the management of patients with JIA,^{15,16} it is essential to understand the significance of Doppler findings in these patients. A description of abnormal Doppler signals and an evaluation of whether these findings reflect active disease are needed.

The objectives of this study were, first, to describe PD ultrasound findings in joint regions with BM synovitis using a standardised scanning protocol and a joint-specific scoring system for synovitis with reference atlas for patients with JIA. Second, to explore whether PD grades were associated with BM grades and with the presence of clinical arthritis. Further, to examine associations between PD grades and age, sex, JIA subgroups, disease duration and measures of disease activity.

METHODS

In this cross-sectional study, 27 patients with JIA, classified according to the International League of Associations for Rheumatology (ILAR),¹⁷ who had suspected clinical arthritis, that is, an assumed flare that required treatment adjustment, were consecutively recruited from the inpatient and outpatient clinic at the Department of Rheumatology at Oslo University Hospital, Norway between September 2020 and May 2022.

Clinical and laboratory assessment

The patient's age, sex, JIA subgroup, disease duration and medications used were registered at the study visit. Clinical 71 joint evaluation¹⁸ was performed by experienced rheumatologists who were blinded to ultrasound findings. Clinical arthritis was defined as the presence of joint swelling, or of joint tenderness and limited range of motion.¹⁹ Disease activity was assessed using the 10-joint

Juvenile Arthritis Disease Activity Score (JADAS10), (range 0–40) with the new cutoffs for disease activity states in JIA.^{18,20} The JADAS10 includes the following four measures; the number of joints with clinical arthritis (the count of joints with clinical arthritis up to a maximum of ten joints, any joint count higher than 10 gives 10 points in the score), physician global assessment (PhGA) of disease activity (0–10 cm Visual Analogue Scale (VAS) where 0=no activity and 10=maximum activity), parent/patient global assessment (PGA) of the patients well-being (0–10 cm VAS where 0=verywell, 10=very poor) and the normalised erythrocyte sedimentation rate (0–10).^{18,20}

Ultrasound examination

All patients underwent an ultrasound examination within 2 days after the clinical assessment. The ultrasound examinations were performed by the same rheumatologist (NKS) with extensive ultrasound experience. Inter-reader and intra-reader reliability evaluation have been reported in a previous study.¹⁴ The ultrasonographer was blinded to clinical findings, but the patient's age was known. The same ultrasound machine, a GE Logiq S8 machine with linear probe (6–15 MHz) and hockey stick (8–18 MHz), with standardised settings for BM and PD (pulse repetition frequency 0.6 kHz, frequency 7.7 MHz and low wall filter) was used in all examinations. PD was chosen instead of colour Doppler because the ultrasonographer had most experience with PD. The ultrasound examinations were done in 18 joint regions bilaterally according to an image acquisition protocol for patients with JIA including the anterior elbow, posterior elbow, radiocarpal, midcarpal, metacarpophalangeal (MCP)2 and MCP3 (dorsal), proximal interphalangeal (PIP)2 and PIP3 (dorsal and volar), knee (suprapatellar and lateral parapatellar recess), tibiotalar, talonavicular, anterior subtalar, posterior subtalar, metatarsophalangeal (MTP)2 and MTP3 (dorsal) joints.¹⁴ Synovitis detection on ultrasound was defined according to the preliminary ultrasound definitions for synovitis in children.¹² The ultrasound findings were scored at the time of acquisition according to a joint-specific semiquantitative scoring system for BM synovitis and PD activity with reference atlas for patients with JIA ranging from grade 0 (normal) to grade 3 (severe) for each joint region.¹⁴ PD activity was scored accordingly: grade 0: no Doppler signal. Grade 1: 1–3 signals within the area of synovial hypertrophy only. Grade 2: >3 signals or confluent signals present in <50% of the area of synovial hypertrophy. Grade 3: confluent signals present in >50% of the area of synovial hypertrophy.²¹ The synovial abnormalities threshold for BM and PD findings was chosen to be grade ≥ 1 . PD findings were only scored within synovial hypertrophy in joint regions with BM synovitis (grade ≥ 1). The EULAR recommendations checklist for reporting of ultrasound studies in rheumatic and musculoskeletal diseases was used.²²

Statistical analysis

Baseline patient characteristics were expressed as the number (%) or median (IQR). Further analyses were performed on a joint level. This included the 18 joint regions that were examined with ultrasound (anterior elbow, posterior elbow, radiocarpal, midcarpal, MCP2-3 (dorsal), PIP2-3 (dorsal and volar), knee (suprapatellar and lateral parapatellar recess), tibiotalar, talonavicular, anterior subtalar, posterior subtalar and MTP2-3 (dorsal)). Only joint regions with BM synovitis (grade \geq 1) were included in the analyses. The proportion of PD findings (grades 0–3) in joint regions with BM synovitis and in joint regions with clinical arthritis was described. Joint regions within the same clinically assessed joint (elbow anterior/posterior, knee suprapatellar/lateral parapatellar recess, subtalar anterior/posterior, PIP dorsal/volar) were attributed to the same clinical finding. To account for within-patient effect (random intercept), we used multilevel mixed-effects ordered logistic regression analyses. Cross-sectional associations between PD grades and BM grades and clinical arthritis were examined with adjustment for joint regions and side (left and right). We also performed analysis with further adjustment for age and sex to examine if the associations were altered. Associations between PD grades and age, sex, JIA subgroups, disease duration and measures of disease activity (JADAS10) were also explored. P values <0.05 were regarded as statistically significant. For missing PhGA, PGA and biochemical values, the JADAS10 was not estimated. One joint region (anterior elbow) was not assessed by ultrasound because of band-aid in the elbow, but for joint regions assessed by ultrasound there were no missing values for BM grades, PD grades or findings of clinical arthritis. Statistical analyses were performed using STATA V.17.

Patient and public involvement

Patients did not actively participate in the planning of this study. However, the participants and the Norwegian Rheumatism Association have communicated that this is of interest to the patient community, especially due to the difference in the use and interpretation of ultrasound in children. Study results will be disseminated to patients and the public through the patient organisation's website and newsletter.

RESULTS

Table 1 shows demographic and clinical characteristics of the 27 patients. A total of 971 joint regions were evaluated by ultrasound. Of these, 129 joint regions had BM synovitis and were included in further analyses (flowchart of joint region assessment in online supplemental figure 1).

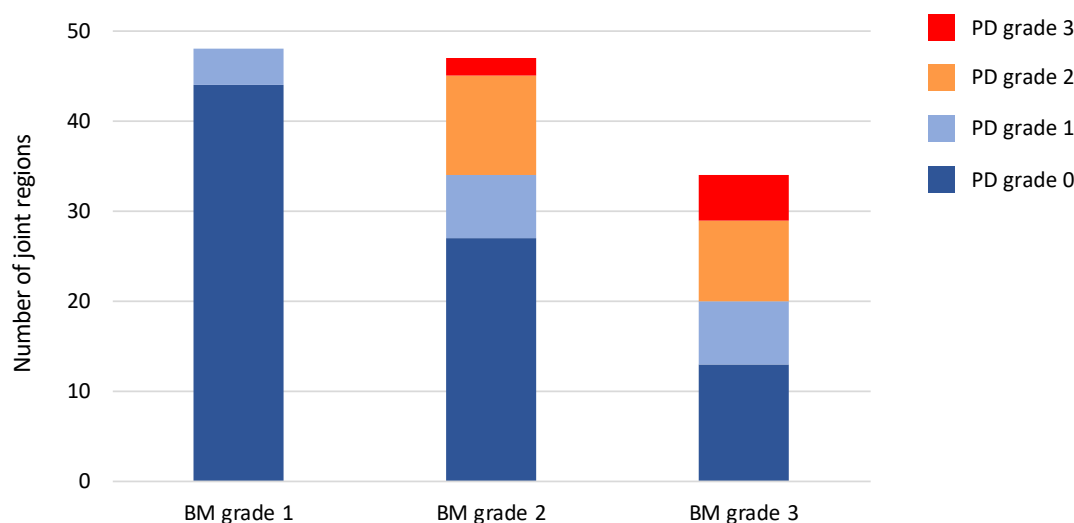
Abnormal PD signals were present in 45 of 129 joint regions with BM synovitis (34.9%), of which 18, 20 and 7 joint regions had PD grades 1, 2 and 3, respectively. Of the 129 joint regions with BM synovitis, 84 of 129 joint

Table 1 Demographic and clinical characteristics of the 27 patients with JIA

Characteristics	Value
Girls, n (%)	21 (77.8)
Age, median years (IQR)	8 (6–12)
Age groups, n (%)	
2–4 years	6 (22.2)
5–8 years	9 (33.3)
9–12 years	6 (22.2)
13–18 years	6 (22.2)
JIA subgroups, n (%)	
Oligoarthritis	17 (63.0)
Polyarthritis RF negative	5 (18.5)
Polyarthritis RF positive	3 (11.1)
Psoriatic arthritis	2 (7.4)
Disease duration, median months (IQR)	2 (0–50)
JADAS10, median (IQR)	9.8 (6.9–12.8)
Disease activity group, n (%)	
Minimal	3 (11.1)
Moderate	15 (55.6)
High	4 (14.8)
Missing	5 (18.5)
ESR, mm/hour, median (IQR)	12 (4.5–24)
CRP, mg/L, median (IQR)	1.2 (0–6.6)
Medication, n (%)	
Methotrexate	12 (44.4)
TNF alfa inhibitor	4 (14.8)
NSAIDS	7 (25.9)
No medication	6 (22.2)
Patient/parent global, median VAS 0–10 cm (IQR)	4.8 (1.1–6.1)
Physician global, median VAS 0–10 cm (IQR)	3.6 (2.5–5.4)
Joints with clinical arthritis, median number (IQR)	2(1–4)
CRP, C reactive protein; ESR, erythrocyte sedimentation rate; JADAS10, 10-joint Juvenile Arthritis Disease Activity Score; JIA, juvenile idiopathic arthritis; NSAIDS, non-steroidal anti-inflammatory drugs; RF, rheumatoid factor; TNF, tumour necrosis factor; VAS, Visual Analogue Scale.	

regions (65.1%) did not have PD findings (PD grade=0). PD grade 1 was found in 4 of 48 (8.3%), 7 of 47 (14.9%) and 7 of 34 (20.6%) joint regions with BM grades 1, 2 and 3, respectively. PD grades 2 and 3 were only present in joint regions with BM grades 2 and 3 (figure 1A). Increasing PD grades were associated with higher BM grades (OR 5.0, 95% CI 2.7 to 9.1, $p<0.001$). Additional adjustment for age and sex did not alter the results (data not shown).

Figure 1A.



1B.

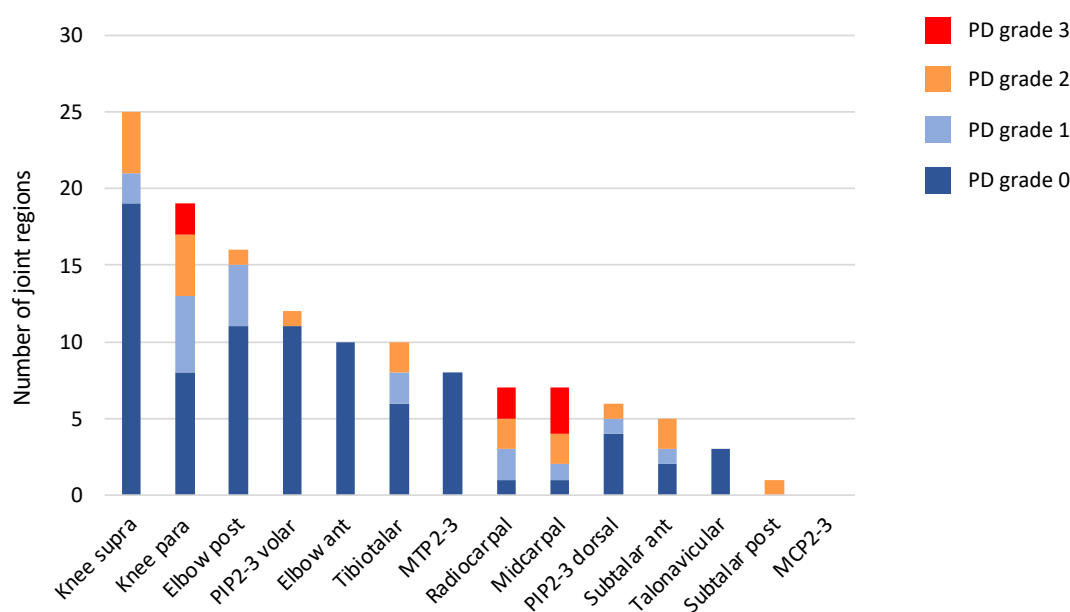


Figure 1 (A). Power Doppler (PD) ultrasound findings (grades 0–3) in 129 joint regions with B-mode (BM) synovitis (grades 1–3) in patients with juvenile idiopathic arthritis (JIA). (B). Distribution of PD ultrasound findings (grades 0–3) in 129 joint regions with BM synovitis in patients with JIA. ant, anterior; MCP, metacarpophalangeal; MTP, metatarsophalangeal; para, parapatellar recess; PIP, proximal interphalangeal; Post, posterior; supra, suprapatellar recess.

Converted

The lateral parapatellar recess of the knee was the joint region with most PD findings (11 of 45 joint regions (24.4%)), followed by the radiocarpal (6 of 45 joint regions (13.3%)), the midcarpal (6 of 45 joint regions (13.3%)) and the suprapatellar recess of the knee (6 of 45

joint regions (13.3%)). The joint region with most findings of BM synovitis without abnormal PD signals was the suprapatellar recess of the knee (19 of 84 joint regions (22.6%)). Synovitis based on BM findings without PD findings and synovitis based on BM and PD findings are

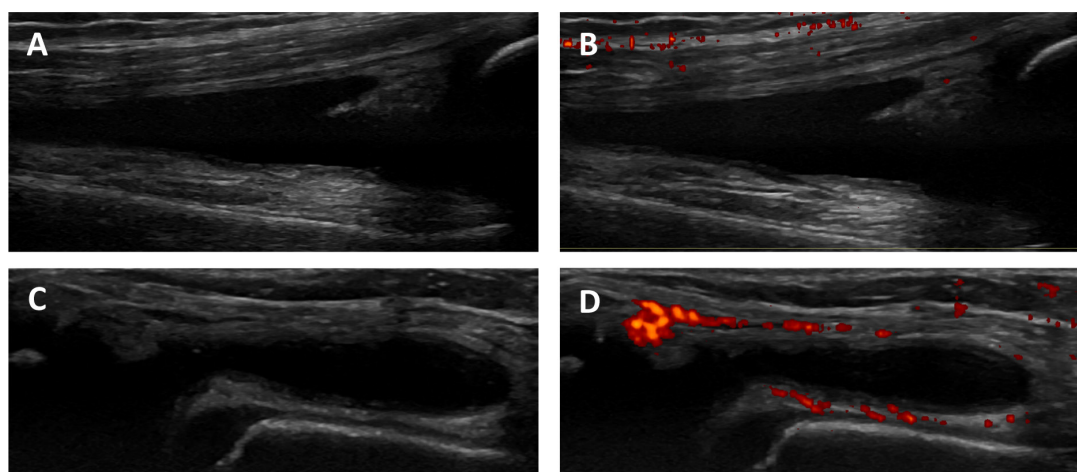


Figure 2 Illustration of variations in power Doppler (PD) ultrasound findings in two joint regions of the knee in a 10-year-old with juvenile idiopathic arthritis (JIA). Longitudinal dorsal scan of the knee joint (suprapatellar recess) showing B-mode (BM) synovitis (A), and BM synovitis without abnormal PD signals (grade 0) (B). Longitudinal dorsal scan of the knee joint (lateral parapatellar recess) showing BM synovitis (C), and BM synovitis with abnormal PD signals (grade 3) (D).

illustrated in [figure 2](#). There were no BM or PD findings in the MCP2 or MCP3 joints. Distribution of PD findings (grades 0–3) in the 129 joint regions with BM synovitis are illustrated in [figure 1B](#).

Of joint regions with PD grades 1, 2 and 3, clinical arthritis was present in 13 of 18 (72.2%), 17 of 20 (85.0%) and 7 of 7 (100.0%), respectively. Of joint regions considered as clinical arthritis, 37 of 78 joint regions (47.4%) had PD findings. The lateral parapatellar recess of the knee had the highest frequency of PD findings (10 of 37 (27.0%)), followed by the radiocarpal (6 of 37 (16.2%)), the midcarpal (6 of 37 (16.2%)) and the suprapatellar recess of the knee (6 of 37 (16.2%)) in joints with clinical arthritis. Increasing PD grades were significantly associated with the presence of clinical arthritis (OR 7.4, 95% CI 2.6 to 21.0, $p < 0.001$). Additional adjustment for age and sex did not alter the results (data not shown).

Abnormal PD signals were present in all age groups. Joint regions with PD findings were seen in 9 of 27 (33.3%), 11 of 35 (31.4%), 14 of 27 (51.9%) and 11 of 40 (27.5%) in the age groups 2–4, 5–8, 9–12 and 13–18 years, respectively. Boys had PD findings in 13 of 32 joint regions (40.6%) whereas girls had PD findings in 32 of 97 joint regions (33.0%). Oligoarthritis was the JIA subgroup that had most PD findings (29 of 73 joint regions (39.7%)), followed by polyarthritis rheumatoid factor (RF) positive (10 of 33 joint regions (30.3%)), polyarthritis RF negative (5 of 17 joint regions (29.4%)) and psoriatic arthritis (1 of 6 joint regions (16.7%)). Joint regions with PD findings were seen in 1 of 6 (16.7%), 27 of 68 (39.7%) and 9 of 33 (27.3%) in the minimal, moderate and high disease activity groups, respectively. Cross-sectional associations were not found between PD findings and age, sex, JIA subgroups, disease duration or JADAS10.

DISCUSSION

This is the first study to investigate associations between PD grades and BM grades and the presence of clinical arthritis in multiple joint regions using a standardised scanning protocol and a joint-specific scoring system for synovitis with reference atlas for patients with JIA. On joint level, increasing PD grades were strongly associated with higher BM grades. We also demonstrated a clear association between increasing PD grades and the presence of clinical arthritis. This suggests that the scoring system corresponds well with the severity of synovitis.

The preliminary ultrasound definitions for synovitis in children emphasise that synovitis can include BM findings alone, but not PD findings alone.¹² In our study, we found many joint regions with BM synovitis without abnormal PD signals. This could represent residual findings of previous active arthritis,²³ or that our patients had a low-grade severity arthritis. It could also indicate that BM synovitis alone without PD findings is more common in patients with JIA, or that synovial effusion without synovial hypertrophy is a prominent feature in joints with active arthritis since Doppler signals must be detected within synovial hypertrophy to be considered as a sign of synovitis.

In joint regions that had PD findings, most had findings of clinical arthritis. The knee, radiocarpal and midcarpal joints had the highest frequency of PD findings in joints with clinical arthritis. The wrist joint is difficult to evaluate clinically and has been identified as an indicator of poor outcome and a vulnerable site of structural damage.^{24 25} Ultrasound can be an important and helpful tool in the evaluation of this joint as ultrasound has been shown to be more sensitive than clinical examination in the evaluation of joint inflammation in peripheral joints.²⁶ Our findings might suggest that the presence of abnormal PD signals is a sign of disease

severity, but longitudinal studies are needed to examine this further.

We found that increasing PD signals were associated with the presence of clinical arthritis, but not with the composite disease activity score JADAS10. This could be because clinical joint examination and ultrasound evaluate the precise site of inflammation, while the JADAS measures the disease activity more widely and may also be affected by confounding factors. Other studies have reported poor correlation between ultrasound findings and JADAS.⁷ In this study, we explored associations on joint level, if we had investigated on patient level with ultrasound sum scores, we might have obtained other results. This could be addressed in a future study.

We found a high number of PD findings in the lateral parapatellar recess of the knee joint. The highest number of BM synovitis without PD findings was found in the suprapatellar recess of the knee joint. This may be because the parapatellar recess is more superficial than the suprapatellar recess and therefore easier to detect Doppler signals there. This supports the added value of scanning both the suprapatellar and the parapatellar recess when evaluating the knee joint with ultrasound in children, as has also been suggested by others.²¹

We did not find BM synovitis, and therefore, no abnormal PD signals, in the MCP joints. This was unexpected since these joints are superficial and PD findings are then often easier to interpret, in addition, the MCP2 joint is often affected in patients with JIA.^{6 27 28} This could be a random finding in our sample, but the small size of the joint, few vessels and slow blood flow velocity could have made it difficult to evaluate. However, we did find synovitis in the PIP joints which are even smaller. The PIP joints were assessed from both the dorsal and volar views. The MCP joints were only evaluated from the dorsal view. In adults with RA, a dorsal approach is recommended over the volar approach to evaluate finger joints with ultrasound.²⁹ To our knowledge, this has not been investigated in children, and the use of only the dorsal or both the dorsal and the volar approaches are inconsistent.^{12 27 28 30} In a clinical setting it can be difficult to evaluate several joints from more views because young children are often impatient. Larger studies to evaluate the different views to include for each joint are needed.

A clear definition of abnormal Doppler signals and a scoring system for Doppler findings is important to discriminate between physiological and pathological vascularisation in children.^{1 12} Magni-Manzoni *et al* evaluated patients with JIA in remission and found that patients with PD findings had less flares than patients without PD findings.³¹ However, most of the PD signals were found in the youngest patients and were scored as a grade 1 and may have represented normal vascularisation. In a study evaluating physiological Doppler signals in healthy children, most Doppler signals were detected in the age group 2–12 years.⁵ We were concerned that physiological Doppler signals in the youngest age groups could affect our interpretation of abnormal PD signals.

However, when performing the ultrasound examinations this was not an issue. This could be because the ultrasonographer only considered Doppler signals within synovial hypertrophy as pathologic in accordance with the preliminary definitions for synovitis in children,¹² and because a standardised scanning approach and scoring system with reference atlas were used during the examinations.¹⁴ In this study, most PD findings were seen in the age group 9–12 years old, but no significant association between PD findings and age was found.

There are some limitations in this study. First, the study was cross-sectional. Consequently, we cannot say anything about the longitudinal associations between PD findings and measures of disease activity, but this was outside the scope of this study. Second, we did not include healthy controls to investigate BM and PD findings in healthy children. It can, therefore, be difficult to conclude with what is a normal finding. However, the purpose of this study was to describe PD findings in joint regions with BM synovitis on ultrasound in patients with JIA, and since Doppler signals must be within synovial hypertrophy to be considered as a sign of synovitis, joint regions without BM synovitis were excluded. Another limitation is that only one rheumatologist performed the ultrasound examinations. The ultrasonographer in this study has shown moderate to excellent inter-reader reliability in a previous ultrasound study.¹⁴ In addition, it is challenging and not feasible to perform several ultrasound examinations in children. Another limitation of this study is the limited number of patients. This might explain why we did not detect pathological ultrasound findings in the MCP2-3 joints, and that there were few findings in some joints. Since the patients in this study were consecutively included from our inpatient and outpatient clinic, we believe that our sample is representative of patients with JIA seen in clinical practice. However, larger studies are needed to explore all joints that can be affected in JIA. Finally, we did not use other modalities like dynamic contrast-enhanced MRI to compare our findings. This should be addressed in a future study.

The strengths of this study include the use of the same ultrasound machine in all assessments, that the ultrasonographer was blinded to clinical findings, and that multiple joint regions were evaluated in a live-exercise. In addition, the image acquisition protocol and the joint-specific scoring system for synovitis with reference atlas ensured a standardised examination and scoring in all patients.

In conclusion, we found that increasing PD grades were significantly associated with higher BM grades and with the presence of clinical arthritis, suggesting that PD signals detected using a standardised ultrasound examination and scoring system can reflect active disease in patients with JIA. However, further studies are needed to understand more about the clinical implications of Doppler findings in these patients.

Acknowledgements The authors thank all the patients and their families who contributed to this study. The support from the Norwegian Rheumatism Association and the Simon Fougner Hartmann's Family Foundation is gratefully acknowledged by the authors.

Contributors NKS designed the study, made substantial contribution to acquisition, analyses and interpretation of data, and writing the manuscript. PB and VL designed the study and made substantial contributions to acquisition and interpretation of data and writing the manuscript. BF, A-BA and EK participated in the study design and made substantial contributions to acquisition of data and writing the manuscript. All authors read and revised the article critically and approved the final manuscript. PB is the guarantor of the study.

Funding This study was funded by the DAM foundation.

Competing interests A-BA reports personal fees from Abbvie, personal fees from Eli Lilly, personal fees from Novartis and personal fees from Pfizer.

Patient consent for publication Not applicable.

Ethics approval The study was approved by the Norwegian Regional Committee for Medical and Health Ethics (REK 2018/805) and done in accordance with the Declaration of Helsinki. Signed informed consent was obtained by patients and/or parents.

Provenance and peer review Not commissioned; externally peer reviewed.

Data availability statement Data are available on reasonable request. Quantified ultrasound data may be available on reasonable request, but patients' data are not publicly available.

Supplemental material This content has been supplied by the author(s). It has not been vetted by BMJ Publishing Group Limited (BMJ) and may not have been peer-reviewed. Any opinions or recommendations discussed are solely those of the author(s) and are not endorsed by BMJ. BMJ disclaims all liability and responsibility arising from any reliance placed on the content. Where the content includes any translated material, BMJ does not warrant the accuracy and reliability of the translations (including but not limited to local regulations, clinical guidelines, terminology, drug names and drug dosages), and is not responsible for any error and/or omissions arising from translation and adaptation or otherwise.

Open access This is an open access article distributed in accordance with the Creative Commons Attribution Non Commercial (CC BY-NC 4.0) license, which permits others to distribute, remix, adapt, build upon this work non-commercially, and license their derivative works on different terms, provided the original work is properly cited, appropriate credit is given, any changes made indicated, and the use is non-commercial. See: <http://creativecommons.org/licenses/by-nc/4.0/>.

ORCID iDs

Nina Krafft Sande <http://orcid.org/0000-0003-3461-9525>

Anna-Birgitte Aga <http://orcid.org/0000-0003-0234-4993>

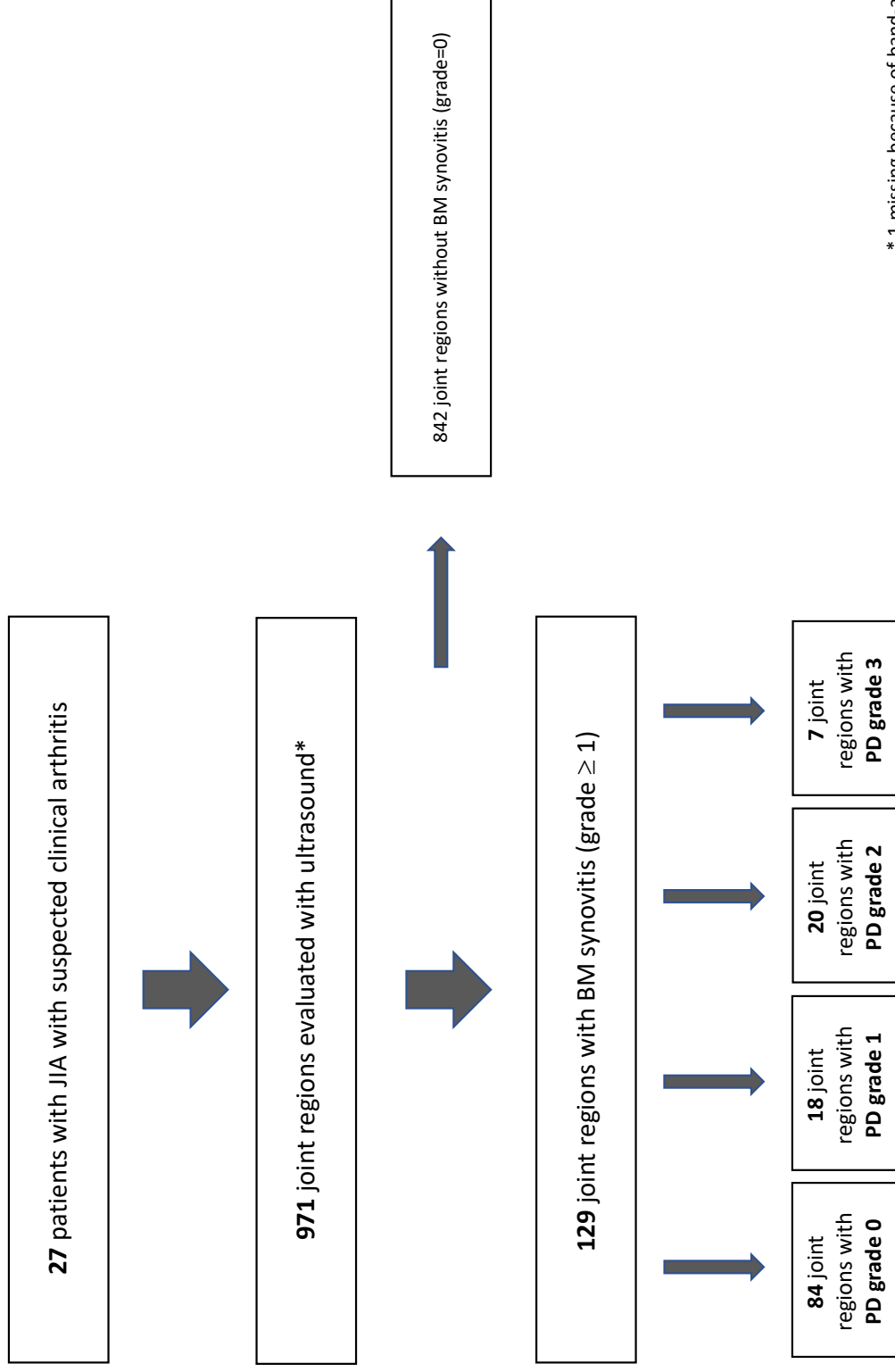
Pernille Bøyesen <http://orcid.org/0000-0002-9751-5144>

REFERENCES

- Roth J, Jousse-Joulin S, Magni-Manzoni S, *et al*. Definitions for the sonographic features of joints in healthy children. *Arthritis Care Res (Hoboken)* 2015;67:136–42.
- Windschall D, Trauzeddel R, Haller M, *et al*. Pediatric musculoskeletal ultrasound: age- and sex-related normal B-mode findings of the knee. *Rheumatol Int* 2016;36:1569–77.
- Magni-Manzoni S. Ultrasound in juvenile idiopathic arthritis. *Pediatr Rheumatol Online J* 2016;14:33.
- Collado P, Windschall D, Vojinovic J, *et al*. Amendment of the OMERACT ultrasound definitions of joints' features in healthy children when using the Doppler technique. *Pediatr Rheumatol Online J* 2018;16:23.
- Windschall D, Collado P, Vojinovic J, *et al*. Age-Related vascularization and ossification of joints in children: an international pilot study to test multiobserver ultrasound reliability. *Arthritis Care Res (Hoboken)* 2020;72:498–506.
- Collado P, Vojinovic J, Nieto JC, *et al*. Toward standardized musculoskeletal ultrasound in pediatric rheumatology: normal age-related ultrasound findings. *Arthritis Care Res (Hoboken)* 2016;68:348–56.
- Magni-Manzoni S, Epis O, Ravelli A, *et al*. Comparison of clinical versus ultrasound-determined synovitis in juvenile idiopathic arthritis. *Arthritis Rheum* 2009;61:1497–504.
- Laurell L, Court-Payen M, Nielsen S, *et al*. Ultrasonography and color Doppler in juvenile idiopathic arthritis: diagnosis and follow-

- up of ultrasound-guided steroid injection in the wrist region. A descriptive interventional study. *Pediatr Rheumatol Online J* 2012;10:11.
- Collado P, Naredo E, Calvo C, *et al*. Reduced joint assessment vs comprehensive assessment for ultrasound detection of synovitis in juvenile idiopathic arthritis. *Rheumatology (Oxford)* 2013;52:1477–84.
- Lanni S, Marafon DP, Civino A, *et al*. Comparison between clinical and ultrasound assessment of the ankle region in children with juvenile idiopathic arthritis. *Arthritis Care Res (Hoboken)* 2021;73:1180–6.
- Shanmugavel C, Sodhi KS, Sandhu MS, *et al*. Role of power Doppler sonography in evaluation of therapeutic response of the knee in juvenile rheumatoid arthritis. *Rheumatol Int* 2008;28:573–8.
- Roth J, Ravagnani V, Backhaus M, *et al*. Preliminary definitions for the sonographic features of synovitis in children. *Arthritis Care Res (Hoboken)* 2017;69:1217–23.
- Wakefield RJ, Balint PV, Szkudlarek M, *et al*. Musculoskeletal ultrasound including definitions for ultrasonographic pathology. *J Rheumatol* 2005;32:2485–7.
- Sande NK, Bøyesen P, Aga A-B, *et al*. Development and reliability of a novel ultrasonographic joint-specific scoring system for synovitis with reference atlas for patients with juvenile idiopathic arthritis. *RMD Open* 2021;7:e001581.
- Windschall D, Malattia C. Ultrasound imaging in paediatric rheumatology. *Best Pract Res Clin Rheumatol* 2020;34:101570.
- Lanni S. The recent evolution of ultrasound in juvenile idiopathic arthritis. *Clin Exp Rheumatol* 2021;39:1413–21.
- Petty RE, Southwood TR, Manners P, *et al*. International league of associations for rheumatology classification of juvenile idiopathic arthritis: second revision, edmonton, 2001. *J Rheumatol* 2004;31:390–2.
- Consolaro A, Ruperto N, Bazso A, *et al*. Development and validation of a composite disease activity score for juvenile idiopathic arthritis. *Arthritis Rheum* 2009;61:658–66.
- Ravelli A, Viola S, Ruperto N, *et al*. Correlation between conventional disease activity measures in juvenile chronic arthritis. *Ann Rheum Dis* 1997;56:197–200.
- Trincianti C, Van Dijkhuizen EHP, Alongi A, *et al*. Definition and validation of the American College of rheumatology 2021 juvenile arthritis disease activity score cutoffs for disease activity states in juvenile idiopathic arthritis. *Arthritis Rheumatol* 2021;73:1966–75.
- Ting TV, Vega-Fernandez P, Oberle EJ, *et al*. Novel ultrasound image acquisition protocol and scoring system for the pediatric knee. *Arthritis Care Res (Hoboken)* 2019;71:977–85.
- Costantino F, Carmona L, Boers M, *et al*. EULAR recommendations for the reporting of ultrasound studies in rheumatic and musculoskeletal diseases (rmds). *Ann Rheum Dis* 2021;80:840–7.
- Rebollo-Polo M, Koujok K, Weisser C, *et al*. Ultrasound findings on patients with juvenile idiopathic arthritis in clinical remission. *Arthritis Care Res (Hoboken)* 2011;63:1013–9.
- Selvaag AM, Flato B, Dale K, *et al*. Radiographic and clinical outcome in early juvenile rheumatoid arthritis and juvenile spondyloarthritis: a 3-year prospective study. *J Rheumatol* 2006;33:1382–91.
- Ravelli A, Martini A. Juvenile idiopathic arthritis. *Lancet* 2007;369:767–78.
- Colebatch-Bourn AN, Edwards CJ, Collado P, *et al*. EULAR-pres points to consider for the use of imaging in the diagnosis and management of juvenile idiopathic arthritis in clinical practice. *Ann Rheum Dis* 2015;74:1946–57.
- Karmazyn B, Bowyer SL, Schmidt KM, *et al*. Us findings of metacarpophalangeal joints in children with idiopathic juvenile arthritis. *Pediatr Radiol* 2007;37:475–82.
- Rossi-Semerano L, Breton S, Semerano L, *et al*. Application of the OMERACT synovitis ultrasound scoring system in juvenile idiopathic arthritis: a multicenter reliability exercise. *Rheumatology (Oxford)* 2021;60:3579–87.
- Witt MN, Mueller F, Weinert P, *et al*. Ultrasound of synovitis in rheumatoid arthritis: advantages of the dorsal over the palmar approach to finger joints. *J Rheumatol* 2014;41:422–8.
- Ventura-Rios L, Faugier E, Barzola L, *et al*. Reliability of ultrasonography to detect inflammatory lesions and structural damage in juvenile idiopathic arthritis. *Pediatr Rheumatol Online J* 2018;16:58.
- Magni-Manzoni S, Scirè CA, Ravelli A, *et al*. Ultrasound-detected synovial abnormalities are frequent in clinically inactive juvenile idiopathic arthritis, but do not predict a flare of synovitis. *Ann Rheum Dis* 2013;72:223–8.

Supplementary Figure 1. Flowchart of joint region assessment by B-mode (BM) and power Doppler (PD) ultrasound



* 1 missing because of band-aid in the elbow

1 Original research

2 **Validity of ultrasound synovitis in juvenile idiopathic arthritis: comparison**
3 **with whole-body magnetic resonance imaging and clinical assessment**

4

5 Nina Krafft Sande^{1,2}, Eva Kirkhus³, Vibke Lilleby¹, Anders H. Tomterstad³, Anna-Birgitte
6 Aga¹, Berit Flatø^{1,2}, Pernille Bøyesen¹

7

8 **Affiliations:**

9 1. Department of Rheumatology, Oslo University Hospital, Oslo, Norway.

10 2. Institute of Clinical Medicine, Faculty of Medicine, University of Oslo, Oslo, Norway.

11 3. Department of Radiology, Oslo University Hospital, Oslo, Norway.

12

13 **Corresponding author:** Nina Krafft Sande

14 Address: Oslo University Hospital, Department of Rheumatology, Pb 4950 Nydalen 0424
15 Oslo, Norway

16 E-mail: ninamkrafft@hotmail.com

17 Phone: 0047 92423660

18

19 Word count manuscript: 3734

20

21 **ABSTRACT:**

22 **Objective:** To assess the validity of ultrasound in juvenile idiopathic arthritis (JIA) by
23 comparing ultrasound detected synovitis with whole-body magnetic resonance imaging (MRI)
24 and clinical assessment of disease activity.

25 **Methods:** In a cross-sectional study, 27 patients with active JIA underwent clinical 71-joints
26 examination, non-contrast enhanced whole-body MRI and ultrasound evaluation of 28 joints
27 (elbow, radiocarpal, midcarpal, metacarpophalangeal 2-3, proximal interphalangeal 2-3, hip,
28 knee, tibiotalar, talonavicular, subtalar and metatarsophalangeal 2-3). One rheumatologist,
29 blinded to clinical findings, performed ultrasound and scored synovitis (B-mode and power
30 Doppler) findings using a semiquantitative joint-specific scoring system for synovitis in JIA.
31 A radiologist scored effusion/synovial thickening on whole-body MRI using a scoring system
32 for whole-body MRI in JIA. At patient level, associations between ultrasound synovitis sum
33 scores, whole-body MRI effusion/synovial thickening sum scores, clinical arthritis sum
34 scores, and the 71-joints Juvenile Arthritis Disease Activity Score (JADAS71) were calculated
35 using Spearman's correlation coefficients (r_s). To explore associations at joint level, sensitivity
36 and specificity were calculated for ultrasound using whole-body MRI or clinical joint
37 examination as reference.

38 **Results:** Ultrasound synovitis sum scores correlated strongly with whole-body MRI
39 effusion/synovial thickening sum scores ($r_s=0.74$, $p<0.01$) and the JADAS71 ($r_s=0.71$,
40 $p<0.01$), and moderately with clinical arthritis sum scores ($r_s=0.57$, $p<0.01$).
41 Sensitivity/specificity of ultrasound in detecting synovitis were 0.57/0.96 and 0.55/0.96 using
42 whole-body MRI or clinical joint examination as reference, respectively.

43

44 **Conclusion:** Our findings suggest that ultrasound is a valid instrument to detect synovitis, and
45 that ultrasound synovitis sum scores can reflect disease activity and may be an outcome
46 measure in JIA.

47 **Key messages**

48 **What is already known on this topic**

49 Ultrasound is increasingly being used in the management of patients with juvenile idiopathic
50 arthritis (JIA). However, the correlation between ultrasound findings and other imaging
51 modalities and the validity of ultrasound detected synovitis in patients with JIA is not well
52 known.

53

54 **What this study adds**

55 Ultrasound synovitis sum scores correlated strongly with whole-body MRI effusion/synovial
56 thickening sum scores and the 71-joints Juvenile Arthritis Disease Activity Score (JADAS71).
57 A novel ultrasonographic joint-specific scoring system with age-divided reference atlas may
58 provide a valid assessment of synovitis in patients with JIA.

59

60 **How this study might affect research, practice or policy**

61 Our findings suggest that ultrasound synovitis sum scores can reflect overall disease activity
62 and may be an important outcome measure in clinical practice and research.

63

64

65

66

67

68

69

70 **INTRODUCTION**

71 Patients with juvenile idiopathic arthritis (JIA) demonstrate a wide range of disease
72 manifestations and the clinical symptoms and signs can be variable. The number of joints with
73 inflammation and the pattern of joint involvement are known to be of prognostic importance
74 and guide the physician in treatment decisions.(1, 2) Detection of joints with inflammation is
75 therefore important for the diagnosis, treatment and follow up of these patients.(3)
76 Consequently, valid methods to detect and quantify joints with inflammation, and to assess
77 disease activity in patients with JIA are needed.

78

79 Traditionally, clinical joint examination with the evaluation of joint swelling, tenderness and
80 limited range of motion in 71 joints is the standard disease activity assessment in patients with
81 JIA, but can be challenging in children due to vague symptoms and complex anatomic
82 regions.(4-6) Contrast enhanced magnetic resonance imaging (MRI) is considered to be the
83 gold standard in detecting synovitis when imaging a target joint,(7, 8) but a limitation is that
84 only one joint or a limited number of joints can be evaluated in each session. Ultrasound is a
85 readily available imaging modality that can assess many joints, is well accepted by children,
86 and has demonstrated to be more sensitive in the evaluation of joint inflammation than clinical
87 examination.(9)

88

89 The process of standardising the use of ultrasound in children has evolved in recent years.(10-
90 15) Standardised ultrasound scanning approaches and scoring systems have shown to provide
91 reliable findings of synovitis.(13-15) However, it is less known whether ultrasound detected
92 synovitis in children correlates with other imaging modalities and validated measures of
93 disease activity.

94

95 Few studies validating ultrasound findings of synovitis in children are available, and the
96 studies conducted are difficult to compare as they vary in ultrasound definitions of synovitis,
97 number of joints assessed, scoring systems, and type of comparator used.(5, 6, 16-23) Most
98 previous studies evaluating the validity of ultrasound have assessed single joints with
99 ultrasound using clinical examination or contrast enhanced MRI as comparators.(5, 16, 17, 20,
100 23) Other studies have examined multiple joints with ultrasound using clinical examination as
101 a comparator.(18, 21, 22) To our knowledge, no studies have examined multiple joints with
102 ultrasound using MRI as a comparator. This is now possible with whole-body MRI, which can
103 depict the entire axial skeleton and peripheral joints in each session.(8) The use of contrast
104 in whole-body MRI is challenging as prolonged scan time can lead to incorrect interpretation
105 of synovial contrast enhancement.(24) However, inflammation can be evaluated without
106 contrast by detecting and quantifying effusion and synovial thickening.

107

108 The objective of this study was to assess the construct validity of ultrasound in patients with
109 JIA, using a standardised scanning approach and a joint-specific semiquantitative scoring
110 system for synovitis with age-divided reference atlas, by comparing ultrasound detected
111 synovitis with non-contrast enhanced whole-body MRI findings of effusion/synovial
112 thickening and clinical assessment of disease activity.

113

114 **METHODS**

115 This cross-sectional study was conducted at the Department of Rheumatology, Oslo
116 University Hospital (OUH) Rikshospitalet from September 2021 to December 2022. Patients
117 fulfilling the International League of Associations for Rheumatology (ILAR) criteria for
118 JIA,(25) who were referred to an MRI of a joint or a whole-body MRI on clinical indication
119 and attending the paediatric rheumatology clinic at OUH were consecutively included. Signed

120 informed consent was obtained from parents and from patients when aged 16 years and older.
121 The study was done in accordance with the Declaration of Helsinki and approved by the
122 Norwegian Regional Committee for Medical and Health Research Ethics (REK 2018/805).

123

124 **Study assessment**

125 Upon study inclusion, the assigned MRI examination was converted to a non-contrast
126 enhanced whole-body MRI since the intention was to evaluate many joints. Each patient was
127 first assessed clinically by their treating rheumatologist, then ultrasound and whole-body MRI
128 examinations were performed within an average of 1-2 days. No changes were made to the
129 patient's medications between the clinical, ultrasound and whole-body MRI assessments. The
130 rheumatologists, the ultrasonographer and the radiologist were blinded to each other's
131 findings, but the age of the patient was known to all assessors. The ultrasonographer and the
132 radiologist were also blinded to clinical information.

133

134 **Clinical and laboratory assessment**

135 Each patient was assessed by experienced rheumatologists who performed clinical 71-joints
136 examination including the following joints: the temporomandibular, sternoclavicular,
137 acromioclavicular, shoulder, elbow, wrist, metacarpophalangeal (MCP) 1-5, proximal
138 interphalangeal (PIP) 1-5, distal interphalangeal (DIP) 2-5, hip, knee, ankle, subtalar,
139 intertarsal, metatarsophalangeal (MTP) 1-5, toe 1-5, and the cervical spine. Clinical active
140 arthritis (active joint) was defined as the presence of joint swelling or, if no swelling was
141 present, the presence of joint pain/tenderness and limited range of motion.(26) Presence or
142 absence of active joints was recorded and an active joint sum score was calculated for each
143 patient (range 0-71). Patient and disease variables including age, sex, JIA subgroup, disease
144 duration, medications, duration of morning stiffness (minutes), patient/parent global

145 assessment (PGA) of well-being (0-10 cm visual analogue scale (VAS), 0 = very well and 10
146 = very poor) and the physician global assessment (PhGA) of disease activity (0-10 cm VAS,
147 0 = no activity and 10 = maximum activity) were recorded. Biochemical analyses included
148 erythrocyte sedimentation rate (ESR), C-reactive protein (CRP), Antinuclear antibody (ANA),
149 Rheumatoid factor (RF) and Anti-cyclic citrullinated peptide (Anti-CCP). Disease activity was
150 measured using the 71-joints Juvenile Arthritis Disease Activity Score (JADAS71), with a
151 total score of 0-101.(27) The JADAS71 is calculated as the sum of the score of the four
152 following components: the number of joints with active arthritis up to a maximum of 71 joints,
153 PGA (0-10 cm VAS), PhGA (0-10 cm VAS) and the normalised ESR (0-10).(27)

154

155 **Ultrasound assessment**

156 One rheumatologist (NKS), with broad experience in musculoskeletal ultrasound (9 years),
157 performed the ultrasound examinations according to a recently published standardised
158 scanning protocol for patients with JIA.(14) The following 14 joints (19 joint regions) were
159 assessed bilaterally: anterior elbow, posterior elbow, radiocarpal, midcarpal, MCP2-3 (dorsal),
160 PIP2-3 (dorsal and volar), hip, knee (suprapatellar recess and lateral parapatellar recess),
161 tibiotalar, talonavicular, anterior subtalar, posterior subtalar, and MTP2-3 (dorsal). Synovitis
162 detection by ultrasound included B-mode (BM) and power Doppler (PD) findings. BM
163 findings included synovial effusion and/or synovial hypertrophy, defined according to the
164 preliminary definitions for synovitis in children, and PD signals had to be detected within
165 synovial hypertrophy to be considered as a sign of synovitis.(12) The images were scored at
166 the time of acquisition for BM and PD findings according to a semiquantitative joint-specific
167 scoring system for BM synovitis (grades 0-3) and PD activity (grades 0-3) with age-divided
168 reference atlas for patients with JIA for each joint region.(14) A printed version of the scoring
169 system with reference atlas was available during the ultrasound assessment and the

170 examination took an average of 27 minutes (range 13-39 minutes). Ultrasound synovitis sum
171 scores were calculated for each patient for BM scores and PD scores (range 0-84) and for a
172 combined score (BM + PD scores (range 0-168)). To avoid increased weighting of joints that
173 were assessed from more than one view by ultrasound (elbow anterior/posterior, PIP2-3
174 dorsal/volar, knee suprapatellar/lateral parapatellar recess, subtalar anterior/posterior), the
175 highest BM and PD value for each joint region was selected. The rheumatologist used the
176 same ultrasound machine, a GE Logiq S8 machine with multifrequency linear probe (6-15
177 MHz) and hockey stick (8-18 MHz), and standardised settings for BM and PD (pulse repetition
178 frequency (PRF) 0,6 kHz, frequency 7,7 MHz and low wall filter) in all examinations. To
179 ensure a clear description of the study, the European Alliance of Associations for
180 Rheumatology (EULAR) recommendations checklist for the reporting of ultrasound studies
181 in rheumatic and musculoskeletal diseases was used.(28)

182

183 **Whole-body MRI acquisition and assessment**

184 Non-contrast enhanced whole-body MRI was performed using Avanto fit 1.5T, Aera 1.5T and
185 Vida Fit 3T (Siemens Healthineers, Erlangen, Germany), with local receiver coils covering
186 the entire body. General anaesthesia was given to the youngest patients (under 5 years of age)
187 to avoid motion artefacts during the examination. The protocol included T2 Turbo spin echo
188 (TSE) Dixon sequences: coronal plane from the skull base to the thighs; sagittal plane in both
189 knees and ankles; oblique coronal plane in the sacroiliac joints; and sagittal plane in the spine.
190 The image acquisition parameters were preset: repetition time (TR) >2000ms/echo time (TE)
191 92-111ms, field of view (FOV) 15-35 cm, slice thickness 3-4 mm, and in-plane resolution
192 0.39-0.55 mm². Acquisition time was approximately 30 minutes. Images were deidentified
193 and analysed using Sectra Picture Archiving and Communications Systems (PACS). Joint
194 inflammation on whole-body MRI included effusion/synovial thickening defined as

195 hyperintense signal intensity within the joint space distending the joint capsule on fluid
196 sensitive sequence, as suggested by the MRI in JIA (JAMRI) Outcome Measures in
197 Rheumatology (OMERACT) working group.(29) The whole-body MRI images were scored
198 by a radiologist (EK) with extensive experience in musculoskeletal MRI (more than 20 years).
199 Effusion/synovial thickening was scored as absent, mild or moderate (grades 0-2) in large
200 joints (elbows, hips and knees) and as absent or present (grades 0-1) in small joints according
201 to a newly developed semiquantitative whole-body MRI scoring system for JIA.(29)
202 Effusion/synovial thickening scores from the same 28 joints that were assessed with
203 ultrasound were included in the analyses, and a whole-body MRI effusion/synovial thickening
204 sum score was calculated for each patient (range 0-34). Whole-body MRI was performed in
205 all patients except for one where the consent to the examination was withdrawn by the parents.

206

207 **Patient and public involvement**

208 Patients did not actively participate in the planning of this study, but the participants and the
209 Norwegian Rheumatism Association have shown great interest in the study and supported the
210 project. Study results will be disseminated to patients and the public through the patient
211 organisation's website and newsletter.

212

213 **Statistical analysis**

214 Descriptive statistics were calculated as number (%), mean (range) or median (interquartile
215 range (IQR)) as appropriate. At patient level, Spearman's correlation coefficient (r_s) was used
216 to calculate associations between ultrasound synovitis sum scores and whole-body MRI
217 effusion/synovial thickening sum scores, and clinical active joint sum scores. In addition,
218 associations between ultrasound synovitis sum scores and the JADAS71, CRP, ESR, PhGA,
219 and PGA were calculated. The strength of r_s was defined as: very weak 0.0-0.19; weak 0.20-

220 0.39; moderate 0.40-0.59; strong 0.60-0.79 and very strong 0.80-1.0. P-values < 0.05 were
221 regarded as statistically significant. Sum scores for ultrasound, whole-body MRI and clinical
222 joint examination were calculated without any missing values. The JADAS71 was not
223 calculated for patients missing PhGA or PGA (n=2 in total).

224

225 At joint level, the 28 joints (elbow, radiocarpal, midcarpal, MCP2-3, PIP2-3, hip, knee,
226 tibiotalar, talonavicular, subtalar, and MTP2-3 joints) assessed in each patient, with complete
227 ultrasound, whole-body MRI and clinical joint examination data, were included in the
228 analyses, whereas joints with missing data were excluded. Findings in the wrist joint was
229 recorded as one joint in the clinical assessment but in the analysis at joint level, this finding
230 was allocated to both the radiocarpal and the midcarpal joints. Semiquantitative scores on
231 ultrasound and whole-body MRI were dichotomised for further analyses. The threshold for
232 abnormality was chosen to be BM grade ≥ 2 for ultrasound findings, and grade ≥ 1 for whole-
233 body MRI findings. Sensitivity, specificity, positive predictive value and negative predictive
234 value were calculated for findings of synovitis on ultrasound using whole-body MRI or
235 clinical joint examination as reference. Analyses were performed using SPSS V29.

236

237 **RESULTS**

238 Twenty-seven patients (89% girls), with a median age 12 years (IQR 3-14) were included. The
239 median number of active joints was 4 (IQR 2-6) and the median JADAS71 was 13.4 (IQR 9.4-
240 28.6). Demographic and clinical characteristics are described in **Table 1**.

241

242

243

244 **Table 1.** Demographic and clinical characteristics of the patients with juvenile idiopathic
 245 arthritis (n=27).

Characteristics	Value
Sex	
Girls, n (%)	24 (89)
Age, median years (IQR)	12 (3-14)
JIA subgroups, n (%)	
Oligoarthritis	13 (48.1)
Polyarthritis RF negative	5 (18.5)
Polyarthritis RF positive	5 (18.5)
Psoriatic arthritis	3 (11.1)
Undifferentiated arthritis	1 (3.7)
Disease duration, median months (IQR)	0 (0-9)
ESR, mm/hour, median (IQR)	17 (7-59)
CRP, mg/L, median (IQR)	2.1 (0.6-13)
ANA positive, n (%)	14 (51.9)
RF positive, n (%)	5 (18.5)
Anti-CCP positive, n (%)	7 (25.9)
Medications, n (%)	
Methotrexate	11 (40.7)
TNF alfa inhibitor	3 (11.1)
NSAIDS	13 (48.1)
No medication	3 (11.1)
Morning stiffness, minutes (IQR)	30 (15-120)
Patient/parent global, median VAS 0-10 cm (IQR)	5.1 (2.1-6.9)
Physician global, median VAS 0-10 cm (IQR)	4.8 (2.8-6.8)
Active joints, median number (IQR)	4 (2-6)
JADAS71, median (IQR)	13.4 (9.4-28.6)

246 N, number; IQR, interquartile range; JIA, juvenile idiopathic arthritis; RF, rheumatoid factor; ESR, erythrocyte
 247 sedimentation rate; CRP, C-reactive protein; ANA, antinuclear antibody; Anti-CCP, anti-cyclic citrullinated
 248 peptide; TNF, tumour necrosis factor; NSAIDS, non-steroidal anti-inflammatory drugs; VAS, Visual Analogue
 249 Scale; JADAS71, Juvenile Arthritis Disease Activity Score for 71 joints.
 250
 251

252 Patient level

253 The median ultrasound synovitis sum score was 7.0 (IQR 4.0-12.0), 1.0 (IQR 0.0-5.0) and 9.0
 254 (IQR 4.0-17.0), for BM synovitis sum scores, PD synovitis sum scores and combined synovitis
 255 sum scores, respectively. The median whole-body MRI effusion/synovial thickening sum
 256 score was 2.5 (IQR 0.8-7.0). Ultrasound combined synovitis sum scores correlated strongly
 257 with whole-body MRI effusion/synovial thickening sum scores ($r_s = 0.74$, $p < 0.01$), and
 258 moderately with clinical active joint sum scores ($r_s = 0.57$, $p < 0.01$). The correlation between

259 ultrasound combined synovitis sum scores and the JADAS71 was also strong ($r_s = 0.71$,
 260 $p < 0.01$). Correlations between ultrasound synovitis sum scores and measures of disease
 261 activity are presented in **Table 2**.

262
 263 **Table 2.** Spearman's correlations (r_s) between ultrasound synovitis sum scores ((B-mode
 264 (BM), power Doppler (PD) and combined (BM + PD) synovitis sum score) and whole-body
 265 magnetic resonance imaging (MRI) effusion/synovial thickening sum scores, active joint sum
 266 scores and other measures of disease activity at patient level.

	Ultrasound BM synovitis sum scores (p-value)	Ultrasound PD synovitis sum scores (p-value)	Ultrasound combined synovitis sum scores (p-value)
Whole-body MRI effusion/synovial thickening sum scores	0.72 (p<0.01)	0.60 (p<0.01)	0.74 (p<0.01)
Active joint sum scores	0.61 (p<0.01)	0.39 (p=0.04)	0.57 (p<0.01)
JADAS71	0.68 (p<0.01)	0.54 (p=0.01)	0.71 (p<0.01)
ESR	0.55 (p<0.01)	0.53 (p=0.01)	0.59 (p<0.01)
CRP	0.70 (p<0.01)	0.51 (p=0.01)	0.70 (p<0.01)
PhGA VAS	0.63 (p<0.01)	0.58 (p<0.01)	0.68 (p<0.01)
PGA VAS	0.32 (p=0.11)	0.20 (p=0.34)	0.36 (p=0.07)

267
 268 BM, B-mode; PD, power Doppler; MRI, magnetic resonance imaging; JADAS71, Juvenile Arthritis Disease
 269 Activity Score for 71 joints; ESR, erythrocyte sedimentation rate; CRP, C-reactive protein; PhGA, physician
 270 global assessment of disease activity; VAS, 0-10 Visual Analogue Scale; PGA, patient/parent global
 271 assessment of well-being. Strength of Spearman's correlation defined as: very weak 0.0-0.19; weak 0.20-0.39;
 272 moderate 0.40-0.59; strong 0.60-0.79; very strong 0.80-1.0. P-value <0.05 considered significant.
 273

274 **Joint level**

275 A total of 1017 joint regions were assessed with ultrasound, 1917 joints were examined
 276 clinically, and 2605 joints were examined with whole-body MRI. In total, 692 joints were
 277 assessed with ultrasound, whole-body MRI and clinical examination, identifying 533 joints
 278 with normal findings.

279

280 For whole-body MRI, 32 joints were missing as they were outside the field of view (elbows)
281 or of poor image quality (PIP and MTP joints). For ultrasound, one MCP2, one MCP3, one
282 PIP2 and one PIP3 joint were missing due to a venous catheter in the hand of a small patient
283 (2 years old) that made it impossible to assess these joints.

284

285 Ultrasound findings of synovitis at joint level demonstrated a sensitivity of 0.57 and a
286 specificity of 0.96, a positive predictive value of 0.71 and a negative predictive value of 0.93
287 using whole-body MRI findings of effusion/synovial thickening as reference. When using
288 active joints found on clinical examination as reference, ultrasound findings of synovitis at
289 joint level had a sensitivity and specificity of 0.55 and 0.96, respectively, while the positive
290 predictive value was 0.71 and the negative predictive value was 0.92.

291

292 Synovitis was most frequently found in the knee (n=16) and the tibiotalar (n=12) joints with
293 ultrasound, while effusion/synovial thickening was most frequently seen in the knee (n=19)
294 and the subtalar joints (n=17) with whole-body MRI (**Figure 1**). Active joints were most
295 frequently found in the knee (n=18) and the subtalar joints (n=14). The overall frequency of
296 normal and inflammatory findings in the 14 joints assessed with ultrasound, whole-body MRI
297 and clinical examination, are presented in **Figure 2**.

298

299 On ultrasound and whole-body MRI, 58/692 joints (8.4%) had findings of synovitis or
300 effusion/synovial thickening, while 566/692 joints (81.8%) had normal findings on both
301 modalities. Ultrasound detected synovitis in 24/590 joints (4.1%) that were normal on whole-
302 body MRI, while effusion/synovial thickening was found in 44/610 joints (7.2%) on whole-
303 body MRI that were considered normal on ultrasound.

304

305 In total, 534/571 joints (93.5%) that were scored as BM grade 0 on ultrasound had normal
306 findings on whole-body MRI. Of the joints scored as BM grade 1 on ultrasound, 32/39 joints
307 (82.1%) were scored as normal on whole-body MRI. Of all joints scored as BM grade 2 or
308 BM grade 3 on ultrasound, 21/38 (55.3%) and 37/44 joints (84.1%) were scored with findings
309 of effusion/synovial thickening on whole-body MRI, respectively. In large joints (the elbow,
310 hip and knee) scored as BM grade 3 on ultrasound, 8/12 joints (66.7%) were scored as grade
311 2 on whole-body MRI and 4/12 joints (33.3%) were scored as grade 1 on whole-body MRI.
312 No joint scored as BM grade 3 on ultrasound had normal findings on whole-body MRI for
313 these joints.

314

315 Joint inflammation was found in 58/692 joints (8.4%) on both ultrasound and clinical
316 examination, whereas 562/692 joints (81.2%) had normal findings. Ultrasound detected
317 synovitis in 24/586 joints (4.1%) that were normal on clinical examination. In joints deemed
318 normal on ultrasound, 48/610 (7.9%) were considered as active on clinical examination.

319

320 **DISCUSSION**

321 To our knowledge, this is the first study comparing ultrasound assessment of multiple joints
322 with non-contrast enhanced whole-body MRI and clinical assessment of disease activity in
323 patients with JIA. Our study shows that ultrasound synovitis sum scores are strongly correlated
324 with whole-body MRI effusion/synovial thickening sum scores and clinical measures of
325 disease activity in children and adolescents with JIA.

326

327 A strong association between ultrasound synovitis sum scores and whole-body MRI joint
328 inflammation sum scores has also been reported in adults with rheumatoid arthritis.(30) To
329 the best of our knowledge, no study has compared ultrasound findings of synovitis in multiple

330 joints with MRI in patients with JIA. Laurell et al. compared ultrasound with contrast
331 enhanced MRI of the wrist, knee and ankle joints to evaluate disease activity in JIA, but only
332 one joint was assessed with MRI in each patient. Their results were descriptive but indicated
333 that MRI and ultrasound might be valuable in the evaluation of disease activity in JIA.(31)

334

335 Reliable and validated tools to assess disease activity are needed for optimal management of
336 patients with JIA. The ultrasonographic scoring system for synovitis with age-divided
337 reference atlas used in this study has previously shown moderate to excellent reliability. The
338 next step in the validation process was therefore to test the scoring system in relation to other
339 imaging modalities and measures of disease activity. We found a strong correlation between
340 ultrasound synovitis sum scores and whole-body MRI effusion/synovial thickening sum
341 scores, CRP, PhGA and the JADAS71. Magni-Manzoni et al. found a poor correlation
342 between ultrasound synovitis findings and the JADAS,(18) others have found a moderate
343 correlation.(15) The weak correlation between ultrasound synovitis findings and PGA in our
344 study is in line with previously published findings.(18) While ultrasound evaluates the level
345 of inflammation, PGA might also be affected by other confounding factors.

346

347 Ultrasound demonstrated high specificity, but lower sensitivity in detecting synovitis using
348 whole-body MRI or clinical joint examination as reference. It has previously been shown that
349 ultrasound is more sensitive than clinical examination in the evaluation of joint
350 inflammation.(9) Vega-Fernandez et al. found that ultrasound had a sensitivity of 0.83 for
351 diagnosing synovitis in the knee joint when using contrast-enhanced MRI as reference.(23)
352 The sensitivity demonstrated in this study may have many contributing explanations. The
353 participants were referred to an MRI or whole-body MRI on clinical indication prior to
354 inclusion. MRI is most often performed when there is diagnostic doubt, and this usually

355 applies to joints or joint regions that are difficult to assess clinically and with ultrasound. The
356 affected joints could therefore have been complex and challenging to evaluate. The treating
357 rheumatologist that performed the clinical joint examination was not blinded to the medical
358 history, reason for admission or clinical symptoms of the patients. The ultrasonographer was
359 blinded to all clinical information except for the age of the patient, which was known. This
360 may have influenced the findings. Additional explanations may be involvement of several
361 complex joints, the age of the patient and cooperation during the examinations.

362

363 Contrast enhanced MRI is considered the gold standard for assessing synovitis,(7, 8) and since
364 whole-body MRI can assess many joints in each examination we found it suitable as a
365 comparator to ultrasound and our joint-specific scoring system where many joints are being
366 evaluated. The most frequently detected joint with inflammation on ultrasound, whole-body
367 MRI and clinical examination was the knee joint, which is also the most commonly affected
368 joint in JIA.(3) Whole-body MRI detected inflammation in the knee joint more often than
369 ultrasound. This is in line with others who found that contrast enhanced MRI was superior to
370 ultrasound in the evaluation of the knee joint.(16) Whole-body MRI also detected
371 effusion/synovial thickening more often in the subtalar and the talonavicular joints than
372 ultrasound detected synovitis, but ultrasound found more frequently synovitis in the tibiotalar
373 joint. This may be due to the complex anatomy in the ankle joint.(5, 6, 32, 33) In addition, the
374 positioning of the knee and the ankle joint during the ultrasound and whole-body MRI
375 examinations differed, which may have affected the distribution and organisation of the
376 effusion, as also suggested by others.(31)

377

378 Most of the joints with severe findings on ultrasound (BM grade 3) were also scored with
379 effusion/synovial thickening findings on whole-body MRI (84.1%), and a high number of

380 joints with BM grade 0 and BM grade 1 on ultrasound had normal findings on whole-body
381 MRI. For large joints (the elbow, hip and knee), all joints scored as a BM grade 3 on ultrasound
382 had corresponding effusion/synovial thickening on whole-body MRI. This suggests that the
383 scoring system corresponds well with the severity of synovitis. Interestingly, 32/39 joints
384 (82.1%) with a BM grade 1 on ultrasound (defined as normal in this study) were scored as
385 normal on whole-body MRI. However, if PD signals are detected within synovial hypertrophy
386 in a joint scored as BM grade 1 on ultrasound, it is considered abnormal.(12, 34) This was not
387 an issue in this study, but it can be discussed whether a BM grade 1 on ultrasound represents
388 a normal finding or mild synovitis since there is a lack of defined cut-off levels. In addition,
389 most of the joints were scored binary on whole-body MRI potentially leading to the loss of
390 minimal findings, as also indicated by others.(35)

391

392 Limitations of this study include that only one rheumatologist performed the ultrasound
393 examinations. However, this was done for feasibility reasons and the rheumatologist has
394 shown moderate to excellent reliability in a previous study.(14) Another limitation is that only
395 one radiologist scored the whole-body MRI images. The radiologist has extensive experience
396 in musculoskeletal MRI in children. Not all ultrasound and whole-body MRI examinations
397 were performed on the same day, which may have caused discrepancies in the findings.
398 However, there were no adjustments in the patients' medications in the time between the
399 examinations. The whole-body MRI missed many elbow joints because the joint often was
400 outside the field of view. In addition, small joints (PIP) were difficult to visualise on whole-
401 body MRI compared to standard MRI. Further, we did not use contrast during the whole-body
402 MRI examinations, which might have made it more difficult to evaluate joint pathology.
403 However, since we wanted to assess many joints in one session, this was not possible. The
404 small number of patients in this study may also provide uncertain results. Lastly, since this

405 was not a longitudinal study, we cannot say if ultrasound is responsive to change, this should
406 be addressed in a future study.

407

408 The strengths of this study are that many joints were assessed with the same ultrasound
409 machine, using a standardised scanning approach. In addition, that ultrasound definitions for
410 synovitis in children were used and findings scored semiquantitatively with a joint-specific
411 scoring system for synovitis with reference atlas for patients with JIA. Further, that the whole-
412 body MRI images were scored according to a newly developed whole-body MRI scoring
413 system for patients with JIA and that a standardised scanning method was used.

414

415 In summary, our findings provide a validation of ultrasound in JIA showing that ultrasound
416 synovitis sum scores correlate strongly with non-contrast enhanced whole-body MRI
417 effusion/synovial thickening sum scores and clinical measures of disease activity. This
418 indicates that the scanning protocol and scoring system provides a valid assessment of
419 synovitis and suggests that ultrasound synovitis sum scores can reflect overall disease activity
420 and may be a useful outcome measure in clinical practice and research.

421

422

423 **Acknowledgements**

424 We would like to thank all the patients and their families who contributed to this study. We
425 also thank Lien My Diep, Researcher (statistician), MSc, for statistical advice. The authors are
426 grateful for the support from the Norwegian Rheumatism Association and the Simon Fougner
427 Hartmann's Family Foundation.

428

429

430 **Contributors**

431 All authors were involved in drafting the article or revising it critically for important
432 intellectual content, approved the final manuscript to be published and agreed to be
433 accountable for all aspects of the work. NKS designed the study, made substantial contribution
434 to acquisition, analyses and interpretation of data. PB designed the study and made substantial
435 contribution to acquisition and interpretation of data. EK, VL, and BF participated in the study
436 design and made substantial contributions to acquisition and interpretation of data. AHT
437 participated in the study design and made substantial contribution to acquisition of data. ABA
438 made substantial contribution to acquisition and interpretation of data. PB is the guarantor of
439 the study.

440

441 **Funding**

442 This study was funded by the DAM foundation.

443

444 **Competing interests**

445 ABA reports personal fees from AbbVie, Eli Lilly, Novartis and Pfizer.

446

447 **Patient consent for publication**

448 Not applicable

449

450 **Ethics approval and consent to participate**

451 The study was approved by the Norwegian Regional Committee for Medical and Health Ethics
452 (REK 2018/805) and done in accordance with the Declaration of Helsinki. Signed informed
453 consent was obtained from parents and from patients when aged 16 years and older.

454

455 **Data availability statement**

456 Data are available on reasonable request.

457

458 **REFERENCES**

- 459 1. Flatø B, Lien G, Smerdel A, et al. Prognostic factors in juvenile rheumatoid arthritis: a case-
460 control study revealing early predictors and outcome after 14.9 years. *J Rheumatol.* 2003;30:386-93.
- 461 2. Eng SWM, Aeschlimann FA, van Veenendaal M, et al. Patterns of joint involvement in
462 juvenile idiopathic arthritis and prediction of disease course: A prospective study with multilayer non-
463 negative matrix factorization. *PLoS Med.* 2019;16:e1002750.
- 464 3. Ravelli A, Martini A. Juvenile idiopathic arthritis. *Lancet.* 2007;369:767-78.
- 465 4. Rooney ME, McAllister C, Burns JF. Ankle disease in juvenile idiopathic arthritis: ultrasound
466 findings in clinically swollen ankles. *J Rheumatol.* 2009;36:1725-9.
- 467 5. Pascoli L, Wright S, McAllister C, et al. Prospective evaluation of clinical and ultrasound
468 findings in ankle disease in juvenile idiopathic arthritis: importance of ankle ultrasound. *J Rheumatol.*
469 2010;37:2409-14.
- 470 6. Lanni S, Marafon DP, Civino A, et al. Comparison Between Clinical and Ultrasound
471 Assessment of the Ankle Region in Children With Juvenile Idiopathic Arthritis. *Arthritis Care Res*
472 (Hoboken). 2021;73:1180-6.
- 473 7. Damasio MB, Malattia C, Martini A, et al. Synovial and inflammatory diseases in childhood:
474 role of new imaging modalities in the assessment of patients with juvenile idiopathic arthritis. *Pediatr*
475 *Radiol.* 2010;40:985-98.
- 476 8. Malattia C, Tolend M, Mazzoni M, et al. Current status of MR imaging of juvenile idiopathic
477 arthritis. *Best Pract Res Clin Rheumatol.* 2020;34:101629.
- 478 9. Colebatch-Bourn AN, Edwards CJ, Collado P, et al. EULAR-PreS points to consider for the
479 use of imaging in the diagnosis and management of juvenile idiopathic arthritis in clinical practice.
480 *Ann Rheum Dis.* 2015;74:1946-57.
- 481 10. Roth J, Jousse-Joulin S, Magni-Manzoni S, et al. Definitions for the sonographic features of
482 joints in healthy children. *Arthritis Care Res (Hoboken).* 2015;67:136-42.
- 483 11. Collado P, Vojinovic J, Nieto JC, et al. Toward Standardized Musculoskeletal Ultrasound in
484 Pediatric Rheumatology: Normal Age-Related Ultrasound Findings. *Arthritis Care Res (Hoboken).*
485 2016;68:348-56.
- 486 12. Roth J, Ravagnani V, Backhaus M, et al. Preliminary Definitions for the Sonographic Features
487 of Synovitis in Children. *Arthritis Care Res (Hoboken).* 2017;69:1217-23.
- 488 13. Ting TV, Vega-Fernandez P, Oberle EJ, et al. Novel Ultrasound Image Acquisition Protocol
489 and Scoring System for the Pediatric Knee. *Arthritis Care Res (Hoboken).* 2019;71:977-85.
- 490 14. Sande NK, Bøyesen P, Aga AB, et al. Development and reliability of a novel ultrasonographic
491 joint-specific scoring system for synovitis with reference atlas for patients with juvenile idiopathic
492 arthritis. *RMD Open.* 2021;7.
- 493 15. Vega-Fernandez P, Ting TV, Oberle EJ, et al. Musculoskeletal Ultrasound in Childhood
494 Arthritis Limited Examination: A Comprehensive, Reliable, Time-Efficient Assessment of Synovitis.
495 *Arthritis Care Res (Hoboken).* 2021.
- 496 16. El-Miedany YM, Housny IH, Mansour HM, et al. Ultrasound versus MRI in the evaluation of
497 juvenile idiopathic arthritis of the knee. *Joint Bone Spine.* 2001;68:222-30.
- 498 17. Karmazyn B, Bowyer SL, Schmidt KM, et al. US findings of metacarpophalangeal joints in
499 children with idiopathic juvenile arthritis. *Pediatr Radiol.* 2007;37:475-82.
- 500 18. Magni-Manzoni S, Epis O, Ravelli A, et al. Comparison of clinical versus ultrasound-
501 determined synovitis in juvenile idiopathic arthritis. *Arthritis Rheum.* 2009;61:1497-504.
- 502 19. Collado P, Jousse-Joulin S, Alcalde M, et al. Is ultrasound a validated imaging tool for the
503 diagnosis and management of synovitis in juvenile idiopathic arthritis? A systematic literature review.
504 *Arthritis Care Res (Hoboken).* 2012;64:1011-9.

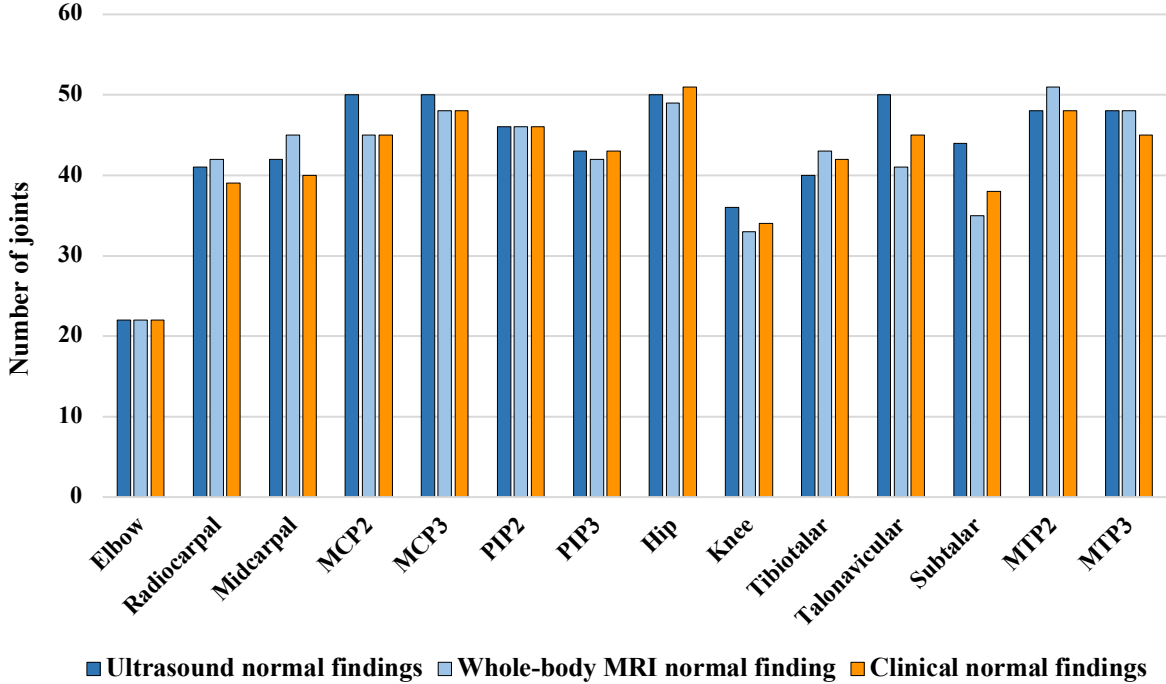
- 505 20. Eich GF, Hallé F, Hodler J, et al. Juvenile chronic arthritis: imaging of the knees and hips
506 before and after intraarticular steroid injection. *Pediatr Radiol*. 1994;24:558-63.
- 507 21. Haslam KE, McCann LJ, Wyatt S, et al. The detection of subclinical synovitis by ultrasound
508 in oligoarticular juvenile idiopathic arthritis: a pilot study. *Rheumatology (Oxford)*. 2010;49:123-7.
- 509 22. Filippou G, Cantarini L, Bertoldi I, et al. Ultrasonography vs. clinical examination in children
510 with suspected arthritis. Does it make sense to use poliarticular ultrasonographic screening? *Clin Exp*
511 *Rheumatol*. 2011;29:345-50.
- 512 23. Vega-Fernandez P, Rogers K, Sproles A, et al. Diagnostic Accuracy Study of the Pediatric-
513 Specific Ultrasound Scoring System for the Knee Joint in Children With Juvenile Idiopathic Arthritis.
514 *Arthritis Care Res (Hoboken)*. 2023.
- 515 24. Panwar J, Patel H, Tolend M, et al. Toward Developing a Semiquantitative Whole Body-MRI
516 Scoring for Juvenile Idiopathic Arthritis: Critical Appraisal of the State of the Art, Challenges, and
517 Opportunities. *Acad Radiol*. 2021;28:271-86.
- 518 25. Petty RE, Southwood TR, Manners P, et al. International League of Associations for
519 Rheumatology classification of juvenile idiopathic arthritis: second revision, Edmonton, 2001. *J*
520 *Rheumatol*. 2004;31:390-2.
- 521 26. Ravelli A, Viola S, Ruperto N, et al. Correlation between conventional disease activity
522 measures in juvenile chronic arthritis. *Ann Rheum Dis*. 1997;56:197-200.
- 523 27. Consolaro A, Ruperto N, Bazso A, et al. Development and validation of a composite disease
524 activity score for juvenile idiopathic arthritis. *Arthritis Rheum*. 2009;61:658-66.
- 525 28. Costantino F, Carmona L, Boers M, et al. EULAR recommendations for the reporting of
526 ultrasound studies in rheumatic and musculoskeletal diseases (RMDs). *Ann Rheum Dis*. 2021.
- 527 29. Panwar J, Tolend M, Redd B, et al. Consensus-driven conceptual development of a
528 standardized whole body-MRI scoring system for assessment of disease activity in juvenile idiopathic
529 arthritis: MRI in JIA OMERACT working group. *Semin Arthritis Rheum*. 2021;51:1350-9.
- 530 30. Ng SN, Axelsen MB, Østergaard M, et al. Whole-Body Magnetic Resonance Imaging
531 Assessment of Joint Inflammation in Rheumatoid Arthritis-Agreement With Ultrasonography and
532 Clinical Evaluation. *Front Med (Lausanne)*. 2020;7:285.
- 533 31. Laurell L, Court-Payen M, Nielsen S, et al. Comparison of ultrasonography with Doppler and
534 MRI for assessment of disease activity in juvenile idiopathic arthritis: a pilot study. *Pediatr Rheumatol*
535 *Online J*. 2012;10:23.
- 536 32. Lanni S, Bovis F, Ravelli A, et al. Delineating the Application of Ultrasound in Detecting
537 Synovial Abnormalities of the Subtalar Joint in Juvenile Idiopathic Arthritis. *Arthritis Care Res*
538 *(Hoboken)*. 2016;68:1346-53.
- 539 33. Remedios D, Martin K, Kaplan G, et al. Juvenile chronic arthritis: diagnosis and management
540 of tibio-talar and sub-talar disease. *Br J Rheumatol*. 1997;36:1214-7.
- 541 34. Sande NK, Lilleby V, Aga AB, et al. Associations between power Doppler ultrasound findings
542 and B-mode synovitis and clinical arthritis in juvenile idiopathic arthritis using a standardised scanning
543 approach and scoring system. *RMD Open*. 2023;9.
- 544 35. D'Agostino MA, Terslev L, Aegerter P, et al. Scoring ultrasound synovitis in rheumatoid
545 arthritis: a EULAR-OMERACT ultrasound taskforce-Part 1: definition and development of a
546 standardised, consensus-based scoring system. *RMD Open*. 2017;3:e000428.
- 547

Figure 1.



Figure 1. Illustration of ultrasound detected synovitis (images A and C) (arrows) and non-contrast enhanced whole-body magnetic resonance imaging (MRI) findings of effusion/synovial thickening (images B and D) (arrows) in three joints in a 15-year old with juvenile idiopathic arthritis. Longitudinal (suprapatellar recess) and transverse (lateral parapatellar recess) ultrasound scan of the knee joint showing B-mode (BM) grade 3 (A). Sagittal MRI scan showing effusion in the knee joint (B). Longitudinal dorsal ultrasound scan of the tibiotalar joint showing BM grade 2, and lateral ultrasound scan of the posterior subtalar joint showing BM grade 3 (C). Sagittal MRI scan showing effusion in the tibiotalar and subtalar joints (D).

Figure 2A.



2B.

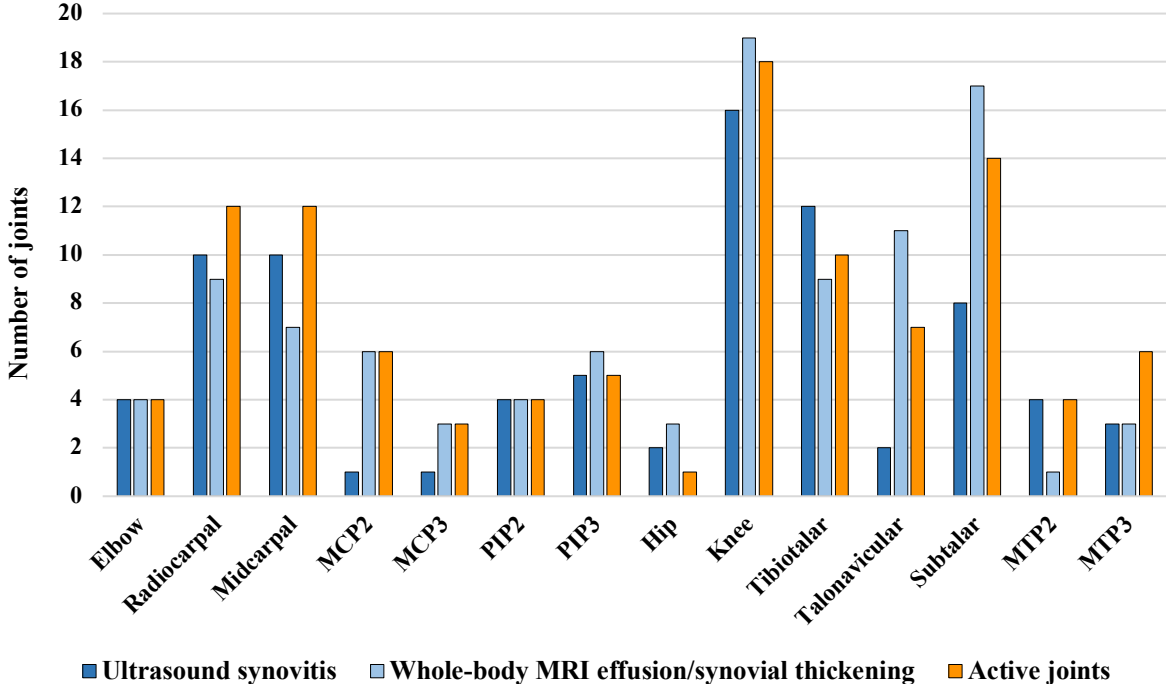


Figure 2. (A) Frequency of normal findings in 14 joints assessed with ultrasound, non-contrast enhanced whole-body magnetic resonance imaging (MRI) and clinical joint examination. (B) Frequency of joint inflammation in 14 joints assessed with ultrasound, non-contrast enhanced whole-body MRI and clinical joint examination. MCP, metacarpophalangeal; PIP, proximal interphalangeal; MTP, metatarsophalangeal; MRI, magnetic resonance imaging